Network Selection and Optimisation of 4G Heterogeneous Multi-hop Broadband Wireless Networks

by

Alvin Ting Kee Ngoh

A Thesis presented to the University of Strathclyde in fulfilment of the requirements for the degree of Doctor of Philosophy in the

Department of Electronic and Electrical Engineering

Centre for Intelligent Dynamic Communications

December 2014

Declaration

This Thesis is the result of the author's original research. It has been composed by the author and has not been previously submitted for examination which has led to the award of a degree.

Alvin Ting Kee Ngoh December 2014

Acknowledgment

First and above all, I praise God, the almighty for his abundant blessing and granting me the opportunity and capability to proceed successfully.

Completing this Thesis has been a greatly rewarding experience. For this, I would like to express my deep and special appreciation and thanks to my supervisor Prof. Ivan Andonovic. I would also like to express my special gratitude for the efforts by Dr. David Chieng (MIMOS Berhad), who has served as a second supervisor, and Dr. Kwong Kae Hsiang. Together, they have provided great support and patience, providing me with an excellent atmosphere for doing research. They have also provided valuable guidance not only regarding various technical issues, but also with respect to the overall research approach.

I am very grateful to several others that have also been involved my research. I especially would like to thank Dr. Mazlan Abbas, Dr. Daniel Wong, Dr. Ng Seh Chung, Abdulziz M Ghaleb and Ayad Atiyah Abdulkafi who have contributed directly and indirectly with ideas and feedback on the research, my Thesis and publications. In addition, the measurements provided by S. Dawood Sajjadi, Lo Ka Kien are much appreciated.

I would also like to express my thanks to Charlie, Wong Ing Liang, Jane, Leo and Gavin for their kindness and help, making my stay in Glasgow unforgettable.

The financial support from the MIMOS Berhad (National Research Institude of Malaysia) is gratefully acknowledged. I am also thankful for the excellent administrative support from Ms Morag Aitken (University of Strathclyde) and Anis Abdullah (MIMOS Berhad).

I want to thank my family who have supported me throughout in an extraordinary manner. I thank my lovely son, Jedd Ting, for his lovely smile and as a source of daily laughter. Finally, I would like to express my deepest love for my wife, Eileen Lau, for her support and taking care of my son during the period I was away from home, based in University of Strathclyde.

Abstract

Wireless Heterogeneous Networking (HetNet) offers the potential to be one of the most promising approaches to meeting escalating network capacity demands cost-effectively. The main challenge facing the deployment of HetNets is provisioning backhaul connectivity for small cells and the selection is governed by availability and cost, not solely by capacity requirements.

In practical deployments, the adoption of mixture of backhaul technologies is likely, creating a non-uniform capacity distribution of small cells. The challenge becomes even more demanding if the backhaul is in the form of a multi-hop network. The research therefore proposes two algorithms which ensure that users enjoy the best possible quality of experience represented in terms of connection throughput and fairness considering the issues owing to small cells backhauling.

The performance of types of HetNet, the Hotspot Wireless HetNet (HWH) and Multi-hop Wireless HetNet (MWH) corresponding to direct and multi-hop backhauling of small cells is evaluated. For HWH, an algorithm – the Dynamic Backhaul Capacity Sensitive Network Selection Scheme (DyBaCS) - is developed to manage the non-uniform backhaul capacity distribution ensuring a consistently fair network bandwidth distribution whilst maintaining throughput. The performance of DyBaCS and two other commonly used network selection schemes (NSSs) is evaluated and compared. Results show that DyBaCS provides superior fairness and a user throughput performance comparable to other reported schemes.

For the more complex MWH architecture, a joint Multi-hop Bandwidth Allocation (MBA) and DyBaCS algorithm is developed to manage network performance. The performance of the algorithm is compared to results obtained using the Cuckoo Search optimisation algorithm and the Fair Share bandwidth allocation scheme. Results show that the algorithm is resilient in improving cell throughput whilst maintaining high levels of fairness.

Table of Contents

List of Figures

List of Tables

List of Algorithms

Abbreviations

3GPP	3rd Generation Partnership Project
AAA	Authentication, Authorization and Accounting
A-MPDU	Aggregated MAC Protocol Data Unit
A-MSDU	Aggregated MAC Service Data Unit
ANDSF	Access Network Discovery and Selection Function
AP	Access Point
BA	Bandwidth Allocation
BE	Best Effort
BS	Base Station
CS	Cuckoo Search
DCU	Distinct Carrier Usage
DL	Downlink
DSL	Digital Subscriber Line
DSMIP	Dual Stack Mobile IP
DSMIPv6	Dual Stack Mobile IPv6
DyBaCS NSS	Dynamic Backhaul Capacity Sensitive NSS
ECC	Error Correction Code
EDGE	Enhanced Data Rate for Global Evolution
EIRP	Equivalent Isotropically Radiated Power
EPC	Evolved Packet Core
ePDG	EPC PDG
EV-DO	Enhanced Voice-Data Optimized

FM	Fade Margin
FS	Fair Share
GPRS	General Packet Radio Service
GPS	Global Positioning System
GSMA	Global System for Mobile Association
GTP	GPRS Tunnelling Protocol
GW	Gateway
HCU	Hybrid Carrier Usage
HetNet	Heterogeneous Network
HPBW	Half Power Beamwidth
HPLMN	Home Public Land Mobile Network
HSDPA	High Speed Downlink Packet Access
HSPA	High Speed Packet Access
HWH	Hotspot Wireless HetNet
IBA	Initial Bandwidth Allocation
ICP	Interoperability Compliance Program
IEEE	Institute of Electrical and Electronics Engineers
IEEE-SA	Electrical and Electronics Engineers Standards Association
IETF	Internet Engineering Task Force
IFW	Integrated Femto-WiFi
IP	Internet Protocol
ISM	Industrial, Scientific and Medical
ITU	International Telecommunication Union
IWLAN	Intergrated Wireless LAN

LOS	Line of Sight
LTE	Long Term Evolution
MAC	Medium Access Control
MAP	Mesh Access Point
MBA	Multi-hop Bandwidth Allocation
MCS	Modulation and Coding Scheme
MIMO	Multiple-Input and Multiple-Output
MMS	Multimedia Messaging Service
MN	Mesh Node
MNO	Mobile Network Operator
MWH	Multi-hop Wireless HetNet
NGH	Next Generation Hotspot
NSS	Network Selection Scheme
OFDM	Orthogonal Frequency Division Multiplexing
PDG	PDN Gateway
PDN	Packet Data Network
PDU	Protocol Data Unit
PMIP	Proxy Mobile IP
PRB	Physical Resource Block
QAM	Quadrature Amplitude Modulation
QoE	Quality of Experience
QoS	Quality of Service
RADIUS	Remote Authentication Dial-In User Service
RAT	Radio Access Technologies

RIFS	Reduced Inter-Frame Space
RSSI	Received signal strength indication
SC-FM	Single-Carrier FDM
SCU	Single Carrier Usage
SIFS	Short Inter-Frame Space
SINR	Signal to Interference and Noise Ratio
SISO	Single-input and single-output
SM	Spatial Multiplexing
SSPNs	Subscription Service Provider Networks
TDMA	Time Division Multiple Access
UE	User Equipment
UL	Uplink
UMTS	Universal Mobile Telecommunications System
UNII	Unlicensed National Information Infrastructure
USD	United States Dollar
WAG	WiFi Access Gateway
WBA	Wireless Broadband Alliance
WCDMA	Wideband Code Division Multiple Access
WFA	WiFi Alliance
WiFi	Wireless Fidelity
WiMAX	Worldwide Interoperability for Microwave Access
WISPr	Wireless Internet Service Provider roaming
WLAN	Wireless Local Area Network
WMN	Wireless Mesh Network

Notations and Symbols

α	Path loss coefficient
σ_L	local variability for shadowing model
φ	WiFi IP layer efficiency
φ_{CP}	Efficiency factor due to Cyclic Prefix
φ_{Pilot}	Efficiency factor due to Pilot carriers
$\varphi_{Spectrum}$	Spectrum Efficiency
θ, ϕ	Angles for the spherical coordination
z	Gaussian random variable
A	Total signal attenuation along transmission path (in watt)
b	Backhaul branch index from GW
B	Channel bandwidth
BW_{Eff}	Effective Channel Bandwidth
c	Edge colour
C_{Av}^{Phy}	Average user throughput (Physical Layer)
C_{Av}	Average user throughput (IP Layer)
C_{Bh}^{i}	Initial backhaul capacity allocated to MAP i
C_{Bh}^{j}	Bandwidth assign to MNj
$C_{Eff,bh}^{i}$	Effective backhaul capacity of MNi
C_{GW}	Total capacity of mesh GW

$C_{i,j}^{b}$	Remaining capacity available on backhaul link $L_{i,j}^{b}$
C_{link}^{WiFi}	IP layer throughput of a WiFi link
C_{link}^{LTE}	IP layer throughput of a LTE link
C_{S^i}	The sum of IBAs for all MNs in S^i
C_{sys}^{Phy}	System throughput (Physical Layer)
d	Distance between receiver and transmitter
D	Antenna directivity
E	Set of Edges representing interference amongst APs
f	Carrier frequency in Hertz
F	Set of WiFi channels
f_c	LTE Carrier frequency in Gigahertz
F'	Set of orthogonal WiFi channels
F_x	Number of slots allocated to user x
FM	Fade Margin
G	Interference Graph
G_{MIMO}	MIMO gain factor
G_{Rx}	Receive antenna gain
G_{Tx}	Transmit antenna gain
h	Average building height in meters
h_{BS}	Antenna heights of BS in meters
h_{UT}	Antenna heights of user terminal in meters
I_j	logical number indicating whether signal strength of AP j is strong enough to cause interference

I_{TBS}	transport block size index
IM	Implementation Margin
k	Boltzmann Constant
L	Total signal attenuation along transmission path (in decibel)
L_{All}	Loss considering path loss and shadowing loss
$L_{i,j}^{b}$	Branch b backhaul link connecting MNi and MNj
L_{Int}	Interference Loss
L_{l}^{j}	Logical number indicating whether AP j is on the same channel
L_{Tx}	Transmit line loss
L_{Rx}	Receive line loss
L_{Shadow}	Shadowing loss
M	Total number of APs
N	Number of users terminal in a cell
NF	Noise figure
NFl	Noise Floor
P_{l}^{i}	Total interference power to AP i on channel l
P_{j}	Interference power from AP j
PL	Path loss
P_{Rx}	Received power
P_{Tx}	Transmit power
P_{x}	Relative frequency of user packets of class x
R	WiFi raw data rate

$\mathcal{R}^i$	Bandwidth allocation weight on MAP i
R_x	User data rate
S^i	Set of sub-ordinate MNs connected to MNi
T	Temperature in ℃Kelvin
U	Set represents all mesh nodes
V	Set of Vertices
W	Street width in meters

Chapter 1

Introduction

1.1 Overview

The success of mobile telephony has dramatically transformed lifestyles and behaviours. Users now stay connected accessing information anytime, anywhere and with integrated GPS, location based services are provisioned routinely; locating the nearest restaurant is now as easy as performing a search on the Internet. Ubiquitous connectivity through mobile telephony has also sparked the emergence of various innovative mobile applications such as free navigation [Waze, 2008] and Easy Taxi [Easy Taxi, 2012], to highlight a few.

The range of services and ease of use provided by mobile networks has stimulated massive growth in the number of mobile subscribers. According to the International Telecommunication Union (ITU) World Telecommunication/ICT Indicators database (Figure 1.1), the total number of mobile subscribers now exceeds the world population [ITU-D, 2013].

The proliferation of multimedia applications and services over new mobile devices such as smart phones and tablets has generated a massive amount of data traffic which in turn continually challenges Mobile Network Operators (MNOs) to keep pace with the rapidly growing demand for access capacity. MNOs are facing

increasing pressure to upgrade their mobile networks in order to service consumer demand for faster access to a rich mix of services. According to Cisco [Cisco, 2014], global mobile data traffic will increase nearly 11-fold from 2013 to 2018 (Figure 1.2); however, global mobile network connection speeds are predicted to increase only by 2-fold by 2018. If this mismatch is not addressed, the gap is expected to grow wider due to the ever increasing proliferation of devices supporting multimedia content.

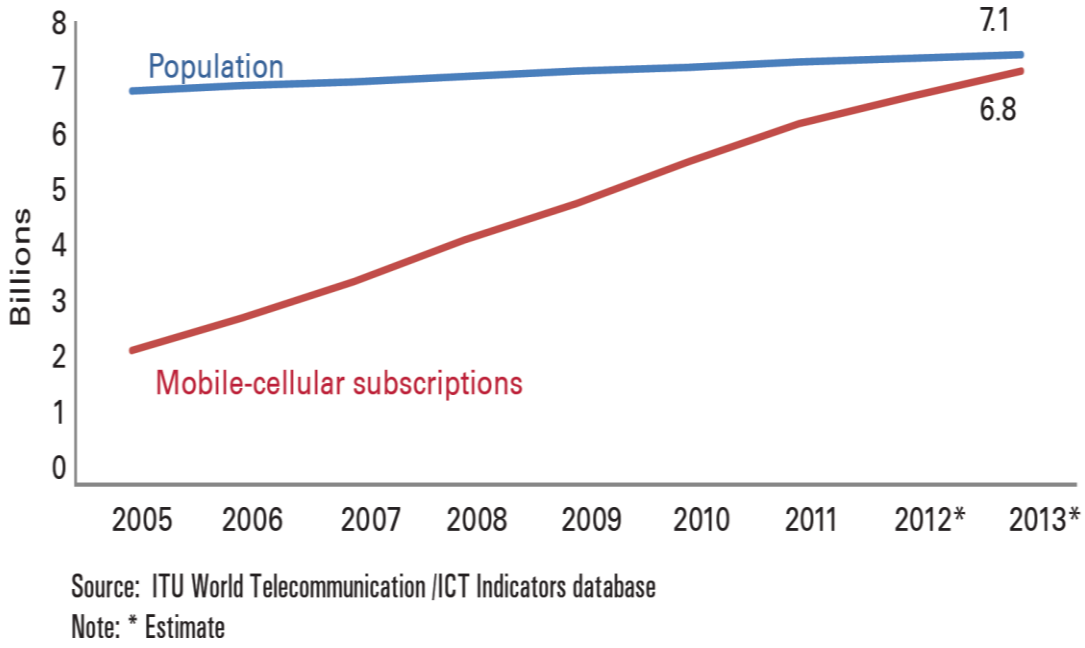

Figure 1.1: Number of mobile-cellular subscriptions compared to the world population.

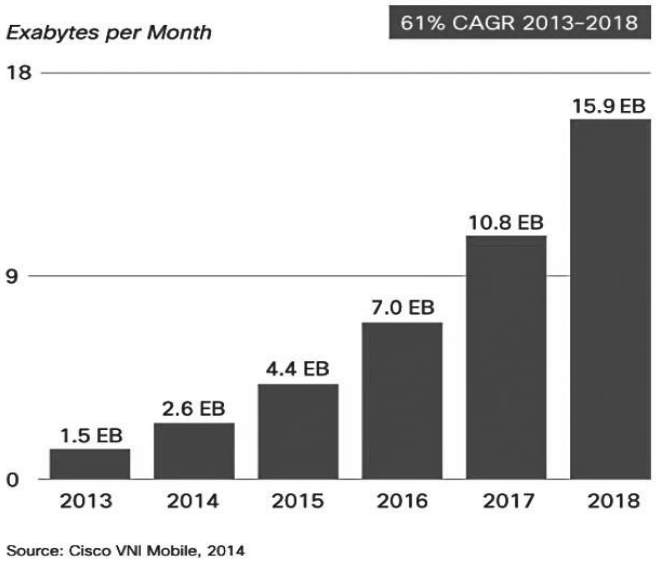

Figure 1.2: Growth of mobile data traffic per month from 2013-2018. (Source: Cisco VNI Mobile Forecast, 2013)

1.2 Network Capacity Enhancement Approaches

In modern wireless communications, as data traffic increases, the spectral efficiency of wireless systems must be improved. The following solutions are typically adopted by current mobile operators to improve mobile network capacity.

1.2.1 Cell Splitting and Cell Sectorisation

The main characteristic of a cellular network is the ability to re-use frequencies to increase both coverage and capacity by deploying multiple cells over a coverage area [MacDonald, 1979]. Each cell is served by a transceiver – the base station (BS) – which transmits at a power level that does not interfere with other cells operating at

the same frequency. Hence, frequency channels can be reused by splitting or sectoring cells.

Cell splitting is the process of dividing a large cell area into several smaller segments to provide additional capacity within the region of the original cell coverage; each smaller cell has its own BS with reduced antenna height and transmitter power. Following cell splitting, the new smaller cells are reassigned new frequencies that do not cause co-channel interference with adjacent cells. Consequently the capacity of the system is increased through reuse of available channels.

Cell Sectorisation is an alternative technique to enhance capacity without deploying new sites, a more cost effective and less time consuming solution. Sectorisation divides a cell into several sectors through directional antennas [Huang et al., 2010] [A.Wacker et al., 1999]. A BS is typically sectorised into three or six sectors and different channels are used by two adjacent sectors in order to avoid co-channel interference, thus improving system capacity.

Although cell splitting and sectorisation are attractive solutions, there are limitations to both methods. In theory, the capacity of a network can be increased without limit by cell splitting as long as the frequency planning is executed properly. However in practice, adding another BS in a dense deployment area can significantly reduce cell splitting gains due to severe inter-cell interference. Cell splitting can only be performed up to a certain dimension, limited by the density of the cell within an area unless systems with power control and active smart antennas are implemented [Caretti et al., 2012]. Furthermore, site acquisition costs in a capacity-limited dense

urban area can be prohibitively expensive. Similar to cell sectoring, a typical number of sectors in a cell are usually three to six.

1.2.2 Improved Modulation Techniques

The capacity of a wireless network is closely related to its spectral efficiency measured by bits per second per Hertz (bps/Hz) [Agilent, 2001]; the type of radio modulation used is a primary factor in the attainable spectral efficiency. Digital modulation used in present advanced wireless communications involves modifying a radio waveform – referred to as a symbol [Agilent, 2001] – in order to encode bits of information. While the rate of symbol transmission is proportional to channel bandwidth, the total number of bits that can be encoded onto a symbol is a function of the type of modulation. The maximum bit rate is the product of symbol rate and number of encoded bits per symbol.

A higher-order modulation such as the 64 Quadrature Amplitude Modulation (64-QAM) encodes more bits (6 bits) compared to the lower-order modulation 16-QAM (4 bits). A higher-order modulation generally requires a higher Signal-to-Interference-plus-Noise Ratio (SINR) [Tse and Viswanath, 2005]; hence the highest-order modulation cannot always be utilised and is dependent on received signal quality. To improve the reliability of a link, Error Correction Codes (ECC) is normally applied to the transmitted data allowing the detection of errors in receiving data and consequently correction of these errors without retransmission. ECC introduces overheads that reduce the effective throughput as part of the bandwidth is

used by the correction task; a trade-off between link reliability and effective throughput exists.

Figure 1.3 [3GPP, 2010b] compares the spectral efficiencies of a Shannon bounded channel [Pahlavan and Levesque, 2005a] with various Modulation and Coding Schemes (MCS) commonly used in the Long Term Evolution (LTE) standards [3GPP, 2013], High-Speed Downlink Packet Access (HSDPA) [Holma and Toskala, 2006], Enhanced Voice-Data Optimized (EV-DO) [Bi, 2005], IEEE802.16e-2005 [IEEE Std, 2005b] and other wireless technologies. The comparison shows that advanced wireless technologies are only 2 dB or 3 dB below the Shannon capacity bound. Consequently state-of-the-art modulation and coding techniques are already operating close to the theoretical limit, leaving very limited room for further improvement.

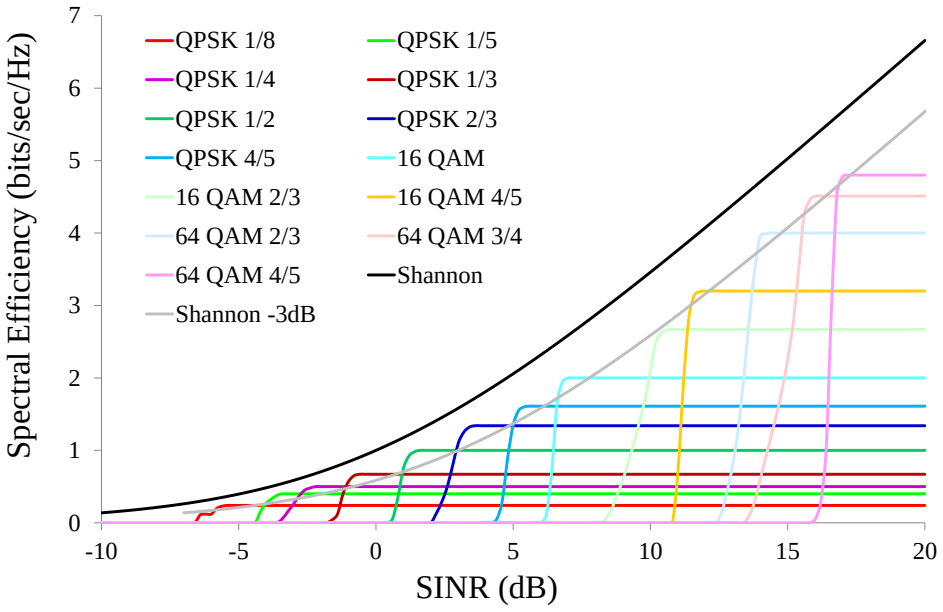

Figure 1.3: Spectral efficiency of a set of Modulation and Coding techniques used in LTE-Advanced systems as compared to Shannon theoretical limits [3GPP, 2010b].

1.2.3 Multiple-Input Multiple-Output (MIMO)

MIMO principles have become an indispensable part of existing and future broadband wireless communication systems. A MIMO strategy improves the performance of a wireless system through for example, Spatial Multiplexing (SM), spatial diversity and beam forming. Spatial diversity provides gain that improves link reliability and beam forming increases transmission range by focussing the radiated power of an antenna array to the desired direction. The only MIMO technique that increases spectral efficiency in wireless networks is SM, improving capacity by enabling independent transmission of separately encoded data streams using multiple antennas.

A MIMO system with n_T transmit and n_R receive antennas and channel $H(n)$ can be treated as an $n_R \times n_T$ matrix, its capacity represented as [Barbarossa, 2005]:

$$C(H) = q \cdot B \cdot log_2\left(\frac{S}{N}\right) + B \cdot \sum_{i=1}^{q} log_2\left(\frac{P_{Tx}}{n_T}\right) bps \qquad (1.1)$$

where B is the channel bandwidth, S is signal power, N is noise power and $\frac{S}{N}$ is the Signal-to-Noise Ratio, P_{Tx} is the transmit power, n_T is number of transmit antennas and q is the rank of matrix H, the maximum value for the rank is $min(n_T, n_R)$. If the second term on the right-hand side of Equation (1.1) is neglected for the moment and if $SNR \gg 1$, a MIMO channel results in a potential increase of channel capacity at high SNR, with respect to the Single-Input and Single-Output (SISO) case in

Equation (1.2) [Barbarossa, 2005], by a factor equal to the rank q of the channel matrix H;

$$C(H) = B \cdot log_2\left(1 + \frac{S}{N}\right) \quad (1.2)$$

Although Equation (1.1) shows that it is possible to linearly improve the capacity by adding more antennas within a MIMO architecture, implementing multiple antenna elements on handheld devices with small form factors is a major practical challenge [Jamil A et al., 2010].

1.2.4 Carrier/Channel Aggregation

Shannon's Law (Equation (1.2)) shows that in a communication system, the wider the channel bandwidth B the greater the capacity. Therefore, when more capacity is required, the most straightforward solution is to increase channel bandwidth.

For example, the Universal Mobile Telecommunications System (UMTS) [Holma and Toskala, 2006] uses Wideband Code Division Multiple Access (WCDMA) [Harri Holma and Antti Toskala, 2004] to provision data speeds up to 2Mbps. The subsequent HSDPA standard [Holma and Toskala, 2006] increases the data transmission speeds to 14.1Mbps via a 5 MHz channel bandwidth [3GPP, 2001]. The 3GPP LTE standard [3GPP, 2013] is designed to provide a channel bandwidth up to 20MHz (1.4 MHz, 3 MHz, 5 MHz, 10 MHz, 15 MHz and 20 MHz). As specified in LTE Release 8, the theoretical bit rates of an LTE system can go up to 100 Mbps on

the downlink and 50 Mbps on the uplink [Rohde & Schwarz, 2008]. In fact, up to 170Mbps in the uplink and 300Mbps in the downlink [3GPP, 2013] can be achieved if MIMO is used. The latest LTE-Advanced (3GPP Release 10) [3GPP, 2012a] system includes carrier or channel aggregation techniques which enable bandwidth aggregation of up to five 20MHz Component Carriers (CC) [3GPP, 2012c] in order to achieve the peak data rate of 1Gbps for low mobility and 100Mbps for high mobility communication.

Although providing a wider channel bandwidth is one way to release capacity, it is economically challenging to do so due to the high cost of securing spectrum [Ofcom, 2013; Rishabh, 2010].

1.2.5 The Wireless Heterogeneous Network (HetNet)

The Wireless Heterogeneous Network (HetNet) is an emerging concept which adopts a variety of BS types, radio access technology (RAT), transmission solutions and power levels to provision an extensive wireless network.

The heterogeneity of HetNet can be categorised into two groups, single-RAT multi-tier and multi-RAT HetNet [Yeh et al., 2011]. In a single-RAT multi-tier HetNet, BSs with the same radio technology but different coverage footprint are overlaid across the same geographical area. Devices within the network share the same carrier frequency, also referred to as a Single Carrier Usage (SCU) HetNet (Section 2.3.1). In a multi-RAT HetNet, different radio access technologies operating in different spectrum bands are adopted, also referred to as Distinct Carrier Usage (DCU)

(Section 2.3.2). The focus of the study is mainly on the multi-RAT HetNet, discussed in Chapter 2.

In HetNets, low power and low cost small cells are placed at coverage gaps or high capacity-demand hotspots to complement the conventional larger BS i.e. Macro BSs which provides the blanket coverage. Thus part of the overall traffic is offloaded to small cells to manage traffic congestion at the BS. The performance of HetNets using small cells has been studied [H. Claussen, 2007] [Gora and Kolding, 2009] [Qualcomm, 2011] [Kyunghan Lee et al., 2010] with results showing that the spectral efficiency can be improved further.

The small cells in HetNets can be based on licensed or unlicensed technologies e.g. WiFi operating in an unlicensed spectrum and LTE Femto and Pico cells usually operating within a licensed spectrum. A recent survey of mobile operators, vendors, and regulators [Ruckus] which focused on the provision of data services shows that Wi-Fi offload and small cells are considered the most effective solutions to increasing capacity in the RAN. Wi-Fi offload is expected to provide 34% capacity increase and a 27% increase from small cells (Figure 1.4). The expectation is that in the near future, Wi-Fi will assume a more significant role in offloading traffic compared to licensed small cells.

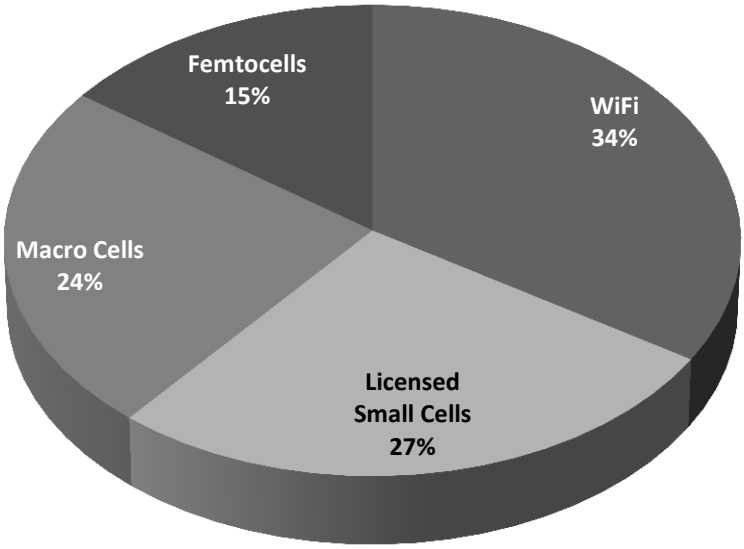

Figure 1.4: Capacity increases due to data offload or technology improvement [Ruckus].

1.3 Research Motivation

As discussed in Section 1.1, most network cellular operators are struggling to cope with the huge demand for increasing data rate especially at wireless hotspots. Radio link improvements via modulation and coding techniques are approaching the theoretical limit and additional spectrum is often limited and expensive. Advanced antenna architectures are also believed to be approaching their practical limits due to the small form factor of mobile devices. Conventional base station deployments in high data demand areas through cell splitting and sectorisation are either hitting the saturation point or becoming unsustainable. On the backdrop of the growing demand for network capacity, MNOs are also facing flattening revenue per bit due largely to

the proliferation of flat-rate data-centric service plans. Therefore, whilst enhancing network capacity, at the same time MNOs have to keep the cost as low as possible.

All of the above dynamics inevitably stimulate a network topology migration to a HetNet consisting of a mixture of macro cells and small cells capable of providing a step increase in capacity in a cost-effective manner [Yeh et al., 2011]. Small cells are attractive because of the small coverage size, ease of deployment, low equipment and operating cost compared to a normal BS. WiFi cells utilising the spectrum free of charge are already providing widespread coverage at many locations. The availability of multi-RAT (Radio Access Technology) allows user devices to connect to different wireless networks such as 3G, LTE, WiMAX, and WiFi either one at a time or simultaneously also serves as a catalyst to further fuels the migration of the existing network to wireless HetNets. In addition to providing a means of offloading traffic from the Macro/Micro cell, small cells operating at lower power with reduced footprints also have a positive impact on battery life of mobile devices since small cell transceivers are closer to end users [Alcatel Lucent, 2013].

In view of the many benefits offered by HetNets, this evolution has the potential to be one of the most promising routes to managing mobile data capacity growth. Hence, the evalaution of the performance of HetNets is the main research topic presented in the dissertation.

1.4 Thesis Outline

Two classes of HetNet, namely Hotspot Wireless HetNet (HWH) and Multi-hop Wireless HetNet (MWH) are explored. In HWH, different commonly applied end users' Network Selection Schemes (NSSs) are studied and compared to a proposed NSS which aims to optimise network performance whilst maintaining fairness. The study is then extended to a more complex MWH scenario where a combined NSS and backhaul bandwidth assignment scheme is required to optimise performance.

Chapter 2 provides background on HetNets presenting existing architectures followed by the reasons why a specific HetNet architecture is chosen for the research. Subsequently the technology components – LTE and WiFi – within the selected HetNet architecture are described along with the issues and challenges faced by this class of implementation.

In Chapter 3, the state-of-the-art related to cellular-WLAN wireless HetNets is discussed in detail. The existing 3GPP and IEEE standards that support Cellular-WLAN interworking are presented and the latest standards implementations by 3GPP and IEEE are introduced. The mapping of existing standards and the detail of the implementation permits the research scope to narrow to a specific problem related to backhauling of small cells within HetNets. A literature review on related research is then carried out.

Chapter 4 presents the modelling approaches used in the performance evaluation of the proposed implementation. The models are divided into two categories viz. Macro cell and Small cell. LTE is chosen as the underlying radio technology for the Macro cell, while Small cells are assumed to be based on WiFi standards, predominately owing to their widespread popularity and market penetration. For both technologies, the modelling detail of the Physical layer, MAC layer, wireless propagation and channel are discussed. Further, resource allocation and sharing amongst users are also discussed for both technologies. Finally, the approach of combining both Macro and Small cells to form a HetNet is presented.

Chapter 5 presents the proposed Network Selection Scheme (NSS) referred to as the Dynamic Backhaul Capacity Sensitive (DyBaCS) NSS. DyBaCS takes into consideration network information such as effective backhaul capacity, network load and access link capacity from both the Macro BS and Small Cells in reaching a decision and in so doing, ensures a consistently fair network bandwidth distribution whilst maintaining network throughput. The study compares the performance of DyBaCS with two of the most common network selection schemes. Results show that DyBaCS provides the best fairness while preserving average user throughput compared with other well-known NSSs.

Chapter 6 presents the new algorithm for the optimisation of the performance of a Multi-hop Wireless HetNet applying a joint Multi-hop Bandwidth Allocation (MBA) and DyBaCS Network Selection Scheme. The simulation methodology used in the evaluation is detailed. For comparison purposes, the Cuckoo Search algorithm is implemented and used to determine the performance upper bound of the MWH.

Finally simulation results are compared to the results obtained using the Cuckoo search. The Chapter concludes with discussions.

Chapter 7 highlights important results, summarises the contributions, followed by suggestions for future work.

1.5 Thesis Contributions

The Thesis proposes two algorithms which aim to optimise throughput and fairness of HetNets considering issues and challenges owing to small cells backhauling. The methodology adopted in the development is;

I. Two distinct wireless heterogeneous network architectures are modelled

- The spatial model of HetNet consisting of a LTE advanced network according to Release 10 [3GPP, 2010b] and IEEE802.11g [IEEE Std, 2003] based WiFi Hotspots. In this architecture the small hotspot cells are directly backhauled to the core network.

- The spatial model of a multi-hop wireless HetNet consisting of a LTE advanced network based on Release 10 and IEEE 802.11n [IEEE Std, 2009], WiFi mesh network with 2.4GHz for access radio and 5GHz for backhaul radio. In this scenario only the Mesh Gateway is backhaul to the core network.

Both HetNet models consider the physical layer consisting of multiple MCS instead of a simplified unit circle radio coverage area model adopted in many existing research. The spatial model offers higher accuracy in interference modeling since antenna radiation patterns (directional or omni-directional) are considered.

II. A new NSS scheme referred to as the Dynamic Backhaul Capacity Sensitive (DyBaCS) NSS is developed to take the backhaul capacity of small cells into consideration during network selection and treat the non-uniform backhaul capacity distributions in HetNet when different technologies are used to ensure every user has a fair network bandwidth distribution whilst maintaining overall network throughput. The proposed DyBaCS takes into consideration network information such as effective backhaul capacity, network load and access link capacity from both Macro BS and Small cells when making a decision.

III. An algorithm is developed based on the Cuckoo Search principle to compute the upper bound capacity for the Multi-hop Wireless HetNet. Given the fixed WiFi Gateway capacity allocation, the algorithm optimises the Small cells backhaul bandwidth allocation dynamically as the number of users joining the network varies. Although the Cuckoo Search algorithm provides the optimal result the time used to locate the optimum point is relative long and it is not suitable for fast changing dynamic HetNets; therefore the results obtained serve solely as the upper bound reference.

IV. A new algorithm with joint Multi-hop Bandwidth Assignment and DyBaCS for Multi-hop Wireless HetNet capacity and fairness optimisation is proposed. The output of the proposed algorithm is compared to the result obtained using the well-known Cuckoo Search optimisation. The proposed algorithm is computationally simpler and suitable for dynamic fast changing wireless environments compared to a Cuckoo Search.

Overall, the dissertation provides a rigorous optimisation study and performance evaluation of HetNets considering direct backhaul and multi-hop backhaul to Small cells.

1.6 Publications

[David Chieng et al., 2011]

David Chieng, Alvin Ting, Kwong Kae Hsiang, Mazlan Abbas, Ivan Andonovic, (2011, December). "Scalability Analysis of Multi-Tier Hybrid WiMAX-WiFi Multi-Hop Network", IEEE Global Telecommunications Conference (GLOBECOM 2011), 2011 (pp. 1-6).

[Ting et al., 2012]

Alvin Ting, David Chieng, Kwong Kae Hsiang & Ivan Andonovic, (2012, November), "Optimization of heterogeneous multi-radio multi-hop rural wireless network", IEEE 14th International Conference on Communication Technology (ICCT) 2012, (pp. 1159-1165).

[Ting et al., 2013]

Alvin Ting, David Chieng, Kwong Kae Hsiang, Ivan Andonovic, & Wong K. D. (2013, September). "Dynamic backhaul sensitive Network Selection Scheme in LTE-WiFi wireless HetNet", IEEE Personal Indoor and Mobile Radio Communications (PIMRC), 2013 IEEE 24th International Symposium on (pp. 3061-3065).

Alvin Ting, David Chieng, Kwong Kae Hsiang, Ivan Andonovic, Wong K. D, "Scalability analysis of backhaul sensitive network selection scheme in LTE-WiFi HetNet" submitted to Transactions on Emerging Telecommunications Technologies, Wiley.

Alvin Ting, David Chieng, Kwong Kae Hsiang, Ivan Andonovic, "LTE-WiFi Multi-Hop Heterogeneous Wireless Network Performance Optimisation" submitted to IEEE Transactions on Communications.

Chapter 2

Wireless Heterogeneous Networks (HetNets)

2.1 Introduction

In the Chapter, the most relevant Wireless Heterogeneous Networks (HetNets) architectures are detailed, their advantages and disadvantages are discussed and the motivation behind the research is developed. The characteristics of the underlying radio technologies such as LTE and WiFi which form the proposed HetNet implementation are presented as well as the issues and challenges faced by HetNet deployments.

2.2 Background

The evolution of mobile cellular networks over the last few decades has been staggering. The number of mobile-cellular subscribers worldwide has grown exponentially, surpassing 6.8 billion in 2013 [ITU-D, 2013] and the number of mobile phones has exceeded the world population [Cisco, 2014]. The cellular network has evolved from the 2G Enhanced Data Rate for Global Evolution (EDGE) technology offering 472kbps peak downlink rate [Holma and Toskala, 2009] to the

current 3G/3.5G technologies such as High Speed Packet Access (HSPA) [Holma and Toskala, 2006] and the Long Term Evolution (LTE) standard which offer peak rates of 2Mbps and 42Mbps respectively (Figure 2.1). In the near future, 4G such as LTE-Advanced will be offering a peak downlink rate of 1 Gbps [Sesia et al., 2009].

While 4G is being adopted by mobile network operators, emerging 5G concepts are beginning to be defined. [Thompson et al., 2014a] [Thompson et al., 2014b] indicate that the drivers for 5G systems are much more diverse than simply the demand for data services over the Internet e.g. greener wireless networks, support for machine-to-machine communications, device-centric network design and adopt higher-frequency millimeter wave bands.

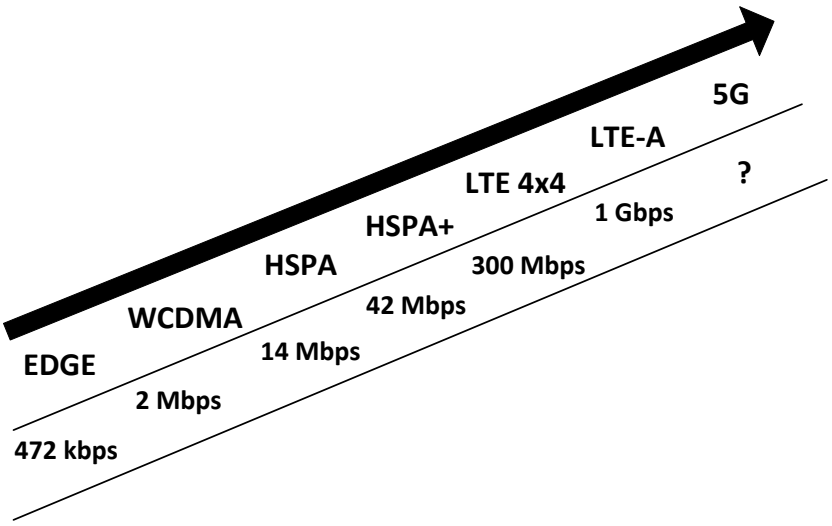

Figure 2.1: Evolution of cellular network data rates (Reference to [Holma and Toskala, 2009]).

The advancement of cellular technologies as well as the development of user devices such as smart phones and tablets has enhanced the Internet surfing experience and stimulated the exponential growth of data traffic which in turn creates huge challenges for cellular network providers. Hence there is an increasing urgency for mobile network operators (MNO) to improve network capacity.

One route to increase network capacity is to deploy many small cells i.e. WLAN [Geier, 2002], Pico Cell [Damnjanovic et al., 2011] and Femto Cell [Chandrasekhar et al., 2008] in order to offload data traffic from Macro Cells i.e.3G [Damnjanovic et al., 2011], LTE [Sesia et al., 2009] or WiMAX Base Stations [Chen et al., 2008]. The increasing pressure for mobile network operators to offload data traffic to small cell networks indicates that future mobile broadband networks are largely going to be heterogeneous [Aviat Networks, 2011] [Informa telecoms & media, 2013]. Such migration is further fuelled by the availability of multi-RAT (Radio Access Technology), which allow user devices to connect to 3G, LTE, WiMAX, WiFi, either one at a time or simultaneously.

2.3 Wireless Heterogeneous Network (HetNet) Architectures

HetNet promotes cooperation between Macro/Micro Cell and lower power small cells in addressing the issues of coverage gaps and capacity hotspots. Figure 2.2 shows an example of a HetNet deployment comprising a LTE Macro base station covering a wide area with LTE Pico Cells, LTE Femto Cells and WiFi networks

covering much smaller areas such as main streets, train stations and residential areas, where the demand for capacity is usually high.

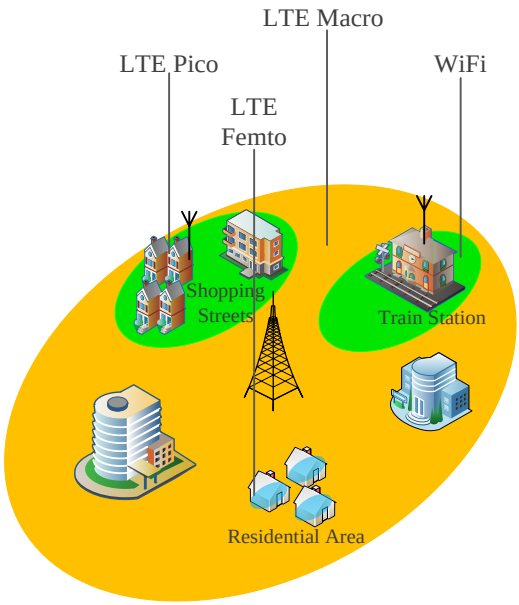

Figure 2.2: An example of a Wireless Heterogeneous Network (HetNet).

HetNets can be categorised into three classes largely based on spectrum usage; Single Carrier Usage (SCU), Distinct Carrier Usage (DCU) [Yeh et al., 2011] or a combination of both here referred to as Hybrid Carrier Usage (HCU).

2.3.1 Single Carrier Usage (SCU) HetNet

A HetNet consisting of pure 3rd Generation Partnership Project (3GPP) components such as a Macro/Micro Cell, Pico Cells and Femto Cells is defined as a Single Carrier Usage (SCU) HetNet [Yeh et al., 2011]. All components in the network belong to 3GPP family and share the same carrier frequency. SCU HetNets follow the general network evolution trends for a network in terms of improved coverage

and greater capacity. Femto Cells deployed within the network provide both general Internet access as well as access to services provided by a mobile network operator.

The advantage of the SCU HetNet is the availability of standards for interoperability as well as the compatibility of all network components. User experience (Quality-of-Experience (QoE)) is adequately satisfied as services can be provisioned seamlessly when a user is moving within the HetNet. Handover can be performed smoothly with session continuity. However, there are some drawbacks; Femto Cells require the use of the same costly and limited licensed spectrum as the Macro/Micro Cells reducing the spectrum utilisation efficiency. Macro/Micro Cell interference from Femto Cells is another concern and consequently the latter are confined to indoor use only.

2.3.2 Distinct Carrier Usage (DCU) HetNet

DCU combines different radio access technologies (RAT) operating in different frequency bands such as LTE and WiFi. DCU HetNets - or more commonly known as Cellular-WiFi Integration – combine a cellular Macro/Micro Cell with smaller WiFi cells. User devices can either connect to WiFi or the cellular network depending on the coverage of the network. DCU is attractive to many MNOs as a cost-effective means of offloading significant amounts of mobile data traffic owing to the widespread WiFi deployments and most devices on the market such as laptops, smart phones and tablets feature integrated WiFi radio interfaces.

Since WiFi uses unlicensed spectrum, DCU has a clear advantage on enhancing capacity without interfering with existing cellular networks. Unlike Femto Cells

which are limited to indoor usage in order to keep the Femto-to-Macro interference level as low as possible, WiFi cells can be deployed freely outdoors [Ruckus, 2014] [Firetide, 2014] [Strix System, 2014].

However, the use of the unlicensed spectrum by WiFi brings its own drawbacks. The spectrum at 2.4 GHz is often crowded with devices such as Bluetooth, cordless phones and a range of other devices equipped with WiFi interfaces creating interference and performance degradation. While 5GHz is less crowded (with less interference), only the newer consumer devices support 5 GHz, including Samsung and Apple smartphones and the iPad [Cisco, 2012b]; the 5 GHz band will become more congested in the future.

At present, WiFi cells mainly transport traffic not on the core cellular infrastructure but on a separate network as the WiFi network may not always belong to the operator. Generally, Cellular-WiFi interworking can be categorised into two modes referred to as loosely and tightly coupled networks.

In a loosely coupled network, WiFi traffic is usually beyond the 3GPP operator's control and only the Best Effort (BE) traffic class is supported. The main objective is for the operators to offload cellular traffic, especially for Internet access [4G Americas, 2013]. In a tightly coupled network, WiFi traffic is usually controlled by the 3GPP operator. WiFi access networks may be integrated into the 3GPP core providing services from mobile network operators, IP session continuity and seamless end user experience irrespective of network type. With such control over the network, carriers can also make RAT selection in order to optimise overall

network performance and provide the greatest QoE for a given subscriber/service at a given time or location.

To date, seamless interworking between WiFi and cellular networks remains a big challenge. As the network operators become more aware of the potential of WiFi networks, standardisation activities that focus on WiFi and 3GPP interworking are beginning to gain momentum, to be discussed in more detail in Chapter 3.

2.3.3 Hybrid Carrier Usage (Femto-WiFi Integration)

Hybrid Carrier Usage (HCU) is the combination of both SCU and DCU. HCU or more commonly known as Femto-WiFi integration is the integration of Femto and WiFi into a single cell [Small Cell Forum, 2012]. Since Femto and WiFi technologies were both designed for small coverage areas serving users through Digital Subscriber Line (DSL)/Ethernet backhaul, mobile network operators soon realised that both technologies could co-exist to bring benefits to end-users, operators, service providers as well as technology providers.

In an integrated cell, a WiFi Access Point (AP) is used to provide general Internet access while Femto APs provide both Internet access as well as access to services provided by the mobile network operator. This is a primary motivation for Integrated-Femto-WiFi Networks because both WiFi and Cellular terminals are served, provisioning services to users through Femto Cells and low cost general Internet access over WiFi. Interference between Femto and Macro-Cellular networks can also be reduced by offloading certain traffic to the WiFi network.

The disadvantages of Integrated Femto-WiFi (IFW) lie in the integration of WiFi modems with the Femto provisioning system that operates with a separate provisioning profile. Since the two networks are different in terms of policies and procedures, a common auto-configuration server for provisioning both WiFi and Femto can be costly [Small Cell Forum, 2012]. Furthermore, interference from Femto Cells to Macro/Micro Cell remains an issue despite traffic being offloaded to the WiFi network.

A comparison for three types of HetNet is summarised in Table 2.1.

Table 2.1: HetNet classification and summary comparison.

HetNet Type	Characteristics	Advantages	Disadvantages
SCU	Macro Cell and Small Cells operating on a common licensed frequency band.	Smooth and seamless Handover between BSs for better user experience.	Less efficient spectrum utilisation due to interference and Femto cells limited to indoor usage.
DCU	Small Cells operate in frequency bands (normally unlicensed) different to Macro cell.	Cost effective due to licensed free spectrum. Efficient spectrum utilisation as no interference between Small Cells and Macro Cell. Widespread WiFi hotspot deployments and common WiFi embedded devices.	Seamless interworking between network components is challenging. Operates in the unlicensed spectrum which is crowded and subject to interferences from other devices.

HCU	Small Cells operate in both licensed and unlicensed frequency band.	MNO services are accessible through Femto Cells and Internet is accessible through inexpensive WiFi access.	Costly to integrate both Femto and WiFi provision system. Interference still exist within HetNet although is it less compared to SCU.

2.4 Scope of HetNet Architecture Implementations

From the above consideration summarised in Table 2.1, DCU seems to be the most promising solution on meeting the demands of cellular network capacity, the main reason being that WiFi 802.11n networks [IEEE Std, 2009] are already supporting up to hundreds of megabits per second data rates within an unlicensed spectrum band. The widespread availability of WiFi radio interfaces in existing user devices implies that WiFi offloading is a natural solution to managing Cellular traffic congestion. Moreover WiFi is an economical solution [Gao et al., 2013] and does not create additional interference between the WiFi and cellular Macro Cell.

SCU which uses a single carrier throughout the whole network is less efficient in spectrum utilisation and is therefore not pursued further. Similary, the more complicated and costly HCU architecture will not be studied.

Consequently, the research focus centres on the design and performance evaluation of HetNets comprising Macro Cell and WiFi small cells. The HetNet architecture under study uses LTE as the Macro/Micro BS, deployed as the main cell that provides blanket coverage with overlapping WiFi cells providing coverage at high demand hotspots. LTE is preferred since it is universally accepted as the core next generation wireless technology - IMT-Advanced – and the standards are being continually defined by the International Telecommunication Union Radio Section (ITU-R) [ITU-R, 2003].

Within the scope of DCU, the WiFi network can be further categorised into two common types viz. WiFi Hotspot and Multi-hop/Mesh WiFi Network corresponding to the Extended Service Set (ESS) and Independent Basic Service Set (IBSS) topologies supported by the IEEE802.11 standards [IEEE Std, 1997].

2.4.1 Hotspot Wireless HetNet (HWH)

WiFi hotspots are widely deployed and readily accepted worldwide [Gabriel, 2013]. One of the common HetNet architectures is a combination of a Macro Cell and WiFi hotspots [Bennis et al., 2013], defined as the Hotspot Wireless HetNet (HWH) for the purposes of the research. Figure 2.3 shows a DCU-type HetNet comprising LTE and WiFi-Hotspost. All WiFi hotspots can be backhauled individually through various wired or wireless technologies such as fibre, cable, copper, xDSL, microwave and multi-hop wireless links. WiFi cells are integrated into the core network through their individual backhaul links.

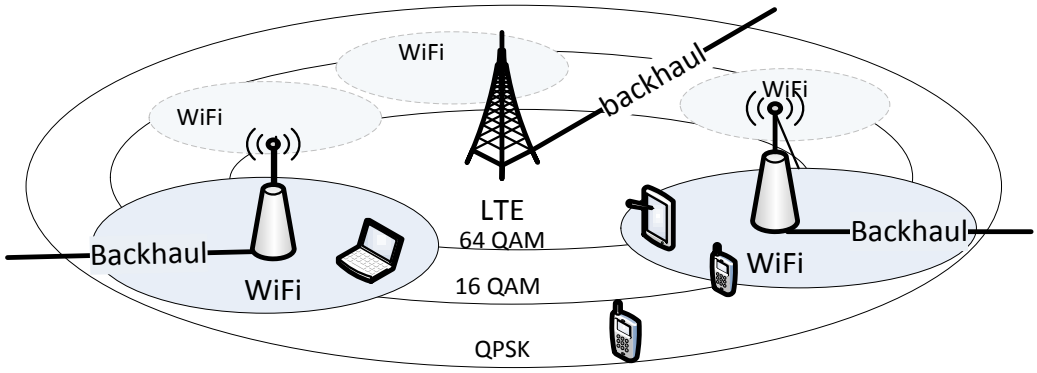

Figure 2.3: A Hotspot Wireless Heterogeneous Network.

2.4.2 Multi-hop Wireless HetNet (MWH)

Wireless mesh networks have been in existence for a number of years [Akyildiz et al., 2005] and a number of commercial wireless mesh networking solutions are currently on offer [Cisco Meraki, 2014], Motorola [Motorola Solutions, 2014], Firetide [Firetide, 2014], Tropos Networks [Tropos, 2014] and Strix Systems [Strix System, 2014].

Due to the growing interest in Wireless Mesh Networking (WMN) technologies, an alternative Multi-hop Wireless HetNet (MWH) architecture consisting of LTE and WiFi Mesh is proposed (Figure 2.4). Within the MWH, several WiFi Mesh nodes are interconnected to form a Multi-hop/Mesh network. WiFi Mesh networks are divided into clusters with a Gateway (GW) acting as a cluster head, also providing backhaul connectivity to the core network. In order to access the Internet, users that are more than one hop away from a GW rely on intermediate Mesh Nodes to forward traffic between the service Mesh AP and the GW.

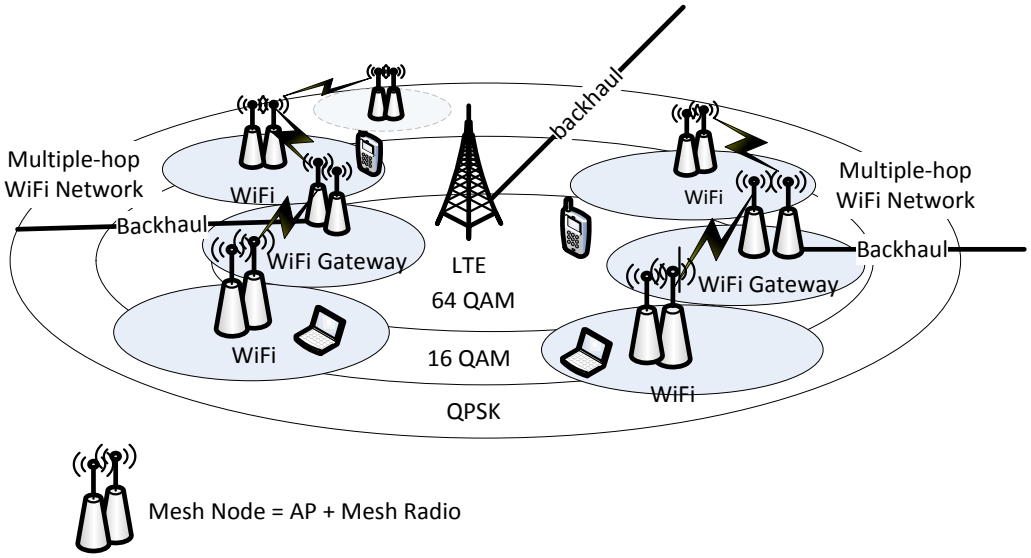

Figure 2.4: Multi-hop Wireless Heterogeneous Network.

2.5 HetNet Radio Technologies

2.5.1 LTE Overview

The Long Term Evolution (LTE) standard was developed by 3GPP for fourth-generation (4G) cellular networking with the aim to improve transmission efficiency and to increase cellular network capacity [3GPP, 2008a]. The radio interface for LTE is based on Orthogonal Frequency Division Multiplexing (OFDM) for downlink (DL) and Single-Carrier FDM (SC-FM) for uplink (UL).

LTE offers higher peak data rates compared to third-generation (3G) High Speed Downlink Packet Access (HSDPA) by mainly utilising a wider channel bandwidth and higher order Multiple-Input and Multiple-Output (MIMO) antenna geometries. A component carrier can have a bandwidth of 1.4 MHz, 3 MHz, 5 MHz, 10 MHz, 15

MHz or 20 MHz and up to five component carriers can be aggregated (equivalent to a maximum bandwidth of 100MHz) [3GPP, 2010b] and up to 8x8 MIMO in the DL and 4x4 in the UL is allowed. The LTE BS can be divided into Macro Cell, Micro Cell, Pico Cell and Femto Cell through the control of power levels.

2.5.1.1 Macro Cell

A Macro Cell is a large base station transmitting at a typical power of ~43 dBm [Quek et al., 2013] that provides excellent coverage range up to several kilometres and supports high mobility.

2.5.1.2 Micro Cell

A Micro Cell is usually smaller than Macro Cell with a typical coverage range of less than two kilometres and inter-site distance of no less than 500 m [Lei et al., 2013]. Micro Cells are backhauled by fibre or microwave dependent on the available infrastructure.

2.5.1.3 Pico Cell

Pico Cells are smaller than Macro Cells with a transmit power ranging from ~23 dBm to ~30 dBm (Table 2.2) and a coverage range of ~200 meters or less. It is an outdoor base station, open to the public. Usually Pico Cells are included inside the Macro Cell to provide hotspot coverage such as in an airport, malls or stadia.

2.5.1.4 Femto Cell

Femto Cells, as its name suggests are the smallest cell within the LTE BS family. Femto Cell equipment is relatively new, constituting very small cellular base stations that support small numbers of users (compared to traditional cell towers). The Femto BSs is designed to serve mobile devices within a home or small business and are usually placed indoor, operating at low transmitted power of < 23 dBm.

The advantage of Femto BSs is the increase in the data rate due to the short distance between User Equipment (UE) and BS. Moreover the battery life of the UE improves due to the lower transmit power requirement. The main advantages of Femto Cells are low cost and can be deployed quickly at exact locations where coverage and capacity are needed. In most cases, Femto BSs may be purchased by customers and self-installed.

A comparison of the different types of BS is presented in Table 2.2.

Table 2.2: Comparison of different type of BSs. [Quek et al., 2013]

Type of Nodes	**Transmit Power/10MHz**	**Coverage Range**
Macro Cell	43dBm	Few km
Micro Cell	38dBm	200 - 2km
Pico Cell	23 - 30dBm	< 300m
Femto Cell	< 23 dBm	< 50m

2.5.2 IEEE 802.11 Overview

Wireless Local Area Networks (WLANs), more commonly known as Wireless Fidelity (WiFi), have emerged as a viable replacement to wired solutions for last mile Internet access. In the late 1980s, the Institute for Electrical and Electronic Engineers (IEEE) 802.11 Working Group responsible for the development of LAN standards began to develop the standards for WLANs. The group, as the name suggests, belongs to the group of popular IEEE 802.x standards, e.g., IEEE 802.3 Ethernet [IEEE Std, 1985a] and IEEE 802.5 Token Ring [IEEE Std, 1985b]. The main objective of the IEEE 802.11 Working Group was to define the wireless LAN Medium Access Control (MAC) and Physical Layer specifications. The first IEEE 802.11 Wireless Local Area Network (WLAN) standard [IEEE Std, 1997] supported a maximum data rate up to 2Mbps operating in the license free 2.4GHz Industrial, Scientific and Medical (ISM) frequency band.

The technology continues to evolve and a series of new Physical Layer specifications were released to increase the performance. For example, two enhanced Physical Layer specifications, IEEE 802.11a [IEEE Std, 1999a] and IEEE 802.11b [IEEE Std, 1999b] increased the data rate up to 11Mbps and 54Mbps respectively. 802.11b is based on a Direct Sequence Spread Spectrum (DSSS) technology [Geier, 2002] operating in the 2.4GHz band, while 802.11a is a technology based on OFDM and operates in the 5GHz band. The 802.11g standard [IEEE Std, 2003] extended the 802.11b Physical Layer to support data transmission rates up to 54 Mbps in the 2.4 GHz band. Well-known releases such as 802.11e for Quality of Service (QoS) improvement [IEEE Std, 2005a], 802.11s for mesh networking [IEEE Std, 2011]

and 802.11n [IEEE Std, 2009] that uses multiple-input multiple-output (MIMO) technology to increase data rates further address the shortcomings of 802.11. A long list of completed 802.11 standards is now in place and active sub working groups [IEEE Working Group, 2013] continue to specify IP-based broadband services at high bit rates ranging from 54Mbps on IEEE802.11a/g and up to 600Mbps on 802.11n.

In the early of 2000s', WLAN radio cards were expensive compared to now, WLANs at that time would only be considered if the mobility provided tremendous gains in efficiency and resulted in huge cost savings. However, with falling prices of technology and improved performance, WLAN gradually began to secure traction in the market. Today, IEEE 802.11 hotspots can be readily found at offices, stadia, university campuses, libraries, airports, hotels, public transport stations, cafes and residential areas. It is one of the world's most widely deployed wireless network technologies to date. WLAN technologies provide higher access data rates but have lower coverage compared to cellular networks.

IEEE 802.11 defines two architectures i.e. Basic Service Set (BSS) and Independent Basic Service Set (IBSS) [IEEE Std, 1997]. In a BSS, a number of wireless stations (STAs) are associated to an AP which acts as a master to control all connected STAs. All communications take place through the AP. The IBSS on the other hand does not rely on a pre-existing infrastructure such as an AP. STAs can communicate directly with each other and forward data on behalf of other STAs as long as they are within each other's transmission range. This type of wireless network is also commonly referred to as a wireless ad-hoc network.

For the purposes of the research, the IEEE802.11g and IEEE 802.11n are adopted for the study as these two technologies are most widely deployed worldwide. Although IEEE 802.11g is being slowly replaced by the more efficient IEEE 802.11n, many former systems are still in operation.

2.5.2.1 IEEE 802.11g

IEEE 802.11g is the third modulation standard for wireless LANs [Agrawal and Zeng, 2015]. Figure 2.5 shows the channel structure of both 802.11b and 802.11g [IEEE Std, 2003].

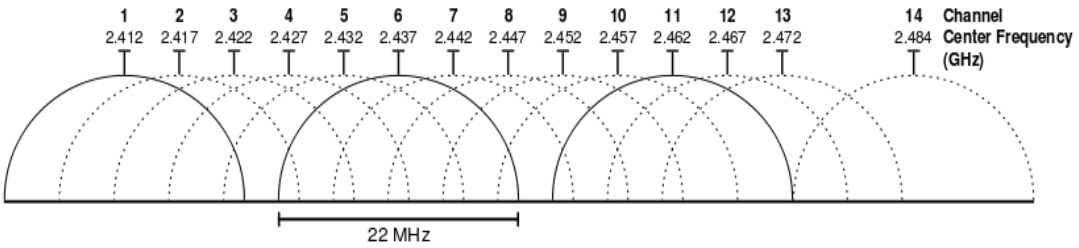

Figure 2.5: Channels in the 2.4 GHz band (Picture source:[Wikipedia, 2014]).

802.11g uses Orthogonal Frequency-Division Multiplexing (OFDM) with data rates of 6 Mbps, 9 Mbps, 12 Mbps, 18 Mbps, 24 Mbps, 36 Mbps, 48 Mbps, and 54 Mbps available. The 802.11g standard is based on IEEE 802.11a which only operates in the 5 GHz band and offers a much shorter coverage range. Since 802.11g operates in the 2.4 GHz band, coverage ranges is much better than IEEE 802.11a but with comparable data rates. Use of the 2.4 GHz frequency also makes 802.11g backward compatible to 802.11b.

2.5.2.2 IEEE 802.11n

802.11n operates in both 2.4 GHz and 5 GHz bands; however, the support for the 5GHz band is optional. 802.11n offers a major improvement over previous 802.11a/b/g standards through several key enhancements such as MIMO, frame aggregation, block ACK and channel bonding [IEEE Std, 2009].

MIMO

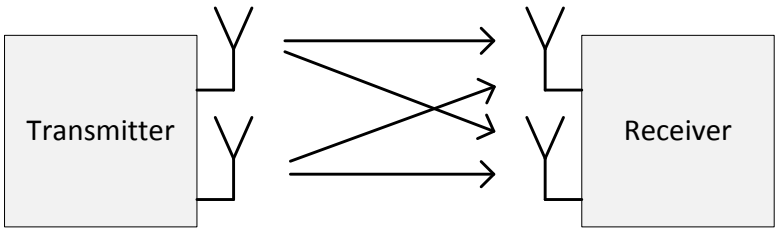

Figure 2.6: 2x2 Multiple Input Multiple Output (MIMO) system. (Source: [Conniq.com, 2015])

Physical data rates in 802.11n are significantly improved over 802.11a and 802.11g through the use of MIMO Spatial Multiplexing (SM) which multiplexes multiple independent spatially separated data streams and transmits them simultaneously using multiple antenna elements within one spectral channel of bandwidth (Figure 2.6). In MIMO, each transmission propagates along a different path and hence the individual streams at the receiver experience sufficiently distinct spatial signatures. With a SM enabled receiver, the original data streams can be recovered. By spatial multiplexing two data streams onto a single radio channel, the original capacity is effectively doubled. For example, a data rate higher than 100 Mbps is achievable

using a 20MHz channel and two SM streams, transmitting over 64QAM-5/6 MCS (Figure 2.8) in contrast to just 54Mbps with 802.11a/g. Up to four SM streams have been defined in the standard which further improve the capacity (Figure 2.9) but the support for 3 or higher SM streams is optional.

In addition to SM, MIMO also supports a Space-Time Block Coding (STBC) [Sandhu et al., 2003] option in the Physical Layer (PHY) to further improve the robustness of a link. Low Density Parity Check (LDPC) [Perahia and Stacey, 2013] codes are adopted for that purpose. Furthermore, the standard also caters for transmit beam forming, where both PHY and MAC enhancements are introduced to further improve link robustness.

Channel Bonding

IEEE 802.11n enables two 20 MHz channels to be combined to form a 40 MHz channel in either the ISM or Unlicensed National Information Infrastructure (UNII) band [FCC, 2013] to improve data rates.

Before 802.11n was fully defined, WiFi (802.11b/g) products used channels approximately 20 MHz wide occupying 11 channels (three non-overlapping: 1, 6, 11) within the 2.4GHz frequency band (Figure 2.5); in the 5 GHz UNII band, there are 12 non-overlapping 20 MHz channels (varies depending on countries and region) that can be used (Figure 2.7).

The 40 MHz channel was initially intended only for the 5 GHz band due to the larger spectrum available; however, 40 MHz channel operation at 2.4GHz is permitted in the standard. Due to the limited number of non-overlapping channels, special care has to be taken during deployment as options for channel planning are low.

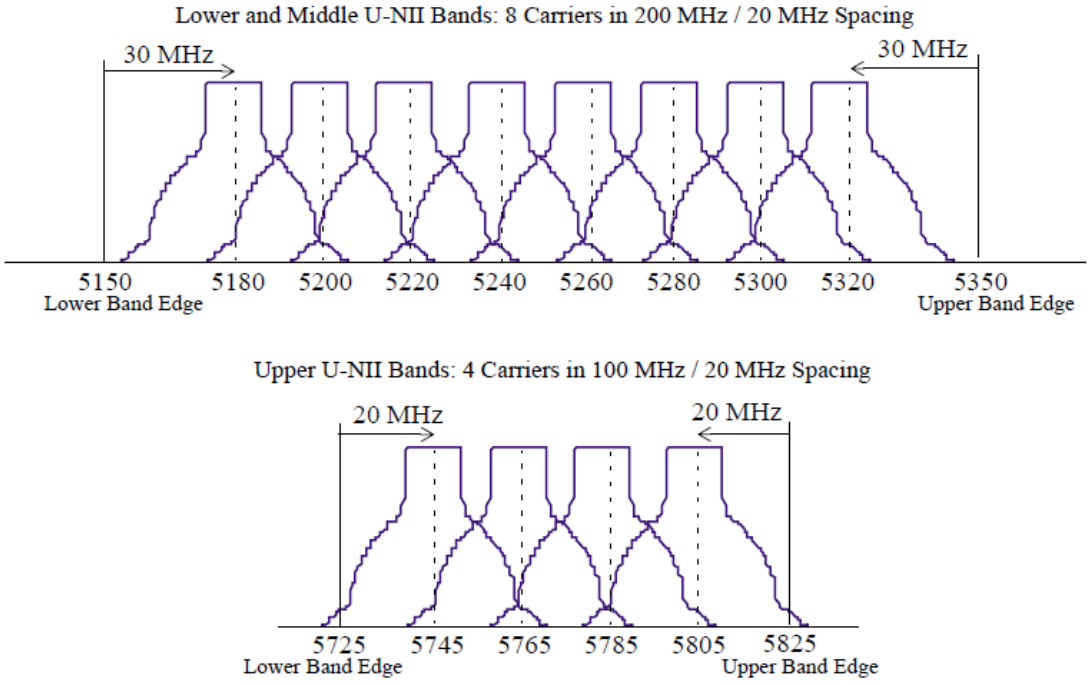

Figure 2.7: OFDM PHY frequency channel for the United States [IEEE Std, 1999a].

Frame Aggregation and Block Acknowledgement

In addition to improvements in the RF performance, MAC efficiency and throughput performance have also been improved by aggregating multiple frames into a single transmission with block acknowledgement [Perahia and Stacey, 2013]. In frame aggregation, multiple frames can be sent through a single access to the medium by

combining frames into one larger frame. There are two forms of frame aggregation: Aggregated MAC Service Data Unit (A-MSDU) and Aggregated MAC Protocol Data Unit (A-MPDU) [Perahia and Stacey, 2013].

A-MSDU

With A-MSDU, MAC frames from the same physical source, same destination end points and same traffic class are integrated into one larger frame with a common MAC header. In other words, multiple MSDUs are aggregated at the MAC layer and inserted into a single MPDU which in turn will be passed to the PHY layer. An A-MSDU packet has a single frame header with multiple frames destined for the same client at the same service class. The sender is acknowledged once the whole A-MSDU is received successfully. A more detail description of A-MSDU is provided in Appendix A.

A-MPDU

A-MPDU is basically a chain of individual 802.11 frames transmitted by piggy backing each other at one access to the medium. Similar to an A-MSDU, the destination address as well as the traffic class (QoS) must be common. However, unlike the A-MSDU, each PDU frame has its own Cyclic Redundancy Check (CRC) resulting in increased robustness on packet transmission as an error in one PDU does not affect others in the group. However, A-MPDU is less efficient due to a higher overhead introduced by individual PDU frame headers.

A-MPDU is more efficient in high bit error rate environments as each data frame within an A-MPDU is acknowledged or re-transmitted separately if an error is detected. A-MSDU on the other hand, is more suitable for a radio environment where the bit error rate is low as only one acknowledgement is sent upon the successful recovery of the entire A-MSDU. Under poor radio channel conditions, frequent retransmission is expected, very costly for huge frames [Jackman et al., 2011] [Daldoul et al., 2011].

Block ACK

802.11n introduces a block acknowledgement mechanism in which multiple frames can be transmitted and acknowledged by a single frame instead of an ACK frame for each transmitted data frame [Perahia and Stacey, 2013]. A reduction in the transmission overhead results since only missing frames or frames with errors are re-transmitted by checking a compressed bit map embedded in the block acknowledgement.

Other enhancements by 802.11n include a shorter guard interval in PHY only to be used under certain channel conditions. If backward compatibility is not a concern, a Greenfield preamble shorter than the mandatory mixed format preamble, is an option for performance improvement [Eldad and Robert, 2008]. A Reduced Inter-Frame Space (RIFS) instead of a Short Inter-Frame Space (SIFS) can also be used when transmitting a burst of frames to reduce the overhead.

With these enhancements, the maximum data rate of 802.11n has been increased from 54 Mbps to 600 Mbps. However, data rates up to 600 Mbps are only achievable with the maximum four spatial streams operating in the 40 MHz channel. Various modulation schemes and coding rates have been defined and are represented by a Modulation and Coding Scheme (MCS) index value ranging from 0 to 31 [Eldad and Robert, 2008]. Figure 2.8 and Figure 2.9 show the achievable 802.11n data rates for a 20 MHz and 40 MHz channel bandwidth using a short Guard Interval (GI) [AirMagnet, 2008].

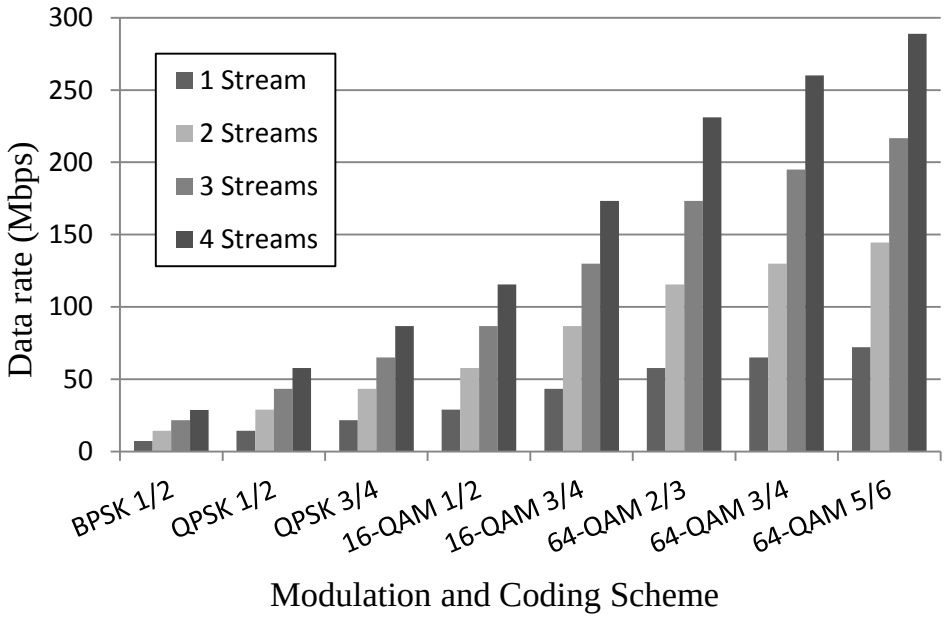

Figure 2.8: 802.11n data rates with 20MHz channel bandwidth, 400ns Guard Interval.

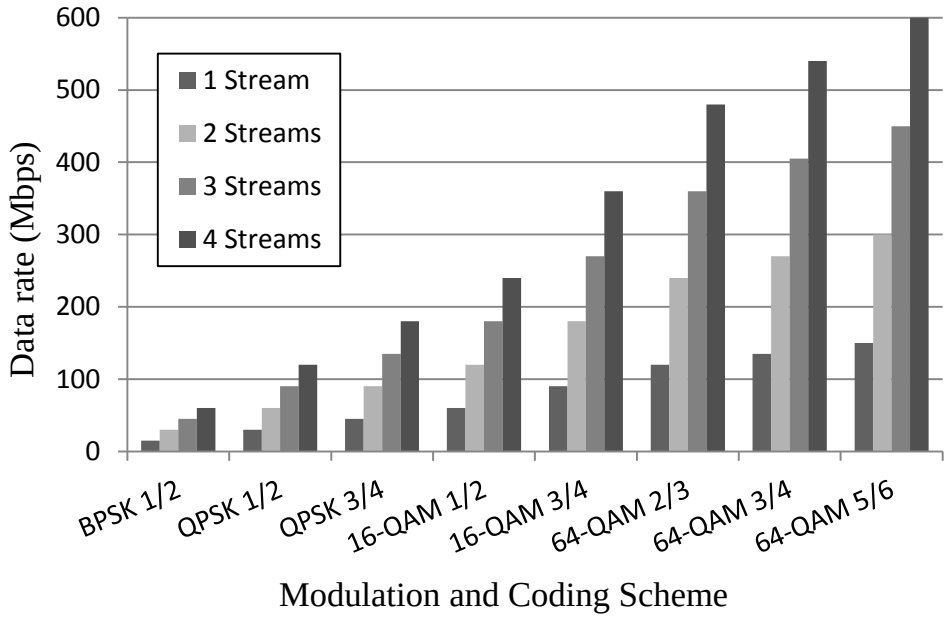

Figure 2.9: 802.11n data rates with 40MHz channel bandwidth, 400ns Guard Interval.

2.6 General HetNet Issues and Challenges

HetNet is a large, complex next generation network that consists of multiple access nodes that differ in technology type, transmit power level and link capacity. With integrated WiFi, the user experience can be maximised by supporting the cellular network to deliver higher capacity through harnessing the widely available unlicensed spectrum. Although HetNet is a promising technology, several challenges need to be addressed.

2.6.1 Cellular WiFi Interworking

Cellular and WiFi are two technologies designed with different objectives; the former is designed for mobile telephony whilst the latter is aimed for last mile wireless access for broadband data communications. Since WiFi is not part of the

cellular network, the integration of WiFi with the cellular network presents several interworking challenges and requires a new set of standards to address the mismatch.

For example, in order to provision services from MNOs, reliable access to the cellular core network through a 3GPP or non-3GPP network is desirable. Fortunately, MNOs recognised the importance of integrating WiFi into Cellular networks and standards were drafted and approved in 3GPP and IEEE to facilitate Cellular WiFi interworking (Section 3.2). However, those standards addressed basic interworking issues, such as authentication, authorisation, billing, basic mobility support and simple network detection and selection algorithm. A more intelligent interworking system is required to optimise network performance [4G Americas, 2013]. For instance, providing end to-end integration from the mobile packet core network to the individual cell or AP, encompassing controllers and management systems are needed for a seamless user experience. Real time network status information from all cells in the HetNet must be provided to the network management system in order to achieve optimum inter-networking. WiFi broadband modems and Femto systems are governed by separate provisioning profiles, policies and procedures such as different start up procedures, device ID, data models, QoS policies and DSL rate plan. The integration of modems and Femto systems are costly [Small Cell Forum, 2012] and pose a challenge since reducing network operating and management cost is important to MNOs.

2.6.2 Mobility (Handover)

The Cellular network is known for its reliable mobility support providing smooth and uninterrupted voice and data support even when a user moves across several BSs. In HetNets, mobility support is far more challenging compared to a Macro-cell-only network due to its complex and nested network topology [Andrews, 2013]. Handover comes at the expense of a system overhead consisting of control and signalling messages that slice the network resource. Furthermore owing to the large number of small cells within HetNet, handover can be too frequent resulting in massive system overheads [Andrews, 2013]. Hence a trade-off between network performance and user experience exists and a major challenge is to determine the optimum balance between them.

Managing vertical handover seamlessly whilst providing a good quality service is also presents a challenge. Vertical handover occurs between a Macro Cell and small cells when a user moves through a HetNet. In view of the differences between WiFi and Cellular network technologies, seamless vertical handover relies on synchronisation and signalling between the two networks and any delay causes interruptions to real time services [Qualcomm, 2011]. Hence in vertical handover scenarios, operators need to differentiate services by application or application type before making any handover decision. Unlike the Macro-only network, handovers may occur in HetNet even when a user is static in order to achieve traffic load balancing across the entire HetNet e.g. users at the more congested cells are shifted to the less congested cells.

2.6.3 QoS Support

Future networks must provide a range of services, from basic voice communications, web access, business transactions, through to online gaming and video streaming. Networks are expected to support traffic with various Quality of Service (QoS) and Quality of Experience (QoE) requirements and is therefore of high importance for MNOs.

Ensuring end-to-end QoS is thus one of the main challenges. WiFi and Cellular have been designed for different purposes and consequently operate with very different QoS characteristics; hence QoS mapping is required [4G Americas, 2013]. Further, WiFi cells are normally backhauled by DSL which have their own QoS mechanisms over IP networks; thus end-to-end QoS preservation is a huge challenge in HetNets.

As a consequence of the large number of small cells that increase the frequency of handovers, the probability of handover failure in HetNet is higher, in turn degrading the QoS. This is confirmed by 3GPP studies, showing that the failure rate in Macro-Pico HetNet doubles compared to a Macro-only network [3GPP, 2012b]. The handoff procedure may also cause extra delay, packet loss, and even connection interruption especially in the vertical handover between Macro and small cells during which the signalling is likely to travel through a longer path compared to a horizontal handover [Yan Zhang et al., 2008].

Despite the challenges of providing QoS in HetNets, the focus of the study is mainly on non-delay-sensitive applications such as web-browsing, email access, file transfer

and best effort VoIP. Thus QoS is not considered or assumed to be provided on a best effort (BE) basis.

2.6.4 Offloading Decision

Offloading decisions are core in HetNet in order to ease the traffic congestion. From the network point of view, any offloading decision has to consider overall network performance such as optimising network throughput by offloading the user to a best network as well as balancing the load within the entire HetNet. Further, all optimisation processes need to consider QoS and user satisfaction (QoE). Decisions are based on a number of criteria; the user preference, the traffic type, the best time, how much traffic in total should be offloaded from the cellular network and to which small cell(s)?

Communication between HetNet and user devices is vital for overall network performance for user centric Network Selection (NS). Here user preferences must be a consideration as some users may not be willing to switch to a lower QoS guarantee network such as a WiFi network. Incentive schemes may be required to encourage users to deprioritise in relation to other users on more QoS sensitive applications [Zhuo et al., 2013].

Fairness on accessing network resource amongst users is also important and is a major consideration during offloading. In most cases, a network with optimum capacity performance may not be the fairest and often maximum throughput has to

be traded-off for fairness. Hence, a balance between network performance and fairness is required.

Fairness is one of the core performance metrics used in the study (Section 5.6.1). The principal is that in commercial applications when a user is being charged relatively equal amounts of money for services from a network, each should be treated fairly.

2.6.5 Backhauling

In HetNets, backhauling a large number of small cells is challenging. For deployment of small cells in indoor environments, access to the power supply and wired network backhauling is required, which may be potentially expensive. Although eliminating backhaul costs by relying on consumers to provide the broadband connection to indoor small cells may be an option, difficulties in ensuring an acceptable quality of service (QoS) over customer backhaul is a major issue.

For outdoor small cells deployments, backhauling is even more challenging as backhauling access points may not be readily available at the most suitable locations [Infonetics Research, 2013] [NGMN Alliance, 2012]. Due to the extensive engineering work required, high cost and regulatory barriers, fixed line solutions such as fibre, cable, copper or xDSL are often not the best options. Furthermore, a relatively large number of WiFi hotspots may be too costly for operators to backhaul over a wired infrastructure [Nitin Bhas, 2011].

In such situations, the solution is likely to be a mix of both wireless and wired backhaul [Andrews, 2013] [Ghosh et al., 2012], in which some cells may have dedicated interfaces to the core network, whilst other cells may rely on multi-hop wireless technology to relay the traffic to the core [Firetide, 2013] [NGMN Alliance, 2012]. The adoption of a mix of technologies to implement backhauling supporting a number of cells results in varying bandwidth and delay constraints. Hence, the planning and design of the HetNet backhaul is challenging and any solution must be cost effective and guarantee performance.

2.7 Conclusions

In this chapter, background technologies underpinning Wireless Heterogeneous Network (HetNet) is presented. HetNet implementations are categorised as SCU, DCU and HCU, their advantages and disadvantages discussed and compared and the motivation behind the selection of the DCU in this research is clearly stated.

Within a DCU HetNet, LTE is chosen as a Macro Cell and WiFi is chosen as the Small Cell. The WiFi Hotspot and WiFi Mesh topologies are introduced and overviews of the chosen underlying radio technologies and their main characteristics are given.

Mobility support, QoS support, traffic offloading decisions and backhauling are general cellular-WiFi interworking challenges faced by MNOs highlighted and summarised in Table 2.3.

Table 2.3: Summary of cellular-WiFi HetNet issues and challenges.

HetNet Issues	Challenges
Cellular WiFi Interworking	• Available standards are for basic Cellular-WiFi interworking, more intelligent interworking standards required for network optimisation. • High provisioning cost due to existence of different systems in HetNet.
Mobility	• Mobility is more challenging than Macro-only network due to its complex and nested network topology. • Large number of small cells may cause frequent handover resulting in massive system overheads.
QoS Support	• End-to-end QoS is challenging over different technologies in HetNet as QoS mapping is required and results in longer handover delay. • Frequent handover due to large number of small cells increases handover failure. • Providing services meeting QoS for multiple traffic types is challenging.
Offloading Decision	• Performing load balancing that takes care of overall HetNet performance is challenging. • Finding that balance between throughput performance and fairness during offloading is not straight forward. • Incentive scheme may be needed for the user being offloaded to less QoS supported network.

Backhauling	• Wired backhaul is expensive and may not ubiquitously available. • Mixture of wired and wireless backhaul is likely and creates non-uniform backhaul capacity over small cells. • Cost-effective and performance guaranty backhauling solution is needed.

Chapter 3

State of The Art and Research Scope

3.1 Introduction

The Chapter provides an overview on state-of-the-art in Cellular-WiFi integration and defines the scope of the research. The Chapter starts with a mapping of existing standards and industrial organisations supporting Cellular-WiFi integration. Related research is presented and discussed, a foundation to develop the motivation and scope of research before conclusions are drawn.

3.2 Standards Supporting Cellular-WiFi Interworking

Due to the popularity and widespread deployment of WiFi worldwide, MNOs were compelled to inter-network instead of competing with WiFi. In order to facilitate cellular-WiFi interworking, both 3GPP and IEEE have acknowledged the evolution by drafting standards to better support Cellular-WiFi integration.

3.2.1 3GPP Standards

The Global System for Mobile Association (GSMA) WLAN Task Force (2002 to 2004) report on WLAN-Cellular interworking highlighted five scenarios that enhance WLAN-Cellular interworking [GSMA, 2003]:

1. Common Billing and Customer Care
2. 3GPP system based Access Control and Charging
3. Access to 3GPP system Packet Switched based services
4. Service Continuity
5. Seamless services

The findings stimulated subsequent standardisation activities that pushed several standards to be pursued based on the above scenarios. Table 3.1 presents the most relevant standards.

Table 3.1: 3GPP technical specifications and their scope.

Technical Specs	Scope
TS 23.234	Scenarios 1, 2 and 3: Common Billing, Access Control and Charging and Access to Packet Switched Services.
TS 23.327, TS 23.261, TS 23.401, TS 23.402	Scenarios 4 and 5: Service Continuity, Seamless Services and Mobility

3.2.1.1 Integrated Wireless LAN (IWLAN) Standard

The main purpose of TS 23.234 is to provide solutions for interworking Scenario 1, Scenario 2 and Scenario 3, addressing Common Billing, Access Control, Charging and Access to Packet Switched Services.

Figure 3.1 shows a WLAN Inter-working reference model from TS 23.234 recommending that 3GPP Authentication, Authorization and Accounting (AAA) be executed by a server for both WLAN access and 3GPP services. Users are able to perform IP access through either "3GPP IP" or "Direct IP" access [InterDigital, 2012]. The former allows users to access Mobile Network Operator packet data services, such as Multimedia Messaging Service (MMS), mobile video, etc. as well as Internet services, whereas the latter provides direct access to the Internet or Intranets. 3GPP IP access is enabled by two entities – the WiFi Access Gateway (WAG) and the Packet Data Network Gateway (PDG) - both functioning as Gateways to the Packet Data Network (PDN). The WAG is a typical gateway connecting the user to the PDG and at the same time it also acts as a firewall, enforcing operator policies which are downloads from the 3GPP AAA servers. PDG is a gateway to a specific Packet Data Network, such as the Internet or an operator service network.

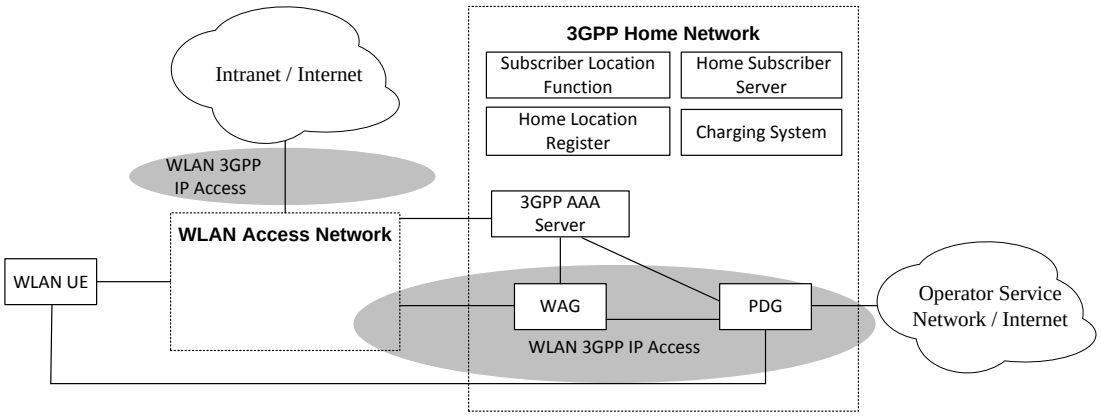

Figure 3.1: WLAN Inter-working reference model (Non-roaming).

TS 23.234 [3GPP, 2008c] only specified how WLAN UEs are permitted to access 3GPP core networks and services, however the dynamic switching of radio connections and user handover between WiFi and 3GPP networks are not defined. The mobility solution is standardised in TS 23.327 [3GPP, 2008e], defining the mobility between Interworking WLAN Networks and 3GPP networks.

IWLAN-3GPP mobility solutions have two basic limitations. Firstly, the Home Agent (HA) is not connected to policy and QoS management entities in the core network (such as Policy and Charging Rules Function (PCRF) [Mulligan, 2012]) preventing advanced policy and QoS based management. Secondly, User Equipment (UE) is restricted to only a single radio connection at any given time, namely either to the WLAN or 3GPP radio interface which limits the possibility of dynamic switching of individual IP-Flows from one radio interface to another as well as multi-homing functionality. These limitations are removed by integrating WLAN into Evolved Packet Core (EPC) core networks.

3.2.1.2 Evolved Packet Core (EPC) Standards

In EPC [3GPP, 2008b], the latest evolution of the 3GPP core network architecture, non-3GPP access networks (access networks not specified in the 3GPP) can be split into two categories, the "trusted" and the "untrusted".

Trusted non-3GPP accesses can interact directly with the EPC while untrusted non-3GPP accesses through EPC have to be done via the Evolved Packet Data Gateway (ePDG) network entity. The main role of the ePDG is to provide security mechanisms such as the Internet Protocol Security tunnel (IPsec tunnelling [Mulligan, 2012]) of connections with the User Equipment (UE) over an untrusted non-3GPP access.

Trusted (non-3GPP) WiFi access is a network managed by the Operator. For example UE can connect to the trusted WiFi Network directly using the radio interface without any additional security measures.

However, for Untrusted WiFi Networks with no trust relationship with the operators, an UE is required to establish an IPSec tunnel to the ePDG in the core network. The ePDG acts as a termination node for IPsec tunnels established with the UE.

The architecture of an EPC core network with trusted and untrusted non-3GPP access is shown in Figure 3.2.

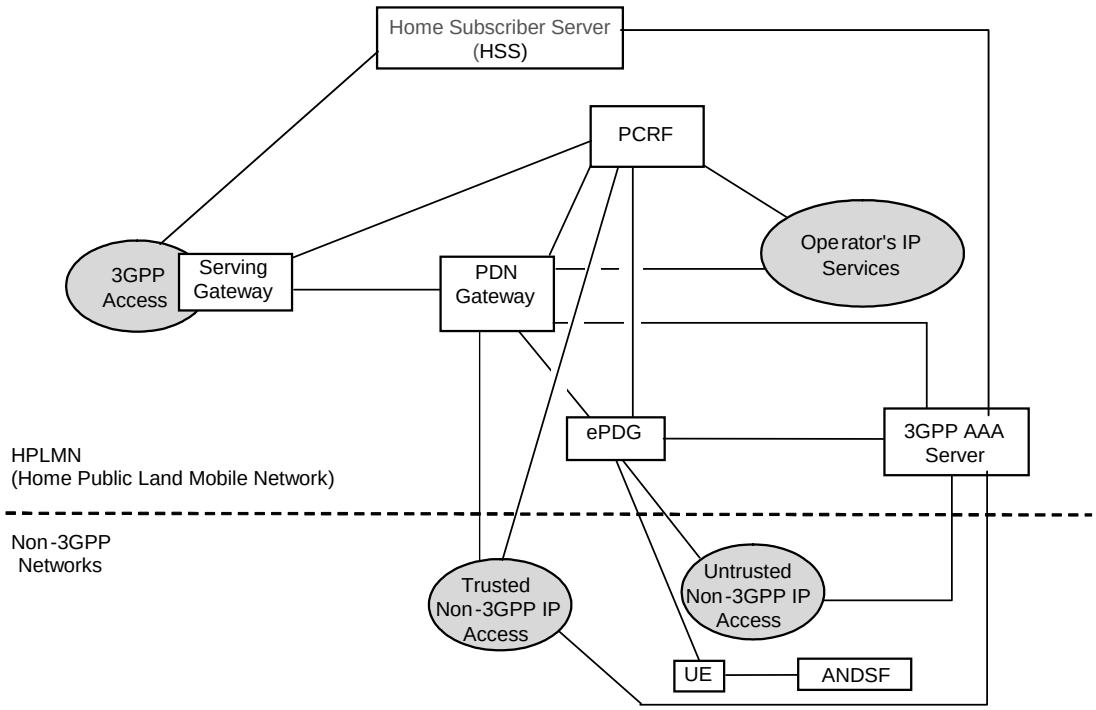

Figure 3.2: EPC architecture for access via trusted and untrusted non-3GPP networks (source: [3GPP, 2008g]).

For mobility, there are two approaches specified for EPC, namely client-based and network-based mobility [3GPP, 2008f; 3GPP, 2008g]. In the client-based approach, the handover during network switching is triggered by the UE and not by the network and software has to be installed in each UE in order to facilitate the mobility.

For client-based mobility, seamless and non-seamless handover solutions between 3GPP and Non-3GPP access networks are described in the 3GPP standard TS 23.401 [3GPP, 2008f], wherein the General Packet Radio Service (GPRS) Tunnelling Protocol (GTP) is used for the handover over interfaces S2a, S2b and S5. A similar solution is documented in TS 23.402 where the Proxy Mobile IP (PMIP) and Dual

Stack Mobile IP (DSMIP) are used [3GPP, 2008g]. Solutions for seamless IP-Flow mobility using DSMIP protocols are described within TS 23.261 [3GPP, 2008d].

In EPC, to facilitate network selection by the UE, Access Network Discovery and Selection Function (ANDSF) protocol [3GPP, 2008h] is proposed to assist user equipment (UE) on network discovery and selection, enabling operators a means of providing guidelines to UEs for WiFi network selection by customising network selection policies and distributing those policies down to devices.

With network-based mobility, UE mobility services are handled by the network for session continuity. No software has to be installed in the UE and hence the implementation of network-based mobility is much easier. Furthermore, since the network often has better insight on overall network usage and the congestion state than the UE, a better handover decision can therefore be made. The network-based mobility approach uses the IETF protocol, Proxy Mobile IPv6 (PMIPv6) [Cisco, 2012a]. PMIPv6 is used on the S2a, S2b and S5 interfaces in EPC.

3.2.2 IEEE 802.11u Standards

The Institute of Electrical and Electronics Engineers Standards Association (IEEE-SA) is an organisation within the IEEE that develops global standards including WLAN standards such as 802.11x. The IEEE 802.11x standards were initially designed to serve as a last mile Ethernet replacement. However, the overwhelming market penetration and worldwide acceptance of these technologies changed the landscape completely. Many operators started to adopt and integrate IEEE 802.11x

into their networks. In order to address the shortcoming of existing 802.11x standards on interworking with other networks, one of the IEEE initiatives centred on 802.11u.

IEEE802.11u [IEEE Std, 2011] is the ninth amendment to the IEEE 802.11-2007 standard, adding features that improve interworking of WLAN with external networks. IEEE 802.11u has defined a new MAC state convergence function aiding network discovery and selection, enabling information transfer from external networks, enabling emergency services via the 802.11 network, and interfacing Subscription Service Provider Networks (SSPNs) to 802.11 networks that support interworking with external networks.

With 802.11u implemented, APs are capable of providing interworking-specific information – such as the type of network offered – in the beacon frame to enable mobile devices to select the network even before attempting association. Service providers and external subscription service providers can also established roaming partnerships and their services can be advertised in the APs' beacon frame.

In a HetNet, 802.11u simplifies network selection especially during vertical handover. For example, a mobile device connected to a cellular network and downloading a file can perform vertical handoff and connect to the WiFi network through the 802.11u standard selecting a better WiFi network.

In terms of adoption by the industry, 802.11u is actively supported by vendors and network operators through the WiFi Alliance (WFA) [WiFi Alliance, 1999] with

Hotspot 2.0 [WiFi Alliance, 2012] specifications and the Passpoint Certification [Wi-Fi Alliance, 2012] process which is detailed in Section 3.3.

3.3 Industrial Forums

The standards as discussed in Section 3.2 are supported by industrial bodies in order to champion their implementation. Industrial bodies that are actively involved are the GSM Association (GSMA) [GSMA, 1995], Small Cell Forum [Small Cell Forum, 2007], WiFi Alliance (WFA) [WiFi Alliance, 1999] and Wireless Broadband Alliance (WBA) [WBA, 2003].

3.3.1 GSM Association (GSMA)

The GSM Association (GSMA) is a community of worldwide mobile operators and related companies representing their interests. GSMA is devoted to supporting the standardisation, deployment and promotion of the GSM mobile telephony systems. Upon realising the mass acceptance of WiFi worldwide, mobile operators and vendors within GSMA initiated a study exploring the potential for cellular-WiFi integration so that an alternative radio access to mobile services could be provided. The "GSMA WLAN Task Force" investigated various use cases of interworking between the WiFi and cellular networks; six different interworking network scenarios and levels of interworking ranging from no, loose and tightly coupled were studied and included consideration of important issues such as authentication, access control, billing, core network accessibility, service continuity and mobility. The study [GSMA, 2003] subsequently led to the various standards within 3GPP to enable interworking between cellular and WiFi (Section 3.2).

3.3.2 Small-Cell Forum

The Small Cell Forum, formerly known as the Femto Forum, was formed to support and accelerate the wide-scale adoption of small cells and to maximise the potential of the mobile Internet [Small Cell Forum].

In support of HetNet standardisation, the Small Cell Forum undertook the study of radio level coexistence between co-located Femto and WiFi APs. The Integrated Femto-WiFi (IFW) action [Small Cell Forum, 2012] investigated the integration of the Small Cells (both 3G and LTE) and WiFi technologies due to the increasing interest from Femto vendors on integrating Femto and WiFi APs in the same equipment as a single unit. The IFW work item generated a white paper, a comprehensive study on various deployment and operational scenarios, user and operator benefits and various service and technology aspects. The Small Cell Forum also interacted with other industry bodies, especially those dealing with WiFi in order to drive their initiatives towards reality.

3.3.3 WiFi Alliance (WFA)

The WiFi Alliance (WFA) is a powerful association that promotes WiFi technologies and ensures the interoperability of IEEE802.11 products through certification processes; any WiFi certified products has to pass the WFA certification process. To support interworking with external networks, WFA has defined Hotspot 2.0 [WiFi Alliance, 2012] based on IEEE802.11u standard.

3.3.3.1 Hotspot 2.0

Hotspot 2.0 enables mobile devices to automatically discover APs associated with user home networks and to establish a connection securely during roaming [WiFi Alliance, 2012]. Before connecting to a WiFi network, the mobile device normally queries APs to discover whether the visited network supports roaming with the device's home network. On selecting the network, the client device is allowed to authenticate to visited network with one or more credentials, such as a SIM card, username/password pair, or X.509 certificate in order to secure the connection.

Hotspot 2.0 (v1.0) focuses on discovery/selection, authentication, and over-the-air security. Subsequent releases will follow with additional capabilities.

3.3.3.2 Passpoint Certification

As for product certification, Hotspot 2.0 is supported by WFA Passpoint™ certification [Wi-Fi Alliance, 2012] which ensures that certified products comply with the technical specifications. Passpoint™ certification is being deployed in phases; the current is Release 1 and Release 2 is expected in 2014.

3.3.4 Wireless Broadband Alliance (WBA)

The Wireless Broadband Alliance (WBA) targets the provision of outstanding user experiences through the global deployment of next generation WiFi. WBA is

essentially a body similar to WFA developing standards to simplify connection and roaming.

WFA Hotspot 2.0/Passpoint is complemented by WBA through its Next Generation Hotspot (NGH) [WBA, 2011] initiative. The NGH protocol in effect carries the end user Hotspot 2.0 identity and ensures inter-operability with other segments of the network through authentication to the operator's Remote Authentication Dial-In User Service (RADIUS) [C. Rigney et al., 1997] servers whilst managing roaming and billing. In NGH, inter-operability requirements between hotspots, cable and 3G/4G mobile operators are defined and comprehensive guidelines are developed for the operators. In full functionality mode, NGH is equivalent to cellular roaming but in a WiFi implementation.

WBA believes that WiFi is a complementary to other wireless and broadband networks including 3GPP/UMTS, WiMAX, DSL and Cable. Thus in addition to the NGH initiative, WBA also initiated the Interoperability Compliance Program (ICP) [WBA, 2012], Wireless Internet Service Provider roaming (WISPr 2.0) [WBA, 2010] and Wireless Roaming Intermediary Exchange (WRiX) [WBA, 2013] which aim to improve inter-operability with other networks. In the long term, WBA aims to integrate both cellular and WiFi as one service, with seamless connectivity, automatic authentication and security.

3.4 Scope of Study

Both IEEE and 3GPP are aggressively working to expedite Cellular-WLAN integration through standardisation activities such as 802.11u and the series of 3GPP technical specifications (Table 3.1). Several other issues inherent with interworking such as security, mobility support, QoS and network selection for offloading are also addressed in the standards. With the support of industrial bodies and forums such as WiFi Alliance, GSM Association, Wireless Broadband Alliance and Small Cell Forum, the standards are currently being implemented e.g. Hotspot 2.0, Next Generation Hotspot and ANDFS module in EPC.

Amongst the major issues (Chapter 2), the backhauling challenge is the least addressed by standard bodies and researchers. Thus developing and analysing solutions to HetNet small cells backhauling form the focus of the study.

For the study, Small Cells are assumed to be deployed outdoor predominantly where finding a backhaul at a strategic location is relatively challenging compared to indoor scenario e.g. train stations, outdoor malls, stadia and theme parks. However, the solution is not exclusively limited to outdoor especially in the case of deploying Small Cells in older buildings with poor infrastructure.

In respect of Small Cells, WiFi is assumed as a Small Cell for the purposes of rest of the dissertation and only two options exist; wireline and wireless backhaul. Due to the intensive engineering work required, high cost and regulatory barriers, fixed line

solutions such as fiber, cable, copper or xDSL are not available extensively, especially outdoors. Further, a relatively large number of WiFi hotspots may prove too costly for operators to backhaul through a wired option.

In such situations, the operators may rely increasingly on point-to-point and point-to-multipoint wireless solutions. Furthermore, the maturity of multi-hop mesh networking promotes the approach as a potential candidate to backhaul WiFi APs [Priscaro, 2013] [Firetide, 2013] [NGMN Alliance, 2012]. However in most scenarios, a mixture of backhaul technologies is expected, as operators are likely to adopt the most suitable backhaul solution based on cost and availability [Infonetics Research, 2013] (Figure 3.3).

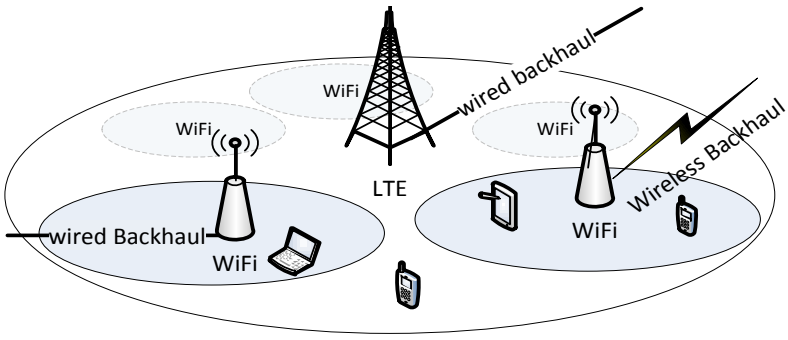

Figure 3.3: LTE-WiFi Heterogeneous Network with various potential backhauling options for WiFi cells.

Currently, WiFi APs are typically backhauled through different technologies offering throughputs ranging from several to tens of mega bit per second [Priscaro, 2013]. However backhauling APs using different technologies within HetNet leads to a non-uniform backhaul capacity distribution. With the most widely deployed IEEE802.11n

WiFi technology provisioning peak physical data rate of 600 Mbps, most existing fixed backhaul services are not able to offer sufficient capacity for these WiFi APs to realise their full potential [Ericsson, 2013]. Therefore consideration of WiFi backhaul capacity is a central consideration during traffic offload decision making. Furthermore, if a multi-hop backhaul option is adopted for backhauling small cells [Cavalcanti et al., 2005], a rigorous investigation into the possible techniques that optimise the performance of Multi-hop Wireless HetNet is necessary.

3.4.1 Specific Research Scope

For both Hotspot Wireless HetNet (HWH) and Multi-hop Wireless HetNet (MWH) network architectures (Section 2.4), the challenges addressed in the research are best defined according to the following high-level problems;

1. Hotspot Wireless HetNet (HWH)
    a. To model (Spatial Model) the Hotspot Wireless HetNet consisting of a LTE advanced network based on Release 10 and Hotspot WLAN based on 802.11g.
    b. To evaluate the impact of non-uniform backhaul capacity distribution within HetNet, ensuring every user is allocated a fair network bandwidth distribution while maintaining overall network throughput. Hence, the aim is to design a Network Selection Scheme (NSS) sensitive to network status such as backhaul capacity, network load and access link capacity in order to optimise network performance.
2. Multi-hop Wireless HetNet (MWH)

a. To model the Multi-hop Wireless HetNet consisting of a LTE advanced network based on Release 10 and Wireless Multi-hop/Mesh Network (WMN) based on 802.11n, 2.4GHz and 5GHz for access and backhaul radio respectively.
b. To optimise MWH performance by an appropriate multi-hop backhaul bandwidth assignment algorithm operating in tandem with an appropriate Network Selection Scheme. The objective is to optimise the bandwidth allocation in multi-hop/mesh network so that throughput and fairness are enhanced.

For the HWH architecture, a Dynamic Backhaul Capacity Sensitive (DyBaCS) NSS is proposed and evaluated. DyBaCS is a NSS that considers available backhaul capacity, access link throughput as well as network load in order to improve network capacity and preserve fairness amongst users.

For the MWM architecture, which relies on the multi-hop network to backhaul the APs, a joint multi-hop bandwidth allocation and network selection algorithm is proposed and evaluated. The algorithm is an extension of the HWH and the multi-hop bandwidth allocation scheme is designed to co-operate with the DyBaCS algorithm.

The HWH and MWH developments are discussed in detail in Chapter 5 and Chapter 6 respectively.

3.5 Related Works

The reported research related to the focus of this study is discussed. There are basically two categories of related research, the first related to network selection schemes in HWHs, the second related to bandwidth allocation in MWHs.

3.5.1 HetNet Network Selection Schemes (NSS)

Handa et al. [A. Handa, 2009] state that most WiFi-enabled smartphones are configured by default to give higher priority to WiFi over the cellular interface for data transmissions, referred to as the WiFi First (WF) NSS in the research. This kind of NSS is in common use as it is user-centric [Piamrat et al., 2011] and can be implemented on the UE alone without modification to the access network; however the network capacity that can be achieved using this NSS is not optimal (Chapter 5).

Network selection strategies for HetNets predominantly driven by data rate or signal strength are reported in [Raiciu et al., 2011] [Nie et al., 2005] and [Jackson Juliet Roy et al., 2006]. This kind of network selection has been shown to lead to poor user experience [Balachandran et al., 2002] [Bejerano et al., 2004] and causes unbalanced load distribution amongst access networks [Judd and Steenkiste, 2002].

Several studies [Kumar et al., 2007] [Premkumar and Kumar, 2006] [Sarabjot Singh et al., 2013] have proposed NSSs that consider optimal network performance; [Kumar et al., 2007] considers globally optimal user-network association in a

WLAN-UMTS hybrid cell. In [Premkumar and Kumar, 2006] a heuristic greedy search algorithm that maximises total user throughput in a heterogeneous wireless access network comprising WiFi APs and 3G BSs is evaluated. However, in both studies, simplified and less realistic models for WLANs are considered because only a single AP transmission rate is assumed. Poisson Point Process (PPP) theory and stochastic geometry is used in [Sarabjot Singh et al., 2013] to model traffic offloading in multiple RAT heterogeneous wireless networks. The study proposed a method to determine an optimum percentage of the traffic that should be offloaded to maximise network coverage whilst meeting user requirements; no network selection algorithm is suggested.

Fairness performance is considered in [Peng Gong et al., 2012] [Xue et al., 2012] [Bejerano and Han, 2009] [Velayos et al., 2004] and [Jin et al., 2011], whilst [Peng Gong et al., 2012] focus on providing max-min fairness for multicast in Orthogonal Frequency Division Multiple Access (OFDMA)-based wireless heterogeneous networks. A proportional user rate based radio resource management strategy is investigated in [Xue et al., 2012] on a LTE-WiFi HetNet, where a sub-optimal network selection algorithm is introduced to improve the minimum normalised user rate and fairness. Bejerano et al. [Bejerano and Han, 2009] propose changes to the transmission power of AP beacon messages in order to minimise the load in congested APs and thus produce an optimal max-min load balancing strategy. A load balancing scheme for overlapping wireless LAN cells is reported in [Velayos et al., 2004] where users on overloaded APs are offloaded. However, the design aim is to balance the throughput of APs not of users and fairness amongst users is

consequently not considered. In [Jin et al., 2011], the performance of load balancing in a multi-service 3G-WLAN HetNet is evaluated using fuzzy logic. However, in the study, only simple models are used to model 3G and WLAN; the link budget, link capacity and backhaul capacity are not considered.

NSSs that consider QoS are reported in [Karam and Jensen, 2012] [Bari and Leung, 2007] [Hu et al., 2008]. Network selection based on multiple parameters such as cost, bandwidth and QoS parameters including packet loss, jitter and delay is reported in [Bari and Leung, 2007]. However, the study focuses only on general heterogeneous networking and no specific type of technology is evaluated. Similarly, the work in [Karam and Jensen, 2012] and [Hu et al., 2008] studies access network selection for optimal service delivery and QoS to users respectively but the overall HetNet performance and fairness is not considered.

In [Porjazoski and Popovski, 2011] a network selection algorithm based on service type, user mobility and network load is proposed. The authors use a two-dimensional Markov chain to analyse the performance of the proposed algorithm proving that it outperforms existing single or two criteria RAT selection algorithms.

Load balancing in Cellular and WLAN HetNet is reported in [Pei et al., 2010] [Zhuo et al., 2013] and [Zunli Yang et al., 2013]. In [Pei et al., 2010] a joint access-control strategy is designed for efficient sharing of the radio resource and load balancing between CDMA Cellular Network and WLANs by considering user preference. In the article, radio-resource usage of the CDMA network is optimised considering inter-cell interference and bandwidth allocation is optimised for WLANs networks

by maximising the aggregate social welfare of the WLANs under the resource usage constraints. However the method used to balance the load amongst mobile nodes was not disclosed. In [Zhuo et al., 2013] the trade-off between the amount of traffic being offloaded and users satisfaction is investigated, and an incentive framework is proposed to motivate users to use delay tolerance WiFi networks for traffic offloading. [Zunli Yang et al., 2013] proposes a load balancing scheme that aims to balance the network load between the LTE network and WiFi hotspots considering access pattern of UEs.

[Ristanovic et al., 2011] propose a simple algorithm to determine the best time to switch interfaces in order to let users trade delay for energy, and thus extend the constrained battery life of smartphones.

In all published material to date, backhaul capacity as a network selection criterion has not been considered. In [Lusheng Wang and Kuo, 2013], a comprehensive survey comparing various mathematical models for heterogeneous wireless networks and network selection schemes is presented; however, WLAN backhaul capacity for network selection is not considered. Bejerano et al. [Bejerano et al., 2004] consider backhaul capacity during AP selection, while [Galeana-Zapién and Ferrús, 2010] propose a backhaul-aware base station (BS) selection algorithm. Although backhaul-aware cell or network selection has been explored in both [Bejerano et al., 2004] and [Galeana-Zapién and Ferrús, 2010] both focus on homogeneous wireless networks, while the focus of this study is on LTE-WiFi heterogeneous networking.

3.5.2 Bandwidth Allocation in Wireless Multi-hop HetNet

The level of research in respect of cellular-WiFi Mesh integration is modest. Nevertheless [David Chieng et al., 2011] [Olariu et al., 2013] study a network consisting of cellular and WiFi Mesh. In [David Chieng et al., 2011] the performance of various integrated WiMAX-WiFi Mesh network topologies is studied. In particular, the performance of these topologies under different required data rate per user under different user densities is considered. In the network, WiFi mesh network is backhauled by a WiMAX BS, a limitation as the capacity of the entire network is limited to the maximum capacity available at the WiMAX BS. Such a topology is mainly aimed to service rural areas where user density is low and backhauling of WiFi APs is challenging. [Olariu et al., 2013] present a novel architecture and mechanisms to enable voice services to be deployed over Femto Cells backhauled by a wireless mesh network. Both [David Chieng et al., 2011] [Olariu et al., 2013] do not consider bandwidth allocation in WMNs.

In relation to bandwidth allocation in a pure WiFi multi-hop/mesh network, [Ernst and Denko, 2011] propose a scheduling scheme, the focus being to schedule the bandwidth usage fairly. The scheduling scheme considers a mesh topology with multiple gateways. In [Qin et al., 2012], a solution for providing fair throughput for users in a WMN by jointly considering the handoff and resource allocation at the APs is proposed. In the study, MSs are assumed to be mobile and handover occurs frequently. Hence, this kind of solution is more suitable for vehicular networks. In [Ernst and Denko, 2011] and [Qin et al., 2012], throughput maximisation is not the focus as the main objective is to enhance fairness in the WMN.

For bandwidth allocation schemes that consider both throughput and fairness in multi-hop/mesh networking, [Tang et al., 2006] propose a multi-channel multi-hop bandwidth allocation scheme in wireless mesh networks to maximise network throughput and enhance fairness at the same time. Polynomial time algorithms were used to compute max-min fair bandwidth allocation which leads to high throughput with maximum guaranteed bandwidth allocation. Further, the max-min fair bandwidth allocation - Lexicographical Max–Min (LMM) model - was also proposed for the same purpose. In [Tang et al., 2007], joint rate control, routing and scheduling in multi-channel wireless mesh network is proposed to find a rate allocation along with a flow allocation and a transmission schedule for a set of end-to-end communication sessions such that the network throughput and fairness is maximised. [Tang et al., 2010] propose a scheme for end-to-end bandwidth allocation in WMNs with cognitive radios, which involves routing, scheduling, and spectrum allocation. Two fair bandwidth-allocation problems are defined based on a simple max–min fairness model and the LMM fairness model, to achieve a good trade-off between fairness and throughput. Joint channel assignment and routing is mathematically formulated in [Alicherry et al., 2005], taking into account interference constraints, the number of channels in the network and the number of radios available at each mesh router. The formulation is then used to develop a solution which optimises overall network throughput with fairness constraint. Although [Tang et al., 2010] and [Alicherry et al., 2005] aim to enhance both throughput and fairness, users are not considered in the research; only node-based bandwidth assignment fairness is considered. Per user fairness is not guaranteed especially when the distribution of users across mesh nodes is not uniform.

[Dzal et al., 2014] consider user-based fairness and propose a scheme that enhances the fairness and throughput in multi-radio, multi-channel WMN considering user traffic demand, interference and link utilisation.

Other resource allocation schemes that consider QoS are reported in [De la Oliva et al., 2012] and [Dai et al., 2008]. [De la Oliva et al., 2012] propose a solution to provide throughput guarantees in heterogeneous wireless mesh networks by jointly optimising the routing and Medium Access Control (MAC) configuration. A linearised capacity region model is proposed to determine if a given flow allocation is feasible, and based on that, multi- and single path routing algorithms are proposed to find optimal paths for all flows in the network given their throughput requirements. [Dai et al., 2008] investigate optimal routing strategies for a wireless mesh network taking traffic demand estimations as inputs. The goal is to perform routing optimisation, which in turn distributes the traffic along different routes, so that minimum congestion is incurred even under dynamic traffic. However, the study is for a limited capacity single-radio single-channel WMN which is less common compared to multiple-radio multiple-channel WMN.

From the review of existing research, there are no reported solutions that optimise fairness and network throughput in cellular-WiFi Mesh networks, clear motivation for the research presented.

3.6 Conclusions

Existing standards and industrial bodies supporting Cellular-WiFi integration are discussed. The rapid development of standards and the aggressive establishment of industrial groups indicate that HetNet with Cellular-WiFi integration has great potential as a high capacity wireless networking solution.

The outputs of the industrial and standards activities to date indicate a major focus on issues inherent with interworking such as security, mobility support, QoS and network selection for offloading and little or no focus is targeted to address the small cell backhauling challenge.

Therefore, the development and evaluation of a solution to small cells backhauling in Cellular-WiFi HetNet forms the focus of research in this thesis. The scope is confined to two specific HetNet architectures viz. Hotspot Wireless HetNet (HWH) and Multi-hop Wireless HetNet (MWH), differing in the way the APs are backhauled with the former being backhauled directly to the core network whilst the latter is backhauled by multi-hop wireless networking.

With the scope of research defined, the reported research relevant to the scope has been discussed and mapped. From the review of reported research, there are no reported solutions that optimise fairness and network throughput based on the backhaul capacity in HWH. Further no reported research exists that aims to improve the performance of MHWs based on cellular-WiFi Mesh networks through proper

network selection and backhaul bandwidth allocation. The reported research related to network selection schemes in HWH and MWH are summarised in Table 3.2.

Table 3.2: Summary of reported research in Network Selection Schemes (NSSs) and Mesh Bandwidth Allocation.

Attribute	**Reported Research**
Network Selection (NS):	
WiFi First NS	[A. Handa, 2009] [Piamrat et al., 2011]
NS based on data rate	[Raiciu et al., 2011] [Nie et al., 2005] [Jackson Juliet Roy et al., 2006]
NS aims to optimize throughput	[Kumar et al., 2007] [Premkumar and Kumar, 2006] [Sarabjot Singh et al., 2013]
NS considering Fairness	[Peng Gong et al., 2012] [Xue et al., 2012] [Bejerano and Han, 2009] [Velayos et al., 2004] [Jin et al., 2011]
NS considering QoS	[Karam and Jensen, 2012] [Bari and Leung, 2007] [Hu et al., 2008]
NS based on service type	[Porjazoski and Popovski, 2011]
Network load balancing	[Pei et al., 2010] [Zhuo et al., 2013] [Zunli Yang et al., 2013]
NS for energy saving	[Ristanovic et al., 2011]
NS considering backhaul capacity	[Lusheng Wang and Kuo, 2013] [Bejerano et al., 2004] [Galeana-Zapién and Ferrús, 2010]
Mesh Bandwidth Allocation:	
Fairness only	[Qin et al., 2012] [Ernst and Denko, 2011]
Throughput and fairness	[Tang et al., 2006] [Tang et al., 2007] [Tang et al., 2010] [Alicherry et al., 2005] [Dzal et al., 2014]
QoS	[De la Oliva et al., 2012] [Dai et al., 2008]
Cellular + WiFi Mesh HetNet:	[David Chieng et al., 2011] [Olariu et al., 2013]

Chapter 4

Modelling of HetNets

4.1 Introduction

In the Chapter, propagation models, physical and MAC models as well as network models used to simulate HetNet operation are presented for both WiFi and LTE. Validation of both models is demonstrated. The integrated HetNet model is also presented before the Chapter is concluded.

4.2 WiFi Models

IEEE802.11g and IEEE802.11n wireless networking standards are used to model the WiFi network as both represent the most widely deployed technologies internationally. IEEE 802.11g is an improvement of 802.11b which uses OFDM in the physical layer, while IEEE 802.11n is an amendment to the IEEE 802.11-2007 wireless networking standard [IEEE Std, 2007a] and a further enhancement of IEEE802.11a/g. IEEE 802.11n improves network throughput over 802.11a/g with a significant increase in the maximum raw data rate from 54 Mbps to 600 Mbps. Throughput improvements are mainly attributed to the introduction of MIMO, channel bonding and packet header reduction through frame aggregation and block acknowledgement (Chapter 2).

The WiFi network models developed consist of the Physical Layer, MAC Layer and Network Layer.

4.2.1 WiFi Path Loss Model

4.2.1.1 Access Path Loss Model

Propagation path loss is the attenuation of power of an electromagnetic wave as it propagates through space. The propagation path loss increases logarithmically with distance yielding signal receiving model as in Equation (4.1) [Rappaport, 1996];

$$P_{Rx} = K \times P_{Tx}/d^{\alpha} \tag{4.1}$$

In general, the received signal power P_{Rx} is a function of transmit signal power P_{Tx}, and transmitter-receiver distance *d*. In typical outdoor scenarios, the path loss exponent α takes values between 2 and 4 [Andersen et al., 1995] depending on the propagation environment. *K* is a constant that depends on the transmission frequency, antenna gain, and antenna height. In dB scale, Equation (4.1) takes the form of Equation (4.2), which exhibits a linear dependency between received signal power in dB and the logarithm of the transmitter-receiver distance. Hence, the path loss given by Equation (4.2) is represented by "$10\alpha log_{10}d + K$";

$$P_{Rx} = P_{Tx} - (10\alpha log_{10}d + K) \tag{4.2}$$

A series of field measurements were carried out in the urban area of Kuala Lumpur, Malaysia. The AP heights are fixed at 3m and

Figure 4.1 shows the path loss obtained.

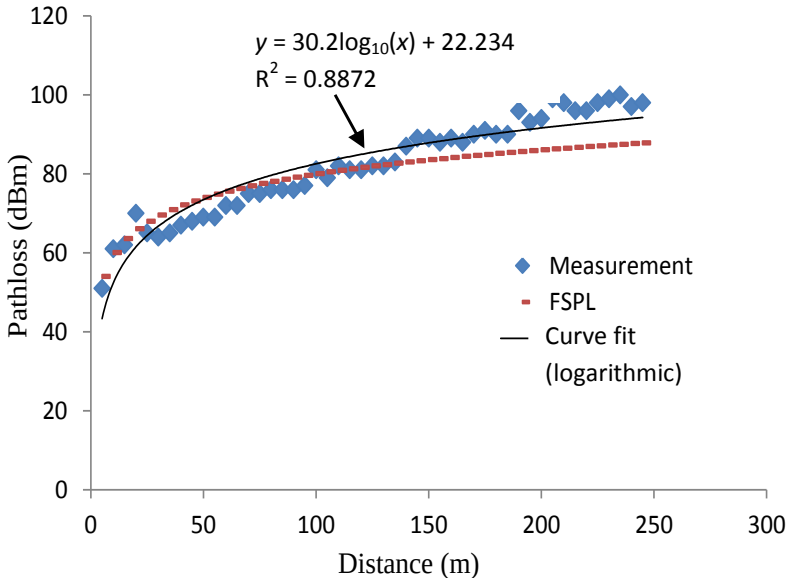

Figure 4.1: Propagation path loss model, 2.4GHz.

Using curve fitting, the path loss exponent, α and K are found to be 3.02 and 22.23 respectively as shown in Equation (4.3) where d is the distance in meters;

$$PL = 30.2 \cdot \log_{10}(d) + 22.234 \quad (4.3)$$

4.2.1.2 Wireless Backhaul Path Loss Model

Mesh nodes are assumed to be in a fixed location and their deployment is pre-planned and as such, Line of Sight (LOS) is assumed between two adjacent WiFi

mesh nodes. Moreover, a directional antenna is used effectively achieving the performance a point to point link (i.e. from a mesh link). Hence, it is acceptable to adopt the free space path loss model as in Equation (4.4) for multi-hop WiFi backhaul [Parsons and Parsons, 2000];

$$PL = 10\alpha \cdot \log_{10}(d) + 20\log_{10}(f) - 147 \qquad (4.4)$$

where, α is the path loss exponent and f is the carrier frequency in Hertz.

4.2.2 WiFi Shadow Fading

Normally, for real environment modelling the effect of shadowing cannot be neglected otherwise the path loss model used simply represents a straight line from transmitter to receiver. Shadow fading, also referred to large-scale fading, is a consequence of blockage or diffraction of a signal by obstacles such as buildings, trees and other objects, resulting in multiple signal paths from transmitter to receiver.

The total attenuation A – assuming the contributions to the signal attenuation along the entire propagation path are considered to act independently – due to N individual contributions i.e. $A_1, \ldots, A_N$ is given by [Saunders and Aragón-Zavala, 2007];

$$A = A_1 \times A_2 \times \cdots \times A_N \qquad (4.5)$$

If shadowing is to be expressed in Decibels (dBs), the result is the sum of the individual losses:

$$L = L_1 + L_2 + \cdots + L_N \tag{4.6}$$

If a sufficient number of diffraction points and/or multi-reflection paths to the receiver exist causing all of the received signals to be considered as random variables, then the Central Limit Theorem [Rice, 2006] holds, justifying the use of Gaussian random variables to represent path loss. In that case, A follows a log-normal relationship, since fading follows a normal distribution in dB (the log domain); hence, large-scale fading is modelled as a log-normal random variable. The standard deviation of the shadowing distribution (in dB) is known as the location variability, denoted by σ_L, a variance used to characterise log-normal fading relative on the mean path loss. The location variability varies with frequency, antenna heights and environment. The value typically ranges from 6 dB to 10 dB [Byeong Gi Lee and Choi, 2008] and in the simulation an σ_L of 6 dB is assumed.

Shadowing loss is modelled as L_{shadow} with z being a Gaussian random variable;

$$L_{shadow} = z\sigma_L \tag{4.7}$$

The total large scale-loss due to both PL (Section 4.2.1) and shadowing can thus be express as L_{All} (in dB) as:

$$L_{All}(dB) = PL + L_{Shadow} \tag{4.8}$$

4.2.3 WiFi Antenna Model

An antenna is used to convert the guided electromagnetic waves in a waveguide, feeder cable or any transmission line into radiating waves which propagate through space to the receiver, or vice versa. The radiation pattern is a plot of the far-field radiation from the antenna [Saunders and Aragón-Zavala, 2007].

There are generally two types of antenna (i) omni-directional, whose radiation pattern is constant in the horizontal plane but may vary vertically and (ii) directional, which radiates greater power in one or more specific directions. Omni-directional antenna can be best represented by the Hertzian dipole as illustrated in Figure 4.2 showing the uniform radiation pattern in X–Y plane.

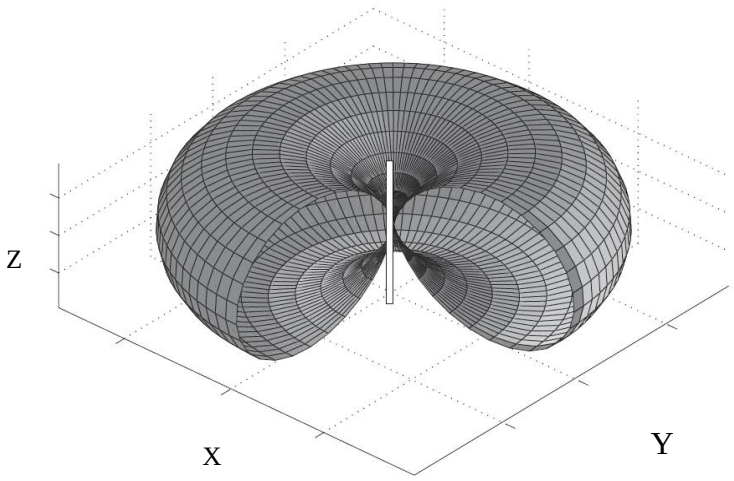

Figure 4.2: Radiation pattern of a Hertzian dipole antenna. The section from $\phi = 0$ to $\phi = \pi/2$ has been cross sectioned for detail revelation. Source: [Saunders and Aragón-Zavala, 2007].

Directional antennas are differentiated by the directivity D of the radiation pattern where D is defined as [Saunders and Aragón-Zavala, 2007]:

$$D(\theta,\phi) = \frac{Radiation\ intensity\ of\ antenna\ in\ direction\ (\theta,\phi)}{Radiation\ intensity\ of\ isotropic\ antenna\ radiating\ the\ same\ total\ power} \quad (4.9)$$

where θ and ϕ are the angles for the spherical coordinates. The directivity is measured in units of dBi [Saunders and Aragón-Zavala, 2007]. Often in practice, the half-power beamwidth (HPBW) or commonly the beamwidth is also used to determine the directivity of an antenna. HPBW is angular separation in which the magnitude of the radiation pattern decreases by 50% (or -3 dB) from the peak of the main lobe.

In the simulation, WiFi access radio antennas are assumed to be omni-directional. For WiFi backhaul, directional antennas with 30 º-3dB beamwidth are assumed and the radiation pattern is shown in Figure 4.3.

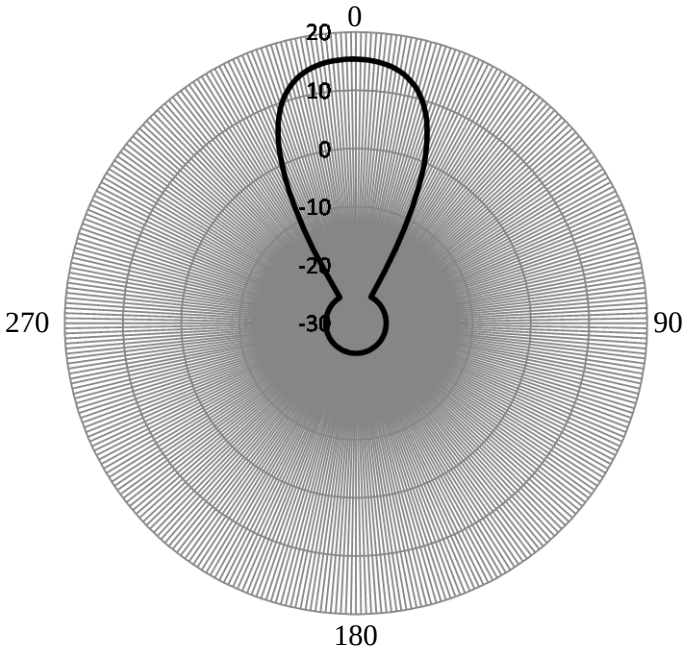

Figure 4.3: Antenna radiation pattern for mesh links; polar plot Azimuth ("*E*" plane).

4.2.4 WiFi Link Budget

A link budget as in Equation (1.1) is adopted for the calculation of received power P_{Rx} (dBm) at user terminals as a function of the transmit power P_{Tx} (dBm). The link budget takes into account the attenuation of the signal through the transmission medium due to path loss PL(dB), shadowing L_{shadow}(dB) and considers transmit and receive antenna gains (G_{Tx}, G_{Rx} (dBi));

$$P_{Rx} = P_{Tx} + G_{Tx} - PL - L_{shadow} + G_{Rx} \quad (4.10)$$

In the study, only large scale fading such as shadowing is considered. Small scale fading such as Rician and Rayleigh [Goldsmith, 2005] describing the fluctuation of signal level at the receiver after encountering obstacles are not considered to keep the model computationally simple.

Equation (4.10) can also be written as Equation (4.11) when the summation of transmit power P_{Tx} and transmit antenna gain G_{Tx} is represented by an Equivalent Isotropic Radiated Power (EIRP) [Saunders and Aragón-Zavala, 2007];

$$P_{Rx} = EIRP - PL - L_{shadow} + G_{Rx} \quad (4.11)$$

Equation (4.11) is adopted to model the WiFi access link. However, in a multi-hop network, the operation of the entire network relies heavily on the wireless backhaul. Therefore the reliability and availability of the backhaul network has to be high. To

meet those requirements, the link budget for the wireless backhaul is more stringent compared to the access network and thus a Fade Margin (FM) is considered in the planning phase. FM buffers against backhaul signal fluctuation and ensures a more robust link quality [Tranzeo, 2010]. The backhaul link budget is typically given by:

$$P_{Rx} = EIRP - PL - L_{shadow} + G_{Rx} - FM \quad (4.12)$$

Typical parameter values for both Equation (4.11) and Equation (4.12) can be obtained from Table 4.5.

4.2.5 WiFi Interference Model

The 2.4 GHz band consisting of eleven channels is used in WiFi access. However, to avoid adjacent channel interference for better performance, only three 20 MHz non-overlapping channels with channel number 1, 6 and 11 [Eldad and Robert, 2008] are considered in the simulation. Since non-overlapping channels are used, only co-channel interference is relevant. The simulated area is divided into 5-by-5 square meter grids. In each grid, an effective Signal-to-Interference Noise Ratio (SINR) is derived as [Tse and Viswanath, 2005]:

$$SINR = \frac{P_u}{\sum_{t=1}^{M} P_t + NFl_u} \quad (4.13)$$

where, p_u is the received power detected by user u from the serving AP located in the grid, M is the total number of co-channel interferer APs within range, p_t is the

interference power at the receiver and NFl_u is the noise floor at the receiver of user u calculated as kTB with k is Boltzmann's constant (1.380662×10^{-23}), T is temperature of the receiver (290 ℃K) and B the effective channel bandwidth. NFl_u represents the thermal noise level falling within the receiver channel bandwidth B and kT is calculated as -174dBm/Hz [Gu, 2005].

The effective SINR is then used to map user data rate (Section 4.2.6) which is subsequently used in user throughput estimation (Section 4.2.8) in WiFi networks. An example coverage plot with and without interference is shown in Figure 4.4. Similarly, the SINR calculation for a link between two mesh nodes is executed using the relationship of Equation (4.13) but u now represents a mesh node instead of a user device.

4.2.6 WiFi Network Channel Assignment Algorithm

When the topology is fixed and APs locations are known, interference aware channel allocation algorithm is implemented to select the best channel for access radio. Firstly, an interference graph G for the entire access domain is generated using the propagation model of Equation (4.3). Given the graph $G = (V, E)$ consists of a set of vertices V representing a total number of M APs, and a set of edges E represents interference amongst APs.

Channel assignment represented by vertex colouring is carried out by referring to the interference graph where the least interference channel is assigned to an AP access radio. In general, a vertex colouring of G is a map $c: V(G) \rightarrow F$ which assigns a

colour $c(V_i)$ to each vertex $V_i \in V$, where F is a set of colours. $F = \{1, 2, \cdots, 11\}$ for IEEE 802.11g, of which the subset $F' = \{1, 6, 11\}$ corresponds to the non-overlapping channels used in the simulation represented by channel index *l* from 1 to 3 respectively in Algorithm 4.1. Colouring is admissible if adjacent vertices have different colours i.e. $c(V_i) \neq c(V_j)$ whenever $V_i, V_j \in E$. For the case where no free channel is available, the least interfering channel within the colour set F' is chosen. To an AP represented by vertex V_i, the aggregated interference value on a particular channel using channel index *l* is calculated as:

$$P_l^i = \sum_{j=1}^{M} P_j \cdot I_j \cdot L_l^j; \ \ where\ l = 1{:}3\ and\ i \neq j \qquad (4.14)$$

where the interference weight P_j denotes received power from vertices V_j and I_j is a binary number indicating whether V_j is a neighbour sufficiently close to interfere and L_l^j is a logical number indicating whether the V_j, vertex under assessment is using the same channel. The channel assignment algorithm itself consists of the steps shown in Algorithm 4.1:

Algorithm 4.1: Channel optimisation algorithm

1 $c(V_i) \leftarrow 0$

2 *for all access interface* $V_i \in V$, *where* $i = 1{:}\,M$ *and* M *is total number of APs*

3 if *AP is not assigned a channel yet*

4 *if any* $c \in F' \neq c(V_j)$; $\forall c(V_j)$ *where* $j = 1{:}\,M$ *and* $j \neq i$

5 $c(V_i) \leftarrow c$

6 *otherwise (if no unused channel)*

7 *for all* $l = 1{:}\,3 \in F'$ *representing 3 orthogonal channels*

8 $P_l^i = \sum_{j=1}^{M} P_j \cdot I_j \cdot L_l^j \; ; \; j \neq i$

9 *end*

10 $c \Leftarrow \min\left(P_l^i;\; l = 1{:}\,3\right)$; *choose channel with least interference*

11 $c(V_i) \leftarrow c$

12 *end*

13 *end*

14 *end*

15 *repeats step 2-15 until no changes of channel to all APs*

Figure 4.4 compares the difference between coverage with and without the application of the WiFi channel optimisation algorithm. The channel assigned to each AP is labelled in the brackets after the AP's name. Without proper channel planning, Figure 4.4(a) shows the coverage of seven WiFi nodes with co-channel interference where adjacent APs are assigned the same channel. Interference at the areas pointed by red arrows results in lower effective WiFi coverage compared to Figure 4.4(b) which follows a better channel plan.

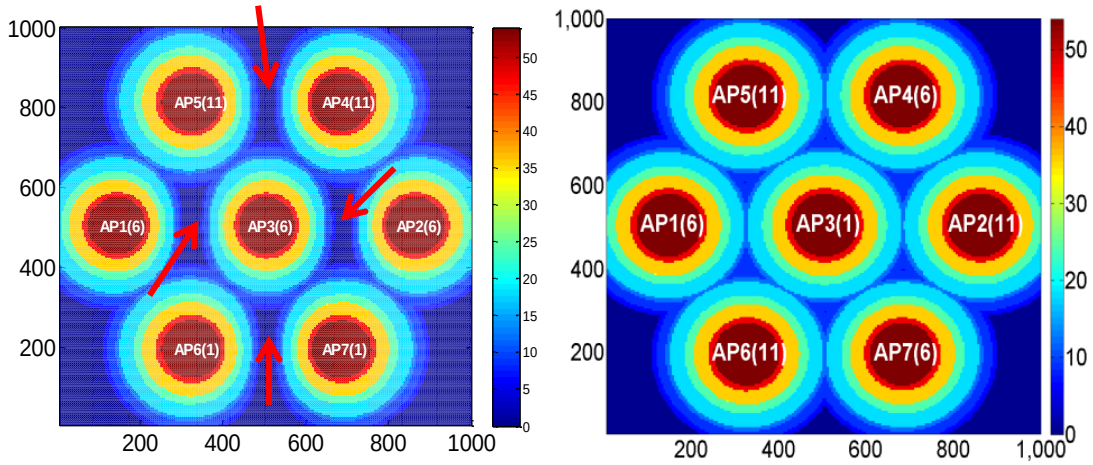

(a) (b)

Figure 4.4: 7-WiFi-Nodes coverage plot (a) with and (b) without co-channel interference (shadowing is not included for clarity).

For backhaul radio channel assignment, a similar algorithm with a directional antenna and a backhaul pathloss model of Equation (4.4) is used. Since the backhaul is operating at 5 GHz, there are more than 10 orthogonal channels (depending on the region) if a 20 MHz channel bandwidth is considered [Cisco, 2008] [IEEE Std, 2007b]. However, for a 40 MHz channel bandwidth (channel aggregation), the number of orthogonal channels is halfed.

4.2.7 WiFi Data Rate

The WiFi data rate achievable at a specific location is largely dependent on received power P_{Rx} at the user terminal. For a particular data rate and modulation coding scheme (MCS), the reference sensitivity level is the minimum received signal strength required to produce a sufficient SINR for the successful recovery of data. Normally the reference sensitivity level is also referred to as the receiver sensitivity. Table 4.1 and Table 4.2 present the receiver sensitivity value per MCS and

corresponding raw data rate for WiFi 802.11g [Networks, 2013] and 802.11n [DNMA-92] respectively.

Table 4.1: WiFi 802.11g receiver sensitivity and data rates.

Index	MCS	11n (20MHz)	
		Receiver Sensitivity (dBm)	Data Rate (Mbps)
1	BPSK1/2	-94	6
2	BPSK 3/4	-93	9
3	QPSK1/2	-91	12
4	QPSK3/4	-90	18
5	16-QAM1/2	-86	24
6	16-QAM3/4	-83	36
7	64-QAM2/3	-77	48
8	64-QAM3/4	-74	54

Table 4.2: WiFi 802.11n (2x2 MIMO) receiver sensitivity and data rates.

Index	MCS	11n (20MHz)		11n (40MHz)	
		Receiver Sensitivity (dBm)	Data Rate (Mbps)	Receiver Sensitivity (dBm)	Data Rate (Mbps)
1	BPSK1/2	-95	14.4	-91	30
2	QPSK1/2	-93	28.9	-90	60
3	QPSK3/4	-90	43.3	-87	90
4	16-QAM1/2	-87	57.8	-84	120
5	16-QAM3/4	-84	86.7	-82	180
6	64-QAM2/3	-80	115.6	-78	240
7	64-QAM3/4	-79	130.0	-76	270
8	64-QAM5/6	-77	144.4	-74	300

Knowledge of both the received power P_{Rx} and receiver sensitivity, allows the achievable raw data rate of a particular user terminal to be estimated by mapping the P_{Rx} to the receiver sensitivity listed in Table 4.1 or Table 4.2.

4.2.8 WiFi Throughput

In the simulation, the IP layer throughput efficiency φ for WiFi is the ratio of the actual IP layer data rate against physical data rate of each MCS scheme after excluding the coding bits, headers and other WiFi specific overheads. In the study, the 802.11g model is used for the access radio in the HWH and 802.11n is modelled for both access and backhaul radios in the MWH.

The throughput efficiency for 802.11g is obtained from the QualNet simulator [Qualnet Network, 2014], while the throughput efficiency of 802.11n is obtained from a theoretical derivation assuming a fixed user packet size of 1000 Bytes at constant bit rate traffic. The detail derivation of 802.11n throughput efficiency can be found in Appendix A. The throughput efficiency of both 802.11g and 802.11n are summarised in Table 4.3 and Table 4.4 respectively.

For a single wireless link capable of supporting a particular MCS, the maximum achieable IP throughput at that modulation is calculated by multiplying the raw data rate R with the corresponding throughput efficiency φ as in Equation (4.15). The maximum achieable IP throughput of both 802.11g and 802.11n are summarised in Table 4.3 and Table 4.4 respectively.

$$C_{link}^{WiFi} = R \times \varphi \tag{4.15}$$

Table 4.3: 802.11g throughput efficiency and IP throughput.

Index	MCS	11g		
		Data Rate, R (Mbps)	Eff, φ	IP Throughput (Mbps)
1	BPSK1/2	6	0.70	4.20
2	BPSK3/4	9	0.64	5.76
3	QPSK1/2	12	0.61	7.32
4	QPSK3/4	18	0.54	9.72
5	16-QAM1/2	24	0.49	11.76
6	16-QAM3/4	36	0.41	14.76
7	64-QAM2/3	48	0.35	16.80
8	64-QAM3/4	54	0.32	17.28

Table 4.4: 802.11n throughput efficiency and IP throughput.

Index	MCS	11n (20MHz), 2.4GHz			11n (40MHz), 5GHz		
		Data Rate (Mbps)	Eff, φ	IP Throughput (Mbps)	Data Rate (Mbps)	Eff, φ	IP Throughput (Mbps)
1	BPSK1/2	14.4	0.84	12.1	30	0.80	24.0
2	QPSK1/2	28.9	0.80	23.1	60	0.74	44.4
3	QPSK3/4	43.3	0.77	33.3	90	0.69	62.1
4	16-QAM1/2	57.8	0.75	43.4	120	0.64	76.8
5	16-QAM3/4	86.7	0.70	60.7	180	0.57	102.6
6	64-QAM2/3	115.6	0.66	76.3	240	0.51	122.4
7	64-QAM3/4	130.0	0.63	81.9	270	0.48	129.6
8	64-QAM5/6	144.4	0.61	88.1	300	0.46	138.0

4.2.9 Single WiFi AP with Max-Min Fairness

In WiFi, users with slower link speed tend to occupy more spectrum resource (in terms of transmit time) than higher speed users for the same amount of data sent. Such a bandwidth sharing scenario amongst all users within a single AP coverage has therefore to be modelled.

Suppose a total of U users connected to an AP are separated by their supportable data rate R_u according to their SINR level. Thus, user u can receive transmission slots at rate R_u bps, where $u = 1,2..U$. Assuming the relative frequency of packets by user u is $\mathcal{P}_u$ and that resources are allocated as a function of the number of slots inversely proportional to user data rate R_u to ensure throughput fairness, let S_u be the number of slots allocated to user u, where $S_u = k/R_u$, k being a constant. In this case, if user packet size is assumed to be the same, the AP throughput at the physical layer is calculated as [Pahlavan and Levesque, 2005b; Bender et al., 2000] (see Section 4.2.11.4 for QualNet simulation verification):

$$C_{sys}^{Phy} = \frac{\sum_{u=1}^{U} \mathcal{P}_u R_u S_u}{\sum_{u=1}^{U} \mathcal{P}_u S_u} \tag{4.16}$$

Substituting $S_u = \frac{k}{R_u}$ into Equation (4.16);

$$C_{sys}^{Phy} = \frac{\sum_{u=1}^{U} \mathcal{P}_u R_u \left(\frac{k}{R_u}\right)}{\sum_{u=1}^{U} \mathcal{P}_u \left(\frac{k}{R_u}\right)} = \frac{k \cdot \sum_{u=1}^{U} \mathcal{P}_u}{k \cdot \sum_{u=1}^{U} \frac{\mathcal{P}_u}{R_u}} = \frac{\sum_{u=1}^{U} \mathcal{P}_u}{\sum_{u=1}^{U} \frac{\mathcal{P}_u}{R_u}} \tag{4.17}$$

Since the sum of the relative frequency of packets (or the probability of accessing the access channel) by all user is $\sum_{u=1}^{U} \mathcal{P}_u = 1$, Equation (4.17) can be further simplified to;

$$C_{sys}^{Phy} = \frac{\sum_{u=1}^{U} 1}{\sum_{u=1}^{U} \frac{\mathcal{P}_u}{R}_u} \tag{4.18}$$

The average physical layer throughput per user C_{Av}^{Phy} is calculated by dividing Equation (4.16) by the total number of users U. Since fair resource sharing is assumed - which in turn implies that the packet sending frequency of every user is the same - the relative frequency of packets $\mathcal{P}_u$ by a user can also be written as $\frac{1}{U}$:

$$C_{Av}^{Phy} = \left(\frac{1}{U}\right) \times \left(\frac{1}{\sum_{u=1}^{U} \frac{1}{\frac{U}{R_u}}}\right) = \frac{1}{\sum_{u=1}^{U} \frac{1}{R_u}} \tag{4.19}$$

The system follows a max-min fairness behaviour at multi-rate operation where all users enjoy a similar amount of traffic, mimicking the WiFi Distributed Coordinated Function (DCF) [Bredel and Fidler, 2008] which allocates all users fair medium access.

Equation (4.19) can be explained using Example 4.1.

Example 4.1: Consider two users connected to an AP with supportable data rate of user 1 and user 2 represented by R_1 = 54 Mbps and R_2 = 6 Mbps.

The number of time slots assigned is inversely proportional to data rate, $S_1 = \frac{k}{R_1} = \frac{k}{54}$ and $S_2 = \frac{k}{R_2} = \frac{k}{6}$ respectively.

The relative frequency of packets of user 1 and user 2 is represented by $\mathcal{P}_1$ and $\mathcal{P}_2$. Since both have equal opportunity to access the AP (or a fair chance to transmit to the AP), $\mathcal{P}_1 = \mathcal{P}_2 = \frac{1}{2}$. With both users taking turns to transmit one packet and assuming their packet sizes are the same, the time slots assigned to each user can be represented by Figure 4.5.

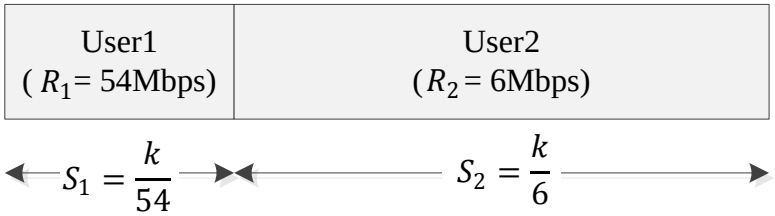

Figure 4.5: Time slots required for two users under an AP with fair throughput

From Figure 4.5, user 2 is allocated more slots than user 1 in order to maintain throughput fairness, in other words, User 1 is being penalised in terms of fairness, which is the characteristic of WiFi DCF system.

The average throughput for both users can be calculated as in Equation (4.20);

$$C_{AV}^{Phy} = \frac{S_1}{S_1 + S_2} \times R_1 = \frac{S_2}{S_1 + S_2} \times R_2 \quad (4.20)$$

By substituding value of S_1, S_2, R_1 and R_2 into Equation (4.20), the average throughput for both users can be calculated as 5.4 Mbps (Equation (4.21));

$$C_{AV}^{Phy} = \frac{\frac{k}{54}}{\frac{k}{54} + \frac{k}{6}} \times 54 = \frac{\frac{k}{6}}{\frac{k}{54} + \frac{k}{6}} \times 6 = \frac{1}{\frac{1}{54} + \frac{1}{6}} = 5.4 \quad (4.21)$$

Similarily, within a single WiFi network, the average IP layer throughput per user C_{Av} (Equation (4.22)) is calculated by multiplying the physical data rate R_u in Equation (4.19) by a corresponding throughput efficiency factor φ_u as described in Section 4.2.8:

$$C_{Av} = \frac{1}{\sum_{u=1}^{U} \frac{1}{R_u \times \varphi_u}} \quad (4.22)$$

4.2.10 General WiFi Simulation Parameters

General parameters used for the WiFi models (Section 4.2) are given in Table 4.5. WiFi access radio is assumed to operate in the 2.4 GHz unlicensed Industrial, Scientific and Medical (ISM) radio bands while the WiFi backhaul radio is assumed

to operate in the Unlicensed National Information Infrastructure (U-NII) band of 5.8 GHz.

Table 4.5: General WiFi simulation parameters.

Parameters	Value	Unit
Carrier frenquency, f (Access/Backhaul)	2.4 / 5.8	GHz
Maximum EIRP for Access Radio	27	dBm
Maximum EIRP for Backhaul Radio	30	dBm
WiFi Access Channel Bandwidth	20	MHz
WiFi Backhaul Channel Bandwidth	40	MHz
Backhaul path loss coeficient, α	2.5	-
Fade Margin (WiFi backhaul)	18	dB
Location variability for Shadowing, σ_L	6	dB
User Terminal Antenna Gain	3	dBi
UDP Packet Size	1000	Bytes

A 20 MHz channel bandwidth is assumed for the access radio. However, for multi-hop backhaul which normally requires higher bandwidths due to the traffic aggregation from APs over multiple hops, a larger channel bandwidth (40 MHz) is assumed. Since the backhaul link is vitally important for the overall performance of WMN, the 5 GHz operating frequency is chosen for backhaul radio as it enjoys lower interference and can utilise a higher the number of orthogonal channels. For both access and backhaul radio with 802.11n, two MIMO streams are assumed for throughput enhancement. In the case where line of sight (LOS) exists between two backhaul radio interfaces, a dual-polarized antenna can be used to realise two-stream MIMO transmission [Nirmal Kumar Das et al., 2006].

The maximum EIRP for the access and backhaul radio is set to 27 dBm and 30 dBm respectively according to the Malaysia regulatory body [SKMM, 2005]. The mesh nodes are assumed to be deployed at fixed locations and LOS is engineered for all WiFi mesh/backhaul links. A typical path loss exponent α for a LOS link ranges from 2 to 2.7 [Schwengler and Glbert, 2000] and in the study, α=2.5 is assumed for all WiFi backhaul links. A FM of 18 dB is assumed for the backhaul link to ensure 99% link availability according to [Tranzeo, 2010] based on the Rayleigh fading model [F. Perez Fontan, 2008]. As explained in Section 4.2.2, σ_L=6 is assumed for location variability as a consequence of shadowing. User terminals are assumed to be mainly laptops, tablets and smart phones. The antenna gain of those devices varies depending on the device form factor. With advanced antenna design for the laptop or smaller devices, an antenna gain beyond 3 dBi is achievable [Guo et al., 2014] [Shun-Min Wang et al., 2013]; hence, an antenna gain for all user terminals is assumed to be 3dBi.

To simplify the simulation, UDP traffic with an arbitrary packet size of 1000 Bytes is assumed in all simulations. The evaluation can be easily extended to study other type of traffic based on, for example, TCP and HTTP.

4.2.11 IEEE 802.11g Model Verification

For the convenience of combining LTE and WiFi models to form a HetNet and ease of evaluating the proposed algorithms, all models are implemented in Matlab [Matlab]. All IEEE802.11g WiFi models used in the Matlab simulator were verified using the QualNet simulator (Version 5.2). The parameters used to synchronise both

simulators in order to execute a fair comparison are discussed in Section 4.2.11.1. Subsequently, several simulation scenarios consisting of a single user and multiple users were executed using both simulators and the results on user(s) throughput and fairness in terms of bandwidth sharing were compared.

4.2.11.1 Parameters Setting

IEEE802.11g WiFi models used in Matlab are verified using QualNet simulator (Version 5.2). In order to execute a fair comparison, the propagation model for both simulators has to be the same; the propagation model used in QualNet is the Two Ray model and hence the Two Ray model was also used in the Matlab simulator, implemented only for comparison purposes. Once results were compared and were proven to be in good agreement, then it is assumed that the Matlab models, especially the MAC layer, are accurate regardless of the propagation model used.

Table 4.6: IEEE802.11g parameters.

MCS Types	**Sensitivity**	**Data Rate (Mbps)**	**IP Eff, φ_{IP}**	**Throughput (Mbps)**
BPSK 1/2	-85	6	0.70	4.20
BPSK 3/4	-84	9	0.64	5.76
QPSK 1/2	-83	12	0.61	7.32
QPSK 3/4	-80	18	0.54	9.72
16QAM 1/2	-78	24	0.49	11.76
16QAM 3/4	-75	36	0.41	14.76
64QAM 2/3	-72	48	0.35	16.80
64 QAM3/4	-69	54	0.32	17.28

Similarly, receiver sensitivities are kept consistent between simulators and set to the values as in Table 4.6. The throughput efficiencies of the Matlab model for respective MCS are also set to the values as in Table 4.10.

4.2.11.2 Single User Throughput Comparison

The propagation range obtained from the two simulators was compared.

Figure **4.6** shows the throughput as a function of distance for both simulators. Two simulations were carried out with the maximum EIRPs set to 20 dBm and 30 dBm respectively and the results between simulators are in good agreement.

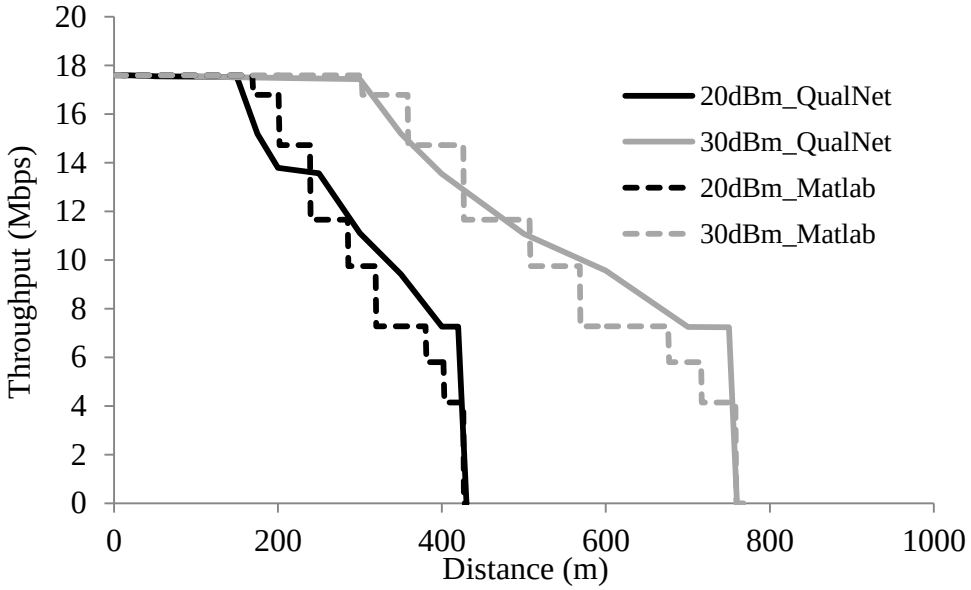

Figure 4.6: IEEE802.11g throughput as a function of distance from two simulators.

4.2.11.3 Multi-users Throughput Comparison

Further validation was carried out through a comparison of the multiple-user throughput with certain number of users distributed within a WiFi cell. A Grid distribution is chosen to tabulate the users. Three scenarios are considered with 16, 26 and 36 users distributed across the coverage area covered by an AP node (EIRP 20 dBm) located in the centre (Figure 4.7).

UDP traffic of 1000 byte packet size is generated for the downlink. Every user is assumed to have the same amount of traffic from the AP and therefore the traffic is generated in such a way as to send the same amount of traffic to each user on the downlink. The total traffic generated is just sufficient to saturate the access link so that the network throughput could be maximised without overloading the AP access link.

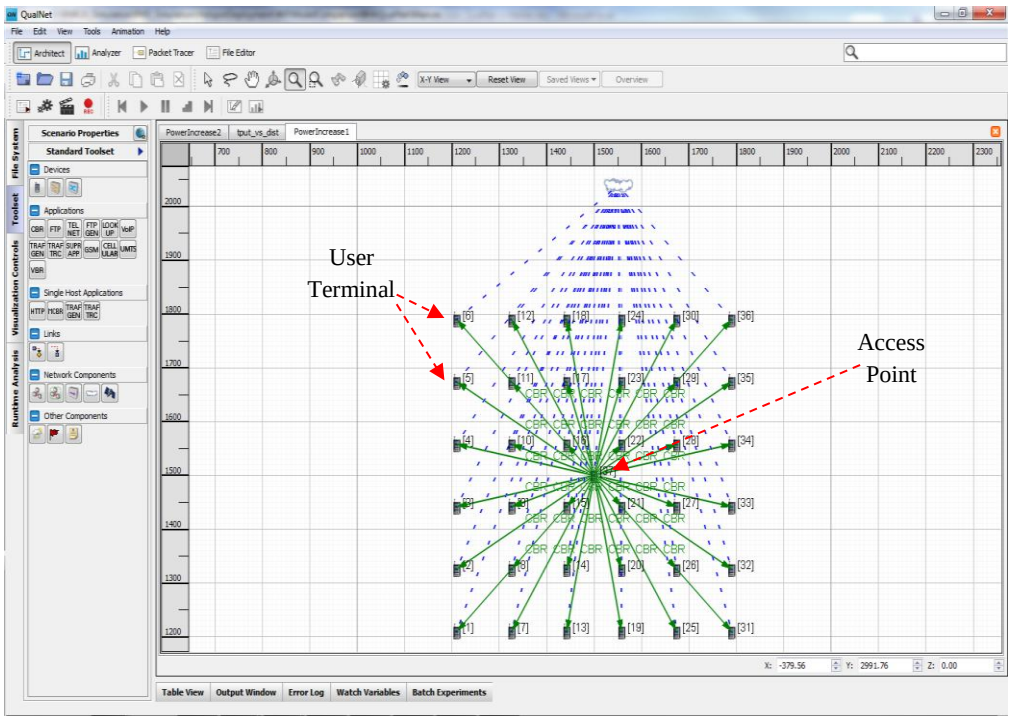

Figure 4.7: Snapshot for QualNet simulation with 36 clients and one AP.

Average Throughput as a Function of the Number of Users

The simulation was carried out at a EIRP of 20 dBm and varying the number of users from 16, 25 and 36. Figure 4.8 shows that the Matlab simulation result is very close to the result generated by QualNet; the differences are 0.06 Mbps, 0.02 Mbps and 0.004 Mbps for 16, 25 and 36 users respectively.

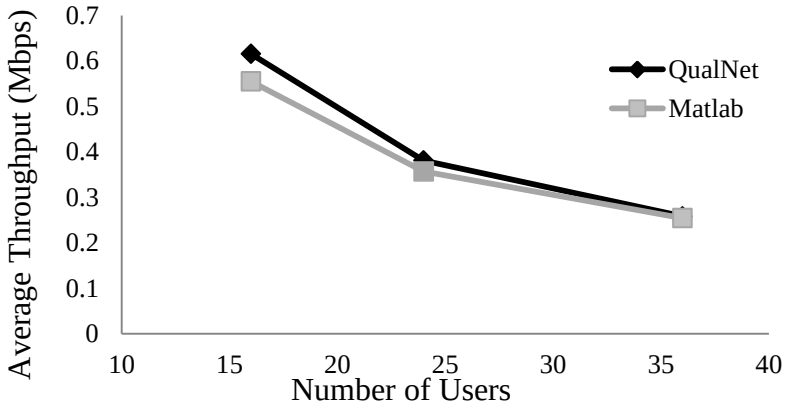

Figure 4.8: Average capacity as a function of the number of users per AP cell for the two simulators.

Figure 4.9 plots the differences (in percentages) between Matlab and QualNet results, showing that as the number of users increases the difference becomes smaller. This behaviour can be explained by referring to the throughput as a function of distance characteristic as shown in

Figure 4.6 where the difference between the two models is larger at the edge of the cell. In the 16-user-scenario, 12 out of 16 users (75%) are located at the edge of the cell, while for the 36-user-scenario only around half of the users (55%) are located at the edge of the cell. Therefore, in the Matlab model when there are a higher

percentage of users are placed closer to the AP, the results are closer to that of QualNet.

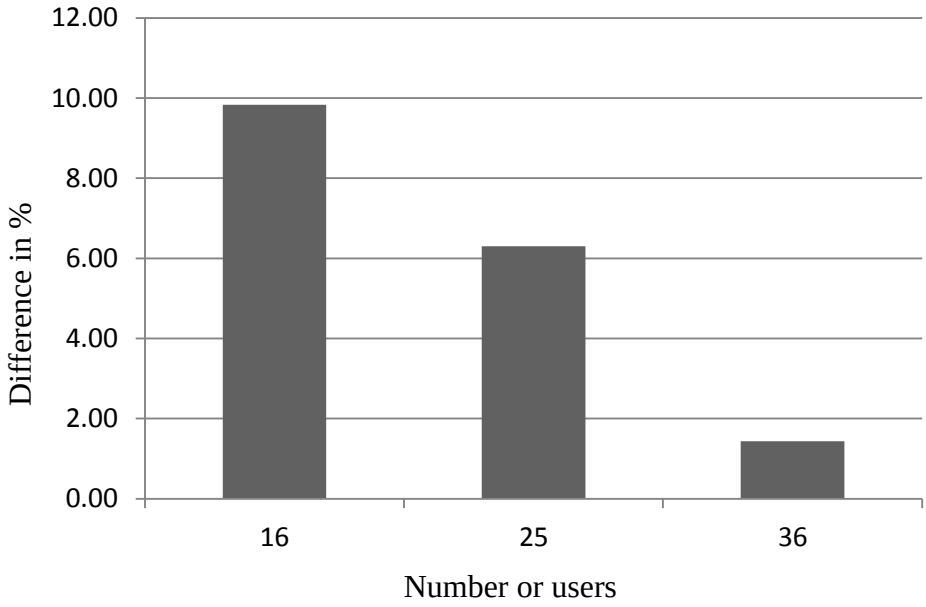

Figure 4.9: Difference in percentage between QualNet and Matlab simulation results.

Average Throughput as a Function of EIRP and Number of Users

This simulation was carried out as a function of increasing AP EIRP - from 20 dBm, 23 dBm, 26 dBm, 29 dBm to 30 dBm - with fixed user locations. Three sets of simulation with 16, 25 and 36 users respectively are executed.

Figure 4.10 shows the average user throughput over the range of EIRP; results show that the Matlab model outputs are very comparable to that of QualNet. Detailed results data for the simulations are presented in Table 4.7, Table 4.8 and Table 4.9.

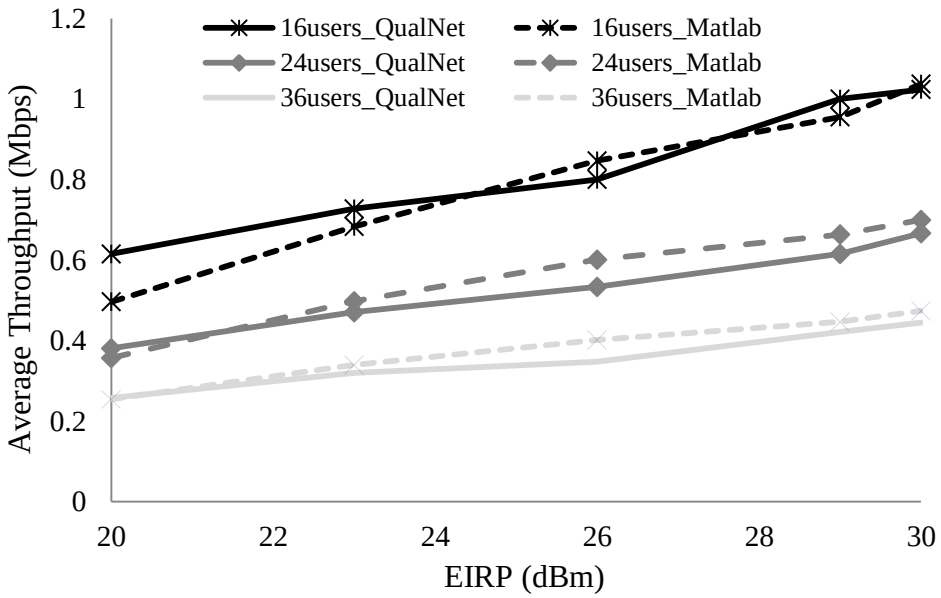

Figure 4.10: Average capacity as a function of EIRP for the two simulators.

Table 4.7: Throughput comparison (16-users scenario).

AP Transmit EIRP (dBm)	Average User Throughput (Mbps)	
	QualNet	Matlab Simulator
20	0.6155	0.4966
23	0.7275	0.6832
26	0.8000	0.8465
29	1.0000	0.9551
30	1.0235	1.0371

Table 4.8: Throughput comparison (24-users scenario).

AP Transmit EIRP (dBm)	Average User Throughput (Mbps)	
	QualNet	Matlab Simulator
20	0.3810	0.3570
23	0.4706	0.4977
26	0.5335	0.6012
29	0.6155	0.6636
30	0.6668	0.6995

Table 4.9: Throughput comparison (36-users scenario).

AP Transmit EIRP (dBm)	Average User Throughput (Mbps)	
	QualNet	Matlab Simulator
20	0.2580	0.2543
23	0.3200	0.3397
26	0.3479	0.4017
29	0.4213	0.4467
30	0.4447	0.4737

4.2.11.4 User Throughput Fairness

In all simulations, equal fairness is achieved for all users connected to the serving AP. Figure 4.11 shows a snapshot of the results generated by QualNet for 36 users. Each user is represented by an index number on the x-axis while the y-axis shows the achievable throughput (bps) of the users. The results show that a good fairness can be achieved amongst all users, in good agreement with the assumption of max-min fairness of Equation (4.22).

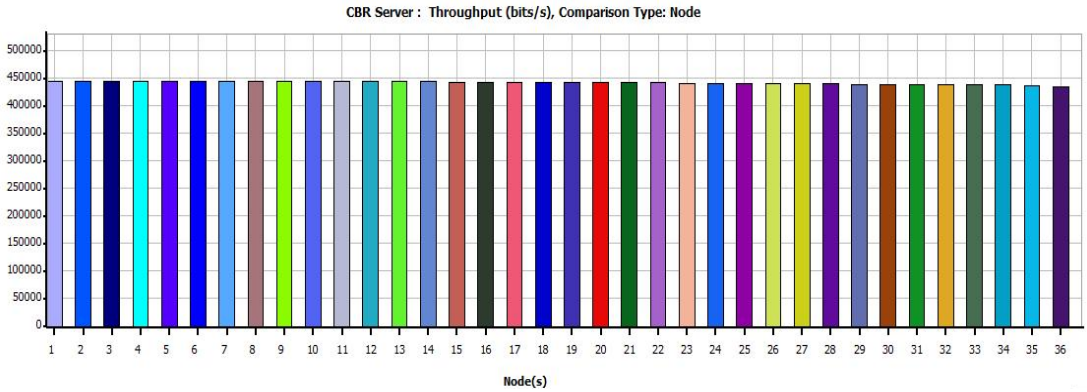

Figure 4.11: Achievable throughput by WiFi users.

4.3 LTE Models

In the HetNet study, LTE is chosen for the macro network providing more extensive coverage than WiFi cells.

4.3.1 LTE Propagation Model

In order to calculate the received power, the ITU recommended LTE Urban Macro (UMa) Non-Line-of-Sight (NLOS) path loss model is used [ITU-R, 2009];

$$\begin{aligned} PL = {} & 161.04 - 7.1log_{10}(W) + 7.5log_{10}(h) \\ & - \left(24.37 - 3.7\left(\frac{h}{h_{BS}}\right)^2\right) log_{10}(h_{BS}) \\ & + \left(43.42 - 3.1log_{10}(h_{BS})\right)(log_{10}(d) - 3) \\ & + 20log_{10}(f_c) \\ & - \left(3.2\left(log_{10}(11.75h_{UT})\right)^2 - 4.97\right) \end{aligned} \tag{4.23}$$

where d is the distance in meters, W is street width in meters, h is average building height in meters, f_c is the centre frequency in Gigahertz, h_{BS} and h_{UT} are the actual antenna heights of BS and user terminal. The simulation parameters are summarised in Table 4.10.

Table 4.10: Parameters for LTE propagation model.

Parameters	Value	Unit
W	20	M
h	20	M
h_{BS}	25	M
h_{UT}	1.5	M
f_c	2.3	GHz

4.3.2 LTE Shadow Fading

As discussed in Section 4.2.2, shadow fading is caused by obstacles such as terrains and buildings in the propagation path between transmitter and receiver which can be interpreted as irregularities to the average path loss obtained from the macroscopic path loss model.

In the model used in the research, a two dimensional Gaussian process with spatial correlation is adopted in order to capture the shadowing effect over two dimensions of the simulated area. The spatial correlation is included to avoid the unrealistic simulation scenarios where spatially close UEs experience uncorrelated shadow fading losses. To introduce the space correlation into the Gaussian process, a low-complexity method which nevertheless still preserves the statistical properties as described in [Claussen, 2005], is used.

Typical LTE shadowing with log-normal distribution of mean 0 dB is approximated by a standard deviation of 6 dB when the Urban Macro (UMa) NLOS path loss model is used [ITU-R, 2009]. Figure 4.12 depicts the resulting space-correlated shadow fading map for the chosen simulation area. Figure 4.13 highlights the LTE received signal considering space correlated shadowing.

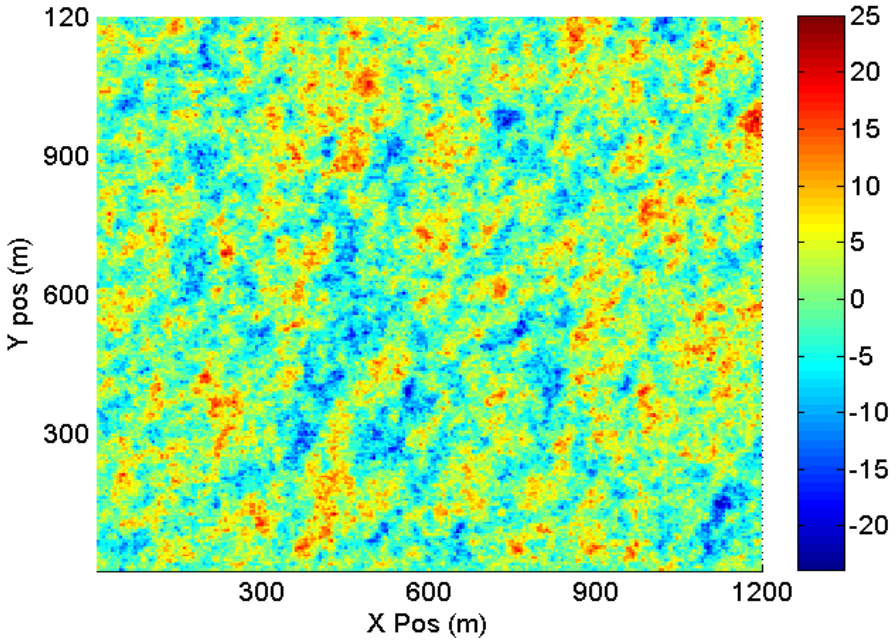

Figure 4.12: Space-correlated shadow fading.

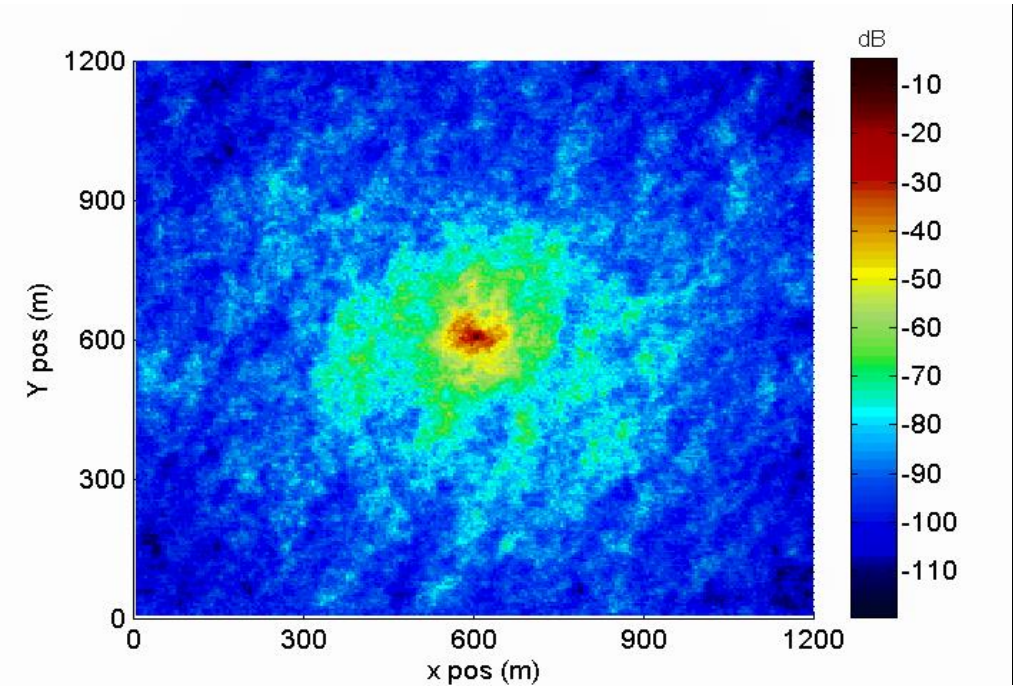

Figure 4.13: LTE received signal considering space-correlated shadowing.

4.3.3 LTE Throughput

Coded data is the combination of data and coding bits. Thus the throughput for a given MCS (Modulation and Coding Scheme) is the product of the symbol rate and the number of data bits per modulation symbol. The net throughput has units of data bits per modulation symbol [Agilent, 2001], commonly normalised to a channel of unity bandwidth, which carries one symbol per second. The units of throughput then become bits per second per Hz.

For a modern communications system with Adaptive Modulations and Coding (AMC) [Sesia et al., 2009] such as LTE, for a MCS to operate at an acceptably low Bit Error Rate (BER) requires a minimum SINR value; higher order MCSs that give higher throughputs need a higher SINR to operate. Therefore with AMC, signals are measured in order to feedback the channel SINR to the transmitter for proper selection of the most suitable MCS to maximise throughput for a particular channel condition. A code set contains many MCSs and is designed to cover a range of SNRs such as the throughput plot [3GPP, 2010a] shown in Figure 4.14. In the simulation, LTE throughput is calculated based on the throughput plot of Figure 4.14 where the SINR ratio at a receiver is used to calculate the achievable throughput.

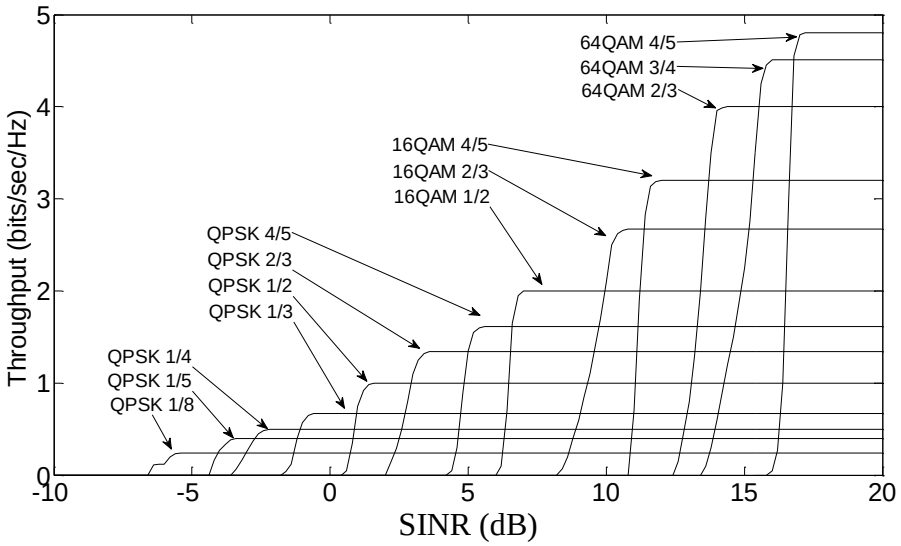

Figure 4.14: LTE throughput as a function of SINR for different Modulation and Coding Schemes (MCS) used in the model.

Equation (4.24) gives the received SINR value from LTE BS:

$$SINR = P_{Rx} - NF - NFl - IM \tag{4.24}$$

where, P_{Rx} is the received signal power and IM is Implementation Margin. From [Sesia et al., 2009], IM ranges from 2.5 dB to 4 dB for different MCS; for simplicity 3 dB is assumed for all MCSs in the simulations. NF (Noise Figure) is the degradation of signal power due to the noise generated in the receiver and a typical NF value for a modern receiver is 8 dB to 10 dB [Takei, 2008]. NFl is the Noise Floor as explained in Section 4.2.5 and P_{Rx} is calculated using;

$$P_{Rx} = P_{Tx} - PL - L_{Int} - L_{Shadow} - FM + G_{Rx} \tag{4.25}$$

where PL is path loss as calculated in Equation (4.23), L_{Int} is the loss due to LTE interference where 3 dB is assumed and L_{Shadow} is the shadowing loss as discussed in

Section 4.3.2. P_{Tx} and G_{Rx} are LTE BS transmit power and receiver antenna gain respectively. FM is the Fade Margin, the safety margin included to account for losses due to multipath fading. Here, a FM of 18 dB is assumed to ensure 99% link availability following [Tranzeo, 2010], based on the Rayleigh fading model.

LTE ideal throughput can be calculated by mapping the SINR value to throughput as in Figure 4.14. However, the spectrum efficiency of LTE is reduced by several factors such as Adjacent Channel Leakage Ratio (ACLR) [Sesia et al., 2009], cyclic prefix and pilot overhead as listed in Table 4.11 [Mogensen et al., 2007]. The ACLR and practical filter implementation restricts the effective bandwidth BW_{Eff} to 90%. The cyclic prefix contributes a ~7% of overhead and reduces the efficiency by a factor of 0.93 (φ_{CP}). With pilot assisted channel estimation, the efficiency is further reduced to a factor (φ_{Pilot}) of 0.94 and 0.89 for single and dual antenna (2x2 MIMO) transmission respectively. At the system level, there is an additional overhead related to common control channels, such as synchronization and broadcast [Mogensen et al., 2007]; such overheads are not considered in the study.

Table 4.11: LTE downlink bandwidth efficiency (10MHz system).

Impairment	**BW Efficiency**
Effective BW, BW_{Eff}	0.90
Cyclic prefix, φ_{CP}	0.93
Pilot overhead, φ_{Pilot}	0.94 (SISO) / 0.89 (2x2 MIMO)
Total	0.79/0.74

In the research, a 20 MHz system is assumed and thus the efficiency will be comparable to those in Table 4.11. The throughput of LTE system is finally calculated using;

$$C_{link}^{LTE} = BW_{Eff} \times \varphi_{Spectrum} \times \varphi_{CP} \times G_{MIMO} \times \varphi_{Pilot} \quad (4.26)$$

where, G_{MIMO} is the MIMO gain factor; a gain factor of two is assumed if 2x2 MIMO is used. The model used for the study (LTE 20 MHz system) is verified in Section 4.3.5, where the throughput is compared to OPNET [OPNET Modeler, 2009] simulation results from [Ghaleb et al., 2013]. Figure 4.15 shows the throughput plot without (Figure 4.15(a)) and with shadowing (Figure 4.15(b)).

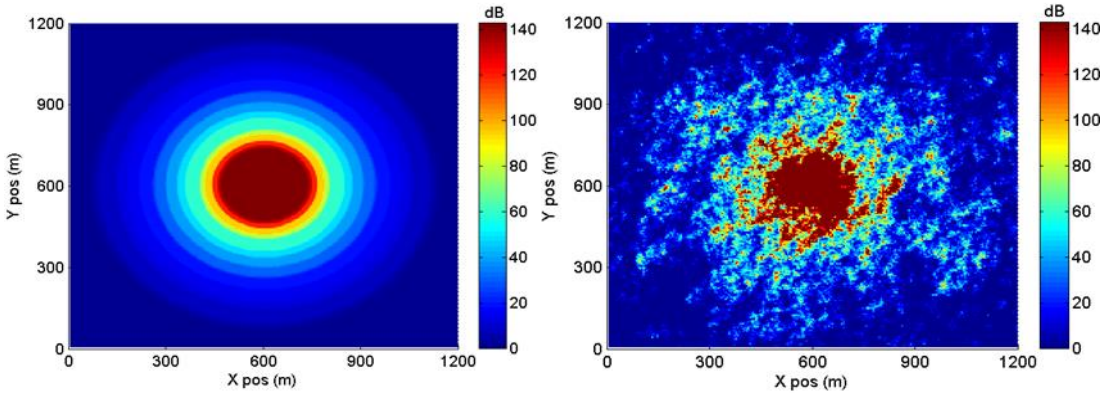

(a) (b)

Figure 4.15: LTE throughput for a 20MHz channel bandwidth and 2x2 MIMO (a) without and (b) with space-coorelated shadow fading.

4.3.4 LTE Cell Max-Min Fairness

In LTE resource is being assigned to users in the form of Physical Resource Blocks (PRB) consisting of many resource elements [Sesia et al., 2009]. Since the objective of the research is to provide fair throughput to all users, the same max-min fair bandwidth resource allocation approach is assumed where in the LTE case, more resource blocks are assigned to users with inferior channels to ensure fairness. This is reasonable, since the scheduler is not fully specified in the standards. In order to simplify the study, the resource element is assumed to be a time fraction and allocation follows a Time Division Multiple Access (TDMA) principle as modelled in [Xue et al., 2012] and the average user throughput is modelled similar to Equation (4.22) as:

$$C_{Av} = \frac{1}{\sum_{u=1}^{U} \frac{1}{T_u}} \tag{4.27}$$

where T_u is the maximum link throughput achievable by LTE user u and U is the total number of LTE users.

General parameters used for LTE modelling (Section 4.3) are summarised in Table 4.12.

Table 4.12: General LTE simulation parameters.

Parameters	Value	Unit
Frequency band, f	2.6	GHz
Channel bandwidth	20	MHz
BS transmit power, P_{Tx}	36	dBm
Tx Antenna Gain, G_{Tx}	8	dBi
Rx Antenna Gain, G_{Rx}	0	dBi
Shadow Fading	6	dB
Fade Margin (fast fading)	18	dB
Bandwidth Efficiency, BW_{Eff}	90	%
Cyclic Prefix Overhead	7	%
Pilot Overhead	7 (SISO) / 11 (2x2MIMO)	%
UE Noise Figure	10	dB
Interference Margin, IM	3	dB
LTE implementation loss	3	dB
2x2 MIMO capacity gain, G_{MIMO}	2	-

4.3.5 LTE Throughput Verification

In 3GPP documentation, LTE eNodeB supports 29 different MCSs with MCS index ranging from 0 to 28 [3GPP, 2012a]. Each MCS is mapped to a transport block size index I_{TBS} ranging from 0 to 26. I_{TBS} together with the number of RBs determine the transport block size, in bits, that can be transmitted within one Transmission Time Interval (TTI); hence the data rate and throughput can be calculated. From the OPNET downlink simulation [Ghaleb et al., 2013], the coding rate for all MCSs operated by the LTE eNodeB are captured in Table 4.13. MCS with the index 0-9 are

modulated using QPSK, index 10-16 with 16QAM and the remainder with 64QAM. The OPNET simulation results which study the maximum throughput that each MCS index can support using 20 MHz error free Channel is presented in Figure 4.16.

Table 4.13: LTE MCS indices and coding rates using OPNET simulator.

MCS Index	**Coding Rate**	**MCS Index**	**Coding Rate**
0	0.167	15	0.583
1	0.200	16	0.633
2	0.233	17	0.422
3	0.267	18	0.489
4	0.333	19	0.500
5	0.400	20	0.556
6	0.467	21	0.600
7	0.533	22	0.644
8	0.600	23	0.711
9	0.667	24	0.756
10	0.333	25	0.800
11	0.350	26	0.844
12	0.417	27	0.889
13	0.483	28	1.000
14	0.517	-	-

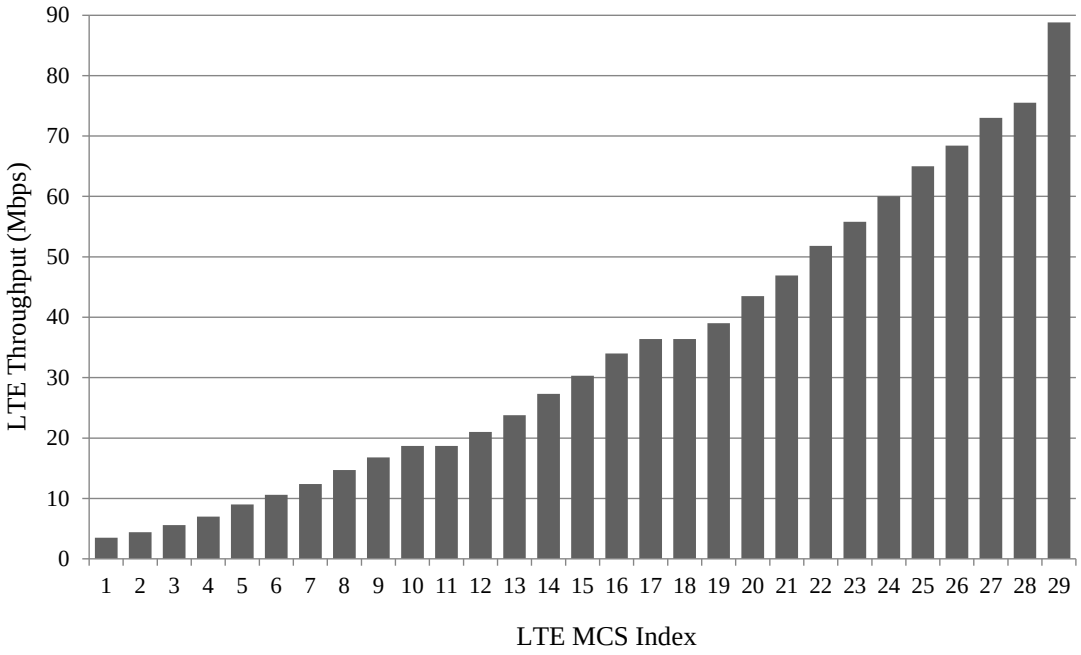

Figure 4.16: LTE throughput as a function of MCS type.

The 3GPP LTE throughput used for the study was obtained by multiplying the 3GPP spectral efficiency plot (Figure 4.14) with a 20 MHz channel. Since only 90% bandwidth efficiency is achievable for 20 MHz LTE and subject to 7% cyclic prefix and 6% pilot overhead, the effective throughput for LTE SISO is plotted in Figure 4.17. The result is compared with OPNET simulation result in Figure 4.16 [Ghaleb et al., 2013], mapped from the minimum SINR (-6.8 dB) to the maximum SINR value (18 dB) and is a good agreement. The only discrepancy relates to the last OPNET MCS value where the simulation result predicts a higher data rate due to the use of un-coded transmission (coding rate of 1). From the comparison, it can be concluded that the 13-MCS-LTE model used in the simulation provides a good representation of the performance of the whole spectrum of MCS types. For 2x2 MIMO, to simplify the simulation study, a throughput gain with a factor of two is applied.

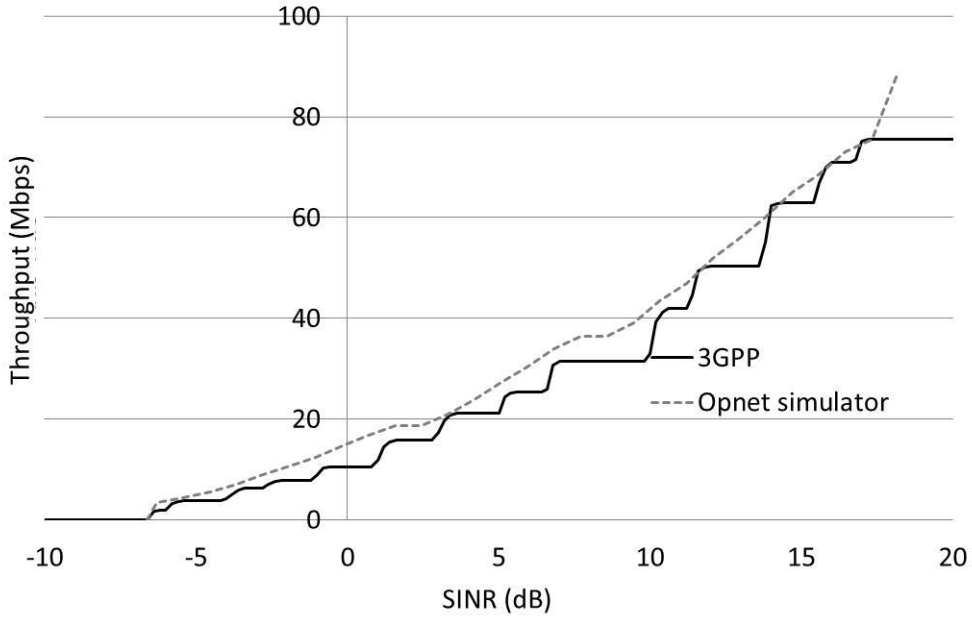

Figure 4.17: LTE throughput comparison between the 3GPP model and OPNET simulation (20MHz SISO).

4.4 Heterogeneous Network Coverage

Using the outputs from the WiFi and LTE models, HetNet coverage is plotted by overlaying WiFi cells on top of the LTE cell. For example, 802.11g and LTE (20 MHz, 2x2 MIMO) coverage based on data rate are plotted in Figure 4.18(a) and Figure 4.18(b) respectively and the combined WiFi and LTE data rates are shown in Figure 4.18(c). In addition to the data rate, the link throughput can also be generated for both WiFi and LTE using a similar approach. With knowledge of the physical data rate, link throughput, network information such as access capacity and backhaul capacity (to be discussed in detail in Chapter 5 and Chapter 6), decisions can be made to select the best network to connect to.

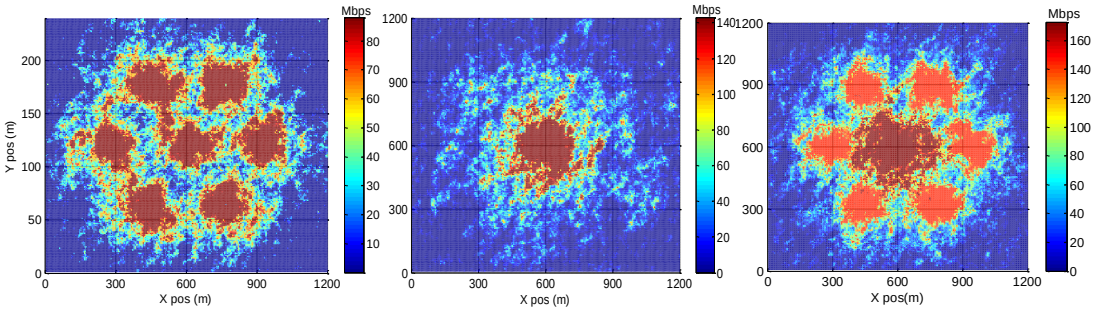

(a) (b) (c)

Figure 4.18: Network coverage based on data rate with X-axis and Y-axis showing coverage size in meters; a) 7-WiFi-Nodes (802.11n), b) LTE network and c) HetNet (LTE+WiFi).

4.5 Conclusions

WiFi and LTE propagation models, physical and MAC models as well as network models used to simulate the HetNet have been detailed. The calculation of throughput for WiFi users is formulated and validation using the QualNet simulator shows that the model is a close match. The LTE throughput model has also been verified with results obtained from the OPNET modeller. The combination of WiFi and LTE models that form a Wireless Heterogeneous Network has been demonstrated and operation validated.

In short, the models and verification exercises show that an accurate and credible model has been established for the research.

Chapter 5

Dynamic Backhaul Capacity Sensitive Network Selection Scheme in Hotspot Wireless HetNet (DyBaCS)

5.1 Introduction

The Chapter introduces a Network Selection Scheme (NSS) - the Dynamic Backhaul Capacity Sensitive (DyBaCS) Scheme - for Hotspot Wireless HetNets (HWHs). The performance of DyBaCS is compared to two other well-known NSSs. The detail of the simulation methodology, simulation parameters and assumptions are presented. Finally, simulation results are discussed before conclusions are drawn.

5.2 Background

The increasing pressure for mobile operators to offload data traffic from their 3G, LTE or WiMAX networks to small cell networks [Aviat Networks, 2011] [Informa telecoms, 2013] indicates that future mobile broadband networks will largely be heterogeneous. This migration is further fuelled by the availability of multi-RAT (Radio Access Technologies) which allow user devices to connect to different wireless networks such as 3G, LTE, WiMAX, WiFi either one at a time or simultaneously. Deployment of small cells such as WiFi raises new challenges for

operators especially on backhauling. There are only two choices as far as backhaul is concerned viz. wireline and wireless backhaul. Due to the intensive engineering work required, high cost and regulatory barriers, fixed line solutions such as fibre, cable, copper or xDSL are not readily available. Further, a relatively large number of WiFi hotspots may prove too costly for operators to backhaul with wired options. In such situations, the operator will increasingly rely on point-to-point and point-to-multipoint wireless solutions. In most scenarios, a mixture of backhaul technologies is expected, as operators will adopt the most suitable solution for small cells considering cost and availability [Infonetics Research, 2013].

Indeed, currently, WiFi APs are typically backhauled through different types of technologies which offer throughputs ranging from several to tens of megabits per second [Priscaro, 2013]. However, backhauling using different technologies within the HWH creates a non-uniform AP capacity distribution. Since the most widely deployed IEEE802.11n WiFi technology provisions a peak physical data rate of 600 Mbps, most existing fixed backhaul services are not able to offer sufficient capacity for these WiFi APs to realise their full throughput [Ericsson, 2013]. Therefore consideration of WiFi backhaul capacity is inevitable during traffic offload decision making. Thus a new network selection strategy which considers small cell backhaul capacity is proposed to ensure that users enjoy the best possible usage experience especially in terms of connection throughput and fairness.

5.3 Contributions

With the implementation of the spatial wireless model at the physical layer and HWH architectures, a new NSS referred to as DyBaCS is developed to manage the non-uniform backhaul capacity distribution in HWHs and hence ensure a consistently fair network bandwidth distribution whilst maintaining network throughput. DyBaCS takes into consideration network information such as effective backhaul capacity, network load and access link capacity from both Macro BS and Small Cells in making a decision.

The study compares the performance of two common NSSs viz. WiFi First (WF) [A. Handa, 2009] [Ericsson, 2013] and Physical Data Rate (PDR) [Raiciu et al., 2011] [Nie et al., 2005] [Jackson Juliet Roy et al., 2006] with DyBaCS in LTE-WiFi HetNet environments. The downlink performance of the HetNet is evaluated in terms of average user throughput and bandwidth sharing fairness amongst users. The effects of varying WiFi backhaul capacity (uniform and non-uniform distribution), WiFi-LTE coverage ratio, user density and WiFi APs density within the HetNet form the focus of the evaluation.

Results show that the DyBaCS provides superior fairness and user throughput performance across the range of backhaul capacities considered. Furthermore DyBaCS is able to scale much better than WF and PDR across different user and WiFi densities.

5.4 Existing and Proposed Network Selection Schemes (NSSs)

In a heterogeneous wireless network comprising two or more technologies, user throughput fairness needs to be considered in two aspects; intra-network and inter-network fairness. Intra-network fairness can be provided by an AP or LTE BS to its associated users as the task is confined locally. Such fairness is achievable amongst users under the same AP or BS using max-min fair capacity sharing for the WiFi and LTE network (Equation (4.22) and Equation (4.27)). However, fair capacity sharing across the entire HetNet is not guaranteed and is strongly dependent on user distribution and the implemented NSS.

5.4.1 WiFi First (WF)

In HetNets, WF connects a user to an AP whenever WiFi coverage is available; in other words, a user will never connect to a LTE network when there is WiFi coverage. This approach is generally adopted by current mobile operators [Choi et al., 2011] [A. Handa, 2009].

5.4.2 Physical Data Rate (PDR)

The selection criterion of PDR is purely governed by the physical data rate of the RAT available to the user [Nie et al., 2005] [Jackson Juliet Roy et al., 2006] i.e. the physical data rate of LTE and WiFi in multi-rate operation is compared and the RAT with higher physical data rate is chosen. The algorithm is a modification of a NSS

based on Received Signal Strength Indication (RSSI) where higher received signal strength is likely to provide a higher physical data rate. However, WiFi and LTE are two different systems with different physical layer capabilities, thus a pure RSSI comparison is not sufficiently accurate. The implication is that the user device is assumed to perform the selection based on the physical data rate supported by the WiFi and LTE networks.

5.4.3 Dynamic Backhaul Capacity Sensitive (DyBaCS) Algorithm

A single LTE network is assumed with I ($I \geq 1$) denoting the total number of WiFi APs in the HWH and i denoting the index of the network, i.e. network $i = 1 \leq i \leq I$ is the i-th WiFi network, while, $u = 1 \leq u \leq U$ represents the u-th user in the HetNet.

Before explaining the DyBaCS algorithm in detail, Algorithm 5.1 is presented first; the User Throughput Estimation Flow (UTEF) algorithm which enables the estimation of WiFi user throughputs $C_{eff,u}^{i}$ and LTE user throughputs $C_{eff,u}^{LTE}$.

Algorithm 5.1: Users Throughput Estimation Flow (UTEF)

---

a) WiFi UTEF:

1) *Let* $u = \{1,2,\ldots,U^i\}$ *is number of WiFi users in Network i*

2) *Average user throughput is :* $C_{Av}^{i} = \frac{1}{\sum_{u=1}^{U^i} \frac{1}{R_u^i \times \varphi_u}}$; *Equation (4.22)*

3) *System throughput for network i is:* $C_{sys}^{i} = C_{Av}^{i} \times U^i$

4) *For* $u = 1\ to\ U^i$

A) *If* $C_{bh}^i \geq C_{sys}^i$

i) $C_{eff,u}^i = \min\left(C_{Av}^i \times OF\ ,\ C_{link,u}^i\right)$

B) *Elseif* $C_{bh}^i < C_{sys}^i$

i) $C_{Av,ltd}^i = C_{bh}^i / U^i$

ii) *if* $C_{Av,ltd}^i \times OF \leq C_{link,u}^i$

a) $C_{eff,u}^i = \min\left(C_{Av,ltd}^i \times OF\ ,\ C_{bh}^i\right)$

iii) *If* $C_{Av,ltd}^i \times OF > C_{link,u}^i$

a) $C_{eff,u}^i = \min\left(C_{link,u}^i\ ,\ C_{bh}^i\right)$

b) LTE UTEF:

1) *Let* $u = \{1,2,\ldots,U^{LTE}\}$ *is number of users in LTE Network*

2) *Average user throughput is :* $C_{Av}^{LTE} = \frac{1}{\sum_{u=1}^{U^{LTE}} \frac{1}{T_u}}$ *; Equation (4.27)*

3) *Average user throughput considering OF is:*

a) $C_{eff,u}^{LTE} = \begin{cases} C_{Av} \times OF : C_{Av} \times OF \geq C_{link,u}^{LTE} \\ C_{link,u}^{LTE} \quad : C_{Av} \times OF < C_{link,u}^{LTE} \end{cases}$

For WiFi UTEF (Algorithm 5.1), the calculation of effective WiFi user throughput $C_{eff,u}^i$ is based on user access link throughput $C_{link,u}^i$, AP backhaul capacity C_{bh}^i and Overbooking Factor (OF). Link throughput $C_{link,u}^i$ (or equivalent to $R_u^i \times \varphi_u$ in Equation (4.22)) of user u is predominately affected by the distance from the AP, channel quality and other channel conditions such as interference. Backhaul capacity

C_{bh}^{i} is defined as the actual available backhaul capacity to APi. Effective user throughput is limited by both factors.

The calculation of effective user throughput can be explained in detail with the aid of the scenario shown in Figure 5.1, where 4 users are connected to APi. User data rate R_u^i and link throughput $C_{link,u}^{i}$ are listed in Table 5.1.

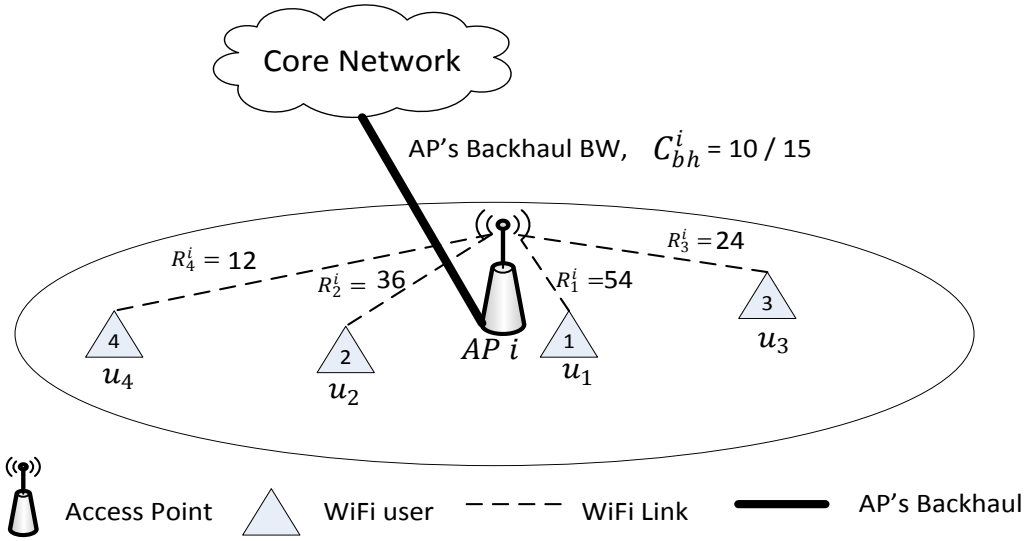

Figure 5.1: AP with 4 users under its coverage

Table 5.1: User data rate and link throughput in Figure 5.1.

User, u	$\boldsymbol{R_u^i}$	$\boldsymbol{C_{link,u}^{i} = R_u^i \times \varphi_u}$
1	54	$54 \times 0.32 = 17.28$
2	36	$36 \times 0.41 = 14.76$
3	24	$24 \times 0.49 = 11.76$
4	12	$12 \times 0.70 = 8.40$

Step 1 and Step 2 in Algorithm 5.1 estimate the average WiFi user throughput by considering access link speed only. As in Equation (4.22), when all users in APi are attempting to access the channel simultaneously, the average user throughput can be calculated as:

$$C_{Av}^{i} = \frac{1}{\sum_{u=1}^{U^i} \frac{1}{R_u^i \times \varphi_u}} = \frac{1}{\frac{1}{R_1^i \times \varphi_1} + \frac{1}{R_2^i \times \varphi_2} + \frac{1}{R_3^i \times \varphi_3} + \frac{1}{R_4^i \times \varphi_4}}$$

$$= \frac{1}{\frac{1}{54 \times 0.32} + \frac{1}{36 \times 0.41} + \frac{1}{24 \times 0.49} + \frac{1}{12 \times 0.61}} = 2.88 \text{ M} \qquad (5.1)$$

Multiplying the average user throughput C_{Av}^{i} by the total number of users under APi, as in Step 3, yields the total system throughput C_{sys}^{i} of APi:

$$C_{sys}^{i} = C_{Av}^{i} \times U^{i} \qquad (5.2)$$

where U^{i} is the number of users connected to the WiFi APi.

In the scenario, $C_{sys}^{i} = 2.88 \times 4 = 11.52$ Mbps. As in Equation (4.22), C_{sys}^{i} is affected by link speed R_u of all users in network i; therefore it is a dynamic value depending on the distribution of users. C_{sys}^{i} also represents the required backhaul capacity for AP i to realise its full access capacity. If the backhaul capacity is sufficient to support the maximum capacity from the AP to clients such that $C_{bh}^{i} \geq C_{sys}^{i}$, then all users enjoy a throughput of C_{Av}^{i}. However, if the backhaul capacity is insufficient, $C_{bh}^{i} \leq C_{sys}^{i}$, then the backhaul capacity C_{bh}^{i} is the limiting factor. The available backhaul capacity C_{bh}^{i} is shared evenly to all users U^{i} and average user throughput in such scenario is limited to a value $C_{Av,ltd}^{i}$ (Equation (5.3)) which is less than C_{Av}^{i}.

$$C_{Av,ltd}^{i} = \frac{C_{bh}^{i}}{U^{i}} \tag{5.3}$$

It is important to note that users will not secure a throughput higher than C_{Av}^{i} even at backhaul capacities greater than C_{sys}^{i} due to the restriction imposed by the WiFi physical and MAC layer capability. Under simultaneous channel access, C_{Av}^{i} or $C_{Av,ltd}^{i}$ is the average user throughput for sufficient and limited backhaul capacity respectively.

In Figure 5.1, assuming that backhaul capacity C_{bh}^{i}= 10 is less than $C_{sys}^{i} = 11.52$, the actual average throughput for the users is limited to $C_{Av,ltd}^{i} = \frac{C_{bh}^{i}}{U^{i}} = \frac{10}{4} = 2.5$ Mbps. Otherwise, each user will enjoy $C_{Av}^{i} = 2.88$ Mbps if $C_{bh}^{i} \geq C_{sys}^{i}$.

In practice, OF is normally considered as not all users access the channel at the same time [Tranzeo, 2007]; by including OF the perceived throughput from the users point of view can be calculated. Considering OF, the calculation of the effective average throughput $C_{eff,u}^{i}$ is not as straightforward as $C_{Av}^{i} \times OF$ or $C_{Av,ltd}^{i} \times OF$ for sufficient and limited backhaul capacity scenarios.

In order to simplify the explaination of Algorithm 5.1 an OF = 5 is adpoted. Taking the example that C_{bh}^{i}= 15 Mbps where $C_{bh}^{i} \geq C_{sys}^{i}$, the effective average throughput $C_{eff,u}^{i}$ of user u is limited by its link throughput $C_{link,u}^{i}$, Step 4A (i) places a constraint to ensure that the value of $C_{Av}^{i} \times OF$ does not exceed $C_{link,u}^{i}$. Table 5.2 shows that effective user throughput $C_{eff,u}^{i}$ is the minimum value between $C_{Av}^{i} \times OF$

and $C^i_{link,u}$. The effective average throughput for user 3 and user 4 is limited to their link throughput which is 11.76 Mbps and 7.32 Mbps respectively.

Table 5.2: Effective user theroughput $C^i_{eff,u}$ under condition $C^i_{bh} \geq C^i_{sys}$.

User, u	C^i_{Av}	$C^i_{link,u}$	C^i_{bh}	$C^i_{Av} \times OF$	$C^i_{eff,u}$
1	2.88	17.28	15	14.40	14.40
2	2.88	14.76	15	14.40	14.40
3	2.88	11.76	15	14.40	11.76
4	2.88	7.32	15	14.40	7.32

Similarly, with limited backhaul capacity, Step 4B (ii) and Step 4B (iii) ensure that $C^i_{Av,ltd} \times OF$ is bound by both $C^i_{link,u}$ and C^i_{bh}, whichever is smaller. The result is shown in Table 5.3.

Table 5.3: Effective user throughput $C^i_{eff,u}$ under condition $C^i_{bh} \leq C^i_{sys}$.

User, u	C^i_{Av}	$C^i_{link,u}$	C^i_{bh}	$C^i_{Av} \times OF$	$C^i_{eff,u}$
1	2.88	17.28	10	12.5	10
2	2.88	14.76	10	12.5	10
3	2.88	11.76	10	12.5	10
4	2.88	7.32	10	12.5	7.32

In short, Step 4 imposes logical considerations to the determination of the effective user average throughput $C^i_{eff,u}$ taking into consideration backhaul capacity, user link speed and OF.

Similarly, the LTE user throughput can also be estimated following the LTE UTEF. LTE backhaul capacity is always assumed to be sufficient; therefore in Step 3, the

only constraint for user throughput on the LTE network is access link throughput $C_{link,u}^{LTE}$.

It is important to note that the estimation of effective user throughput for both WiFi and LTE relies on Equation (4.22) and Equation (4.27). Both equations give a high level throughput estimation assuming the network is fully occupied and users always send traffic to the AP or BS. Hence all users are assumed to be active. However, there is a possibility that an user joins the network offering very little traffic, resulting in an inaccurate estimation of effective user throughput and thus suboptimal decision making. To take care of such a scenario, although a more complex user throughput estimation algorithm or method can be used, the main principles of DyBaCS remain.

The DyBaCS NSS (Algorithm 5.2) initiates by assuming no user is connected to the HetNet; users are admitted to the HetNet one by one and their servicing network is determined by the NSS.

Algorithm 5.2: DyBaCS

---

1) *Initialization*

   a) $\Omega = \emptyset,\ and\ A = \{1,2,\dots,U\}$

   b) $U^i = \emptyset,\ \forall\, i = \{1,2,\dots,I\};\ U^{LTE} = \emptyset$

2) *For* $u = 1$ *to* U

   a) $\Omega_u \leftarrow max\big(\beta_u^i \times C_{link,u}^i\ ,\ C_{link,u}^{LTE}\ \big), \forall\, i = \{1 \dots, I\}$

   End For

3) *For* $u = 1$ *to* U

a) *If user* u *satisfying* $\beta_u^i = 0, \forall i = \{1, 2, \dots I\}$

i. $\alpha_u^{LTE} = 1$

ii. $A = A - \{u\}$

End If

End For

4) *while* $A \neq \emptyset$

a) *find a user* n *where* $|\Omega_n| \geq |\Omega_u|$ *for all* $u \in A$ *and*

b) *Estimate user* n *throughput* $C_{eff,n}^i$ *in i-th WiFi Network assuming user n is included to the network, i.e.* $U^i \cup \{n\}$*; Using WiFi UTEF (Algorithm 5.1a).*

i. $C_n^i \leftarrow C_{eff,n}^i$

c) *Estimate user* n *throughput* $C_{eff,n}^{LTE}$ *in LTE Network assuming user n is included to LTE Network, i.e.* $U^{LTE} \cup \{n\}$*; Using LTE UTEF (Algorithm 5.1b).*

i. $C_n^{LTE} \leftarrow C_{eff,n}^{LTE}$

d) *If* $C_n^{LTE} \geq C_n^i$

i. $\alpha_n^{LTE} = 1$

ii. $U^{LTE} = U^{LTE} \cup \{n\}$

Else

iii. $\alpha_n^i = 1$

iv. $U^i = U^i \cup \{n\}$

End If

e) $A = A - \{n\}$

End while

Step1 initialises variables Ω, A, U^i and U^{LTE}, where Ω is the list of higher speed connections between WiFi and LTE interfaces for all users, A is the set containing all users in the HetNet, U^i is the list of users connected to the WiFi APi and U^{LTE} is the list of users connected to the LTE network.

In Step 2, the link with the highest throughput between user u to LTE ($C^{LTE}_{link,u}$) or WiFi ($C^{i}_{link,u}$) is chosen and placed into Ω, Ω_u representing the throughput value for user u. All users are able to connect to at least the LTE network while access to WiFi depends on availability of WiFi coverage. Hence $\beta^i_u = \{0,1\}$ denotes the connectivity of user u to APi , $\beta^i_u =$ '1' means connection is possible, '0' means the opposite. Since multi-homing is not considered, every user is only allowed to connect to one network at a time. Step 3 assigns all users with no WiFi access to the LTE network and excludes those users from set A. The network selection parameter $\alpha^i_u \in \{0,1\}$ indicates the choice of user u; $\alpha^i_u =$ '1' indicates that user u is connected to network i and value '0' means the opposite.

The remaining users within set A which have not been assigned to any network are addressed in Step 4. Step 4 (a) ensures the user with the highest link throughput is considered first; referred to as user n.

In Step 4 (b) and Step 4 (c) the achievable throughput of user n on WiFi AP i and LTE is estimated using WiFi UTEF and LTE UTEF and represented by $C_{eff,n}^{i}$ and $C_{eff,n}^{LTE}$ respectively. The estimation is executed assuming that user n is added to the corresponding WiFi or LTE network such that the total number of users connected to AP i is user n plus the total number of existing users U^i written as $U^i \cup \{n\}$ and similarly the total number of users in the LTE network is $U^{LTE} \cup \{n\}$. The achievable throughput for user n on the WiFi and LTE network is then assigned to a variable C_n^i and C_n^{LTE}.

Step 4 (d) assigns the user to the network that offers the highest throughput and the corresponding α_n^{LTE} or α_n^i value is set accordingly. The total number of users connected to their respective i-th WiFi network U^i or LTE network U^{LTE} is then updated.

Finally set A is updated by excluding user n in Step 4(f) and the Step 4 processes are repeated until all users are serviced.

5.5 Parameters, Assumptions and Simulation Methodology

5.5.1 Stochastic User Placement Model

A stochastic node location model is used to generate user locations; [Petrova et al., 2007] found that this approach is an acceptable representation of user locations

around a WiFi AP in a city or urban environment. Here users are assumed to be distributed around cluster centres. Two spatial distributions models are adopted; the first is used to generate the number and locations of the cluster centres whilst the second is used for tabulating the number of users around each centre. The initial cluster centre distribution is generated randomly with the total number of cluster centres equal to λ. Subsequently a bivariate Gaussian distribution with covariance matrix $\sum = \mathrm{diag}(\sigma_x^2, \sigma_y^2)$ [Härdle and Simar, 2007] is used to generate actual user locations around the cluster centres. The size and shape of a cluster is characterised by parameters σ_x and σ_y (Figure 5.2). The number of users per cluster follows a Poisson distribution with intensity μ. Parameters σ_x, σ_y and μ are the same for every cluster.

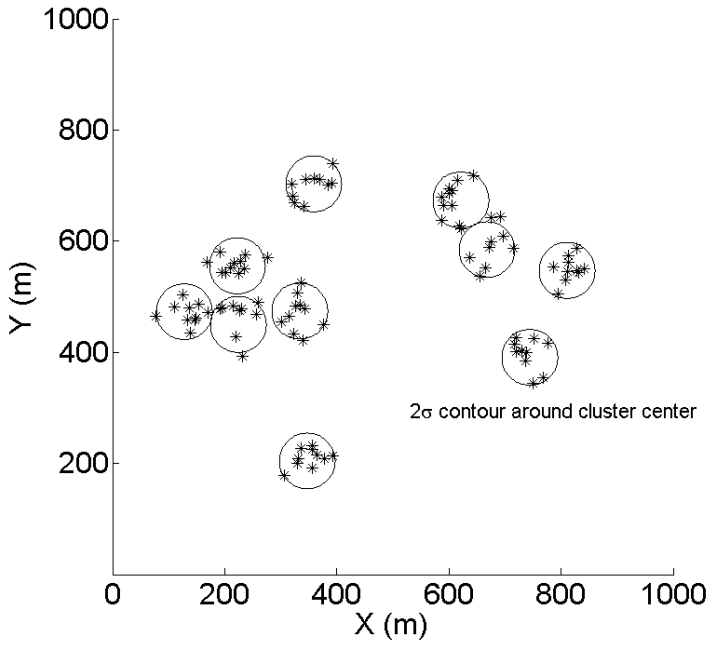

Figure 5.2: User placement within a total number of clusters $\lambda = 10$, cluster size $\mu = 10$ and $\boldsymbol{\sigma_x} = \boldsymbol{\sigma_y} = 25$.

In the simulation, 100 users are placed initially in 1 square kilometre area comprising a number of clusters λ = 10, cluster size μ = 10 and $\sigma_x = \sigma_y$ = 25. Subsequently 50 users are added each time by increasing the number of clusters λ by five whilst keeping the number of users per cluster μ and cluster size σ unchanged, until the total number of users reaches 250 (Figure 5.3). Since all users are distributed within an area of one square kilometre, the terms "number of users" and "user density" are used interchangeably in the rest of the evaluation.

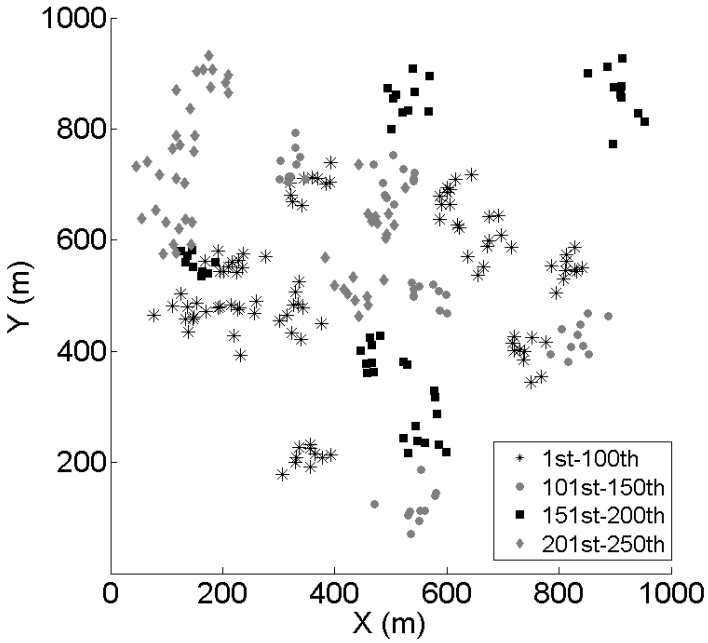

Figure 5.3: User placement ranging from 100 users to 250 users with 50 users added every time; maximum λ = 25, cluster size μ = 10 and $\sigma_x = \sigma_y = 25$.

5.5.2 Placement of WiFi Access Points (APs)

WiFi APs are placed within a LTE cell in three selected topologies shown in Figure 5.4, designs for the blanket-like deployment in round or hexagonal cells.

Figure 5.4(a) shows the topology with 4 APs; Figure 5.4(b) and Figure 5.4(c) showing hexagonal cell layouts with 7 and 13 APs respectively, adopted in a typical cellular network. These WiFi topologies are the basis for the evaluation of performance of the algorithm as a function of WiFi-LTE node ratios (or WiFi node densities). Such topologies are chosen to simplify the study but nevertheless represent meaningful building blocks that form more extensive networks as reported in [David Chieng et al., 2011].

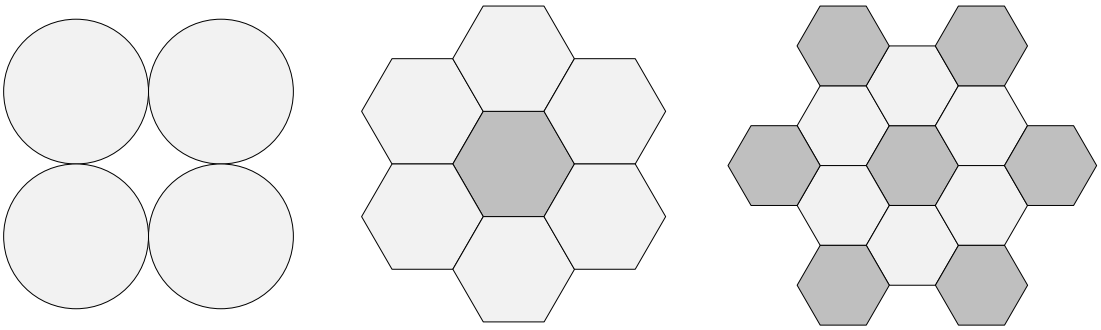

(a) (b) (c)

Figure 5.4: WiFi APs placement within HetNet that comprises the scenarios with 4, 7 and 13 WiFi APs.

By controlling the APs' transmit power, these WiFi topologies are engineered to provide the same coverage as the Macro LTE cell. For example Figure 5.5(a) shows the coverage plot for 4 APs, while the overlay of both WiFi and LTE cell (Figure 5.5 (b)) that forms the HetNet is illustrated in Figure 5.5(c). WiFi coverage plots for 7 and 13 APs are shown in Figure 5.6(a) and Figure 5.6(b) respectively. Although there are no limits on the topologies that can be evaluated, the selected scenarios provide a valuable insight on the relative performance of the NSSs under study.

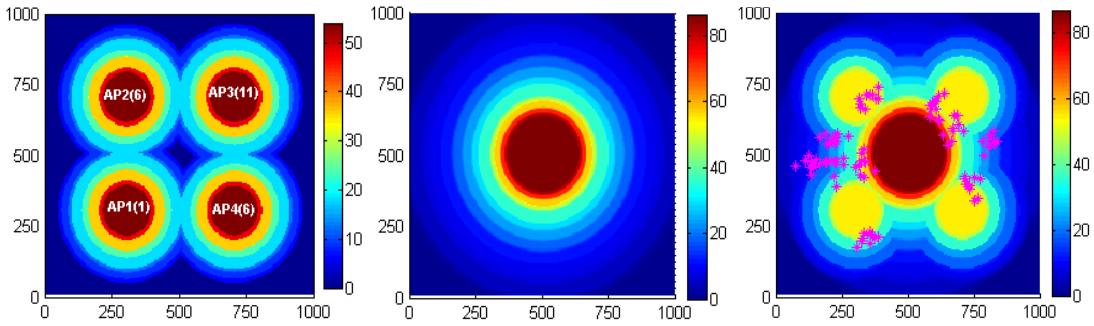

(a) (b) (c)

Figure 5.5: Network coverage based on data rate with x-axis and y-axis showing coverage size in meters; (a) 4-WiFi-Nodes networks with the access channel shown in parentheses, (b) LTE network and (c) HetNet (LTE+WiFi) for a 100 users scenario.

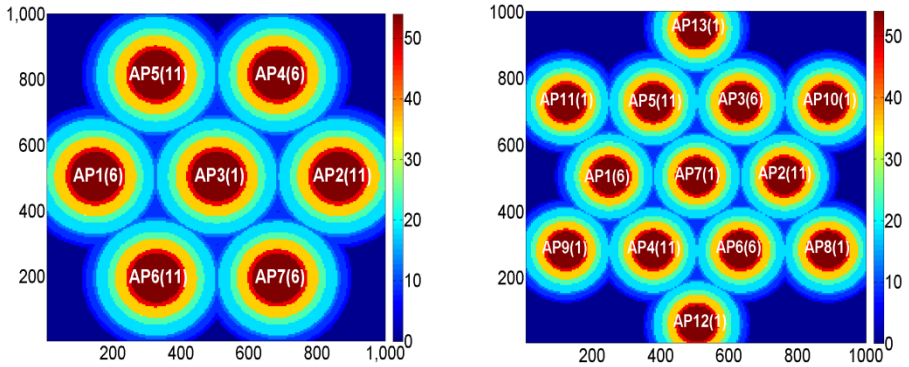

(a) (b)

Figure 5.6: WiFi coverage based on data rate with x-axis and y-axis showing coverage size in meters; (a) 7-WiFi-Nodes networks, (b) 13-WiFi-Nodes networks. The WiFi access channel is shown in parentheses.

5.5.3 WiFi and LTE Backhaul

Two backhaul scenarios are assumed when evaluating the NSSs; 1) uniform and 2) non-uniform WiFi backhaul capacity throughout the HetNet. In the uniform capacity scenario, backhaul capacity is varied from 1 Mbps up to 25 Mbps until the

throughput of the APs saturate. In the case of the non-uniform capacity scenario, backhaul capacity values are randomly chosen as in Table 5.5. The LTE base station (BS) backhaul capacity is always assumed to be sufficient.

5.5.4 Parameters and Assumptions

Table 5.4 summarises the simulation parameters; only the downlink performance is investigated. 2.6 GHz is used for the LTE network, the frequency band allocated in Malaysia. Traffic with fixed packet size of 1000 Bytes at constant bit rate is assumed. From [Tranzeo, 2007], the Overbooking Factor (OF) is a design choice driven by actual user behaviour in the deployed area. OF that varies from 4:1 to 100:1 has been reported by various ISPs and the lower the value, the better the service guarantee [David Chieng et al., 2010]. A factor of 10:1 is adopted to represent relatively heavy usage. User density is varied from 100 to 250 users per square km.

Table 5.4: WiFi and LTE simulation parameters.

	Units	**WiFi Access, 11g**	**LTE**
Frequency band	GHz	2.4	2.6
Channel bandwidth	MHz	20	20
Max EIRP	dBm	27, 24, 18	36
Packet size	Bytes	1000	1000
WiFi backhaul capacity	Mbps	1 – 25	-
LTE backhaul capacity	Mbps	-	Sufficient Capacity Assumed

User Information		
Overbooking Factor, *OF*	-	10:1
User density	Users/sqkm	100, 150, 200, 250

5.6 Results and Analysis

5.6.1 Uniform Backhaul Capacity

Two performance metrics viz. the average user throughput and user throughput fairness in the HetNet cell are used to evaluate the performance of the NSSs. Fairness is derived using Jain fairness index in the form of $\left(\sum_{j=1}^{J} C_{eff,j}\right)^2 / \left(J \sum_{j=1}^{J} \left(C_{eff,j}\right)^2\right)$ [Jain et al., 1999].

Firstly, the performance of all NSSs is evaluated as a function of WiFi backhaul capacity ranging from 1 Mbps to 25 Mbps, with 100% WiFi-LTE coverage overlap and 4 WiFi APs (Figure 5.5(c)). Figure 5.7 shows that the average user throughput of PDR and DyBaCS are similar over the entire range of backhaul capacity and WF provides the lowest average user throughput. The characteristics plateaus when the backhaul capacity reaches 20 Mbps for all NSSs since that is the maximum access throughput achievable by WiFi (IEEE 802.11g). The total WiFi access throughput also depends on user distribution as users with slower bit rates slow down the entire network.

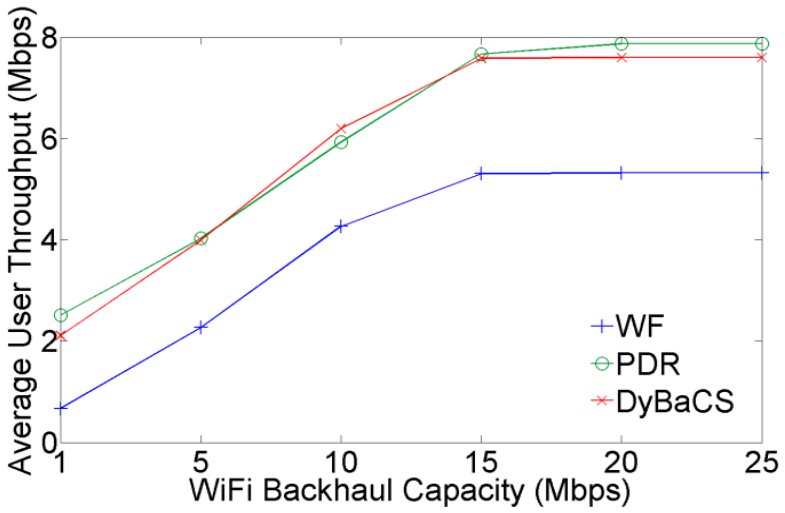

Figure 5.7: HetNet average user throughput as a function of WiFi backhaul capacity (4 WiFi APs, 100% WiFi-LTE overlap, uniform WiFi backhaul capacity).

Figure 5.8 presents an evaluation of the fairness in terms of achievable throughput per user. Results show that the average user throughput of PDR and DyBaCS are similar over the entire range of backhaul capacity while WF provides the lowest average user throughput. DyBaCS outperforms both in terms of fairness with WF exhibiting the worst fairness performance.

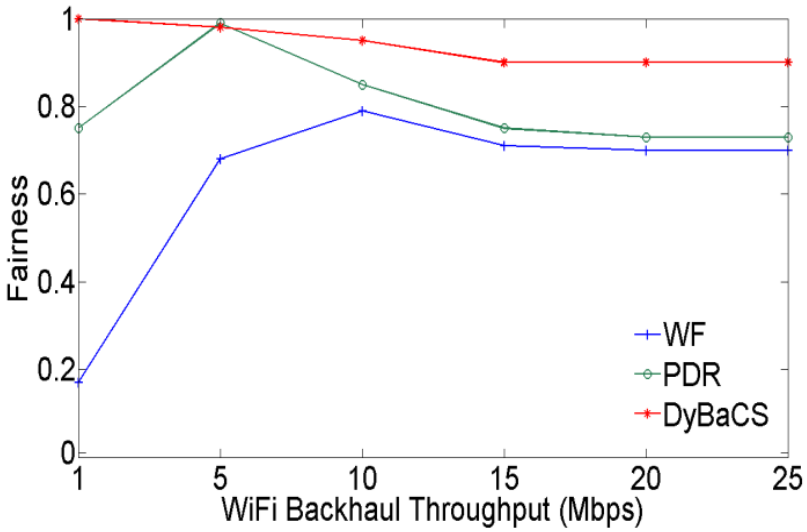

Figure 5.8: Bandwidth sharing fairness as a function of WiFi backhaul capacity (4 WiFi APs, 100% WiFi-LTE overlap, uniform WiFi backhaul capacity).

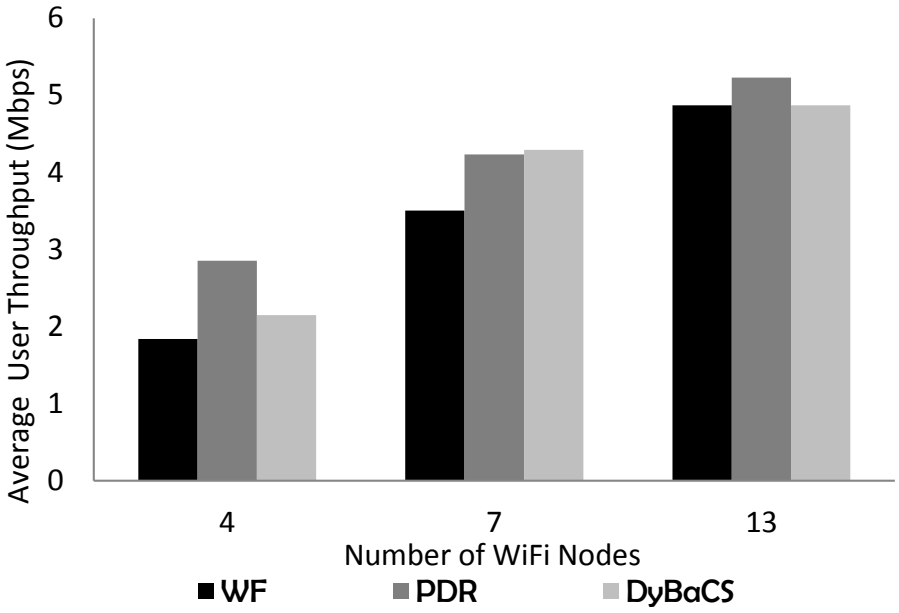

(a) Average User Throughput.

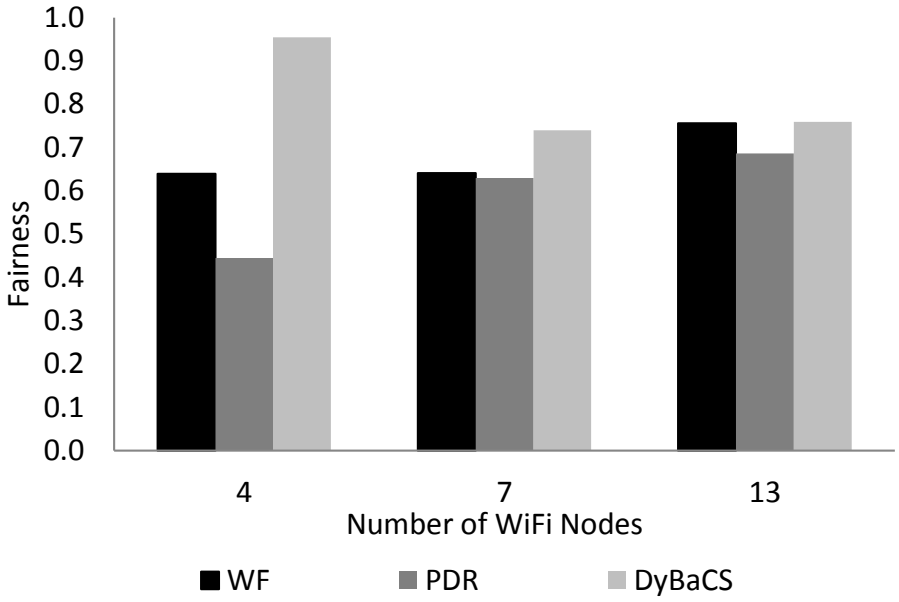

(b) Fairness.

Figure 5.9: Performance comparison between NSSs as a function of total WiFi nodes with 250 Users and fixed backhaul capacity of 20Mbps.

In scenarios where higher user capacity is needed within the HetNet, a denser WiFi APs deployment is required. Figure 5.9 shows the performance of DyBaCS over

varying WiFi-LTE node ratios and 20 Mbps backhaul capacity. The WiFi-LTE node ratio is scaled from 4, 7 to 13 and the EIRP of WiFi APs is set to 27 dBm, 24 dBm and 18 dBm respectively in order to accommodate all APs within a single LTE cell without severe interference amongst APs (Figure 5.5 and Figure 5.6). In all three scenarios, user density is kept at 250 and the coverage overlap between WiFi and LTE networks is maintained at 100%.

The results in Figure 5.9(a) show that, when the WiFi-LTE node ratio is 4, the PDR is the best in terms of average user throughput followed by DyBaCS whlist WF is the worst. At higher WiFi node densities, the advantage of PDR in respect of average user throughput becomes insignificant.

In terms of fairness, Figure 5.9(b) shows that DyBaCS remains the best for the entire range of LTE-WiFi node ratios and the PDR is the worst in terms of fairness. However, fairness with PDR is much lower compared to DyBaCS when the WiFi-LTE node ratio is low e.g. 4; PDR maximises the average user throughput at the expense of fairness. When the WiFi-LTE node ratio is low, the ratio of APs to the number of users is low and the capacity provided by WiFi networks is heavily shared amongst users. When the number of WiFi nodes is increased, unfairness with PDR is less obvious as more capacity is being provided to the HetNet. As the number of users is increased in the 7 and 13 WiFi-LTE node ratios, fairness is compromised.

Evaluation of the performance of DyBaCS such as the effects of WiFi-LTE overlap ratio, WiFi node density and user density are provided in Appendix B.

5.6.2 Non-uniform Backhaul Capacity

In a scenario with 100 users, backhaul capacity of 4 APs covering the entire HetNet are non-uniformly assigned with AP1, AP2, AP3 and AP2 equal to 10 Mbps, 0.5 Mbps, 20 Mbps and 3 Mbps respectively. The results of an evaluation showing average user throughput is presented in Figure 5.10(a), where PDR provides the highest value (4.75 Mbps) followed by DyBaCS (4.22 Mbps) and WF (2.62 Mbps). PDR is expected to offer a higher average user throughput as it selects the network based on the highest physical data rate with the primary intention of maximising average user throughput. However, fairness is compromised in terms of capacity distribution amongst users within the HetNet, highlighted in Figure 5.10(b) where the fairness index of PDR is only 0.59 compared to 0.86 provided by DyBaCS. Although the average throughput of DyBaCS is 11% lower than PDR, the trade-off seems worthwhile as fairness is significantly improved by 45%. WF provides a 0.43 fairness index.

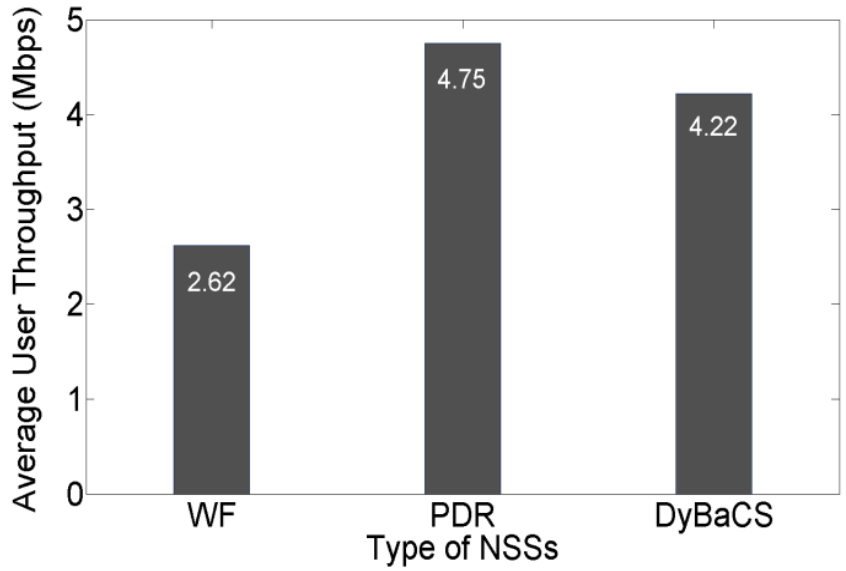

(a) Average User Throughput.

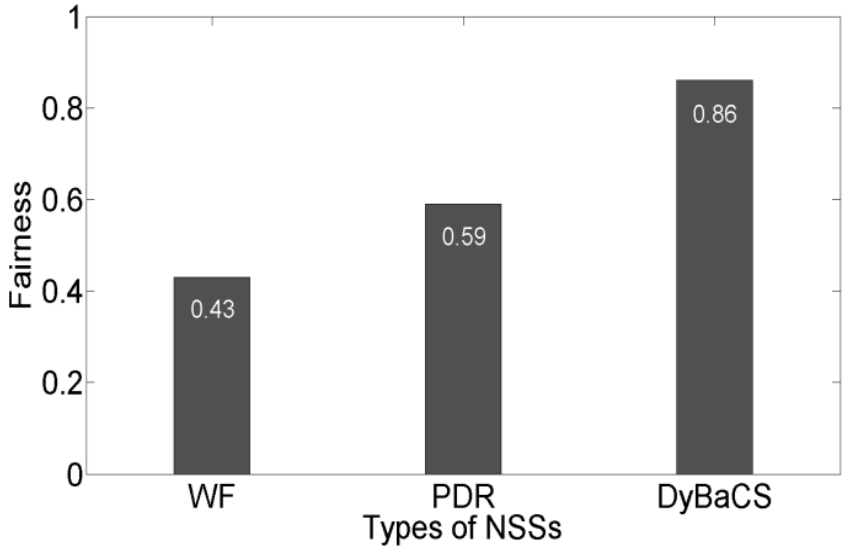

(b) Fairness.

Figure 5.10: (a) Average user throughput and (b) bandwidth sharing Fairness with non-uniform WiFi backhaul capacity (4 Nodes, 100 users).

Under a similar scenario and setting but with 250 users, Figure 5.11 shows an unacceptable fairness index of 0.33 offered by PDR, the poorest amongst all NSSs under study. Although PDR provides the highest average user throughput, the

concomitant compromised fairness remains a big disadvantage. DyBaCS provides a good balance between average user throughput and fairness.

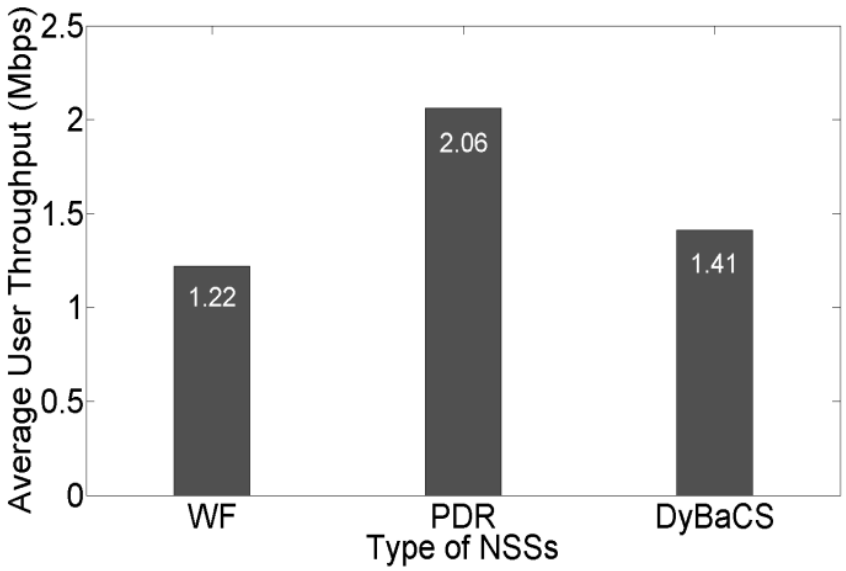

(a) Average user throughput.

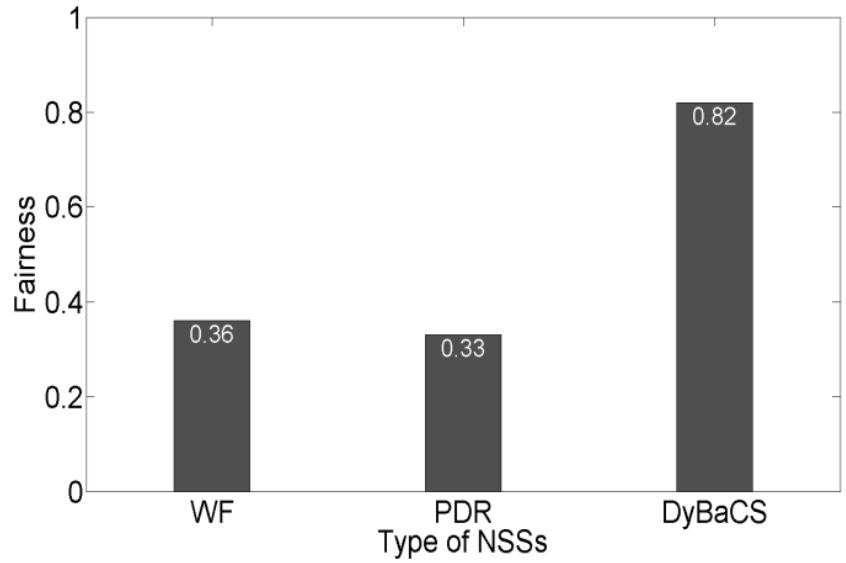

(b) Fairness.

Figure 5.11: (a) Average user throughput and (b) bandwidth sharing fairness with non-uniform WiFi backhaul capacity (4 Nodes, 250 users).

With 13 WiFi nodes and a WiFi backhaul capacity randomly chosen as in Table 5.5, Figure 5.12 shows that DyBaCS offers the best average user throughput and fairness.

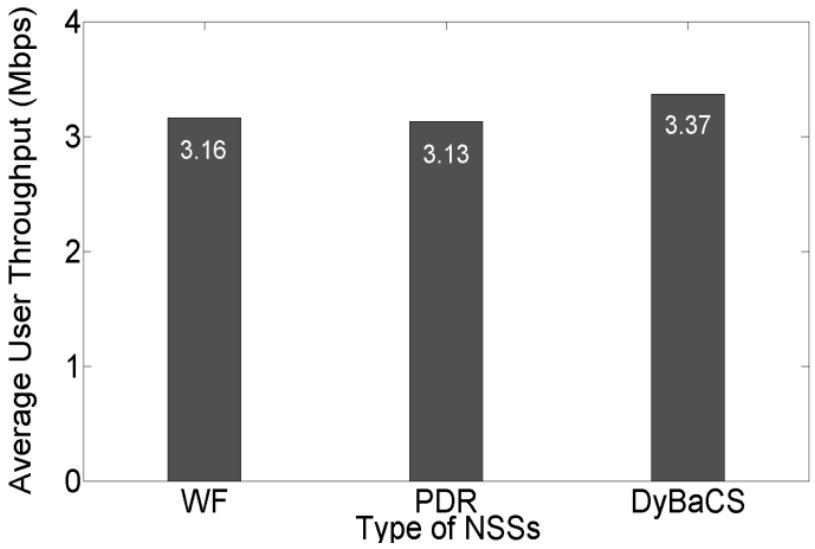

(a) Average user throughput.

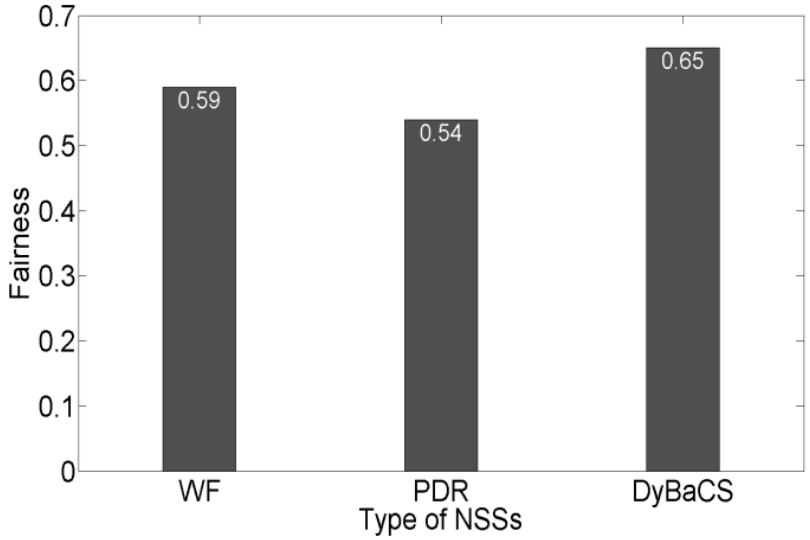

(b) Fairness.

Figure 5.12: (a) Average user throughput and (b) bandwidth sharing fairness with non-uniform WiFi backhaul capacity (13 Nodes, 250 users).

TABLE 5.5: Non-uniform WiFi backhaul capacity for 13 APs.

WiFi APID	1	2	3	4	5	6	7	8	9	10	11	12	13
WiFi Backhaul Capacity (Mbps)	5	10	15	2	5	7	13	6	12	4	9	1	8

The results captured in Figure 5.10, Figure 5.11 and Figure 5.12 consistently indicate that DyBaCS, under non-uniform WiFi backhaul scenarios, provisions best fairness to users with minimal penalty in the average user throughput. DyBaCS provides the best performance on both average throughput and fairness when both user density and WiFi node density is high (similar to the uniform backhaul capacity case). Performance under non-uniform WiFi backhaul is in good agreement with that of the uniform backhaul evaluation detailed in Section 5.6.1. However, it is important to note that changes in user location and distribution of backhaul capacities may affect performance but the general trends remain.

5.7 Conclusions

A backhaul capacity sensitive NSS referred to as DyBaCS designed for operation within a HetNet is presented. To the best of our knowledge, this is the first network selection algorithm that considers backhaul capacity in network selection within a LTE-WiFi Heterogeneous Network environment.

The performance of DyBaCS and two other NSSs are evaluated as a function of WiFi backhaul capacity and WiFi-LTE node ratio. The performance of NSSs is also compared under uniform and non-uniform WiFi backhaul capacity distributions.

In respect of uniform backhaul capacity, the evaluation shows that PDR provides the highest average throughput in most cases but has only a marginal performance edge compared to DyBaCS. However, with increasing backhaul capacity and WiFi-LTE node ratio, the PDR's advantage in relation to average user throughput to DyBaCS is eroded. In terms of fairness, DyBaCS clearly outperforms the others over the entire range of WiFi-LTE node ratio and WiFi backhaul capacity. PDR maximises the average user throughput but at the expense of fairness, thus user fairness is greatly sacrified when number of users is high or WiFi-LTE node ratio is low. WF provides the worst average user throughput and fairness in most cases.

In terms of non-uniform backhaul capacity, the results consistently indicate that DyBaCS provisions best fairness to users with minimal penalty in the average user throughput. DyBaCS provides the best performance on both average throughput and fairness when both user density and WiFi node density is high. The performance is also in good agreement with that of the uniform backhaul evaluation. Although PDR provides the highest average user throughput, the concomitant compromised fairness remains a big disadvantage. DyBaCS provides a good balance between average user throughput and fairness.

As a general conclusion, DyBaCS is the best in terms of fairness whilst maintaining an acceptable average user throughput under uniform and non-uniform WiFi backhaul capacity distributions within HetNet. It has a clear advantage when the number of users is high and capacity in the HetNet is very limited. It is also flexible in managing varying numbers of WiFi nodes and numbers of users, highly relevant in fast changing environments.

Chapter 6

LTE-WiFi Multi-hop Heterogeneous Wireless (MHW) Network Performance Optimisation

6.1 Introduction

In the Chapter, a joint Multi-hop Bandwidth Allocation (MBA) cum DyBaCS Network Selection Scheme (NSS) referred to as the Proposed Jointed Algorithm (PJA) is presented. The PJA aims to improve HetNet-wide throughput performance and fairness. In order to evaluate and compare the performance of the PJA, a Cuckoo Search (CS) optimisation algorithm [Xin-She Yang, 2010] is implemented. With the implementation of CS, the upper bound performance of the Multi-hop Wireless Network (MWH) under study can be determined, and then used to compare with the performance of MWH with PJA implemented. The simulation methodology used for evaluating the performance of the proposed algorithm is also described. Simulation results are then discussed followed by the conclusions.

6.2 Background

In conventional WLAN hotspot networks, the throughput and fairness can be improved by balancing the load amongst WLAN cells through offloading [Huazhi Gong and Kim, 2008] [Velayos et al., 2004] [Bejerano and Han, 2009]. Since the

backhaul bandwidth of WLAN hotspots is fixed, the network performance relies heavily on user network selection. Non-optimal selection results in the overloading of some APs whilst others are lightly loaded which subsequently causes degradation of the overall network performance. Consequently, network-wide performance can be improved by balancing traffic load. It is important to note that such a scenario requires a significant amount of AP coverage overlap, where users have the option of connecting to more than one AP [Velayos et al., 2004].

Normally operators tend to minimise the number of deployed APs while maintaining an acceptable level of user experience. The objective is mainly to reduce capital equipment cost as well as keeping installation and maintenance cost as low as possible [Aruba Networks, 2012] [Cisco, 2005]. One of the ways to reduce the number of APs is to increase inter-AP distance which eventually compromises AP coverage overlap. A lower coverage overlap also helps to keep interference as low as possible especially for WiFi where the number of non-overlapping channels is limited. According to [Cisco, 2005], a 10% - 15% coverage overlap is found to be adequate. As not all users fall within the coverage overlap area and inter-AP offloading cannot be relied on fully. In wireless mesh/multi-hop networks (WMNs), a similar scenario can also be observed and thus alternative performance optimisation strategies in WMNs should be pursued.

Since a WMN is connected to the core/wired network via a Gateway (GW) node, the Gateway bandwidth needs to be shared amongst Mesh Nodes (MNs) within the same cluster. Each MN is only allocated a fraction of time to access GW bandwidth through multi-hop wireless backhaul and hence the effective bandwidth available to a

MN is limited. Since the MN bandwidth also governs the available effective bandwidth for Mesh Access Points (MAPs), MN and MAP is used interchangeability in the remainder of the evaluation.

In WMNs, the available backhaul bandwidth is usually insufficient for MAPs to realise their full access capacity, since the same technology with the same capacity is used for both the access and backhaul radios [D Chieng et al., 2007] [Saumitra M Das et al., 2007]. By extending the WMN to multi-hop operation with multiple APs attached on each mesh node, the bottlenecks are likely to be formed on the wireless backhaul links. Consequently, offloading a user may not always be necessary even when one MAP is subject to a heavier load than the others since more backhaul bandwidth can be allocated to the former. It is therefore worthwhile considering some form of bandwidth allocation (BA) at the expense of some other MAPs bandwidth as long as it yields an overall improvement in the network-wide throughput. Example 6.1 provides a detailed explanation of performance behaviour in such a scenario accentuating that the proper selection of a BA scheme within WMNs is very important to ensure optimum network performance.

6.3 Contributions

The contribution of this Chapter is threefold.

Firstly, the implementation of MWH spatial model consisting of a LTE advanced network based on Release 10 and a IEEE 802.11n [IEEE Std, 2009] WiFi mesh

network with 2.4 GHz for access and 5 GHz for backhaul radio. The WMN is backhauled to the core network by a Gateway (GW).

Secondly, a CS algorithm is implemented and incorporated into the MWH to compute the capacity upper bound. Given the fixed WiFi Gateway capacity allocation, the algorithm optimises the Small cells backhaul BA dynamically as the number of users joining the network changes. Although, the CS provides the optimal result, the optimisation process is significantly more time consuming and is not suitable for fast changing dynamic HetNet applications. Therefore results obtained from CS serve solely as the upper bound reference.

Thirdly, a new algorithm referred to as PJA which integrates MBA and DyBaCS for Multi-hop Wireless HetNet capacity optimisation is developed. The output of the algorithm is compared to upper bound obtained from CS. The proposed computationally simple algorithm provides a solution suitable for dynamic and fast changing wireless environments.

Thus the objective is to develop and evaluate an algorithm to optimise the network performance of Multi-hop Wireless HetNet (MWH) consisting of a hybrid LTE and WiFi Mesh Network (WMN). As discussed, load balancing/offloading is one route to improving the performance of hotspot networks, while in WMNs, backhaul BA plays an important role in optimising network performance. MWH however, presents a very different scenario compared to both WiFi hotspots and homogeneous WMNs as the optimisation process takes into consideration both load balancing/offloading and backhaul BA. The joint load balancing/offloading and backhaul BA algorithm is

implemented through a MBA algorithm designed to operate with the DyBaCS NSS to optimise the throughput and maintain fairness amongst users.

6.4 Multi-hop Bandwidth Allocation (MBA) Algorithm

The proposed MBA algorithm features three strands that cooperatively offer an improvement in the overall network throughput performance and fairness:

i. **Predictive Bandwidth Allocation:** a dynamic bandwidth allocation based on the number of existing users connected to MAPs (or MAPs loading) and the potential user arrival statistics. The DyBaCS NSS on the other hand suggests an optimum number of connected users to the MAPs, which is sensitive to the MAPs' backhaul bandwidth allocation by MBA. Hence, both algorithms jointly promote an overall network performance improvement.

ii. **Dynamic Bandwidth Allocation Capping:** a saturation-aware BA which dynamically caps the allocation based on the maximum bandwidth needed by a MAP. The maximum bandwidth needed is a function of number of users and their channel quality.

iii. **Multi-hop Links Capacity Awareness:** awareness of the effective capacity of multi-hop links ensures that the BA algorithm does not allocate bandwidth in excess of the effective capacity of multi-hop links within a WMN. An algorithm

is executed iteratively to allocate the bandwidth and redistribute any residual bandwidth until all bandwidth from the GW is fully allocated to all MNs.

6.4.1 Predictive Bandwidth Allocation

As a consequence of executing DyBaCS NSS, user association is highly sensitive to MAP backhaul bandwidth as NSS operation is founded on a backhaul capacity-aware algorithm for improved load balancing. To function in tandem with DyBaCS, the proposed MBA should be sensitive to users entering and leaving the network. To balance the traffic load, an ideal bandwidth algorithm should able to predict the user network association and allocate the bandwidth efficiently before users join the network, illustrated in Example 6.1.

Example 6.1: Consider a MWH with two MNs labelled as MN1 and MN2, one macro BS and six users enumerated from 1 to 6 as depicted in Figure 6.1(a). BS coverage is represented by the biggest oval area shown in grey and MAPs coverage is represented by smaller circles in white. User 1, User 2, User 3 and User 4 experience a bit rate of 3 Mbps from MN1 and MN2 respectively (represented by red lines), while User 5 and User 6 experience bit rate of 3 Mbps from the BS (represented by blue lines). The solid lines indicate active connections whilst the dotted lines represent the available network connections. Both MN1 and MN2 are connected to the core network through GW with capacity of 4 Mbps and that capacity is shared evenly i.e. 2 Mbps each. The BS backhaul bandwidth is always assumed to be sufficient to support demand.

For the scenario in Figure 6.1(a) and using Equation (4.22), User 1, User 2, User 3 and User 4 are allocated 1.5 Mbps access capacity by both MN1 and MN2. However, due to the limit of 2 Mbps backhaul capacity for MN1 and MN2 respectively, the effective capacity per user to the core network is limited to 1 Mbps only. Both User 5 and User 6 are allocated 1.5 Mbps. Hence the overall HetNet cell throughput is the sum of all user throughputs viz.7 Mbps.

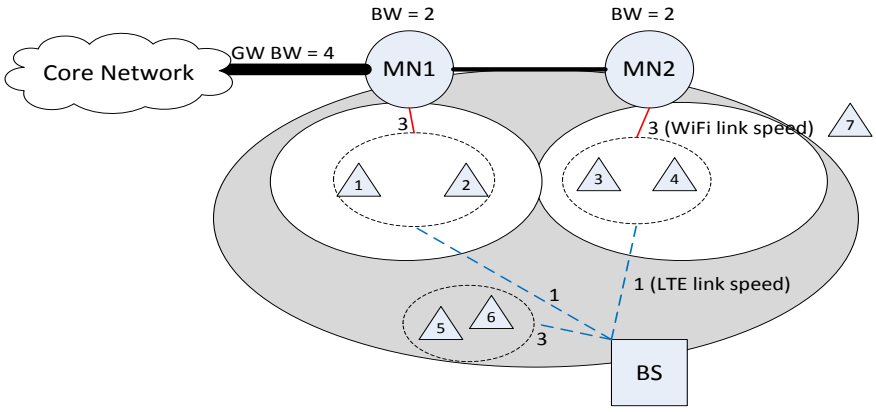

(a) Backhaul bandwidth assignment before arrival of user 7.

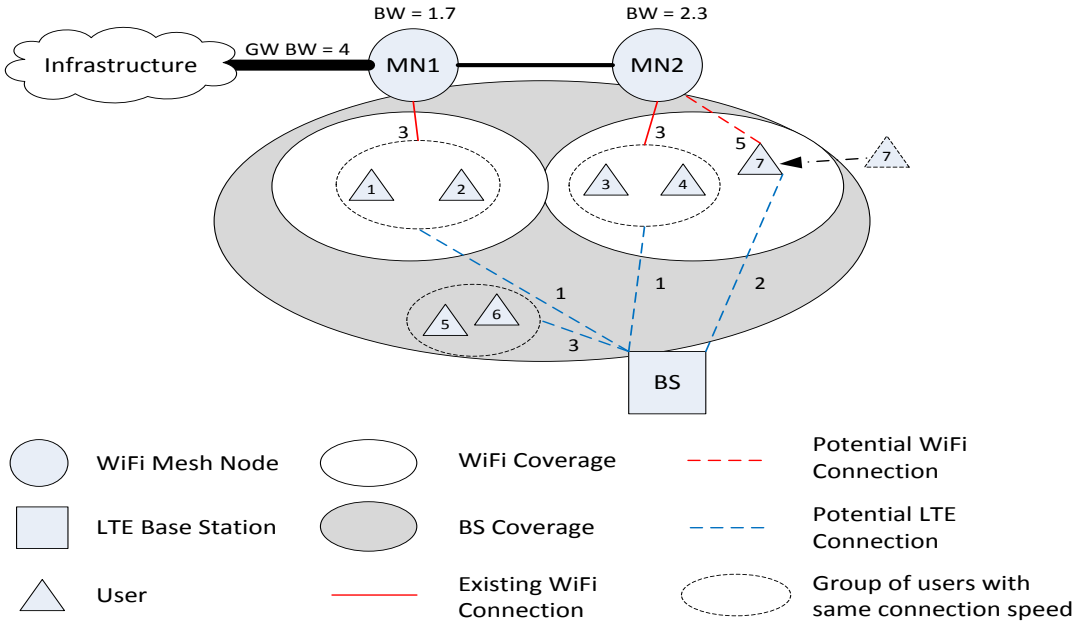

(b) Reallocation of backhaul bandwidth upon arrival of user 7.

Figure 6.1: Example of Multi-hop Wireless HetNet (MWH) system with 2 Mesh Nodes, one Base Station and 6 users.

Now assume that a new User 7 enters the HetNet enjoying access bit rate of 5 Mbps from MN2 and 2 Mbps from the BS. User 7 attempts to connect to either MN1 or BS by searching through the network in order to secure the highest speed connection to the Internet. Due to the 2 Mbps backhaul bandwidth limit at MN2, the effective bandwidth offered to User 7 is 0.77 Mbps, while the BS offers a slightly higher bandwidth at 0.86 Mbps. Hence, the natural tendency is for User 7 to join the BS and thus the HetNet cell throughput becomes 6.57 Mbps (Table 6.1). However, if MN2 can be allocated a higher backhaul bandwidth such as 2.3 Mbps by reducing MN1 backhaul bandwidth to 1.7 Mbps, the effective bandwidth of User 7 increases to 0.88 Mbps; hence User 7 joins MN2 and HetNet system throughput now becomes 7.34 Mbps (Table 6.2). This example highlights that with a slight changes to the BA, User 7 can be offloaded from the BS to the WLAN to increase overall system throughput.

Table 6.1: User bandwidth with MN1 = MN2 = 2 Mbps.

User	**Serving AP/BS**	**Data Rate (Mbps)**	**Eff. BW (Mbps)**
1	MN1	3	1.00
2	MN1	3	1.00
3	MN2	3	1.00
4	MN2	3	1.00
5	BS	3	0.86
6	BS	3	0.86
7	BS	2	0.86
		Cell Throughput	**6.57**

Table 6.2: User bandwidth with MN1 = 1.7 Mbps; MN2 = 2.3 Mbps.

User	Serving AP/BS	Data Rate (Mbps)	Eff. BW (Mbps)
1	MN1	3	0.85
2	MN1	3	0.85
3	MN2	3	0.88
4	MN2	3	0.88
5	BS	3	1.50
6	BS	3	1.50
7	MN2	5	0.88
		Cell Throughput	**7.34**

The above example shows that there is a need for a node-based BA in MWH. Several solutions to the problem based on appropriate BA schemes have been reported [Gambiroza et al., 2004] [Sumit Singh et al., 2012] [Ho et al., 2012] proving that a node-based BA is viable. In node-based BA, when a mesh node is allocated a certain bandwidth, the same amount of capacity is reserved throughout the multi-hop link for the traffic traversing from the node to the GW or vice versa. In the access domain, the mesh AP is in charge of allocating bandwidth fairly to users. A node-based BA is assumed to facilitate the proposed optimisation algorithm; the details of node-based BA are not discussed in the dissertation as it is out of the scope of the study.

In order to allocate bandwidth intelligently and dynamically, the algorithm should have the ability to predict when and where users join the network and pre-allocate sufficient bandwidth to MNs so that the overall HetNet system throughput can be optimised. Therefore in the proposed algorithm, an Initial Bandwidth Allocation (IBA) phase is included as follows:

$$C_{Bh}^{i} = \frac{N^{i} + \mathcal{R}^{i}}{\sum_{i=1}^{I} N^{i} + \sum_{i=1}^{I} \mathcal{R}^{i}} \tag{6.1}$$

where, i is the index of mesh node, I is the total number of mesh nodes, N^{i} is the number of users on MAP i, C_{Bh}^{i} is initial backhaul capacity allocated to MAP i and $\mathcal{R}^{i}$ is bandwidth allocation weight on MAP i.

The variable N^{i} indicates that the AP supporting a higher number of users will be allocated more bandwidth, based on the assumption that every user has the same amount of traffic in the HetNet. This assumption is supported by [A. G. Forte et al., 2006], proving that in highly congested environments, the number of clients still represents a good metric to estimate APs load and is much simpler to adopt for the simulation. N^{i} can also be replaced by different MAP loading measurements if desired.

$\mathcal{R}^{i}$ is the weight on i-th MAP, determining the amount of bandwidth allocated for future users. For example, the i-th MAP can be allocated to a higher $\mathcal{R}^{i}$ value if it is known to be a hotspot. $\mathcal{R}$ is also a weight to prevent the allocation of 'zero bandwidth' to a MAP if no user is connected to it. $\mathcal{R}$ can have any value; larger values make the entire system less sensitive and provides a more even bandwidth allocation. For instance, if R is a very large value i.e. $\lim_{\to\infty} \mathcal{R}$, N^{i} becomes insignificant and Equation (6.1) can be written as Equation (6.2), where each MN shares a portion of GW bandwidth equally;

$$C_{Bh}^{i} = \frac{\mathcal{R}}{I \times \mathcal{R}} = \frac{1}{I} \quad (6.2)$$

Conversely, a small $\mathcal{R}$ causes the system to be very sensitive to the level of MAPs loading; in the extreme of $\lim_{\to 0} \mathcal{R}$, the BA is based solely on MAPs loading.

In the following simulation study, the same value $\mathcal{R}^i = \mathcal{R}$ is used for all MNs as users are distributed according to a stochastic model [Petrova et al., 2007] (Section 5.5.1). The study evaluates the overall cell throughput (Figure 6.2(a)) and fairness (Figure 6.2(b)) for a 7-mesh-node scenario and 250 Mbps GW bandwidth network as a function of the number of users for a $\mathcal{R}$ value ranging from $\mathcal{R}$=5 to $\mathcal{R}$=30. The results show that $\mathcal{R}$=15 is optimum for the scenario under study.

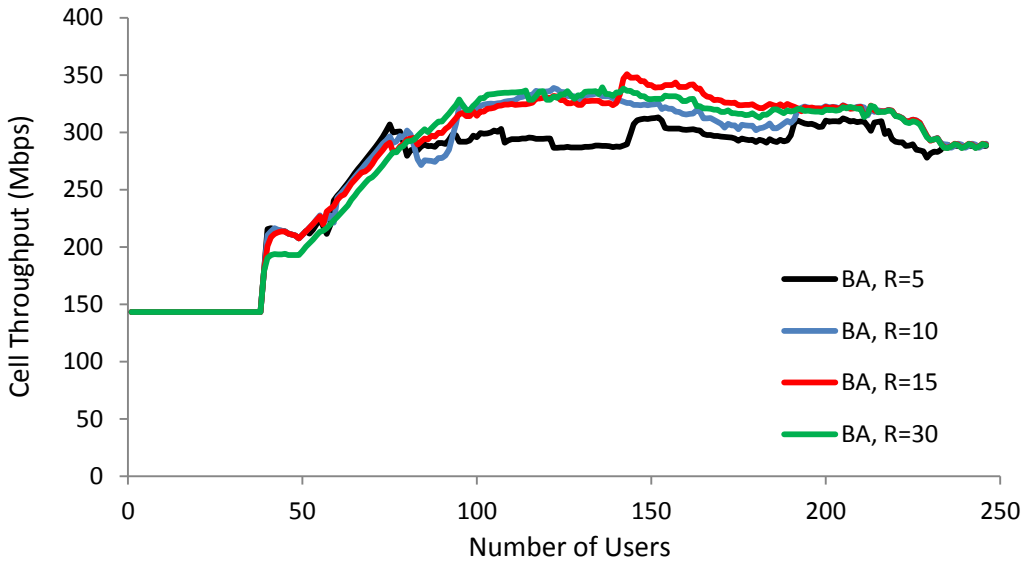

(a)

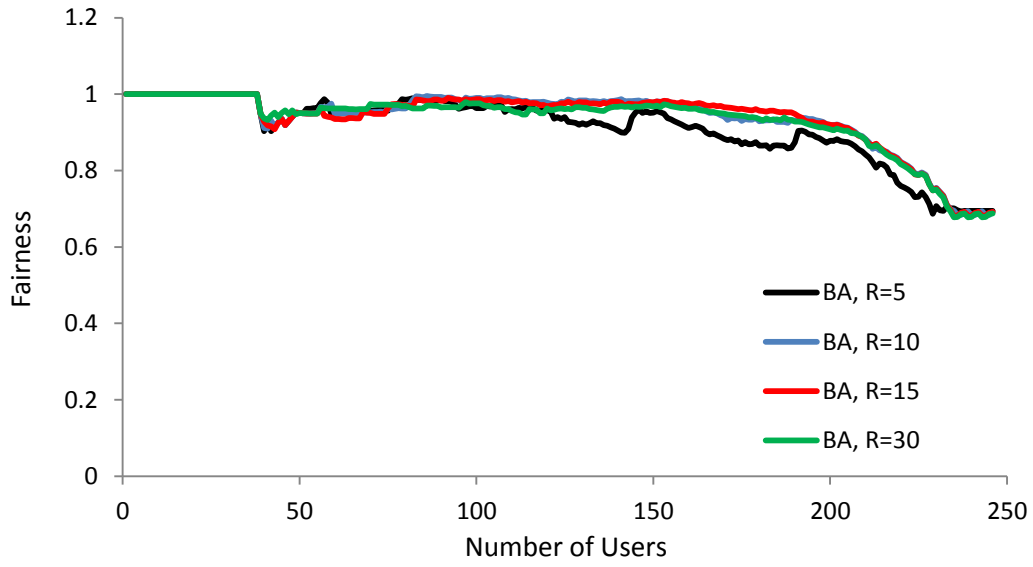

(b)

Figure 6.2: Multi-hop Wireless HetNet (a) Cell throughput and (b) Fairness for a 7-mesh-node scenario; 250 Mbps Gateway bandwidth.

6.4.2 Dynamic Bandwidth Allocation Capping

Since users are distributed within an AP coverage area, not all users enjoy channel access at the highest allowed data rate. Usually users closer to the MAP experience superior channel quality than those further away. Users with bad channel quality and slower access speed compromise overall AP throughput.

When the bandwidth of an AP is shared fairly amongst users, the actual bandwidth required by an MAP is usually much lower than expected. To better explain this, an evaluation was executed by distributing 70 users within an AP coverage area using different types of distributions viz. Grid, Pseudo Random Uniform [Niederreiter, 1992] and Bi-Variate Gaussian [Weisstein, 2014] distribution. Users are admitted to an AP one by one and the corresponding backhaul capacity required by the AP is

calculated. For each scenario, twenty simulations were run with random seeds based on the computer clock and their mean value is taken (Figure 6.3).

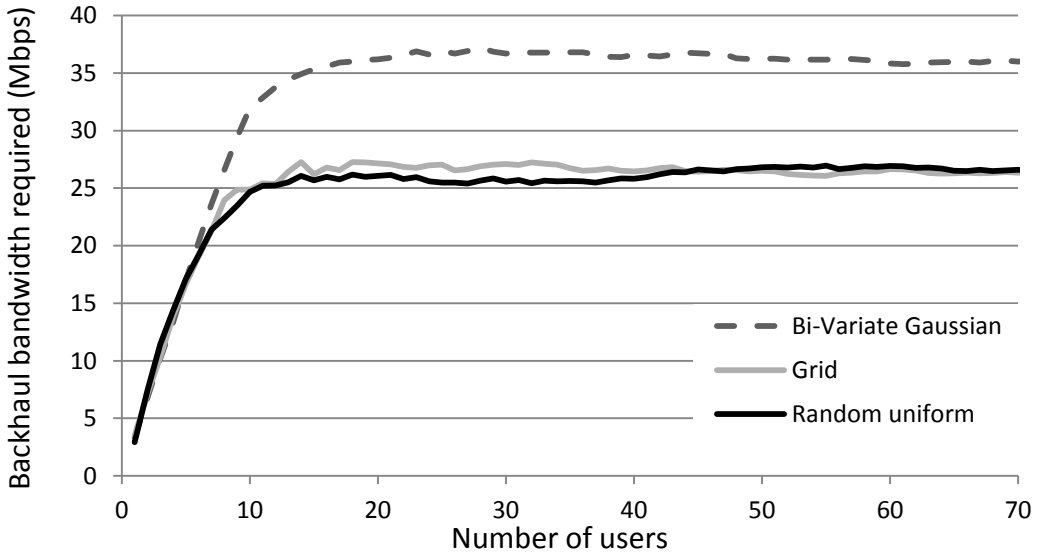

Figure 6.3: Bandwidth required by a MAP as a function of number of users admitted.

Results indicate that the required bandwidth increases linearly for less than 10 users; beyond 10 users, the required bandwidth increases at a slower rate, flattening at around 20 users. In general the required bandwidth of an AP is not linearly proportional to the number of users connected to it. Most importantly, the required bandwidth saturates at a certain point where no additional bandwidth is required even if more users are joining the network. It is also important to note that the required bandwidth saturates at around 30% (26 Mbps/88 Mbps) of the highest possible access throughput supported by an AP for grid and random uniform distribution; and 40% for the Bi-Variate Gaussian distribution. Higher backhaul bandwidth is required for the Bi-Variate Gaussian distribution compared to the other two mainly because the former distribution tends to place users near the APs and as a consequence users enjoy better channel quality. The characteristics may shift slightly upward or

downward depending on user distribution and channel quality experienced by the users.

Equation (6.1) assumes that the BA is based purely on the number of users, but this is only valid when an AP is unsaturated. Therefore, Equation (6.1) has to be applied in tandem with the backhaul bandwidth capping condition. In conclusion, a BA cannot depend solely on number of users connected to an AP and should be capped at its saturation value.

6.4.3 Multi-hop Links Capacity Awareness

In WMNs, it is common to have more than one multi-hop branch extending from the Gateway node. A branch is likely to have one or more sub-branches, similar to the topology shown in Figure 6.4, an example of a branch from a Gateway node. In such a tree topology, wireless backhaul links are shared amongst all MNs. The closer a backhaul link is to the Gateway, the more extensive its bandwidth is shared by MNs as it represents a traffic aggregation point between GW and MNs. Therefore, the total bandwidth allocated to MNs connected directly or indirectly (more than one hop away) to a backhaul link should not exceed the backhaul link capacity; otherwise it cannot be supported. In the proposed Multi-hop Bandwidth Allocation (MBA) algorithm, the wireless backhaul bottleneck condition is examined before any bandwidth is allocated, a scenario explained in Example 6.2.

Example 6.2: MBA considering wireless backhaul link capacity, using a branch of the multi-hop tree topology from Gateway node as shown in Figure 6.4.

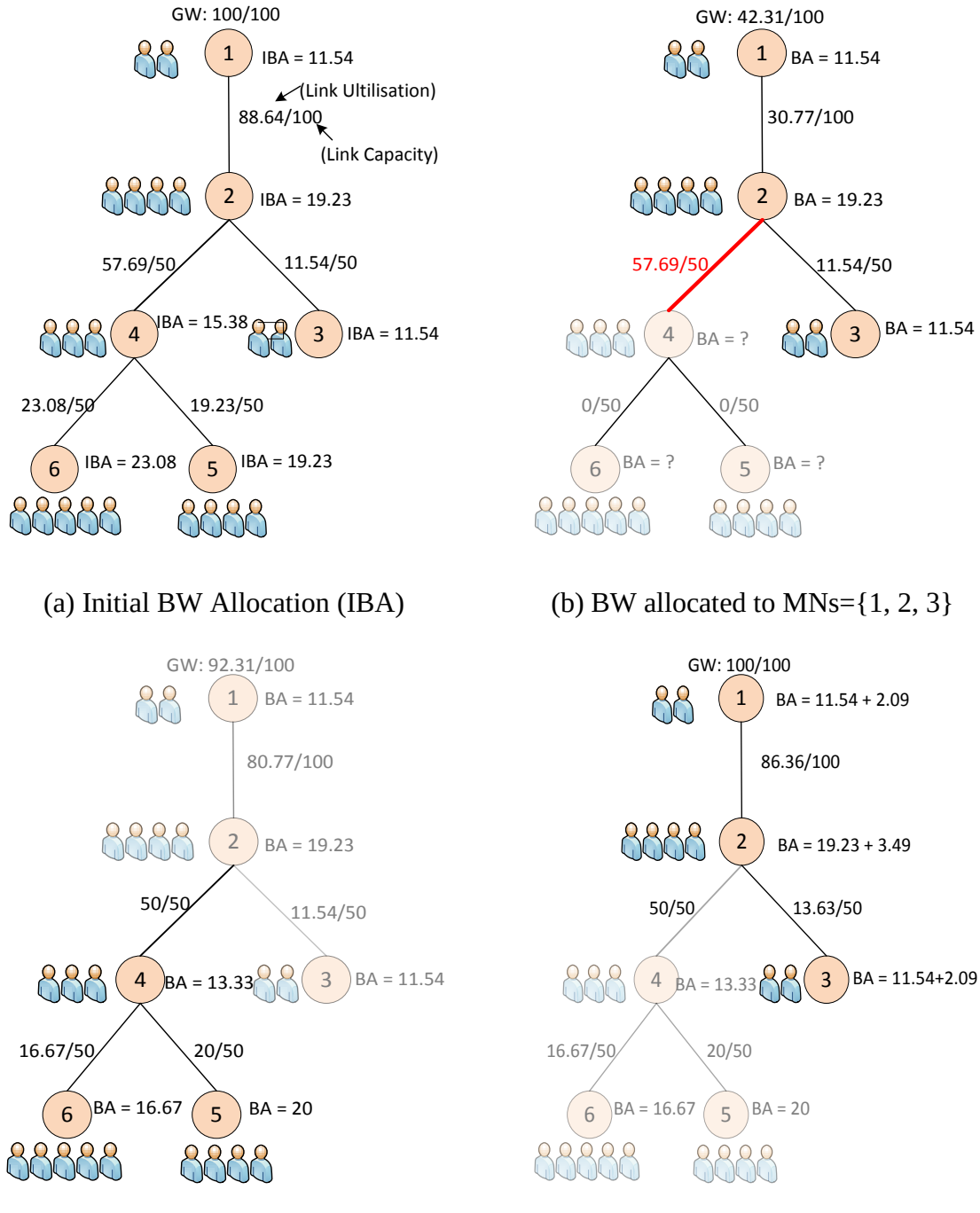

Figure 6.4: Example of Multi-hop Bandwidth Allocation (MBA) on a multi-hop tree topology.

Based on Figure 6.4(a), 6 MNs are represented by set I = {1, 2, 3, …, 6} and each MN is represented by an index $i \in I$, where i=1 is a Gateway node. The total number of users connected to MN1 – MN5 are presented by N= {2, 4, 2, 3, 4, 5} and the number of users connected to MNi is represented by N^i. Similarly, the bandwidth allocated to MNi is written as BA^i.

A wireless backhaul link formed by MNi and MNj is represented by $L_{i,j}$ where MNi is one hop closer to GW than MNj. Similarly, the capacity of backhaul link $L_{i,j}$ is represented by $CA_{i,j}$. For example, in Figure 6.4(a), the capacity for a backhaul link, $L_{1,2}$, written as $CA_{1,2}$ is 100 Mbps. The label 88.64/100 next to $L_{1,2}$ indicates that for the 100 Mbps capacity supported by backhaul link $L_{1,2}$, 88.64 Mbps is being utilised, the total loading of $L_{1,2}$. 88.64 Mbps = $\sum_{i=2}^{6} BA^i$ is calculated by summing the bandwidth allocated to the MNs = {2, 3,…, 6} connected directly and indirectly to $L_{1,2}$.

6.4.3.1 Initial Bandwidth Allocation (IBA)

The first step of the MBA is to calculate the Initial Bandwidth Allocation (IBA) values (using Equation (6.1)). To simplify the calculation in this example, the value of $\mathcal{R}$ is assumed to be equal to one and is applied to all MNs. The results are presented in Table 6.3 and the same IBA values are also stated in Figure 6.4(a).

Table 6.3: Initial Bandwidth Allocation (IBA) values (Figure 6.4(a)).

Mesh Node, i	N^i	BA^i
1	2	11.54
2	4	19.23
3	2	11.54
4	3	15.38
5	4	19.23
6	5	23.08
Total	20	100

The IBA values are not allocated to MNs until the capacity of the underlying multi-hop wireless backhaul links is confirmed to support such a bandwidth allocation. Thus, based on the IBA values, the total loading on all backhaul links is calculated and depicted beside each backhaul link in Figure 6.4(a).

It is found that the total loading on $L_{2,4}$ is equal to 57.69 Mbps, exceeding the maximum support backhaul link capacity of $CA_{2,4}$ = 50 Mbps (highlighted in red in Figure 6.4(b)). Hence, the IBA values cannot be allocated to MNs = {4, 5, 6}. However, IBA values are assigned to MNs = {1, 2, 3} as their backhaul capacity is sufficient for the bandwidth allocation (Figure 6.4(b)).

6.4.3.2 Sub-Branch Calculation

Subsequently (Figure 6.4(c)) the BA calculation progresses by focussing on the performance of the sub-branch consisting of MNs = {4, 5, 6}, not allocated a BA value. Thus, IBA values for MNs = {4, 5, 6} are recalculated using Equation (6.1) based on the maximum supported value $CA_{2,4}$ = 50 Mbps, yielding values of {13.33,

16.67, 20} Mbps respectively. Those IBA values are allocated to the corresponding MNs.

6.4.3.3 Residual Bandwidth Allocation

Thus far, after all MNs are allocated certain BA values, the total bandwidth allocated to all MNs is equal to 92.37 Mbps; a residual bandwidth of 7.63 Mbps remains from the 100 Mbps supported by the GW. In order maximise network throughput, the residual GW bandwidth should be allocated to MNs. Since, $L_{2,4}$ has been fully utilised, all MNs connected to it are excluded for the rest of the BA process (Figure 6.4(d)). Hence, taking into consideration the residual GW capacity of 7.63 Mbps only, the additional IBA values for MNs = {1, 2, 3} are {2.09, 3.49, 2.09} Mbps respectively. These values (as shown in Figure 6.4(d)) are added to the existing BA values since these allocations are supported by their respective backhaul links.

6.4.4 Joint MBA and DyBaCS Algorithm

To implement all the rules discussed in Section 6.4.1 to Section 6.4.3, an algorithm is designed to operate with the DyBaCS NSS. As presented in Chapter 5, DyBaCS can improve HWH throughput while maintaining a high level of fairness.

During the bandwidth allocation and network selection iteration process, the GW bandwidth is first "arbitrarily" shared evenly amongst all MNs; DyBaCS facilitates user network selection based on the allocated bandwidth. Subsequently, based on these user network connections, the MBA will adjust the BA accordingly which in

turn influences the subsequent user network selection. Both MBA and DyBaCS operate in tandem.

The proposed algorithm is described using the pseudo codes in Algorithm 6.1 and Algorithm 6.2. To represent all MNs in the HetNet, set I is used with $i \in I$ as the index representing individual MNs. Since the Gateway (GW) node is the head of a mesh cluster, therefore $i = 1$ represents a GW node. The multi-hop branches extending from the GW or MNs are represented by a set B where $b \in B$ is the index of the branches.

For MNi, let j denote its direct sub-ordinate MN in which MNi is one hop closer to the GW than MNj. MNi and MNj are connected by backhaul link $L_{i,j}^{b}$ where b denotes the branch index. For a backhaul link $L_{i,j}^{b}$, $C_{i,j}^{b}$ denotes the remaining capacity available for all MNs connected to the backhaul link $L_{i,j}^{b}$. After assigning $a\ C_{Bh}^{j}$ amount of bandwidth to a particular MNj connected to $L_{i,j}^{b}$, C_{Bh}^{j} is deducted from $C_{i,j}^{b}$.

For MNi, let S^i denote a set of sub-ordinate MNs connected to MNi directly or indirectly and including MNi itself. Let $C_{S^i} = \sum_{n \in S^i} C_{bh}^{n}$ denote the sum of all Initial Bandwidth Allocations (IBAs) for all MNs in S^i, where an IBA is the preliminary value before it is actually allocated to a MNi. The bandwidth that is actually allocated to a MNi is represented by the effective backhaul capacity $C_{Eff,bh}^{i}$. All users are represented by a set U and $u \in U$ is their index and N^i is total number of users connected to a MNi.

The proposed algorithm is described by the pseudo codes detailed in Algorithm 6.1 and Algorithm 6.2 as follows.

Algorithm 6.1: Joint MBA and DyBaCS algorithm

A1) *Initialization*

a. $C_{GW} \leftarrow 300$ *;* (specify available GW capacity i.e. 300 Mbps)

b. *Initialise* $\mathcal{R}^i;\ \forall\ i \in I;$ (assign BW distribution weight, $\mathcal{R}^i$ value)

A2) *For* $u = 1\ to\ U$ *;* (user entering HetNet)

a. $C^i_{Eff,bh} \leftarrow 0;\ \forall\ i \in I$

b. $\gamma^i \leftarrow 0;\ \forall\ i \in I$

c. *While* $C_{GW} > 0$

i. *Get* $N^i;\ \forall\ i \in I;$(get number of users connected to each MN based on DyBaCS NSS)

ii. *Calculate initial backhaul BW allocation for all MNs (* $C^i_{Bh};\forall\ i \in I$*) based on the number of users connected to MNs* (N^i) *using Equation (6.1):*

$$C^i_{Bh} = \frac{N^i + \mathcal{R}^i}{\sum_{i=1}^{I} N^i + \sum_{i=1}^{I} \mathcal{R}^i} \times C_{GW};\ \forall i \in I$$

iii. *Estimate max required backhaul BW* $C^i_{Bh\_Max};\ \forall i \in I$

iv. *If* $\left(C^i_{Bh} + C^i_{Eff,bh}\right) > C^i_{Bh\_Max};\ \forall i \in I$

- $C^i_{Bh} \leftarrow \left(C^i_{Bh\_Max} - C^i_{Eff,bh}\right)$
- $\gamma^i \leftarrow 1$

End If

v. *Allocate estimated backhaul BW to GW node (node ID* $i = 1$*)*

- $C^1_{Eff,bh} \leftarrow \left(C^1_{Eff,bh} + C^1_{Bh}\right)$
- $C_{GW} \leftarrow (C_{GW} - C^1_{Bh})$
- *BranchHead_ID = GW_ID*

vi. *Call RecursiveBA_Fn(BranchHead_ID) (Algorithm 6.2)*

vii. *Update and mark all links $L^b_{i,j}$ and MNi within branch b if saturated on BW allocation.*

End While

A3) *Call DyBaCS NSS* (Algorithm 5.2)

a. *Executes DyBaCS NSS based on allocated backhaul BW in Step A1-Step A2*

A4) *Return to Step A2 if there are more users to admit otherwise end*

Algorithm 6.1 can be explained as follows:

Step A1); Initialise the available GW capacity and bandwidth distribution weight $\mathcal{R}$ value.

Step A2); Users are admitted one by one until all are admitted

a) Initialise $C^i_{Eff,bh}$ by setting the effective bandwidth allocated to all Mesh Node to zero.

b) Similarly, γ^i is initialised to zero for all $i \in I$. $\gamma^i = \{0,1\}$ denotes whether a node i has been allocated its maximum required bandwidth; a '1' indicates it has been allocated its maximum required bandwidth and '0' otherwise.

c) The bandwidth allocation is executed in an iterative manner using a while loop until all GW bandwidth C_{GW} has been allocated:

i. In this step, the number of users connected to all MNs is obtained and recorded as $N^i;\ \forall\ i \in I$. The number of users connected to MNs is governed by the DyBaCS NSS.

ii. IBA values $C_{Bh}^i;\ \forall i \in I$ are calculated using Equation (6.1) based on the number of users N^i and $\mathcal{R}^i$ value.

iii. Based on the number of users connected to MAPs, the maximum required bandwidth $C_{Bh\_Max}^i$ for all MNs is calculated.

iv. Based on the calculated $C_{Bh\_Max}^i$, the IBA is adjusted so that the overall BA allocation to a MNi never exceeds $C_{Bh\_Max}^i$. If a particular MNi is being allocated its maximum required bandwidth, γ^i is marked as '1'.

v. BA is first applied to the GW node where C_{Bh}^1 is allocated to the GW node on top of previously allocated bandwidth $C_{Eff,bh}^1$ (if any) and the total available GW capacity C_{GW} is updated by subtracting C_{Bh}^1 from it. Subsequently, the GW node ID is set as *BranchHead_ID*, indicative of a branch head.

vi. The *RecursiveBA_Fn* – the recursive function that is the core of Multi-hop Bandwidth Allocation (MBA) – is then invoked. The underpinning *RecursiveBA_Fn* algorithm is discussed in more detail in Algorithm 6.2.

vii. Once a BA iteration is completed – from Step A2.c.i to Step A2.c.vi – the remaining backhaul link capacity $C_{i,j}^b$ in branch b is updated. If a particular link $C_{i,j}^b$ is exhausted i.e. no MN connected to the link can be allocated additional bandwidth, the MNs connected to it are labelled as saturated.

Step A3); DyBaCS NSS is executed after the MBA process.

Step A4); The process is repeated starting from Step 2 if there are additional users to be admitted; otherwise the allocation ends.

Algorithm 6.2: Recursive bandwidth allocation algorithm in MBA

RecursiveBA_Fn (BranchHead_ID)

Step B1) $i \leftarrow$ *BranchHead_ID*

Step B2) *For all branches* $b \in B$ *extended from target MN*i

a. $j \leftarrow$ *Direct_SubNodeID of* MNi in branch b

b. If MNj *is not saturated for existing/additional BW allocation*

i. *Get* $C_{S^j} = \sum_{n \in S^j} C_{Bh}^n$, sum of IBA to MNs in S^j

ii. *Get* $C_{i,j}^b$, *the remaining backhaul link capacity*

iii. $C_{available} = min\left(C_{S^j}\ ,\ C_{i,j}^b\ \right)$; (get lower value between C_{S^j} and $C_{i,j}^b$)

iv. *Calculate IBA value* $\forall\, n \in S^j$ *based on the number of users connected to MNs using Equation (6.1)*

$$C_{Bh}^n = \frac{N^n + \mathcal{R}^n}{\sum_{n \in S^j} N^n + \sum_{n \in S^j} \mathcal{R}^n} \times C_{available};\ \forall n \in S^j;$$ (re-estimate BA for $n \in S^j$ based on $C_{available}$)

v. $C_{Eff,bh}^j \leftarrow \left(C_{Eff,bh}^j + C_{Bh}^j\right)$

vi. $C_{GW} \leftarrow \left(C_{GW} - C_{Bh}^j\right)$; (update available C_{GW})

vii. $C_{i,j}^b \leftarrow \left(C_{i,j}^b - C_{Bh}^j\right)$; (update available link capacity)

viii. *If* $C_{i,j}^b = 0$

- *Marks all sub-ordinate nodes connected to* $L_{i,j}^b$ *as saturated*

End If

ix. *If MNj has one or more sub-branches*

- *BranchHead_ID* ← j
- *calls RecursiveBA_Fn (BranchHead_ID);*

End If

End If

End For

Algorithm 6.2 is a sub-algorithm which carries out bandwidth allocation recursively for multi-hop tree topology that comprises of many branches. Algorithm 6.2 is explained as follows.

Step B1); Once the "*RecursiveBA_Fn"* function is invoked, variable i is set to equal to the *BranchHead_ID* and the value passes from the main algorithm.

Step B2); An iteration ensures that all following steps are performed on all branches $b \in B$ starting from the branch head.

a) For the selected branch b, the direct sub-ordinate ID for the link $L_{i,j}^{b}$ is identified and the variable j is set to be equal to the sub-ordinate node ID.

b) The sub-ordinate MNj is then examined to determine whether it is unsaturated and can still receive additional BA. The subsequent steps are only performed if MNj is not saturated.

i–iii) In order to ensure that the backhaul link $L_{i,j}^{b}$ is able to support the initial BA determined in Step A2.c.ii – iv, total capacity allocated to MNj and its sub-

ordinates (represented by a set S^j) is calculated as C_{Sj} in Step B2.b.i. The available $L^b_{i,j}$ link capacity $C^b_{i,j}$ is then obtained in Step B2.b.ii. Step B2.b.iii then chooses the minimum value between $C^b_{i,j}$ and C_{Sj}, to ensure that the total BA capacity C_{Sj} does not exceed the available backhaul capacity $C^b_{i,j}$ while preventing BA wastage. The chosen value is then assigned to $C_{available}$.

iv-viii) The IBA value for MNs in set S^j is recalculated using $C_{available}$ from Step B2.b.iv. Then, in Step B2.b.v, the bandwidth is allocated to MNj on top of the existing bandwidth allocation $C^j_{Eff,bh}$ (if any). Next, the available GW capacity C_{GW} and backhaul link capacity $C^b_{i,j}$ are updated respectively in Step B2.b.vi and Step B2.b.vii. Step B2.b.viii marks the backhaul link as saturated if $C^b_{i,j} = 0$ viz. no more capacity remains.

ix) MNj is examined to determine whether it has one or more branches. If the condition is true, node ID for MN j is set as *BranchHead_ID* and the *RecursiveBA_Fn* is invoked to address the sub-ordinate MNs. Otherwise, the process continues for other branches from MNi.

6.5 Cuckoo Search (CS) Algorithm

For the purpose of a meaningful comparison of the performance of the proposed algorithm, the upper bound cell capacity for a MWH is estimated providing a benchmark using the Cuckoo Search (CS) optimisation algorithm [Xin-She Yang, 2010] [Xin-She Yang and Deb, 2014] . The CS is one of the latest nature-inspired meta-heuristic algorithms based on the brood parasitism of some cuckoo species

laying their eggs in the nests of other host birds (of other species). Some host birds engage in direct conflict with the intruding cuckoos. For example, if a host bird discovers that eggs are not their own, it will either discard these alien eggs or simply abandon its nest and build a new nest elsewhere. CS idealised such breeding behaviour and thus can be applied in various optimisation problems [Dhivya et al., 2011] [Gandomi et al., 2013] [Vázquez, 2011] [Xin-She Yang and Deb, 2010]. CS applies both local and global searches, controlled by a switching/discovery probability. The local search consumes about 1/4 of the search time (for P_a = 0.25), while the global search consumes about 3/4 of the total search time. The methodology allows the search space to be explored more efficiently on the global scale, and consequently the global optimisation can be located with a higher probability.

In addition, the CS algorithm is enhanced through Lévy flight [Viswanathan et al., 1996] rather than by the original, more conventional isotropic random walk principle. As Lévy flights are characterised by infinite mean and variance, CS can explore the search space more efficiently than algorithms following the standard Gaussian process. This advantage, combined with both local and search capabilities and guaranteed global convergence, makes CS very efficient [Pinar Civicioglu and Besdok, 2011] [Gandomi et al., 2013] [Walton et al., 2011], outperforming other meta-heuristic algorithms in applications. Recent studies show that CS is potentially more efficient than the Particle Swam Optimisation (PSO) and Genetic Algorithm (GA) [Xin-She Yang and Deb, 2014].

The CS follows three idealised rules;

- Each cuckoo lays one egg at a time, and dumps its egg in a randomly chosen nest;
- The best nests with high-quality eggs are carried over to the next generations;
- The number of available host nests is fixed, and the egg laid by a cuckoo is discovered by the host bird with probability $P_a \in [0,1]$. In this case, the host bird can either dispose of the egg, or simply abandon the nest and build a completely new nest. In brief, a fraction P_a of the n host nests are replaced by new nests (with new random solutions).

Based on the above rules, the basic steps of the CS can be summarised as the pseudo code presented in Algorithm 6.3 [Xin-She Yang, 2010].

Algorithm 6.3: Pseudo code of the Cuckoo Search

Objective function: $f(x)$, $x = (x_1, x_2, \dots, x_d)^T$;

Generate an initial population of n *host nests* x_i $(i = 1,2, \dots, n)$;

while ($t <$ *MaxGeneration) or (stopping criterion)*

- *Get a cuckoo randomly (say, i) and replace its solution by performing Lévy flights;*
- *Evaluate its quality/fitness* F_i*; [for maximization,* $F_i \propto f(x_i)$*];*
- *Choose a nest among n* (say, i) *randomly;*
- *If* ($F_i > F_j$),
  Replace j by the new solution;
  End If
- *A fraction* (p_a) *of the worse nests are abandoned and new ones are built;*

- *Keep the best solutions/nests;*
- *Rank the solutions/nests and find the current best;*
- *Pass the current best solutions to the next generation;*

End while

6.5.1 Cuckoo Search Implementation

6.5.1.1 Objective Function

The objective is to optimise cell throughput, the sum of the capacity of all users within the HetNet. Mathematically, the optimisation problem is formulated as Equation (6.3) and is bound by a set of non-linear constraints;

$$Max \sum_{i=0}^{I} \sum_{u=1}^{U} \alpha_u^i \times C_{eff,u}^i \tag{6.3}$$

subject to

$$\frac{\sum_{i=1}^{I} \sum_{u=1}^{U} \alpha_u^i \times C_{eff,u}^i}{OF} \leq \sum_{i=0}^{I} C_{Eff,bh}^i \tag{6.4}$$

$$\sum_{i=1}^{I} C_{Eff,bh}^i = C_{GW} \tag{6.5}$$

$$Ub \geq C_{Eff,bh}^i \geq \frac{C_{GW}}{|I|} \times 0.2 \text{ for all } i \in I \tag{6.6}$$

$$\alpha_u^i = \{0,1\} \text{ for all } i \in I, u \in U \tag{6.7}$$

$$\sum_{i=0}^{I} \alpha_u^i = 1 \text{ for all } u \in U \tag{6.8}$$

where the notation $C_{eff,u}^i$ represents the effective capacity available to user u connected to network i and $C_{eff,u}^i$ is calculated as in Algorithm 5.1. The WiFi network is represented by index i i.e. network $i = 1 \leq i \leq I$ is the i-th WiFi network and I is total number of WiFi networks. $u = 1 \leq u \leq U$ represents the u-th user and U is the total number of users in entire HetNet. α_u^i is a binary indicator that can either be 1 or 0, indicating whether a user u is connecting to a network i.

C_{bh}^i is the backhaul capacity of network i and the constraints in Equation (6.4) stipulate that the sum of the capacity available to all users divided by the OF (Overbooking Factor) is bound by the total backhaul capacity. The constraint in Equation (6.5) ensures that the total backhaul capacity allocated to WiFi Mesh Nodes is equal to the capacity of the mesh Gateway, C_{GW}, i.e. the total backhaul capacity is constrained by the maximum GW capacity available and at the same time ensuring that all the Gateway capacity is fully utilised to avoid wastage. The constraint in Equation (6.6) ensures that the minimum backhaul capacity $C_{Eff,bh}^i$ of a mesh node is guaranteed and at the same time does not exceed the upper bound capacity Ub. In the simulation, the upper bound capacity Ub is set to 100 Mbps as the bandwidth assigned to an AP is rarely larger than this value and at the same time such a value

reduces the search time for the CS. The constraint in Equation (6.8) stipulates that each user can only be connected to one network at a time.

6.5.1.2 Penalty Method

The objective function as described in Section 6.5.1.1 is a nonlinear optimisation problem with equality constraints. The Penalty Method [Xin-She Yang, 2010] is used to simplify the objective function so that the constrained problem is transformed into an unconstrained problem within CS.

The constraint in Equation (6.5) is rewritten as Equation (6.9) and the maximisation problem in Equation (6.3) is transformed into the minimisation problem by rewriting the objective function into Equation (6.10);

$$\sum_{i=1}^{I} C_{bh}^{i} - C_{GW} = 0 \tag{6.9}$$

$$Min\left[\frac{1}{\sum_{i=0}^{I}\sum_{u=1}^{U} C_{eff,u}^{i}} + \mu\left(\sum_{i=1}^{I} C_{bh}^{i} - C_{GW}\right)^{2}\right] \tag{6.10}$$

where $\mu \gg 1$ and in the simulation 10^{15} is used as recommended in [Xin-She Yang, 2010]. With the penalty function included, when an equality constraint is met, its effect or contribution to Equation (6.10) is zero. Otherwise, the penalty is heavy when there is a violation and the value of objective function will increase significantly.

6.5.1.3 Joint Cuckoo Search and DyBaCS Algorithm

The CS is implemented with DyBaCS, is initiated with no users connected to the HetNet and users are admitted one by one. On user admission, CS searches for the best Mesh APs' backhaul BA with the objective to maximise network throughput. Based on the bandwidth allocation, DyBaCS selects the best wireless network connection. After iteration, the CS compares the result with the objective function and refines the BA in the subsequent iteration. The iterations continue until either the objective is achieved or the maximum number of iterations allowed is reached. The best BA is then allocated to the Mesh APs. Flow charts of the joint CS and DyBaCS implementation are presented in Figure 6.5 and Figure 6.6.

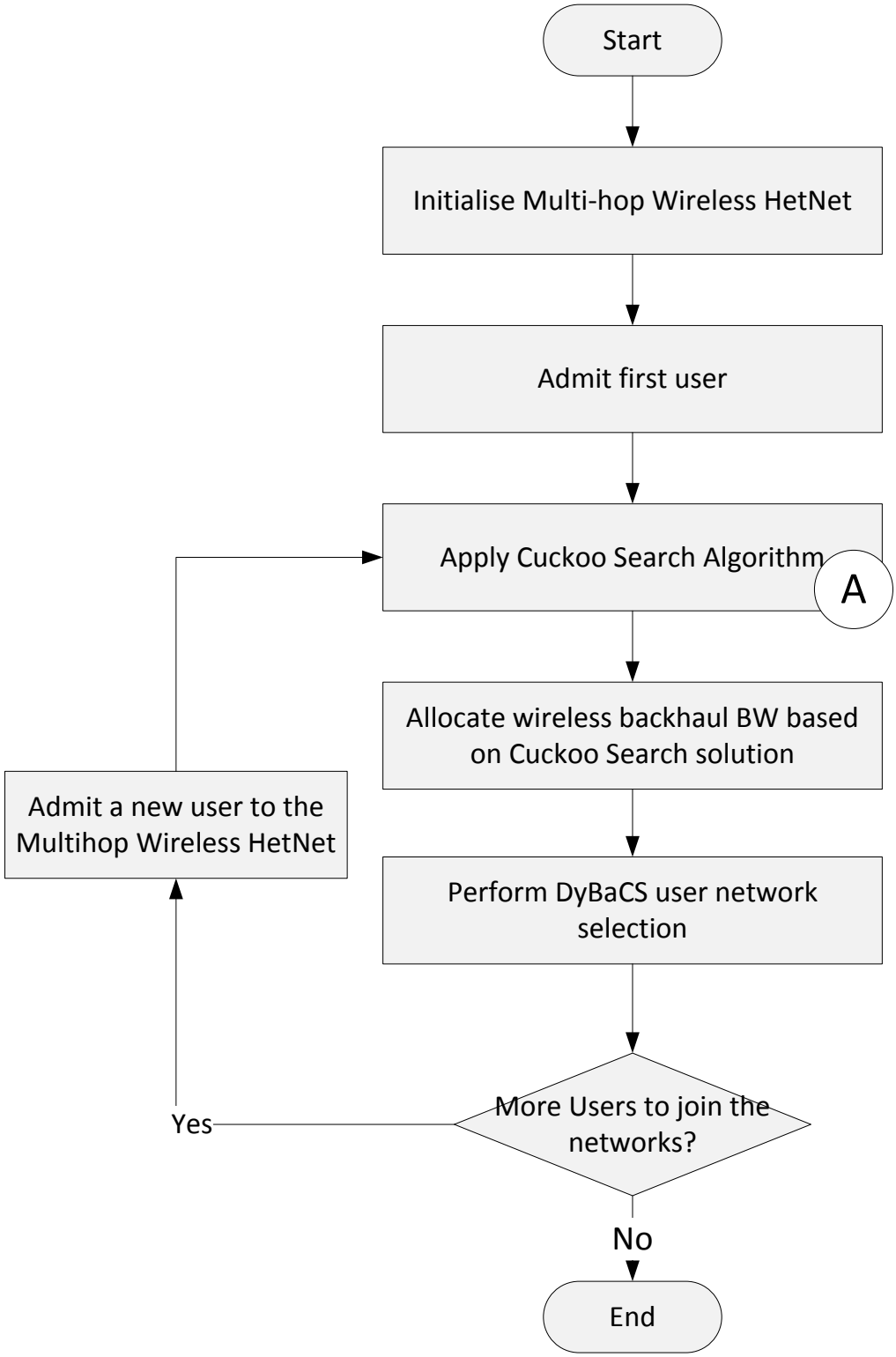

Figure 6.5: Flow chart of Bandwidth Allocation using Cuckoo Search and DyBaCS Network Selection Algorithm. The sub algorithm labelled with 'A' is presented in Figure 6.6.

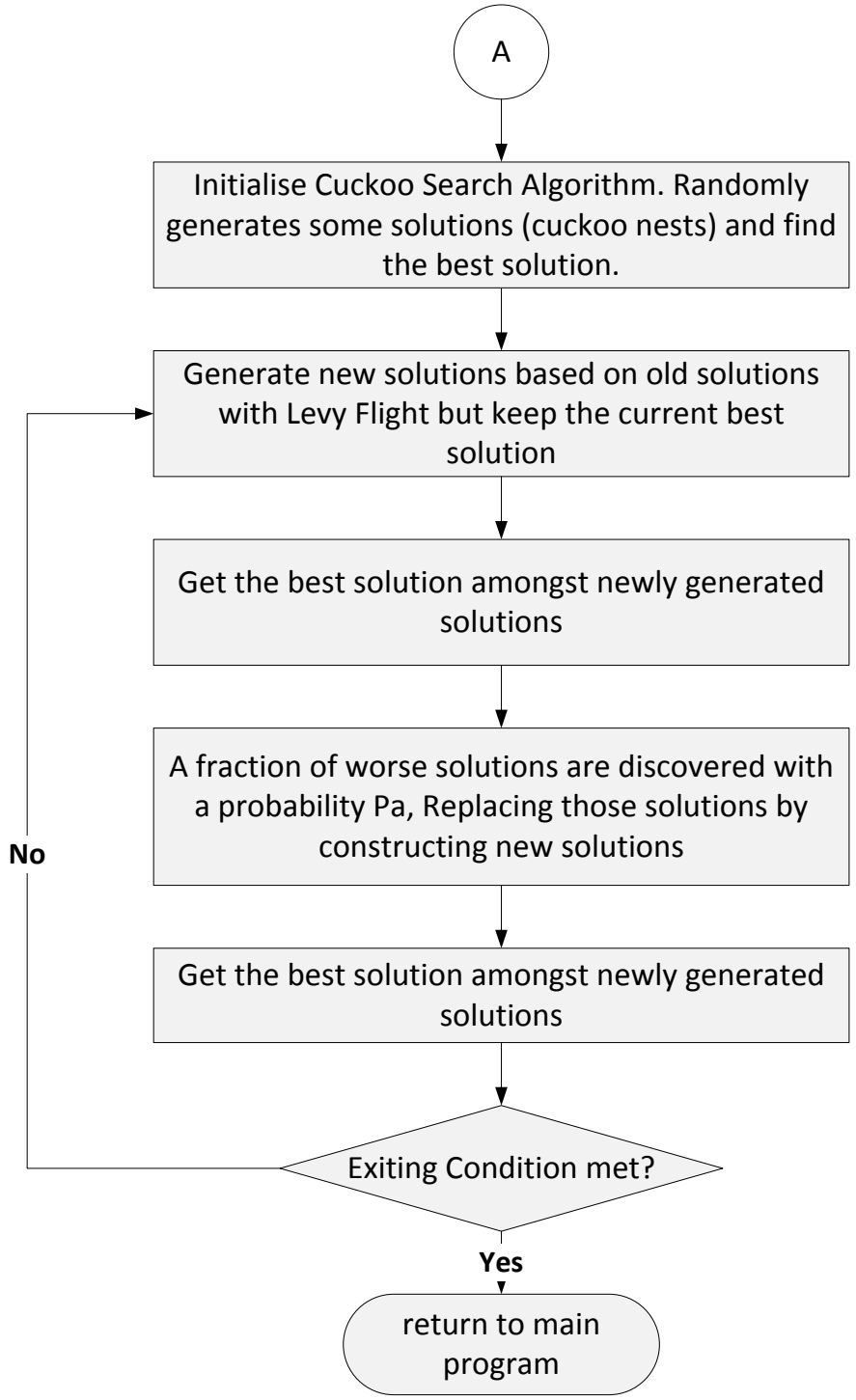

Figure 6.6: Cuckoo Search implementation to optimise the bandwidth allocation in Multi-hop Wireless HetNet.

6.6 Simulation Methodology and Assumptions

6.6.1 Topologies

Two WMN topologies consisting of a 7-cell-tessellation and 19-cell-tessellation are considered for the MWH evaluation. These topologies are selected with the purpose of demonstrating that the proposed algorithm is able to scale in terms of the number of mesh nodes as well as the number of hops. In the 7-cells-tessellation topology, all Mesh Nodes (MNs) are one hop away from the Gateway node, while the 19-cell-tessellation consists of six one-hop nodes and six two-hop nodes (Figure 6.7).

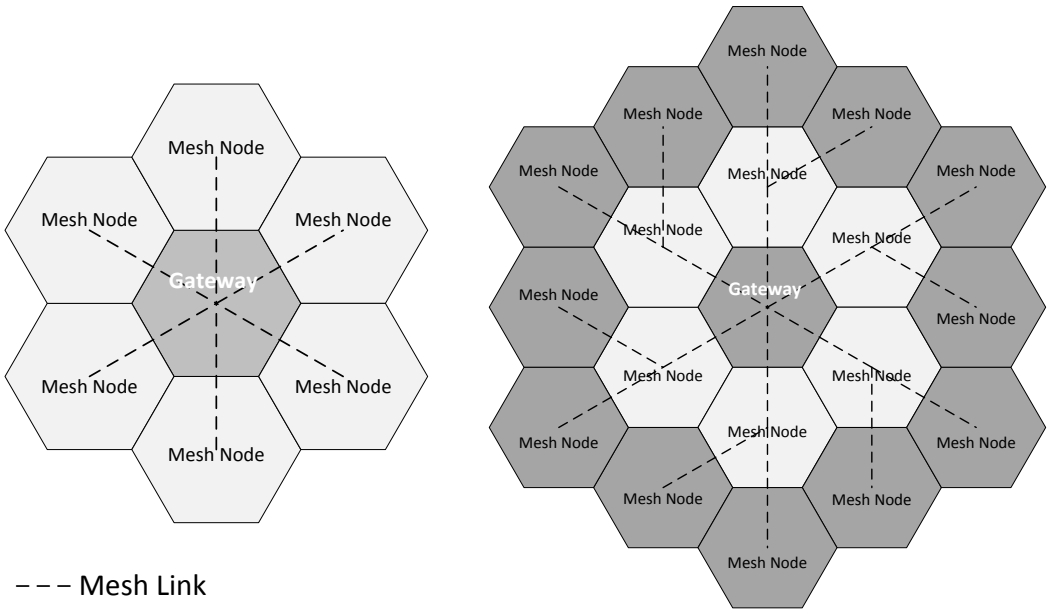

Figure 6.7: 7-cell-tessellation and 19-cell-tessellation mesh topologies.

The static mesh nodes are assumed to be equipped with one access radio and multiple backhaul radio interfaces. Each backhaul radio interface is paired with its neighbouring mesh radio and the total number of backhaul radios per mesh node

depends on the total number of neighbours. With multi-hop links being formed between mesh nodes, the traffic in WMNs is directed from or towards the GW through multi-hop relaying. In the simulation, only the downlink performance of the HetNet is evaluated.

6.6.2 Channel Assignment

Based on the channel assignment algorithm (Section 4.1.3), the best channel is assigned so that non-overlapping channel is used between two adjacent access radios as well as mesh links. There are three 20 MHz non-overlapping channels [IEEE Std, 1999b] in the 2.4 GHz band and twelve 20 MHz non-overlapping channels in the 5 GHz band [IEEE Std, 1999a]. When 40 MHz channel bonding is assumed in the 5 GHz band, the total number of non-overlapping channels is halved.

6.6.3 Mesh Gateway (GW)

The Mesh GW is assumed to be backhauled to the core network with capacity C_{GW} and that capacity is shared among MNs as well as the Gateway node. It is assumed that the Gateway itself or any other intelligent module/algorithm operating in the core network has the capability to allocate a portion of the Gateway bandwidth C_{GW} to all nodes in the mesh network and the proposed algorithm is used to determine the amount of capacity to be assigned to the MNs.

6.6.4 Simulation Parameters

The simulation parameters used for the WiFi mesh and LTE are summarised in Table 6.4.

Table 6.4: Simulation parameters.

	WiFi Access	**WiFi Mesh**	**LTE**	**Unit**
Technology	802.11n	802.11n	Release 10	-
Channel Bandwidth	20	40	20	MHz
Frequency Band	2.4	5	2.6	GHz
MIMO	2x2	2x2	2x2	-
Max EIRP	18, 27	30	36	dBm
WiFi GW Capacity	-	350 (7 MNs), 600 & 900 (19 MNs)	-	Mbps
LTE backhaul capacity	-	-	Sufficient Capacity Assumed	Mbps
Mesh node bandwidth allocation weight, $\mathcal{R}^i$	-	15	-	-
Packet size		1000		Bytes
User Information				
Overbooking Factor, *OF*		10:1		-
User density		250		Users/sqkm

The technology adopted for WiFi access is 802.11n with 20 MHz operating in the 2.4 GHz band, while 802.11n with 40 MHz channel bandwidth is adopted for mesh backhaul operating in the 5 GHz band. 2x2 MIMO is assumed for both access and

backhaul. The LTE uses 2.6GHz and 2x2 MIMO. The rest of the parameters are as detailed in Section 5.5.4, where traffic with fixed packet size of 1000 Bytes with constant bit rate traffic is assumed. A 10:1 OF is adopted to represent a relatively heavy usage scenario for a user density of 250 users per square km. User placement follows the stochastic model described in Section 5.5.1 and depicted in Figure 5.3.

6.6.5 Algorithms under Evaluation

The proposed MBA algorithm is compared to two other BA algorithms viz. Fair Share (FS) and CS. MBA and CS are explained in Section 6.4 and Section 6.5 respectively, while FS is implemented in such a way that the GW bandwidth is allocated fairly to all MNs. In addition to the proposed joint algorithm (PJA - MBA cum DyBaCS algorithm), combinations of different types of BA algorithms (MBA, FS and CS) and NSSs (DyBaCS, WF and PDR) are also evaluated. WF and PDR are explained in Section 5.4.1 and Section 5.4.2. In total, seven combinations are evaluated and listed in Table 6.5.

Table 6.5: Combination of bandwidth allocation and network selection algorithms under evaluation.

Type	**Combination of Algorithm**		**Name in Short**
	Bandwidth Allocation	**Network Selection**	
1	MBA	DyBaCS	PJA
2	CS	DyBaCS	CS
3	FS	DyBaCS	-
4	MBA	WF	-
5	FS	WF	-
6	MBA	PDR	-
7	FS	PDR	-

6.7 Result and Analysis

For the 7-mesh node-scenario, results show that 350 Mbps is the maximum GW bandwidth required; higher GW bandwidths do not yield better cell throughput. Hence these values are chosen for further discussion. For the 19-mesh-node scenario, a maximum GW bandwidth of 900 Mbps is required. However, in order to demonstrate the performance of the proposed algorithm as a function of GW capacity, results for GW bandwidths of 600 Mbps and 900 Mbps are also presented for the 19-mesh-node scenario.

Two performance metrics viz. cell throughput and user throughput fairness within the HetNet are used to evaluate the performance of all algorithms. Cell throughput is calculated by summing all user throughputs and user throughput fairness is calculated based on Jain fairness index as described in Section 5.6.1.

6.7.1 7 Mesh Node Network

Figure 6.8(a) shows the cell throughput for the PJA, CS and a combination of various BA and NSS algorithms for the 7-mesh-node network. Generally, when the number of user in the MWH increases, cell throughput increases and reaches its peak at 140 users. Thereafter cell throughput flattens and starts to drop when the number of users exceeds 150 due to more users with lower link quality joining the HetNet compromising overall network performance.

CS has the highest cell throughput with a maximum at 460 Mbps when the number of users is 140. CS is closely followed by the PJA with a peak cell throughput of 440 Mbps, 4% lower than CS. Removing MBA and Pairing FS with DyBaCS degrades the cell throughput; however with this combination, the cell throughput is still greater than any other combination without DyBaCS, such as MBA+WF, FS+WF, MBA+PDR and FS+PDR. Results show that, although a good network selection algorithm is vital, without the support of an appropriate BA algorithm the throughput performance is not optimal.

Figure 6.8(b) shows the bandwidth fairness sharing characteristics for different algorithms. The PJA yields the best fairness - higher than 0.95 - when the number of users does not exceed 160. Beyond 160 users, the fairness drops gradually to slightly below 0.65 when the number of users reaches 250. The PJA is followed by the CS as well as the combination of FS and DyBaCS; algorithms with WF are the worst in terms of fairness. The fairness of CS is lower than PJA as it has been traded-off for higher cell throughput, a typical challenge in multiple objective optimisation scenarios where the optimisation of one objective is normally at the expense of other objectives. The objective of CS is mainly to optimise cell throughput; hence fairness is sacrificed. The throughput performance of PJA is very close to CS, around 3% lower than CS on average, whilst provisioning the highest fairness amongst all algorithms, thus achieving a good balance between cell throughput and fairness.

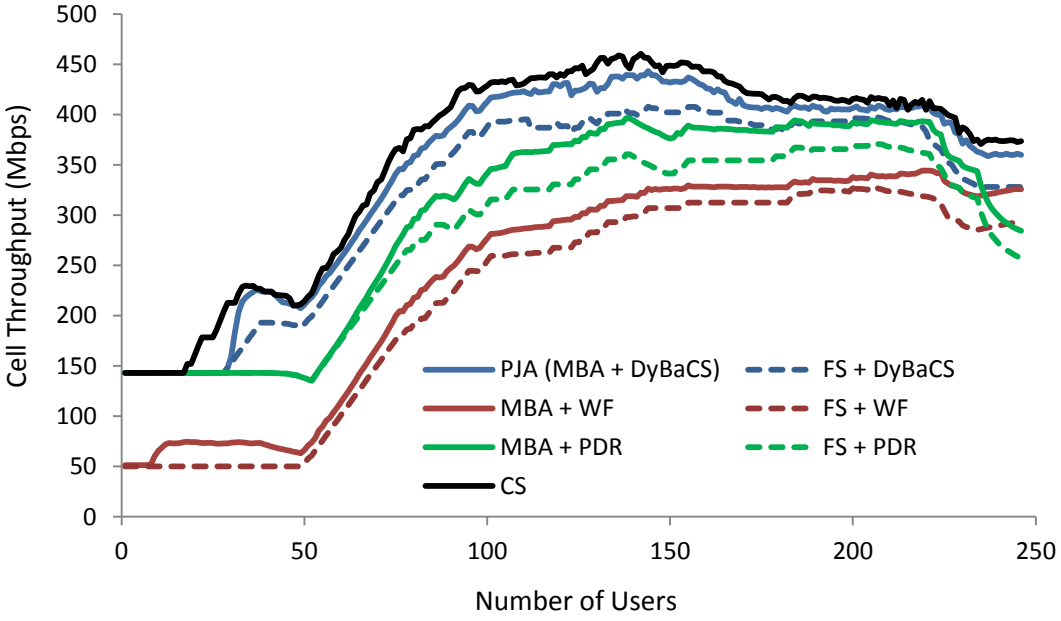

(a) Cell Throughput.

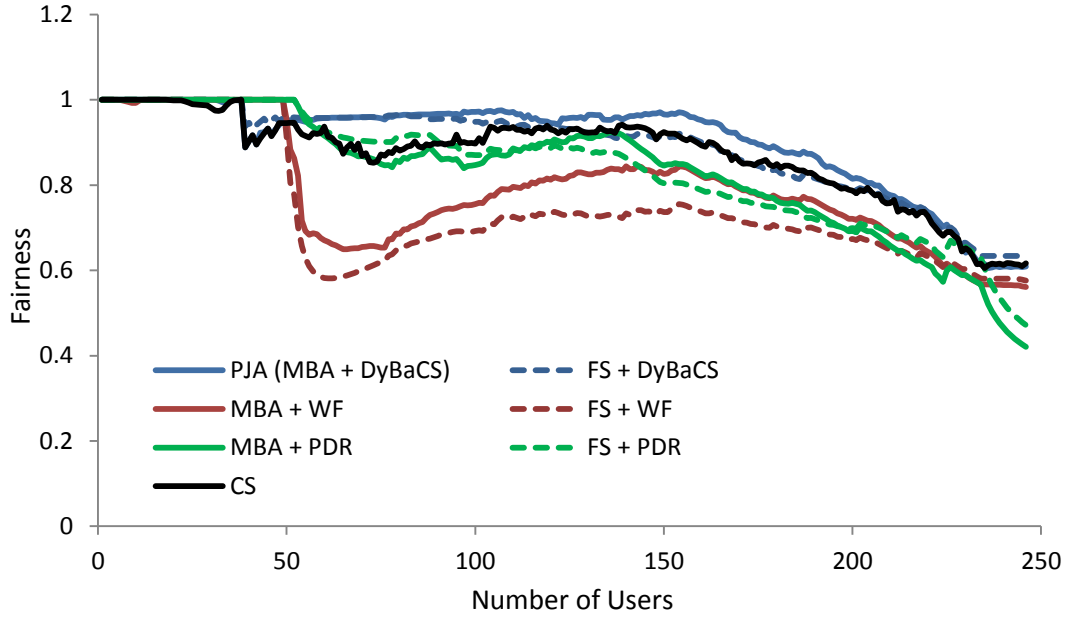

(b) Fairness.

Figure 6.8: Multi-hop Wireless HetNet (a) Cell Throughput and (b) Fairness for 7-mesh-node scenario; for a 350 Mbps GW bandwidth.

6.7.2 19 Mesh Node Network

Figure 6.9 shows the results for the 19-mesh-node network with a GW capacity of 600 Mbps. From Figure 6.9(a), the CS yields the highest cell throughput with the peak throughput reaching 660 Mbps when the number of users is 177, while the PJA provisioning a peak cell throughput of 584 Mbps at 225 users.

The fairness characteristics depicted in Figure 6.9(b) show that the PJA is best with a fairness higher than 0.96 when the number of users is below 230. As the number of users exceeds 230, the PJA derived fairness drops gradually to 0.88 at 250 users. Although the fairness of FS+PDR is higher than PJA when the number of users is less than 120, the fairness drop drastically when the number of users exceeds 120, showing that this algorithm is not as scalable.

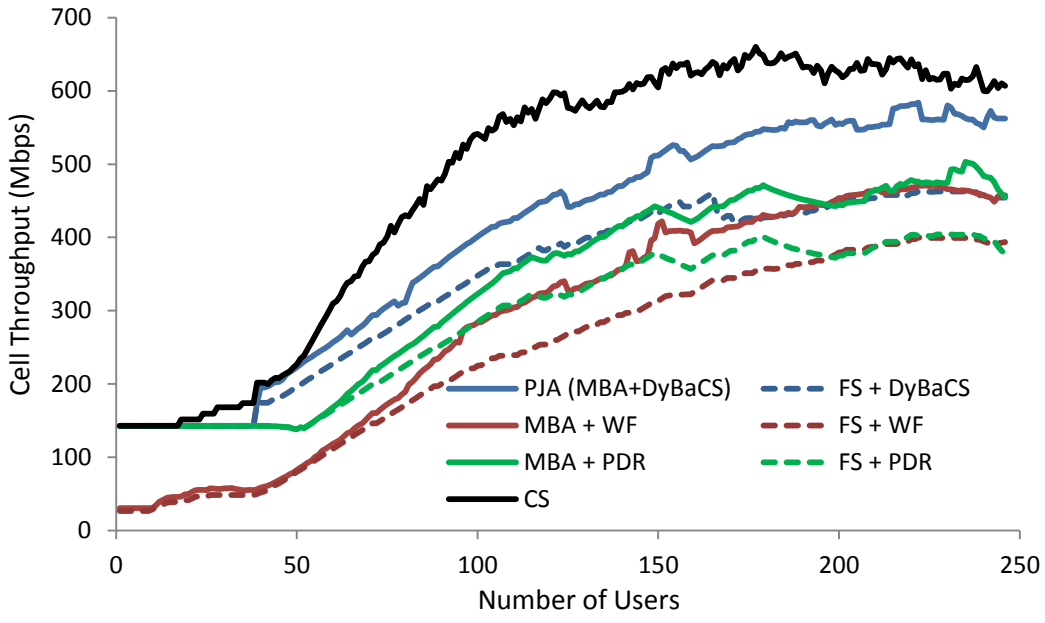

(a) Cell Throughput.

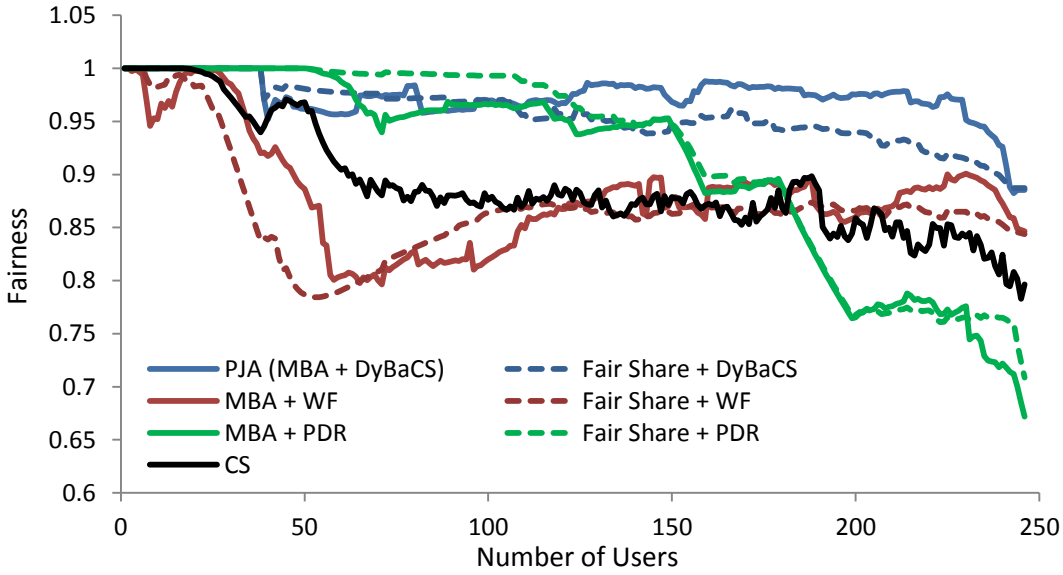

(a) Fairness.

Figure 6.9: Multi-hop Wireless HetNet (a) Cell Throughput and (b) Fairness for 19-mesh-node scenario; for a 600 Mbps GW bandwidth.

CS provides good fairness of 0.85 only at a low number of users and drops when number of users is higher than 100. Again in this scenario, the CS trades-off even more fairness for a higher throughput gain as compared to the 7-mesh-node network because the throughput is much higher than PJA and other algorithms but the fairness is amongst the worst.

Figure 6.10 presents results for an increase in GW capacity to 900 Mbps for the 19-mesh-node topology. Figure 6.10(a) shows that the cell throughput of all algorithms reaches their peak when the number of users is around 185. As expected the CS yields the highest cell throughput with the peak value reaching 780 Mbps, followed by the PJA with the maximum throughput reaching 720 Mbps. The difference in cell throughput for CS and PJA at their peak is around 7.7% and less than 10% on

average. The result shows that the PJA maintains performance with varying GW capacity.

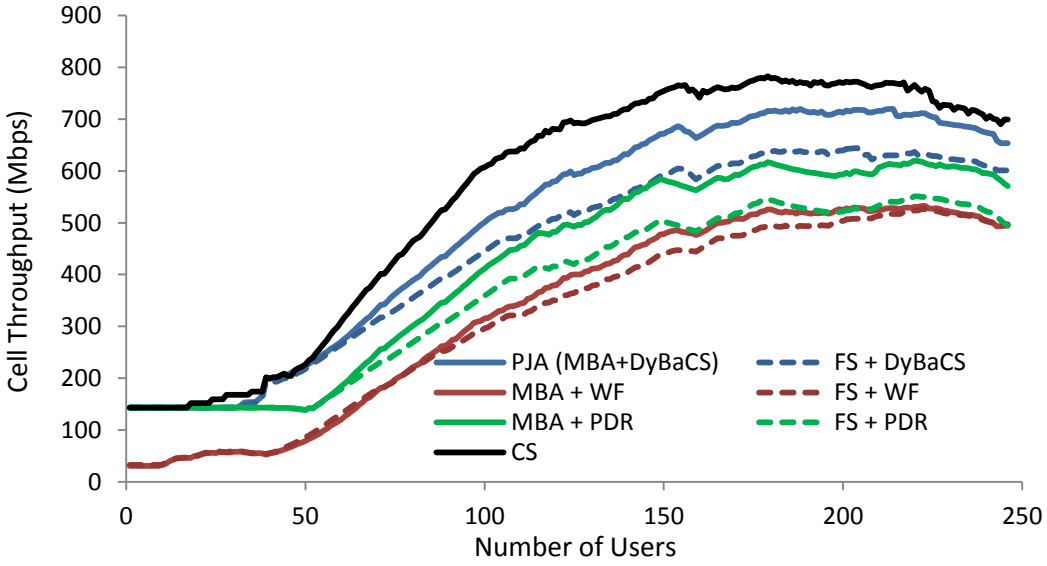

(a) Cell Throughput.

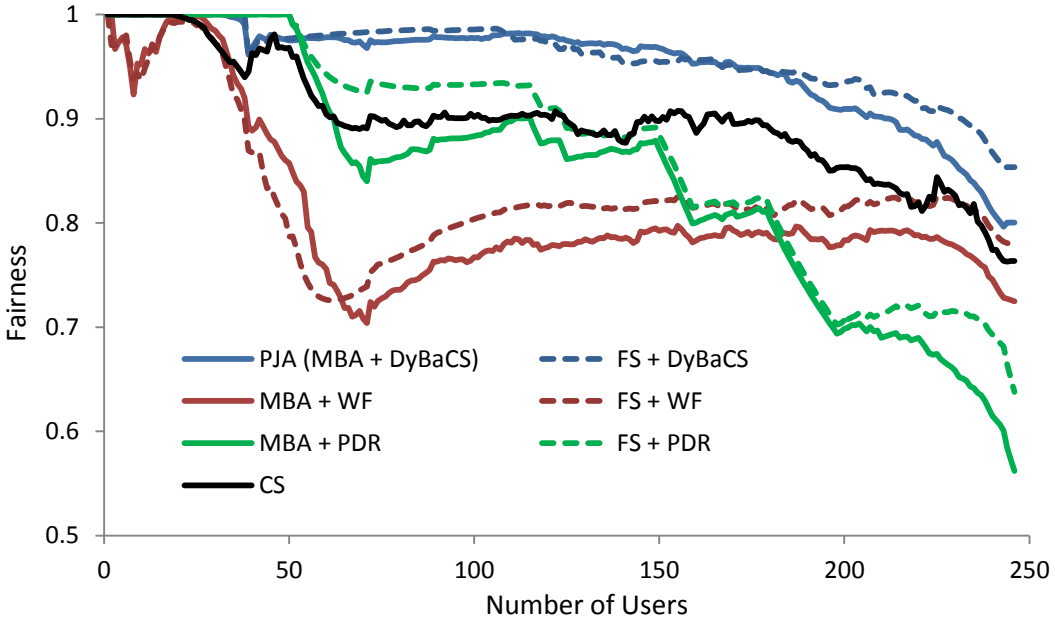

(a) Fairness.

Figure 6.10: Multi-hop Wireless HetNet (a) Cell Throughput and (b) Fairness for 19-mesh-node scenario; for a 900 Mbps GW bandwidth.

Figure 6.10(b) shows that the PJA and FS+DyBaCS are the best in terms of fairness, performing equally well when the number of users is less than 180. However as the number of users exceed 180, FS+DyBaCS remains higher than 0.85 and the PJA is higher than 0.8; the fairness achievable by CS is much lower than PJA.

The throughput difference between PJA and CS actually decreases on increasing the GW capacity from 600 Mbps to 900 Mbps (Figure 6.9 and Figure 6.10). The CS aims to optimise the overall network capacity and fairness is not the objective; however PJA aims to provide a balance between throughput and fairness. Thus, with limited GW capacity the unfairness becomes more severe as shown by large throughput difference; the situation eases with increasing GW capacity to share amongst the users.

In practical deployments, the maximum required GW capacity should be provided as it is a wasteful of resources to invest in a high capacity infrastructure with limited backhaul capacity to the core network.

6.8 Conclusions

Multi-hop Wireless HetNet (MWH) is a topic yet to be widely explored and the research is the first study of its kind addressing the throughput and fairness performance in such network architectures.

A joint MBA cum DyBaCS NSS - referred to as PJA - is proposed to improve the performance of MWHs. The proposed MBA algorithm features three components viz.

Predictive Bandwidth Allocation, Dynamic Bandwidth Capping and Multi-hop Links Capacity Awareness which in combination offer an improvement to the overall MWH throughput performance and fairness.

For the purposes of a rigorous comparison of the performance of the PJA for two key network metrics –throughput and fairness – the well reported and analysed Cuckoo Search (CS) and Fair Share (FS) bandwidth allocation algorithms are selected and implemented. The performance of the PJA is then compared to results obtained using combinations of different types of BA algorithms (CS and FS) and NSSs (DyBaCS, WF and PDR). A summary of all performance results is presented in Table 6.6.

The results show that the PJA is resilient in improving cell throughput whilst maintaining high levels the fairness. As expected the cell throughput achievable using PJA is lower than the CS algorithm owing to the latter's more complicated structure which translates into a longer time to execute, requiring many tens of thousands iterations to obtain the optimal result. Consequently, PJA is more suitable for dynamic wireless environments subject to challenging, real time changes. Furthermore, the CS algorithm used in the comparisons is tuned solely to optimise the cell throughput through trading off fairness; even under such a condition the achievable PJA cell throughput is close to CS especially when the GW is able to provision the maximum required capacity by the mesh network. The throughput difference of PJA and CS in such scenarios is less than 10% and 4% for the 19-node and 7-node-networks respectively.

Table 6.6: Performance summary of algorithms under study.

Algorithm	Throughput	Fairness	Scalability
PJA (MBA+DyBaCS)	High	High	High
CS	High	Medium	Medium
FS+DyBaCS	Medium	High	Medium
MBA + PDR	Medium	Medium	Medium
FS + PDR	Medium	Medium	Medium
MBA + WF	Poor	Poor	Poor
FS + WF	Poor	Poor	Poor

The evaluation of the performance of PJA under two representative MWH scenarios also proves that the algorithm is scalable in terms of both network size and varying GW capacity. Scalability is vital in scenarios with growing capacity demand, allowing progressive, staged deployments by operators.

Chapter 7

Conclusions and Future Work

7.1 Conclusions

The dissertation starts by discussing the challenges facing by existing mobile networks in meeting ever-growing capacity demands, followed by an overview of the technology advancements that support that demand. The review shows that Wireless Heterogeneous Networks (HetNets) are capable of providing a step enhancement in network capacity in a cost-effective manner and are one of the most promising approaches to meeting the growth demands.

Background research to date on HetNet shows that existing HetNet architectures can be categorised into three types; Single Carrier Usage (SCU), Distinct Carrier Usage (DCU) and Hybrid Carrier Usage (HCU); DCU is the most promising solution to enhancing HetNet cell capacity. From existing standards and the activities of industrial bodies supporting Cellular-WiFi integration, it is found that a major focus centres on issues inherent with interworking such as security, mobility support, QoS and network selection for offloading and little attention is being devoted to addressing the challenges of small cell backhauling.

The research therefore discusses and evaluates the performance of two types of HetNets, namely Hotspot Wireless HetNet (HWH) and Multi-hop Wireless HetNet

(MWH). In particular two algorithms which aim to optimise throughput and fairness considering the issues and challenges owing to small cells backhauling are proposed and evaluated.

HWH and MWH are studied in detail using Matlab simulation. Spatial models of LTE and WiFi networks are developed separately and combined to form a HetNet platform. Using the integrated model, a novel Network Selection Scheme (NSS) referred to as DyBaCS is developed taking the backhaul capacity of small cells into consideration during network selection. DyBaCS is also used to manage the non-uniform backhaul capacity distribution in HWHs, especially when a mixture of different wireless and wired technologies are adopted for backhaul. DyBaCS is designed to ensure a consistently fair network bandwidth distribution whilst maintaining network throughput. The performance of DyBaCS and two other network selection schemes (NSSs) is evaluated and compared with different types of commonly used end users' NSSs such as WiFi First and Physical Data Rate (PDR). Results show that the DyBaCS scheme provides superior fairness and user throughput performance across the range of backhaul capacities considered. Furthermore DyBaCS is able to scale better than WF and PDR across different user and WiFi densities. The performance of DyBaCS depends on the WiFi-LTE node ratio or the ratio of the number of WiFi nodes to the number of users. DyBaCS is particular impactful when the ratio of WiFi nodes to the number of user is low, as the algorithm is able to better manage HetNet throughput and fairness compared to other NSS.

The study is then extended to a more complex MWH architecture where an algorithm with joint Multi-hop Bandwidth Allocation (MBA) cum DyBaCS NSS - referred to as Proposed Joint Algorithm (PJA) - is developed for performance improvement. The proposed MBA algorithm features three components viz. Predictive Bandwidth Allocation, Dynamic Bandwidth Capping and Multi-hop Links Capacity Awareness in combination, offering an improvement to the overall MWH throughput performance and fairness. For the purposes of a performance comparison, the Cuckoo Search (CS) and Fair Share (FS) bandwidth allocation schemes are implemented. The simulation performance of the PJA is compared to results obtained using combinations of different types of bandwidth allocation schemes (CS and FS) and NSS schemes (DyBaCS, WF and PDR). Results show that the PJA is resilient in improving cell throughput whilst maintaining high levels the fairness.

Although cell throughput achievable using PJA is lower than CS, the throughput difference between the PJA and CS is less than 10% for various scenarios. CS which is a more complicated algorithm that consumes a much longer execution time to reach an optimal result, while the computationally simple and fast response PJA is more suitable for dynamic wireless environments subject to challenging, real time variations in operational conditions. Furthermore, the CS algorithm trades off fairness in order to optimise cell throughput. The evaluation of the performance of PJA under two representative MWH scenarios as a function of the number of small cells and GW capacity prove that the scheme is scalable in terms of both network size and varying GW capacity. It is worth noting that with algorithms which predominantly optimise network throughput such as CS, low GW capacity increases

the unfairness. It is important to provide the maximum GW capacity supported by the mesh network.

In summary, the research proposes two algorithms which aim to optimise throughput and fairness of an entire HetNet considering issues and challenges owing to small cells backhauling.

The implementation of the proposed algorithms requires signalling and communications amongst users, WiFi APs and LTE BS. In practice, signalling is especially crucial as it informs the system about the users and their activity. Communication between BS, APs and users result in optimum decisions on the admission of a user and network selection.

The proposed algorithms allow network operators to enjoy a higher level of freedom on the selection of their backhaul strategies. The algorithm is able to optimise overall HetNet throughput and fairness irrespective of the type of backhaul, wired or wireless with single hop or multi-hop capability.

7.2 Future Work

The following areas should be explored further to improve the accuracy and practicality of the proposed algorithms:

- Currently, the LTE scheduler is assumed to allocate the resource in a fair share manner. Using the fair share scheduling method, the existence of users

with low data rate greatly slows down the entire network. In future research, consideration of more realistic proportional fairness capacity sharing schemes is desirable with the potential to provide further improvement of HetNet performance.

- Evaluation of algorithm performance under different traffic types also needs to be addressed. Currently, the study focuses on data access for Internet browsing and consequently the traffic is not delay sensitive. In the future, QoS should be considered during both network selection and bandwidth allocation. Practically, network selection or handover of a user device to another network must consider traffic type owing to the application. Currently users switch to the best BS/AP to optimise network throughput and fairness assuming that all users are on non-delay-sensitive applications. Modelling of delay sensitive traffic such as video and voice should be included.

- The application of the proposed algorithms in a multi-homing capable HetNet is also an area of worthwhile research. Multihoming enables a device to simultaneously connect to both the BS and AP. Hence, enabling multi-homing releases higher flexibility in terms of resource allocation as well as potential improvement on user fairness.

References

[3GPP, 2001] 3GPP. (March 2001). Technical Report 25.848, "Physical layer aspects of UTRA High Speed Downlink Packet Access", version 4.0.0.

[3GPP, 2008a] 3GPP, "Evolved Universal Terrestrial Radio Access (E-UTRA); Radio Frequency (RF) system scenarios (Release 8)". 3GPP TR 36.942 V8.1.0 2008.

[3GPP, 2008b] 3GPP. (Dec 2008b). TS 23.002, "Network Architecture (Release 8)".

[3GPP, 2008c] 3GPP. (2008c). TS 23.234, "3GPP system to Wireless Local Area Network (WLAN) Interworking".

[3GPP, 2008d] 3GPP. (2008d). TS 23.261, "IP flow mobility and seamless Wireless Local Area Network (WLAN) offload".

[3GPP, 2008e] 3GPP. (2008e). TS 23.327, "Mobility between 3GPP-Wireless Local Area Network (WLAN) interworking and 3GPP systems".

[3GPP, 2008f] 3GPP. (Dec 2008f). TS 23.401, "GPRS Enhancement for E-UTRAN Access (Release 8)".

[3GPP, 2008g] 3GPP. (Dec 2008g). TS 23.402, "Architecture Enhancement for Non-3GPP Accesses (Release 8)".

[3GPP, 2008h] 3GPP. (2008h). TS 24.312, "Access Network Discovery and Selection Function (ANDSF) Management Object (MO)".

[3GPP, 2010a] 3GPP, "Evolved Universal Terrestrial Radio Access (E-UTRA); Radio Frequency (RF) system scenarios (Release 10)". 3GPP TR 36.942 V10.2.0 2010.

[3GPP, 2010b] 3GPP. (2010b). TR 36.942 V10.2.0, "Evolved Universal Terrestrial Radio Access (E-UTRA); Radio Frequency (RF) System Scenario (Release 10)", 3rd Generation Partnership Project, Technical Specification Group Radio Access Networks, Technical Report, 2010. Available: www.3gpp.org

[3GPP, 2012a] 3GPP, "Evolved Universal Terrestrial Radio Access (E-UTRA): Physical layer procedures (Release 10)", TS 36.213 V10.5.0.

[3GPP, 2012b] 3GPP. (Sept 2012b). TR 36.839 v11.0.0, "Mobility Enhancements in Heterogeneous Networks (Release 11)".

[3GPP, 2012c] 3GPP. (2012c). TR 36.913, "Requirement for further advancements for Evolved Universal Terrestrial Radio Access (E-UTRA) (LTE-Advanced)", www.3gpp.org.

[3GPP, 2013] 3GPP. (2013). *LTE*. Available: http://www.3gpp.org/LTE [Accessed 18th Oct 2013].

[4G Americas, 2013] 4G Americas. (September 2013). "Integration of Cellular and Wi-Fi Networks".

[A. G. Forte et al., 2006] A. G. Forte, S. Shin & H. Schulzrinne. (November 2006). "IEEE 802.11 in the Large: Observations at an IETF Meeting".

[A. Handa, 2009] A. Handa. (Oct 2009). "Mobile Data Offload for 3G Networks: A White Paper". Available: http://www.intellinet-tech.com/Media/PagePDF/Data%20Offload.pdf

[A.Wacker et al., 1999] A.Wacker, Laiho-Steffens, J., Sipilae, K. & Heiska, K. (Year) Published. "The impact of the base station sectorisation on WCDMA radio network performance". *Proc. IEEE Veh, Technol. Conf. Fall*, Sept 1999, Amsterdam, The Netherlands. pp. 2611-2615.

[Afanasyev et al., 2010] Afanasyev, M., Chen, T., Voelker, G. M. & Snoeren, A. C. (2010). "Usage patterns in an urban WiFi network". *IEEE/ACM Transactions on Networking*, vol. 18, pp. 1359-1372.

[Agilent, 2001] Agilent. 2001. Digital modulation in communications system: An introduction. Available: http://cp.literature.agilent.com/litweb/pdf/5965-7160E.pdf.

[Agrawal and Zeng, 2015] Agrawal, D. & Zeng, Q.-A. (2015). *Introduction to wireless and mobile systems*, Cengage Learning.

[AirMagnet, 2008] AirMagnet. 2008. White Paper: "802.11n Primer". Available: http://airmagnet.flukenetworks.com/assets/whitepaper/WP-802.11nPrimer.pdf [Accessed 22 Jan 2014].

[Akyildiz et al., 2005] Akyildiz, I. F., Wang, X. & Wang, W. (2005). "Wireless mesh networks: a survey". *Computer networks*, vol. 47, pp. 445-487.

[Alcatel Lucent, 2013] Alcatel Lucent. 2013. Small Cells: An Introduction. Strategic White Paper.

[Alicherry et al., 2005] Alicherry, M., Bhatia, R. & Li, L. E. (Year) Published. "Joint channel assignment and routing for throughput optimization in multi-radio wireless mesh networks". *Proceedings of the 11th annual international conference on Mobile computing and networking*, 2005. ACM, pp. 58-72.

[Andersen et al., 1995] Andersen, J. B., Rappaport, T. S. & Yoshida, S. (1995). "Propagation measurements and models for wireless communications channels". *Communications Magazine, IEEE,* vol. 33, pp. 42-49.

[Andrews, 2013] Andrews, J. G. (2013). "Seven ways that HetNets are a cellular paradigm shift". *IEEE Communications Magazine,* vol. 51, pp. 136-144.

[Aruba Networks, 2012] Aruba Networks. 2012. The Whys and Hows of Deploying Large-Scale Campus-wide Wi-Fi Networks. Available: http://www.arubanetworks.com/pdf/technology/whitepapers/wp_Large-scale_campus-wide_wifi.pdf [Accessed 25 September 2015].

[Aviat Networks, 2011] Aviat Networks. (6th May 2011). "The LTE capacity shortfall: Why small cell backhaul is the answer". Available from: http://blog.aviatnetworks.com/2011/05/06/lte-capacity-shortfall-why-small-cell-backhaul-is-the-answer/.

[Balachandran et al., 2002] Balachandran, A., Bahl, P. & Voelker, G. M. (2002). "Hot-spot congestion relief and service guarantees in public-area wireless networks". *ACM SIGCOMM Computer Communication Review*, vol. 32, pp. 59-59.

[Barbarossa, 2005] Barbarossa, S. (2005). *Multiantenna wireless communications systems*, Artech House Publishers.

[Bari and Leung, 2007] Bari, F. & Leung, V. (2007). "Automated network selection in a heterogeneous wireless network environment". *IEEE Network: The Magazine of Global Internetworking,* vol. 21, pp. 34-40.

[Bejerano and Han, 2009] Bejerano, Y. & Han, S.-J. (2009). "Cell breathing techniques for load balancing in wireless LANs". *IEEE Transactions on Mobile Computing*, vol. 8, pp. 735-749.

[Bejerano et al., 2004] Bejerano, Y., Han, S.-J. & Li, L. E. (Year) Published. "Fairness and load balancing in wireless LANs using association control". *Proceedings of the 10th annual international conference on Mobile computing and networking*, 2004. ACM, pp. 315-329.

[Bender et al., 2000] Bender, P., Black, P., Grob, M., Padovani, R., Sindhushyana, N. & Viterbi, S. (2000). "CDMA/HDR: a bandwidth efficient high speed wireless data service for nomadic users". *IEEE Communications Magazine*, vol. 38, pp. 70-77.

[Bennis et al., 2013] Bennis, M., Simsek, M., Czylwik, A., Saad, W., Valentin, S. & Debbah, M. (2013). "When cellular meets WiFi in wireless small cell networks". *IEEE Communications Magazine*, vol. 51.

[Bi, 2005] Bi, Q. (2005). "A forward link performance study of the 1xEV‐DO rev. 0 system using field measurements and simulations". *Bell Labs Technical Journal*, vol. 10, pp. 5-19.

[Bredel and Fidler, 2008] Bredel, M. & Fidler, M. (2008). "A measurement study of bandwidth estimation in IEEE 802.11 g wireless LANs using the DCF". *NETWORKING 2008 Ad Hoc and Sensor Networks, Wireless Networks, Next Generation Internet.* pp. 314-325. Springer.

[C. Rigney et al., 1997] C. Rigney, Livingston, A.Rubens & Merit. (1997). IETF RFC 2138, "Remote Authentication Dial In User Service (RADIUS)".

[Caretti et al., 2012] Caretti, M., Crozzoli, M., Dell'Aera, G. & Orlando, A. (Year) Published. "Cell splitting based on active antennas: Performance assessment for LTE system". *Wireless and Microwave Technology Conference (WAMICON), 2012 IEEE 13th Annual*, 2012. IEEE, pp. 1-5.

[Cavalcanti et al., 2005] Cavalcanti, D., Agrawal, D., Cordeiro, C., Xie, B. & Kumar, A. (2005). "Issues in integrating cellular networks WLANs and MANETs: A futuristic heterogeneous wireless network". *IEEE Wireless Communications*, vol. 12, pp. 30-41.

[Chandrasekhar et al., 2008] Chandrasekhar, V., Andrews, J. G. & Gatherer, A. (2008). "Femtocell networks: a survey". *IEEE Communications Magazine*, vol. 46, pp. 59-67.

[Chen et al., 2008] Chen, K.-C., de Marca, J. R. B. & Roberto, J. (2008). *Mobile WiMAX*, Wiley Online Library.

[Chieng et al., 2007] Chieng, D., Hodgkinson, T., Ting, A., Rahim, R. & Kawade, S. (2007). "High-level capacity performance insights into wireless mesh networking". *BT Technology Journal*, vol. 25, pp. 76-86.

[Chieng et al., 2011] Chieng, D., Ting, A., Kwong, K. H., Abbas, M. & Andonovic, I. (Year) Published. "Scalability Analysis of Multi-tier Hybrid WiMAX-WiFi Multi-hop Network". *Global Telecommunications Conference (GLOBECOM)*, 2011. IEEE, pp. 1-6.

[Chieng et al., 2010] Chieng, D., von Hugo, D. & Banchs, A. (Year) Published. "A Cost Sensitivity Analysis for Carrier Grade Wireless Mesh Networks with Tabu Optimization". *2010 INFOCOM IEEE Conference on Computer Communications Workshops*, 2010. IEEE, pp. 1-6.

[Choi et al., 2011] Choi, Y., Ji, H. W., Park, J.-y., Kim, H.-c. & Silvester, J. A. (2011). "A 3W network strategy for mobile data traffic offloading". *IEEE Communications Magazine,* vol. 49, pp. 118-123.

[Cisco, 2005] Cisco. 2005. Deployment Guide: Cisco Aironet 1000 Series Lightweight Access Points. Available: http://www.cisco.com/c/en/us/td/docs/wireless/technology/ap1000/deployment/guide/hah_apdg.pdf [Accessed 25 September 2014].

[Cisco, 2008] Cisco. 2008. Radio Channel Frequencies. Available: http://www.cisco.com/en/US/docs/routers/access/3200/software/wireless/RadioChannelFrequencies.pdf.

[Cisco, 2012a] Cisco. 2012a. Architecture for Mobile Data Offload over Wi-Fi Access Networks. Available: http://www.cisco.com/c/en/us/solutions/collateral/service-provider/service-provider-wi-fi/white_paper_c11-701018.pdf [Accessed 28th Feb 2014].

[Cisco, 2012b] Cisco. 2012b. Challenges of Unlicensed Wi-Fi Deployments: A Practical Guide for Cable Operators Available: http://www.cisco.com/c/en/us/solutions/collateral/service-provider/service-provider-wi-fi/white_paper_c11-716080.pdf.

[Cisco, 2014] Cisco. (5th Feb 2014). "Cisco visual networking index: Global mobile data traffic forecast update, 2013-2018". Available: http://www.cisco.com/c/en/us/solutions/collateral/service-provider/visual-networking-index-vni/white_paper_c11-520862.pdf

[Cisco Meraki, 2014] Cisco Meraki. (2014). *https://meraki.cisco.com/*. [Accessed 24th October 2014].

[Claussen, 2005] Claussen, H. (Year) Published. "Efficient modelling of channel maps with correlated shadow fading in mobile radio systems". *IEEE 16th International Symposium on Personal, Indoor and Mobile Radio Communications (PIMRC)*, 2005. IEEE, pp. 512-516.

[Conniq.com, 2015] Conniq.com. 2015. Introduction to Multiple Antenna Systems: SIMO, MISO, MIMO. Available: http://www.conniq.com/WiMAX/mimo-02.htm.

[Dai et al., 2008] Dai, L., Xue, Y., Chang, B., Cao, Y. & Cui, Y. (2008). "Optimal routing for wireless mesh networks with dynamic traffic demand". *Mobile Networks and Applications,* vol. 13, pp. 97-116.

[Daldoul et al., 2011] Daldoul, Y., Ahmed, T. & Meddour, D.-E. (Year) Published. "IEEE 802.11 n aggregation performance study for the multicast". *2011 IFIP Wireless Days (WD)*, 2011. IEEE, pp. 1-6.

[Damnjanovic et al., 2011] Damnjanovic, A., Montojo, J., Wei, Y., Ji, T., Luo, T., Vajapeyam, M., Yoo, T., Song, O. & Malladi, D. (2011). "A survey on 3GPP heterogeneous networks". *IEEE Wireless Communications,* vol. 18, pp. 10-21.

[Das et al., 2006] Das, N. K., Shinozawa, M., Miyadai, N., Taniguchi, T. & Karasawa, Y. (2006). "Experiments on a MIMO system having dual polarization diversity branches". *IEICE transactions on communications,* vol. 89, pp. 2522-2529.

[Das et al., 2007] Das, S. M., Pucha, H. & Hu, Y. C. (2007). "Mitigating the gateway bottleneck via transparent cooperative caching in wireless mesh networks". *Ad Hoc Networks,* vol. 5, pp. 680-703.

[De la Oliva et al., 2012] De la Oliva, A., Banchs, A., Serrano, P. & Zdarsky, F. A. (2012). "Providing throughput guarantees in heterogeneous wireless mesh networks". *Wireless Communications and Mobile Computing*.

[Dhivya et al., 2011] Dhivya, M., Sundarambal, M. & Anand, L. N. (2011). "Energy efficient computation of data fusion in wireless sensor networks using cuckoo based particle approach (CBPA)". *Int'l J. of Communications, Network and System Sciences,* vol. 4, pp. 249.

[DNMA-92] DNMA-92, U. Unex DNMA-92: 802.11n a/b/g wifi 2x2 mini-PCI module, MB92/AR9220. Available: www.unex.com.tw/product/dnma-92.

[Dzal et al., 2014] Dzal, G. I. M., Feng, S., Tang, W., Feng, W. & Liu, Y. (Year) Published. "Joint Fair Resource Allocation for Multi-radio Multi-channel Mesh Networks with Flow Demand Constraint". *2014 Fourth International Conference on Communication Systems and Network Technologies (CSNT)*, 2014. IEEE, pp. 233-238.

[Easy Taxi, 2012] Easy Taxi. (2012). Available: http://www.easytaxi.com/ [Accessed 19th Jan 2014].

[Eldad and Robert, 2008] Eldad, P. & Robert, S. (2008). *Next generation wireless LANs: Throughput, robustness and reliability in 802.11 n*, Cambridge University Press.

[Ericsson, 2013] Ericsson. 2013. Wi-Fi in Heterogeneous Networks. Available: http://www.ericsson.com/res/docs/whitepapers/wp-wi-fi-in-heterogeneous-networks.pdf [Accessed 3rd April 2014].

[Ernst and Denko, 2011] Ernst, J. B. & Denko, M. K. (2011). "The design and evaluation of fair scheduling in wireless mesh networks". *Journal of Computer and System Sciences*, vol. 77, pp. 652-664.

[F. Perez Fontan, 2008] F. Perez Fontan, P. M. E. (2008). *Modeling the Wireless Propagation Channel: A Simulation Approach with MATLAB*, WILEY.

[FCC, 2013] FCC. 2013. 5 GHz Unlicensed Spectrum (UNII), http://www.fcc.gov/document/5-ghz-unlicensed-spectrum-unii

[Firetide, 2013] Firetide. 2013. Firetide Wireless Mesh Solutions for TELCOS: Access & Small CellBackhaul. Available: https://www.winncom.com/manufacturer/firetide [Accessed Jan 2013].

[Firetide, 2014] Firetide. (2014). *http://www.firetide.com/*. [Accessed 2 April 2014].

[Gabriel, 2013] Gabriel, C. (2013). Wireless broadband alliance industry report 2013: Global trends in public wi-fi.

[Galeana-Zapién and Ferrús, 2010] Galeana-Zapién, H. & Ferrús, R. (2010). "Design and evaluation of a backhaul-aware base station assignment algorithm for OFDMA-based cellular networks". *IEEE Transactions on Wireless Communications*, vol. 9, pp. 3226-3237.

[Gambiroza et al., 2004] Gambiroza, V., Sadeghi, B. & Knightly, E. W. (Year) Published. "End-to-end performance and fairness in multihop wireless backhaul networks". *Proceedings of the 10th annual international conference on Mobile computing and networking*, 2004. ACM, pp. 287-301.

[Gandomi et al., 2013] Gandomi, A. H., Yang, X.-S. & Alavi, A. H. (2013). "Cuckoo search algorithm: a metaheuristic approach to solve structural optimization problems". *Engineering with Computers*, vol. 29, pp. 17-35.

[Gao et al., 2013] Gao, L., Iosifidis, G., Huang, J. & Tassiulas, L. (Year) Published. "Economics of mobile data offloading". *2013 IEEE Conference on Computer Communications Workshops (INFOCOM WKSHPS)*, 2013. IEEE, pp. 351-356.

[Geier, 2002] Geier, J. T. (2002). *Wireless LANs*, Sams Publising.

[Ghaleb et al., 2013] Ghaleb, A. M., Chieng, D., Ting, A., Abdulkafi, A., Lim, K.-C. & Lim, H.-S. (Year) Published. "Throughput performance insights of LTE Release 8: Malaysia's perspective". *2013 9th International Wireless Communications and Mobile Computing Conference (IWCMC)*, 2013. IEEE, pp. 258-263.

[Ghosh et al., 2012] Ghosh, A., Mangalvedhe, N., Ratasuk, R., Mondal, B., Cudak, M., Visotsky, E., Thomas, T. A., Andrews, J. G., Xia, P. & Jo, H. S. (2012). "Heterogeneous cellular networks: From theory to practice". *IEEE Communications Magazine*, vol. 50, pp. 54-64.

[Goldsmith, 2005] Goldsmith, A. (2005). *Wireless communications*, Cambridge university press.

[Gong and Kim, 2008] Gong, H. & Kim, J. (2008). "Dynamic load balancing through association control of mobile users in WiFi networks". *IEEE Transactions on Consumer Electronics*, vol. 54, pp. 342-348.

[Gong et al., 2012] Gong, P., Li, P., Kong, J., Kim, S. H., Jung, H. B., Niu, X. & Kim, D. K. (Year) Published. "Power allocation with max-min fairness for

multicast in heterogeneous network". *2012 14th International Conference on Advanced Communication Technology (ICACT)*, 2012. IEEE, pp. 502-505.

[Gora and Kolding, 2009] Gora, J. & Kolding, T. E. (Year) Published. "Deployment aspects of 3G femtocells". *2009 IEEE 20th International Symposium on Personal, Indoor and Mobile Radio Communications*, 2009. IEEE, pp. 1507-1511.

[GSMA, 1995] GSMA. (1995). *GSM Association*. Available: http://www.gsma.com/ [Accessed 3rd Sept 2013].

[GSMA, 2003] GSMA. (22nd May 2003). PRD:SE.27, PRD SE.27: "Services, Ease of Use, and Operator Considerations in Interworked WLAN-Cellular Systems".

[Gu, 2005] Gu, Q. (2005). *RF system design of transceivers for wireless communications*, Springer.

[Guo et al., 2014] Guo, L., Wang, Y., Du, Z. & Gao, Y. (2014). "A Compact Uniplanar Printed Dual-Antenna Operating at the 2.4/5.2/5.8 GHz WLAN Bands for Laptop Computers".

[H. Claussen, 2007] H. Claussen. (Year) Published. "Performance of macro- and co-channel femtocells in a hierarchical cell structure". *IEEE Int. Symp. Personal, Indoor, Mobile Radio Commun. (PIMRC)*, 2007, Athens, Greece. pp. 1-5.

[Härdle and Simar, 2007] Härdle, W. & Simar, L. (2007). *Applied multivariate statistical analysis*, Springer.

[Harri Holma and Antti Toskala, 2004] Harri Holma & Antti Toskala. (2004). "WCDMA for UMTS, Radio Access for Third Generation Mobile Communications".

[Ho et al., 2012] Ho, P., Holtby, D. W., Lim, K., Kwong, K., Chieng, D., Ting, A. & Chien, S. (Year) Published. "End-to-end throughput and delay analysis of WiFi multi-hop network with deterministic offered load". *IET International Conference on Wireless Communications and Applications (ICWCA 2012)*, 2012. IET, pp. 1-6.

[Holma and Toskala, 2006] Holma, H. & Toskala, A. (2006). *HSDPA/HSUPA for UMTS: High Speed Radio Access for Mobile Communications, John Wiley & Sons.*

[Holma and Toskala, 2009] Holma, H. & Toskala, A. (2009). *LTE for UMTS-OFDMA and SC-FDMA based radio access*, John Wiley & Sons.

[Hu et al., 2008] Hu, H., Zhou, W., Zhang, S. & Song, J. (Year) Published. "A novel network selection algorithm in next generation heterogeneous network for modern service industry". *Proceedings of the 2008 IEEE Asia-Pacific Services Computing Conference*, 2008. IEEE Computer Society, pp. 1263-1268.

[Huang et al., 2010] Huang, H., Alrabadi, O., Samardzija, D., Tran, C., Valenzuela, R. & Walker, S. (Year) Published. "Increasing throughput in cellular network with higher order sectorization". *Proc. 2010 Asilomar Conference on Signals, Systems, and Computers*, 2010. pp. 630 - 635.

[IEEE Std, 2011] IEEE Std, 802.11u, "Part 11: Wireless LAN Medium AccessControl (MAC)and Physical Layer (PHY) Specifications, Amendment 9: Interworking with External Networks". IEEE Inc, 2011.

[IEEE Working Group, 2013] IEEE Working Group. (2013). *Official IEEE 802.11 working group project timelines. 15th November, 2013.* [Accessed 21st Jan 2014].

[IEEE Std, 1985a] IEEE Std, 802.3, "Part 3: Carrier Sense Multiple Access with Collision Detection(CSMA/CD) Access Method and Physical Layer Specifications". IEEE Inc, 1985.

[IEEE Std, 1985b] IEEE Std, 802.5, "Token Ring Access Method and Physical Layer Specificationss". IEEE Inc, 1985.

[IEEE Std, 1997] IEEE Std, "Part 11: Wireless LAN Medium Access Control (MAC) and Physical Layer (PHY) Specifications. IEEE Inc, June 1997".

[IEEE Std, 1999a] IEEE Std, 802.11a, "Part 11: Wireless LAN Medium Access Control (MAC) and Physical Layer (PHY) specifications, High-speed Physical Layer in the 5 GHz Band". IEEE Inc, 1999 (Reaffirmed 12 June 2003).

[IEEE Std, 1999b] IEEE Std, 802.11b, "Supplement to Part 11: Wireless LAN Medium Access Control (MAC) and Physical Layer (PHY) Specifications: Higher-Speed Physical Layer Extension in the 2.4GHz Band". IEEE Inc, Sept 1999.

[IEEE Std, 2003] IEEE Std, 802.11g, "Part 11: Wireless LAN Medium Access Control (MAC) and Physical Layer (PHY) specifications, Amendment 4: Further Higher Data Rate Extension in the 2.4 GHz Band". IEEE Inc, 27 June 2003.

[IEEE Std, 2005a] IEEE Std, 802.11e-2005, "Amendment 8: Medium Access Control (MAC) Quality of Service Enhancements", IEEE Inc, 11 Nov 2005.

[IEEE Std, 2005b] IEEE Std, 802.16e/D12, "IEEE Standard for Local and metropolitan area networks, Part 16: Air Interface for Fixed and Mobile Broadband Wireless Access System", IEEE Press, 2005.

[IEEE Std, 2007a] IEEE Std, 802.11-2007, "Part 11: Wireless LAN Medium Access Control (MAC) and Physical Layer (PHY) Specifications". IEEE Inc, 12 June 2007.

[IEEE Std, 2007b] IEEE Std, Annex J, IEEE Std. "802.11-2007, Part 11: Wireless LAN Medium Access Control (MAC) and Physical Layer (PHY) specifications". IEEE Inc, 12 June 2007.

[IEEE Std, 2009] IEEE Std, "802.11n-2009-Amendment 5: Enhancements for Higher Throughput". IEEE Inc, 29 October 2009.

[IEEE Std, 2011] IEEE Std, 802.11s, "Part 11: Wireless LAN Medium Access Control (MAC) and Physical Layer (PHY) specifications Amendment 10: Mesh Networking", IEEE Inc, 10 Sept 2011.

[Infonetics Research, 2013] Infonetics Research. (16th Jan 2013). "Small cell operators face myriad operational and financial challenges". Available: http://www.infonetics.com/

[Informa telecoms, 2013] Informa telecoms. 2013. Small cell market status. Available: http://www.smallcellforum.org/ [Accessed 2nd October 2013].

[Informa telecoms & media, 2013] Informa telecoms & media. (Feb 2013). "Small cell market status Feb 2013". Available: http://www.smallcellforum.org/smallcellforum_resources/pdfsend01.php?file=050-SCF_2013Q1-market-status%20report.pdf.

[InterDigital, 2012] InterDigital. 2012. Cellular-Wi-Fi Integration: A comprehensive analysis of the technology and standardization roadmap. Available: http://www.interdigital.com/wp-content/uploads/2012/08/Cellular_WiFi_Integration-White-Paper.pdf.

[ITU-D, 2013] ITU-D. (Feb 2013). "The world in 2013: ICT Facts and Figures". Available: http://www.itu.int/en/ITU-D/Statistics/Documents/facts/ICTFactsFigures2013-e.pdf

[ITU-R, 2003] ITU-R. (2003). Recommendation M.1645: "Framework and overall objectives of the future development of IMT-2000 and systems beyond IMT-2000".

[ITU-R, 2009] ITU-R. (December 2009 2009). Report M.2135-1: "Guidelines for evaluation of radio interface technologies for IMT-Advanced", December 2009.

[Jackman et al., 2011] Jackman, S. M., Swartz, M., Burton, M. & Head, T. W. (2011). *CWDP Certified Wireless Design Professional Official Study Guide: Exam PW0-250*, John Wiley & Sons.

[Jackson Juliet Roy et al., 2006] Jackson Juliet Roy, J., Vaidehi, V. & Srikanth, S. (Year) Published. "Always best-connected QoS integration model for the WLAN, WiMAX heterogeneous network". *First International Conference on Industrial and Information Systems*, 2006. IEEE, pp. 361-366.

[Jain et al., 1999] Jain, R., Durresi, A. & Babic, G. (1999). "Throughput fairness index: An explanation, ATM Forum/99-0045".

[Jamil A et al., 2010] Jamil A, Yusoff M.Z & Yahya N. (Year) Published. "Current issues and challenges of MIMO antenna designs". *2010 International*

Conference on Intelligent and Advanced Systems (ICIAS), June 2010. pp. 1,5, 15-17

[Jin et al., 2011] Jin, S., Xuanli, W. & Xuejun, S. (Year) Published. "Load balancing algorithm with multi-service in heterogeneous wireless networks". *2011 6th International ICST Conference on Communications and Networking in China (CHINACOM)*, 2011. IEEE, pp. 703-707.

[Judd and Steenkiste, 2002] Judd, G. & Steenkiste, P. (2002). "Fixing 802. 11 access point selection". *ACM SIGCOMM Computer Communication Review*, vol. 32, pp. 31-31.

[Karam and Jensen, 2012] Karam, F. W. & Jensen, T. (Year) Published. "Performance analysis of ranking for QoS handover algorithm for selection of access network in heterogeneous wireless networks". *2012 21st International Conference on Computer Communications and Networks (ICCCN)*, 2012. IEEE, pp. 1-6.

[Kumar et al., 2007] Kumar, D., Altman, E. & Kelif, J.-M. (2007). "Globally optimal user-network association in an 802.11 WLAN & 3G UMTS hybrid cell". *Managing Traffic Performance in Converged Networks.* pp. 1173-1187. Springer.

[Lee and Choi, 2008] Lee, B. G. & Choi, S. (2008). *Broadband wireless access and local networks: mobile WiMAX and WiFi*, Artech House.

[Lee et al., 2010] Lee, K., Lee, J., Yi, Y., Rhee, I. & Chong, S. (Year) Published. "Mobile data offloading: how much can WiFi deliver?". *Proceedings of the 6th International Conference*, 2010. ACM, pp. 26.

[Lei et al., 2013] Lei, L., Zhong, Z., Zheng, K., Chen, J. & Meng, H. (2013). "Challenges on wireless heterogeneous networks for mobile cloud computing". *IEEE Wireless Communications*, vol. 20.

[MacDonald, 1979] MacDonald, V. H. (1979). " Advanced mobile phone service: The cellular concept". *Bell System Technical Journal, 58.1,* pp. 15-41.

[Matlab] Matlab. Available: http://www.mathworks.com/.

[Mogensen et al., 2007] Mogensen, P., Na, W., Kovács, I. Z., Frederiksen, F., Pokhariyal, A., Pedersen, K. I., Kolding, T., Hugl, K. & Kuusela, M. (Year) Published. "LTE capacity compared to the shannon bound". *VTC2007-Spring. IEEE 65th Vehicular Technology Conference*, 2007. IEEE, pp. 1234-1238.

[Motorola Solutions, 2014] Motorola Solutions. (2014). *http://www.motorolasolutions.com/*. [Accessed 24th Oct 2014].

[Mulligan, 2012] Mulligan, C. (2012). *EPC and 4G Packet Networks: Driving the Mobile Broadband Revolution,* Academic Press.

[Networks, 2013] Networks, U. (2013). *NanoStation2*. Available: www.ubnt.com/products/nano.php [Accessed 23 Feb 2013].

[NGMN Alliance, 2012] NGMN Alliance. (4th June 2012). "Small Cell Backhaul Requirements". Available: https://www.ngmn.org/uploads/media/NGMN_Whitepaper_Small_Cell_Backhaul_Requirements.pdf

[Nie et al., 2005] Nie, J., Wen, J., Dong, Q. & Zho, Z. (2005). " A seamless Handoff in IEEE802.16a and IEEE802.11n Hybrid Networks". *IEEE Communications, Circuits and Systems*, vol. 1, pp. 383-387.

[Niederreiter, 1992] Niederreiter, H. (1992). *Random number generation and quasi-Monte Carlo methods*, SIAM.

[Nitin Bhas, 2011] Nitin Bhas. 2011. Better Backhaul for Mobile, Juniper Research.

[Ofcom, 2013] Ofcom. 2013. Ofcom announces winners of the 4G mobile auction. Available: http://media.ofcom.org.uk/2013/02/20/ofcom-announces-winners-of-the-4g-mobile-auction/ [Accessed 16 April 2014].

[Olariu et al., 2013] Olariu, C., Fitzpatrick, J., Ghamri-Doudane, Y. & Murphy, L. (Year) Published. "Provisioning call quality and capacity for femtocells over wireless mesh backhaul". *2013 IEEE 24th International Symposium on Personal Indoor and Mobile Radio Communications (PIMRC)*, 2013. IEEE, pp. 3071-3076.

[OPNET Modeler, 2009] OPNET Modeler (2009). OPNET Technologies Inc.

[Pahlavan and Levesque, 2005a] Pahlavan, K. & Levesque, A. H. (2005a). *Wireless Information Networks, 2nd Edition*, John Wiley & Sons.

[Pahlavan and Levesque, 2005b] Pahlavan, K. & Levesque, A. H. (2005b). *Wireless Information Networks, 2nd Edition; Chapter 11*, John Wiley & Sons.

[Parsons and Parsons, 2000] Parsons, J. D. & Parsons, P. J. D. (2000). *The mobile radio propagation channel*, John Wiley New York.

[Pei et al., 2010] Pei, X., Jiang, T., Qu, D., Zhu, G. & Liu, J. (2010). "Radio-resource management and access-control mechanism based on a novel economic model in heterogeneous wireless networks". *IEEE Transactions on Vehicular Technology*, vol. 59, pp. 3047-3056.

[Perahia and Stacey, 2013] Perahia, E. & Stacey, R. (2013). *Next Generation Wireless LANs: 802.11 n and 802.11 ac*, Cambridge university press.

[Petrova et al., 2007] Petrova, M., Mahonen, P. & Riihijarvi, J. (Year) Published. "Connectivity analysis of clustered ad hoc and mesh networks". *2007 IEEE Global Telecommunications Conference (GLOBECOM)*, 2007. IEEE, pp. 1139-1143.

[Piamrat et al., 2011] Piamrat, K., Ksentini, A., Bonnin, J.-M. & Viho, C. (2011). "Radio resource management in emerging heterogeneous wireless networks". *Computer Communications*, vol. 34, pp. 1066-1076.

[Pinar Civicioglu and Besdok, 2011] Pinar Civicioglu & Besdok, E. (2011). "A conceptual comparison of the Cuckoo-search, particle swarm optimization, differential evolution and artificial bee colony algorithms". *Springer, Artificial Intelligence Review*.

[Porjazoski and Popovski, 2011] Porjazoski, M. & Popovski, B. (Year) Published. "Radio access technology selection algorithm for heterogeneous wireless networks based on service type, user mobility and network load". *2011 10th International Conference on Telecommunication in Modern Satellite Cable and Broadcasting Services (TELSIKS)*, 2011. IEEE, pp. 475-478.

[Premkumar and Kumar, 2006] Premkumar, K. & Kumar, A. (Year) Published. "Optimum association of mobile wireless devices with a WLAN-3G access

network". *2006 IEEE International Conference on Communications (ICC)*, 2006. IEEE, pp. 2002-2008.

[Priscaro, 2013] Priscaro, M. 2013. Telecom New Zealand and Ruckus Wireless Transform Traditional Phone Booths into Super Fast Wi-Fi Hotspots, Ruckus Wireless. Available: http:// www.ruckuswireless.com/ [Accessed 16th May 2013].

[Qin et al., 2012] Qin, L., Yang, Y. & Zhao, D. (Year) Published. "Joint handoff and resource management for throughput fairness in a wireless mesh network". *2012 IEEE Global Communications Conference (GLOBECOM)*, 2012. IEEE, pp. 5525-5530.

[Qualcomm, 2011] Qualcomm. 2011. A comparison of LTE Advanced HetNet and WiFi. Available: https://www.qualcomm.com/documents/comparison-lte-advanced-hetnets-and-wi-fi [Accessed sept].

[Qualnet Network, 2014] Qualnet Network. (2014). *Scalable Network Technologies*. Available: www.qualnet.com.

[Quek et al., 2013] Quek, T. Q. S., Roche, G. d. l., Güvenç, I. & Kountouris, M. (2013). *Small Cell Network: Deployment, PHY techniques, and Resource Management*, Cambridge.

[Raiciu et al., 2011] Raiciu, C., Niculescu, D., Bagnulo, M. & Handley, M. J. (Year) Published. "Opportunistic mobility with multipath TCP". *Proceedings of the sixth international workshop on MobiArch*, 2011. ACM, pp. 7-12.

[Rappaport, 1996] Rappaport, T. S. (1996). *Wireless Communications: Principles and Practice*, Piscataway, NJ, USA, IEEE Press.

[Rice, 2006] Rice, J. (2006). *Mathematical statistics and data analysis*, Cengage Learning.

[Rishabh, 2010] Rishabh, K. (31st Mar 2010 2010). "Winner's Curse in 3G Auctions: What is expected in India?". Available: http://www.pensions-research.org/3G.pdf

[Ristanovic et al., 2011] Ristanovic, N., Le Boudec, J.-Y., Chaintreau, A. & Erramilli, V. (Year) Published. "Energy efficient offloading of 3g networks". *2011 IEEE 8th International Conference on Mobile Adhoc and Sensor Systems (MASS)*, 2011. IEEE, pp. 202-211.

[Rohde & Schwarz, 2008] Rohde & Schwarz. (2008). "UMTS Long Term Evolution (LTE) Technology Introduction, Rohde & Schwarz". Available: http://www2.rohde-schwarz.com

[Ruckus, 2011] Ruckus. (Nov 2011). "Dealing with Density:The Move to Small-Cell Architectures". Available: http://www.wballiance.com/

[Ruckus, 2014] Ruckus. (2014). *http://www.ruckuswireless.com/*. [Accessed 25 Feb 2014].

[Sandhu et al., 2003] Sandhu, S., Nabar, R., Gore, D. & Paulraj, A. (2003). "Introduction to Space-Time codes". *Applications of Space-Time Adaptive Processing, IEE Publishers*.

[Saunders and Aragón-Zavala, 2007] Saunders, S. & Aragón-Zavala, A. (2007). *Antennas and Propagation for Wireless Communication Systems: 2nd Edition*, John Wiley & Sons.

[Schwengler and Glbert, 2000] Schwengler, T. & Glbert, M. (Year) Published. "Propagation models at 5.8 GHz-path loss and building penetration". *2000 IEEE Radio and Wireless Conference (RAWCON)* 2000. IEEE, pp. 119-124.

[Sesia et al., 2009] Sesia, S., Toufik, I. & Baker, M. (2009). *LTE: The UMTS long term evolution, from theory to practice*, John Wiley & Sons.

[Singh et al., 2013] Singh, S., Dhillon, H. S. & Andrews, J. G. (2013). "Offloading in Heterogeneous Networks: Modeling, Analysis, and Design Insights". *IEEE Transactions on Wireless Communications,* vol. 12.

[Singh et al., 2012] Singh, S., Madhow, U. & Belding, E. M. (2012). "Shaping throughput profiles in multihop wireless networks: a resource-biasing approach". *IEEE Transactions on Mobile Computing,* vol. 11, pp. 367-376.

[SKMM, 2005] SKMM. (2005). "Guideline on the provision of wireless LAN service". Available: http://www.skmm.gov.my

[Small Cell Forum, 2007] Small Cell Forum. (2007). Available: http://www.smallcellforum.org/ [Accessed 28th Feb 2014].

[Small Cell Forum, 2012] Small Cell Forum. (Feb 2012). "Integrated Femto-WiFi (IFW) Networks". Available: www.smallcellforum.org

[Strix System, 2014] Strix System. (2014). *http://www.strixsystems.com/*. [Accessed 2 April 2014].

[Takei, 2008] Takei, J. 2008. Noise Figure, Noise Factor and Sensitivity: Wireless Systems Instructional Design. Available: http://www.intel.com/education/highered/Wireless/lectures/L08-noise_figures.ppt.

[Tang et al., 2010] Tang, J., Hincapié, R., Xue, G., Zhang, W. & Bustamante, R. (2010). "Fair bandwidth allocation in wireless mesh networks with cognitive radios". *IEEE Transactions on Vehicular Technology*, vol. 59, pp. 1487-1496.

[Tang et al., 2006] Tang, J., Xue, G. & Zhang, W. (Year) Published. "Maximum Throughput and Fair Bandwidth Allocation in Multi-Channel Wireless Mesh Networks". *INFOCOM*, 2006. pp. 1-10.

[Tang et al., 2007] Tang, J., Xue, G. & Zhang, W. (2007). "Cross-layer design for end-to-end throughput and fairness enhancement in multi-channel wireless mesh networks". *IEEE Transactions on Wireless Communications*, vol. 6, pp. 3482-3486.

[Thompson et al., 2014a] Thompson, J., Ge, X., Wu, H.-C., Irmer, R., Jiang, H., Fettweis, G. & Alamouti, S. (2014a). "5g wireless communication systems: Prospects and challenges". *Communications Magazine, IEEE*, vol. 52, pp. 62-64.

[Thompson et al., 2014b] Thompson, J., Ge, X., Wu, H.-C., Irmer, R., Jiang, H., Fettweis, G. & Alamouti, S. (2014b). "5G wireless communication systems: prospects and challenges Part 2". *IEEE Communications Magazine*, pp. 24-25.

[Ting et al., 2012] Ting, A., Chieng, D., Kwong, K. H. & Andonovic, I. (Year) Published. "Optimization of heterogeneous multi-radio multi-hop rural wireless network". *14th IEEE International Conference on Communication Technology (ICCT)*, 2012. IEEE, pp. 1159-1165.

[Ting et al., 2013] Ting, A., Chieng, D., Kwong, K. H., Andonovic, I. & Wong, K. (Year) Published. "Dynamic backhaul sensitive Network Selection Scheme in LTE-WiFi wireless HetNet". *2013 IEEE 24th International Symposium on*

Personal Indoor and Mobile Radio Communications (PIMRC), 2013. IEEE, pp. 3061-3065.

[Tranzeo, 2007] Tranzeo. 2007. Example Community Broadband Wireless Mesh Network Design, Version 1.1, 20th June 2007.

[Tranzeo, 2010] Tranzeo. 2010. Wireless Link Budget Analysis, How to Calculate Link Budget for Your Wireless Network. Available: http://www.tranzeo.com/allowed/Tranzeo_Link_Budget_Whitepaper.pdf [Accessed 10 April 2014].

[Tropos, 2014] Tropos. (2014). *https://www.tropos.com/*. [Accessed 24th Oct 2014].

[Tse and Viswanath, 2005] Tse, D. & Viswanath, P. (2005). *Fundamentals of wireless communication*, Cambridge university press.

[Vázquez, 2011] Vázquez, R. A. (Year) Published. "Training spiking neural models using cuckoo search algorithm". *2011 IEEE Congress on Evolutionary Computation (CEC)*, 2011. IEEE, pp. 679-686.

[Velayos et al., 2004] Velayos, H., Aleo, V. & Karlsson, G. (Year) Published. "Load balancing in overlapping wireless LAN cells". *2004 IEEE International Conference on Communications*, 2004. IEEE, pp. 3833-3836.

[Viswanathan et al., 1996] Viswanathan, G., Afanasyev, V., Buldyrev, S., Murphy, E., Prince, P. & Stanley, H. E. (1996). "Lévy flight search patterns of wandering albatrosses". *Nature*, vol. 381, pp. 413-415.

[Walton et al., 2011] Walton, S., Hassan, O., Morgan, K. & Brown, M. (2011). "Modified cuckoo search: A new gradient free optimisation algorithm". *Chaos, Solitons & Fractals*, vol. 44, pp. 710-718.

[Wang and Kuo, 2013] Wang, L. & Kuo, G.-S. (2013). "Mathematical Modeling for Network Selection in Heterogeneous Wireless Networks—A Tutorial". *IEEE Communications Surveys & Tutorials*, vol. 15, pp. 271-292.

[Wang et al., 2013] Wang, S.-M., Hwang, L.-T., Chang, F.-S., Liu, C.-F. & Yen, S.-T. (Year) Published. "A compact printed MIMO antenna integrated into a 2.4 GHz WLAN access point applications". *2013 Asia-Pacific Microwave Conference Proceedings (APMC)*, 2013. IEEE, pp. 639-641.

[Waze, 2008] Waze. (2008). *GPS-based geographical navigation application program for smartphones*. Available: https://www.waze.com/ [Accessed 19th Jan 2014].

[WBA, 2003] WBA. (2003). *Wireless Broadband Alliance*. Available: http://www.wballiance.com/ [Accessed 28th Feb 2014].

[WBA, 2010] WBA, "WISPr (Wireless Internet Service Provider roaming) 2.0",Ref: WBA/RM/WISPr Version 01.00, 8th April, 2010.

[WBA, 2011] WBA. (2011). *Next Generation Hotspot (NGH) Program*. Available: http://www.wballiance.com/programs/next-generation-hotspot/ [Accessed 28th Feb 2014].

[WBA, 2012] WBA. (2012). *Interoperability Compliance Program*. Available: http://www.wballiance.com/programs/interoperability-compliance/ [Accessed 28th Feb 2014].

[WBA, 2013] WBA, "Wireless Roaming Intermediary eXchange (WRIX - i, l, d & f)", October 2013.

[Weisstein, 2014] Weisstein, E. W. (2014). *Bivariate Normal Distribution*. MathWorld,. Available: http://mathworld.wolfram.com/BivariateNormalDistribution.html [Accessed 19 Sept 2014].

[Wi-Fi Alliance, 2012] Wi-Fi Alliance. 2012. Launch of Wi-Fi CERTIFIED Passpoint™ Enables a New Era in Service Provider Wi-Fi, AUSTIN, TX, June 26, 2012 [Accessed 28th Feb 2014].

[WiFi Alliance, 1999] WiFi Alliance. (1999). Available: www.wi-fi.org/ [Accessed 28th Feb 2014].

[WiFi Alliance, 2012] WiFi Alliance, "Wi-Fi Alliance. HotSpot 2.0 Technical Specication. v1.0.0", May 2012.

[Wikipedia, 2014] Wikipedia. (2014). *IEEE 802.11*. Available: http://en.wikipedia.org/wiki/IEEE_802.11 [Accessed 20 March 2014].

[Xiao, 2005] Xiao, Y. (2005). "IEEE 802.11 n: enhancements for higher throughput in wireless LANs". *IEEE Wireless Communications,* vol. 12, pp. 82-91.

[Xue et al., 2012] Xue, P., Gong, P., Park, J. H., Park, D. & Kim, D. K. (2012). "Radio resource management with proportional rate constraint in the heterogeneous networks". *IEEE Transactions on Wireless Communications,* vol. 11, pp. 1066-1075.

[Yan Zhang et al., 2008] Yan Zhang, Laurence T.Yang & Jianhua Ma (2008). *Ulicensed Mobile Access Technology: Protocols, Architectures, Security, Standards and Applications*, CRC Press.

[Yang, 2010] Yang, X.-S. (2010). *Nature-Inspried Metaheuristic Algorithms, 2nd Edition*, Luniver Press.

[Yang and Deb, 2010] Yang, X.-S. & Deb, S. (2010). "Engineering optimisation by cuckoo search". *International Journal of Mathematical Modelling and Numerical Optimisation*, vol. 1, pp. 330-343.

[Yang and Deb, 2014] Yang, X.-S. & Deb, S. (2014). "Cuckoo search: recent advances and applications". *Neural Computing and Applications*, vol. 24, pp. 169-174.

[Yang et al., 2013] Yang, Z., Yang, Q., Fu, F. & Kwak, K. S. (Year) Published. "A novel load balancing scheme in LTE and WiFi coexisted network for OFDMA system". *2013 International Conference on Wireless Communications & Signal Processing (WCSP)*, 2013. IEEE, pp. 1-5.

[Yeh et al., 2011] Yeh, S.-P., Talwar, S., Wu, G., Himayat, N. & Johnsson, K. (2011). "Capacity and coverage enhancement in heterogeneous networks". *IEEE Transactions on Wireless Communications*, vol. 18, pp. 32-38.

[Zhuo et al., 2013] Zhuo, X., Hua, S., Gao, W. & Cao, G. (2013). "An Incentive Framework for Cellular Traffic Offloading". *IEEE Transactions on Mobile Computing*, pp. 1.

Appendix A

A.1 IEEE 802.11n MAC Model

A.1.1 Normal MAC Service Data Unit (MSDU)

In IEEE802.11n [IEEE Std, 2009] the MAC layer (layer 2) data from upper layers (layer 3 and above) will be treated as a MAC Service Data Unit (MSDU). While data is received in MAC layer, the MAC header and Frame Check Sequence (FCS) are added to form a MAC Protocol Data Unit (MPDU) before sending it to the Physical layer (Figure A.1).

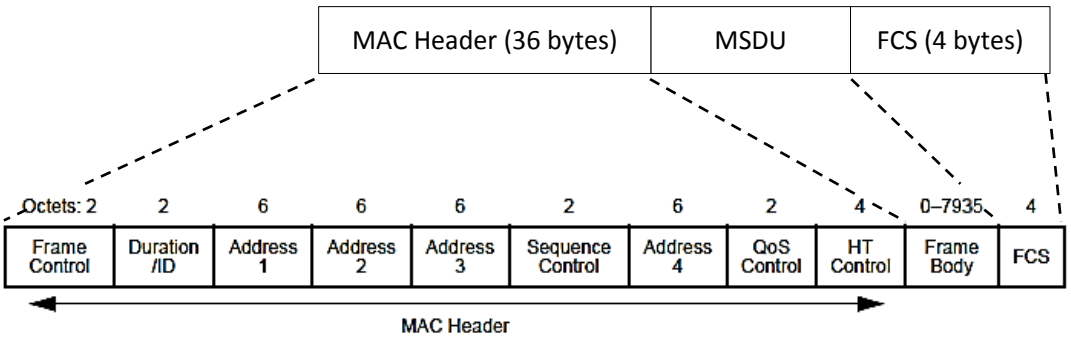

Figure A.1: IEEE802.11n Mac Frame.

The length of MPDU, L_{MPDU}, can be calculated by adding the length of all elements as follows:

$$L_{MPDU} = L_{mac\_hdr} + L_{MSDU} + L_{FCS} \quad \text{(A.1)}$$

where L_{mac_hdr} is the length of MAC header, L_{MSDU} is the length of MSDU and L_{FCS} is the length of FCS. The unit of all the elements are in bytes.

A.1.2 Aggregated MAC Service Data Unit (A-MSDU)

In IEEE802.11n, frame aggregation is introduced to enhance the MAC layer for higher throughput operation. Frame aggregation reduces overheads and enhances the efficiency and channel utilisation. There are two-level aggregation schemes [Xiao, 2005]; Aggregate MAC Service Date Unit (A-MSDU) and MAC Protocol Data Unit (A-MPDU).

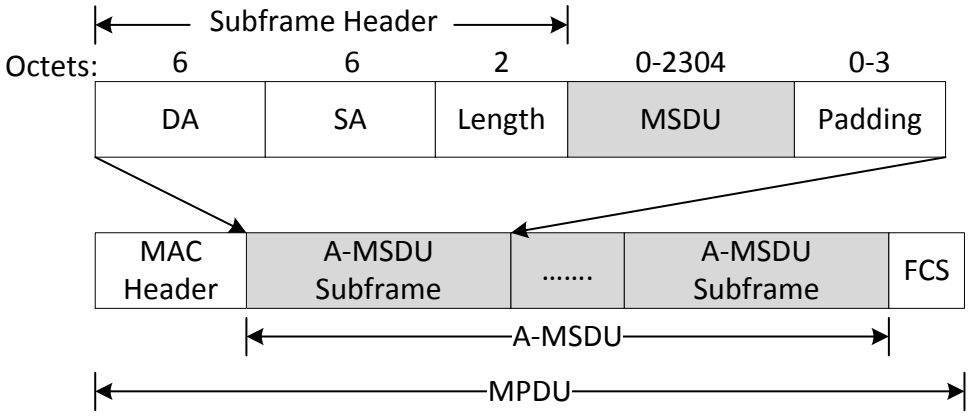

Figure A.2: MSDU aggregation in IEEE 802.11n.

In the simulation, only the A-MSDU mode is assumed (Figure A.2).With A-MSDU, multiple MSDU subframes are aggregated into a larger frame referred to as the A-MSDU frame. The size of a single MSDU, including its own subframe header and padding is a multiple of 4 bytes. The maximum length of an A-MSDU frame can be set to 3839 bytes or 7935 bytes but in the simulation, 7935 bytes is assumed. A MAC header and FCS is added to the A-MSDU frame as in a normal MSDU (Section

A.1.1) to form a MPDU and the length of a MPDU with A-MSDU mode, L'_{MPDU}, can be derived as;

$$L'_{MPDU} = L_{mac\_hdr} + N_{MSDU} \times L_{MSDU} + L_{FCS} \quad \text{(A.2)}$$

Assuming that length of total number of MSDU subframes, $N_{MSDU} \times L_{MSDU}$, is represented by L_{A-MSDU}, Equation (A.2) can be rewritten as;

$$L'_{MPDU} = L_{mac\_hdr} + L_{A-MSDU} + L_{FCS} \quad \text{(A.3)}$$

A.1.3 PPDU Transmit Time

The 802.11n High Throughput (HT) PPDU format shown in Figure A.3 is assumed [IEEE Std, 2009] for the Physical Layer. Also known as the HT-Greenfield mode only 802.11n station are assumed is in the whole network and no 802.11a/b/g stations are going to use the same channel.

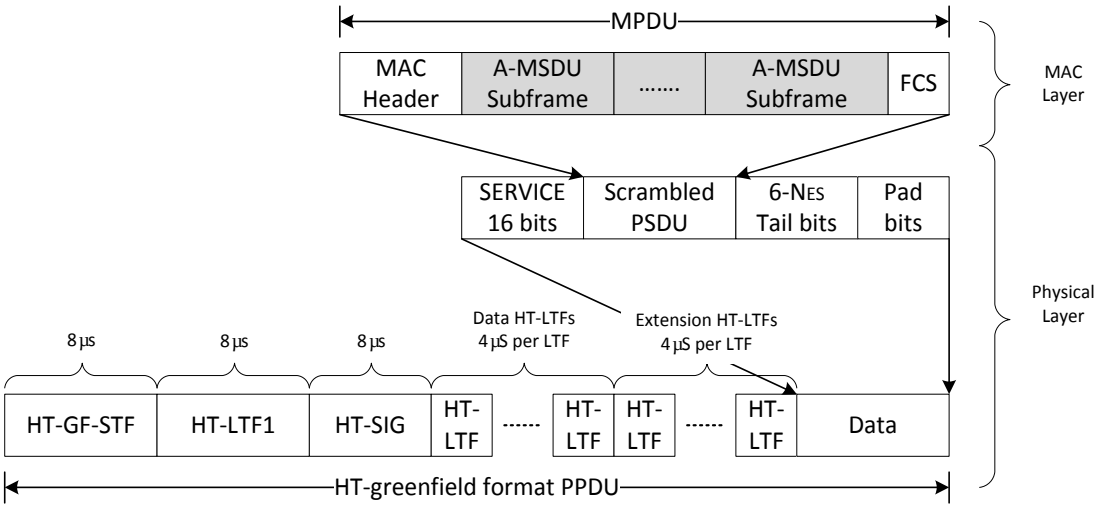

Figure A.3: High Throughput (HT) PPDU format.

The total PPDU transmission can be divided into two parts; the data transmission time and the headers transmission time. The detailed calculation of PPDU Data transmission time and the total PDDU transmission time including all headers is presented in the following sections.

A.1.3.1 PPDU Data Transmit Time

To form the Data field of a PPDU, the MPDU from layer 2 is added with a Service header, Tail bits and Pad bits to form the data field as shown in Figure A.3. The total length of data portion (in bytes) is calculated as;

$$L_{Data} = L_{SERVICE} + L_{PSDU} + L_{Tail} + L_{Pad} \quad \text{(A.4)}$$

where L_{Data} is the length of data packet in the PPDU, $L_{SERVICE}$ is the length of SERVICE header, L_{PSDU} is the length of scrambled PSDU, L_{Tail} is the length of tail bits and L_{Pad} is the length of padding bits.

The time required to transmit L_{Data} is calculated as T_{Data} as follows;

$$T_{Data} = T_{SYM} \times \left\lceil \frac{8 \times L_{Data}}{N_{DBPS}} \right\rceil \quad \text{(A.5)}$$

where N_{DBPS} is number of data bit per symbol and T_{SYM} is the symbol duration. N_{DBPS} of all Modulation and Coding Schemes (MCSs) is tabulated in Table A.1. In Equation (A.5), dividing the length of data L_{Data} (in bits) by N_{DBPS} gives the number of OFDM symbols required to carry the data and the equation can be rewritten as;

$$T_{Data} = T_{SYM} \times N_{SYM} \quad \text{(A.6)}$$

Table A.1: MCS Parameters for 20MHz, N_{SS}=1, N_{ES}=1.

MCS Index	Modulation	R	$N_{BPSCS(i_{SS})}$	N_{SD}	N_{SP}	N_{CBPS}	N_{DBPS}	Data Rate (Mbps)	
								800 ns GI	400 ns GI
0	BPSK	1/2	1	52	4	52	26	6.5	7.2
1	QPSK	1/2	2	52	4	104	52	13.0	14.4
2	QPSK	3/4	2	52	4	104	78	19.5	21.7
3	16-QAM	1/2	4	52	4	208	104	26.0	28.9
4	16-QAM	3/4	4	52	4	208	156	39.0	43.3
5	64-QAM	2/3	6	52	4	312	208	52.0	57.8
6	64-QAM	3/4	6	52	4	312	234	58.5	65.0
7	64-QAM	5/6	6	52	4	312	260	65.0	72.2

A.1.3.2 Total PPDU Transmission Time

A single PPDU transmission time including headers and data can be calculated as follows;

$$T_{PPDU} = T_{GF\_HT\_PREAMBLE} + T_{HT\_SIG} + T_{Data} + (N_{LTF} - 1)T_{HT\_LTFs} \quad \text{(A.7)}$$

where, $T_{GF\_HT\_PREAMBLE}$ is the duration of the preamble in the HT-greenfield format, given by:

$$T_{GF\_HT\_PREAMBLE} = T_{HT\_GF\_STF} + T_{HT\_LTF1} + (N_{HTLTF} - 1)T_{HT\_LTFs} \quad \text{(A.8)}$$

while N_{HTLTF} is defined as:

$$N_{HTLTF} = N_{HTDLFT} + N_{HTELFT} \tag{A.9}$$

A description of every element are presented in Table A.2 and the parameter values including T_{SYM}, $T_{HT\_GF\_STF}$, T_{HT_SIG}, T_{HT_LTFs} and T_{HT_LTF1} are tabulated in Table A.3.

Table A.2: PPDU Element descriptions.

Element	**Description**
HT-GF-STF	HT-Greenfield Short Training field
HT-LTF1	First HT Long Training field (Data)
HT-SIG	HT SIGNAL field
HT-LTFs	Additional HT Long Training fields (Data and Extension)
Data	The Data field includes the PSDU
SIFS	Short Interframe Space

Table A.3: PPDU element transmit times.

PLCP Elements	Duration	Unit
$T_{\text{HT\_GF\_STF}}$	8	µs
T_{SYM}	3.6	µs
T_{HT_SIG}	8	µs
T_{HT_LTF1}	8	µs
T_{HT_DLTF}	4	µs
T_{HT_ELTFs}	4	µs
aSIFSTime	10 (2.4GHz) / 16 (5GHz)	µs
aSlotTime	9	µs

A.1.4 Block Acknowledgement (BAck) Transmission Time

Figure A.4 shows the frame structure of a Block Acknowledgement. The length of the block acknowledgment MAC frame can be calculated by adding the length of fixed fields such as Frame Control, Duration/ID, Recipient STA's Address (RA), Transmitting STA's Address (TA), BAck Control and FCS. BAck Information is a variable depending on the type of BAck used as well as the number of MSDU frames.

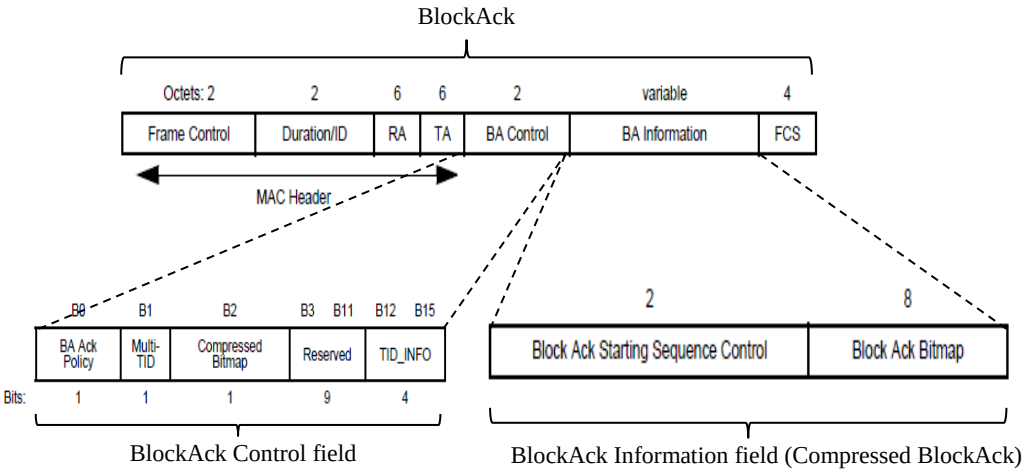

Figure A.4: Block Acknowledgement frame.

In the study, compressed BAck (Figure A.4) is chosen as it is the most efficient among all BAck types introduced in 11n. In the BAck information field, the BAck Bitmap sub-field is 8 octets in length and is used to indicate the received status of up to 64 MSDUs and A-MSDUs. Each bit set to 1 in the compressed BAck bitmap acknowledges the successful reception of a single MSDU or AMSDU in the order of sequence number [IEEE Std, 2009]. The length of the compressed BAck L_{BA} frame is 32 octets as shown in Figure A.4 and the total length of PPDU frame of BAck (in bytes) can be calculated as;

$$L_{PPDU\_BA} = L_{SERVICE} + L_{BA} + L_{Tail} + L_{Pad} \tag{A.10}$$

$$N_{BA\_SYM} = \left\lceil \frac{8 \times L_{PPDU\_BA}}{N_{DBPS}} \right\rceil \tag{A.11}$$

$$T_{MAC\_BA} = T_{SYM} \times N_{BA\_SYM} \tag{A.12}$$

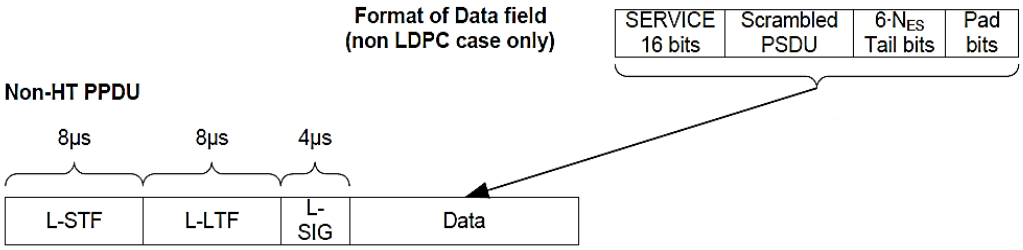

Figure A.5: Non-HT PPDU format.

Total transmission time of BAck frame is;

$$T_{BA} = T_{L\_STF} + T_{L\_LTF} + T_{L\_SIG} + T_{MAC\_BA} \tag{A.13}$$

A.1.5 Total Transmitting time and Throughput Efficiency

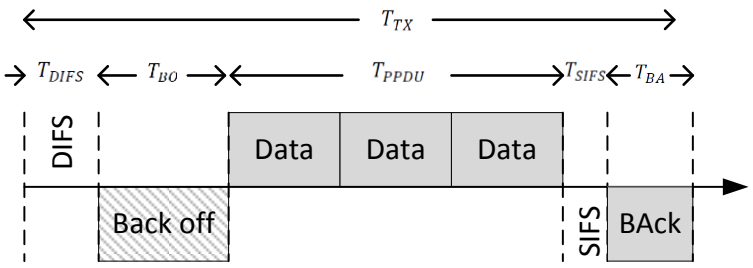

Figure A.6: Timing diagram for A-MSDU and implicit Block Acknowledgement.

To calculate the total time required for a complete transmission of a PPDU frame with A-MSDU, CSMA/CA without RTS/CTS is considered assuming no hidden nodes at the surrounding area. The total transmission cycle is shown in Figure A.6 and the time needed for the entire transmission cycle can be written as;

$$T_{TX} = T_{BO} + T_{DIFS} + T_{PPDU} + T_{SIFS} + T_{BA} \quad \text{(A.14)}$$

where T_{TX} is total cycle time, T_{BO} is the back off time during the contention period and T_{SIFS} is the Short Inter-frame Space.

Usually the backoff time is first selected randomly by a station (STA) following a uniform distribution from 0 to $CW_{\min}$ giving an expected value of $CW_{\min}/2$. In the simulation, T_{BO} is assumed to be equal to $\frac{CW_{\min}}{2} \times T_{SLOT}$ where T_{SLOT} is the slot time as defined in Table A.3.

The theoretical throughput of the 11n MAC layer or IP layer can be calculated by dividing the total data transmitted from the respective layer within entire transmission circle T_{TX}. MAC layer throughput C_{MAC} is derived in Equation (A.15) and IP layer throughput can be calculated by deducting the length of IP header L_{IP_hdr} as in Equation (A.16);

$$C_{MAC} = \frac{N_{MSDU} \times L_{MSDU} \times 8}{T_{TX}} \quad \text{(A.15)}$$

$$C_{IP} = \frac{N_{MSDU} \times \left(L_{MSDU} - L_{IP\_hdr}\right) \times 8}{T_{TX}} \quad \text{(A.16)}$$

The efficiency of MAC layer (φ_{MAC}) and IP layer (φ) with respect to the physical data rate can be determined by can be dividing C_{MAC} and C_{IP} respectively by physical data rate of the link as shown in Equation (A.17) and Equation (A.18). To

calculate the efficiency of each Modulation and Coding Scheme (MCS), link data rate, DR, of respective MCS can be chosen.

$$\varphi_{MAC} = \frac{C_{MAC}}{DR} \tag{A.17}$$

$$\varphi \quad = \frac{C_{IP}}{DR} \tag{A.18}$$

Appendix B

Besides the results in Chapter 5, other evaluation results especially on the scalability of DyBaCS are included in this section.

B.1 WiFi-LTE Overlap Ratio within a HetNet Cell.

Since the coverage overlap between WiFi and LTE is likely to vary in practice, it is therefore important to investigate how NSSs perform as a function of different overlap conditions. Here the coverage area is defined as a percentage e.g. 25% means 25% of LTE coverage is also covered by WiFi and 100% means all LTE coverage is overlapped by WiFi. The simulation is carried out by switching on APs deployed within the LTE cell one by one until the entire LTE cell overlaps with WiFi coverage. The activation sequence for APs is based on the number of users that fall within an individual AP coverage. An AP which covers most users is switched on first, followed by APs with lesser users in descending order.

Figure B.1(a) shows that in general, the average user throughput increases linearly for all NSSs as backhaul capacity increases and begins to plateau at 15 Mbps. The maximum average user throughput for PDR, DyBaCS and WF are 7.87 Mbps, 7.60 Mbps and 5.32 Mbps respectively at 100% WiFi-LTE coverage overlap and 20 Mbps backhaul capacity. PDR, which provides the highest average throughput, has a marginal performance edge compared to DyBaCS. The difference in performance

diminishes when WiFi-LTE coverage overlap increases. WF provides the worst average user throughput in most cases, except when the WiFi-LTE coverage overlap is 25%, but the throughput difference is negligible compared to the two other NSSs. An interesting point to note is for WF at 1 Mbps backhaul capacity, increases in WiFi coverage result in a drop in the average user throughput owing to the fact that WF connects all users to WiFi networks regardless of its backhaul capacity. Consequently, with WiFi backhaul capacity as low as 1 Mbps, WF causes users to suffer from low average throughput, becoming more severe as WiFi coverage increases.

Figure B.1(b) shows that DyBaCS provides the highest fairness for the entire range of WiFi-LTE overlap ratios and backhaul capacities. In the case of WF, higher fairness can be achieved at higher WiFi backhaul capacity because an appropriate level of capacity is shared amongst users. It is also found that fairness of PDR is close to that of DyBaCS when backhaul capacity is low but the difference becomes more significant as backhaul capacity increases because the PDR capacity distribution is less fair. At 25 Mbps backhaul capacity and 100% WiFi-LTE coverage overlap, both WF and PDR achieve 0.7 and 0.73 in terms of fairness respectively, significantly lower than the 0.9 fairness provided by DyBaCS.

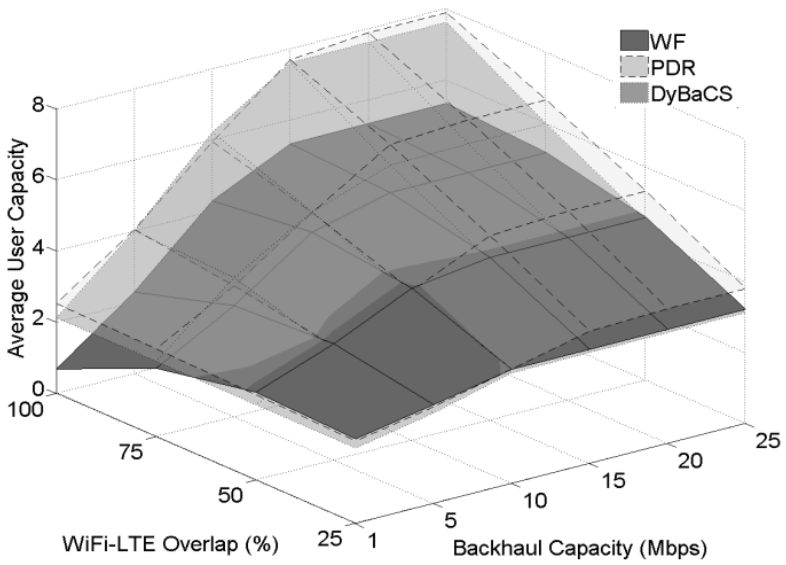

(a) Average user throughput.

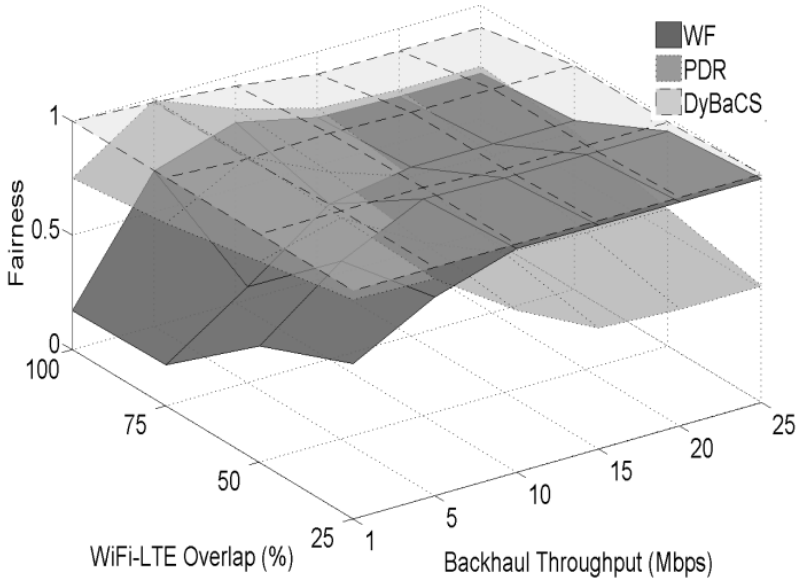

(b) Fairness.

Figure B.1: NSSs performance as a function of backhaul capacity and WiFi-LTE overlap percentage (Maximum 4 WiFi APs, uniform WiFi backhaul capacity).

B.2 WiFi Node Density per HetNet Cell

In this section, DyBaCS performance as a function of WiFi node density per LTE cell viz. WiFi-LTE node ratio and WiFi backhaul capacity is evaluated. The WiFi-LTE node ratio is scaled from 4, 7 to 13 and the EIRP of WiFi APs is set to 27 dBm, 24 dBm and 18 dBm respectively. In all scenarios, user density is kept at 100 and the coverage overlap between WiFi and LTE networks is maintained at 100%.

Figure B.2(a) shows that for all NSSs under investigation, the average user throughput generally improves as the number of WiFi APs increases from 4, 7 to 13 nodes. PDR achieves the highest average user throughput for the entire range of WiFi node densities and backhaul capacities, followed closely by DyBaCS. WF yields the worst average user throughput.

In terms of fairness as shown in Figure B.2(b), DyBaCS clearly outperforms the others over the entire range of WiFi-LTE node ratios and WiFi backhaul capacity, followed by PDR and WF. It is worth noting that the fairness of DyBaCS at 1 Mbps WiFi backhaul capacity is not affected by the WiFi-LTE node ratio, due to the fact that no user is assigned to the WiFi network as backhaul capacity is too low; assigning any user under this scenario to a WiFi network results in lower user throughput than connecting all of them to LTE network.

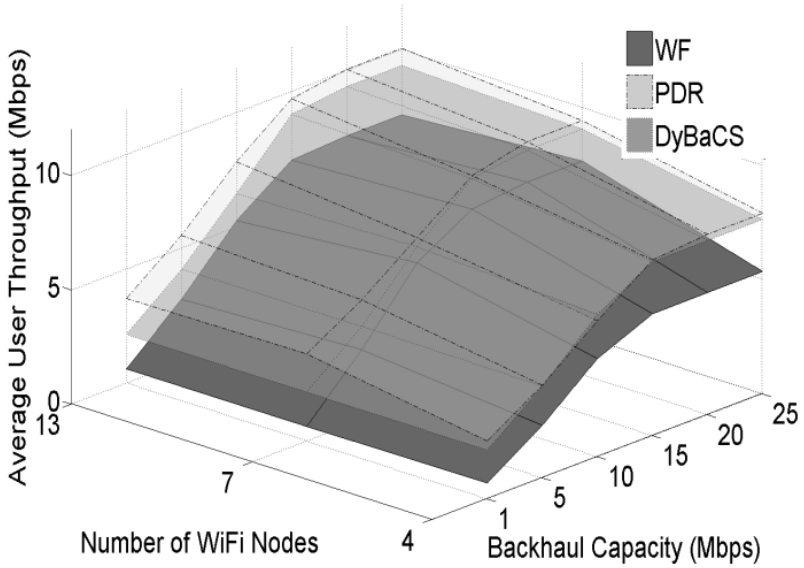

(a) Average user throughput.

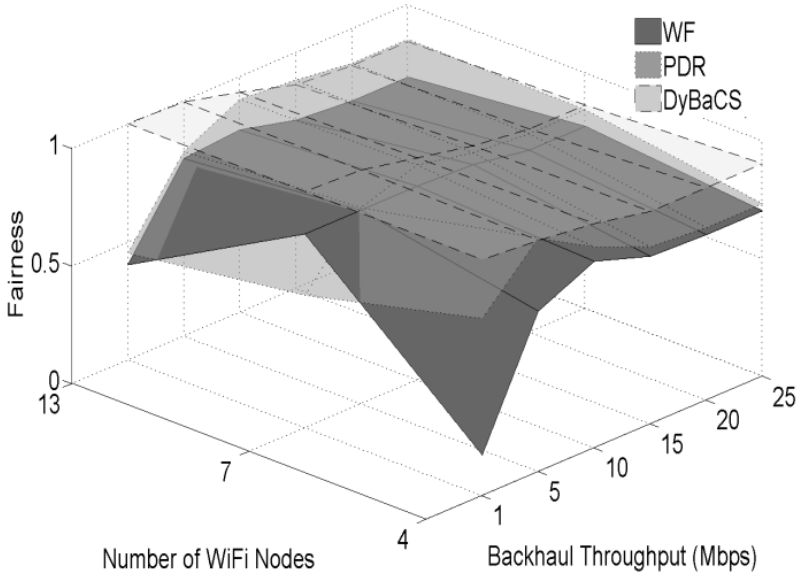

(b) Fairness.

Figure B.2: NSS performances as a function of WiFi-LTE Node Ratio and Backhaul Capacity (100 user density, 100% WiFi-LTE coverage ratio).

B.3 User Density

There is a high probability that the number of users in a network will vary significantly from peak to off peak hours, especially in urban areas [Afanasyev et al., 2010]. Furthermore, the number of users may also increase, but more gradually, in residential areas due to the growth in population. To evaluate how the NSSs under study cope with the variation of user density, an evaluation is carried out by varying the number of users within the HetNet cell. A scenario with 7 WiFi APs, a medium WiFi density is chosen and WiFi-LTE coverage overlap is set to 100%. The number of users is then increased from 100 to 250, in 50 user increments (Figure 5.3).

Results in Figure B.3 shows that PDR provides an advantage on average user throughput over DyBaCS when WiFi backhaul capacity values are low viz. 1 Mbps to 5 Mbps regardless of user density. However, when the WiFi backhaul capacity is increased, the difference in average user throughput between PDR and DyBaCS becomes negligible (similar trends also observed in Figure B.2(a)). At the highest user density – 250 users per square kilometer – the average user throughput of DyBaCS is greater than PDR when the WiFi backhaul capacity exceeds 10 Mbps. WF remains the worst in providing capacity to users. DyBaCS remains the best in terms of fairness for the entire range of user density and backhaul capacity.

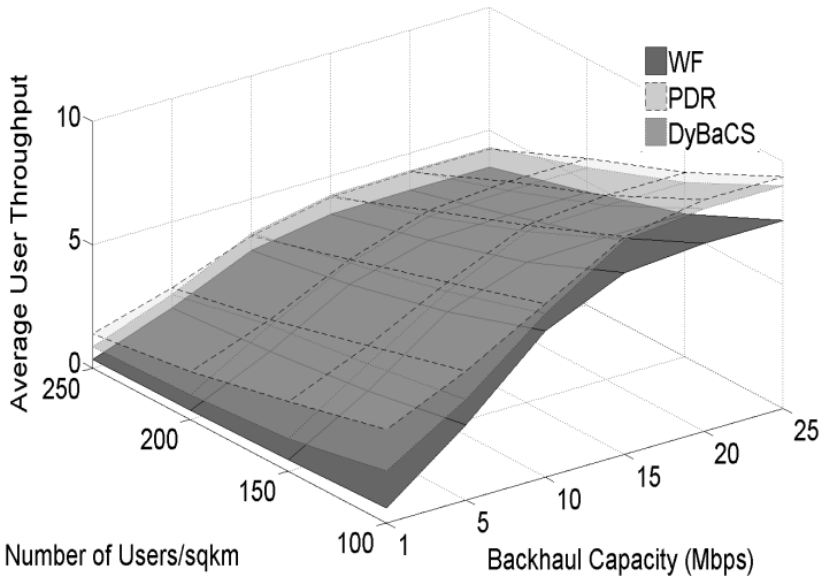

(a) Average User Throughput.

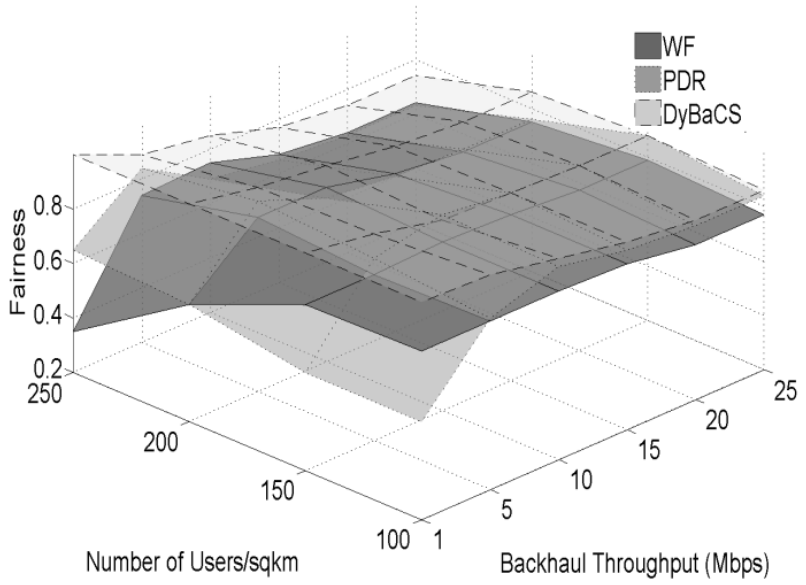

(b) Fairness.

Figure B.3: NSS performance as a function of number of users and backhaul capacity (7 WiFi APs, 100% WiFi-LTE coverage ratio).

Figure B.3 implies that with an increasing number of users, PDR is actually losing its advantage in relation to average user throughput and fairness to DyBaCS and WF respectively.

B.4 DyBaCS User Network Selection Characteristic

Figure B.4 shows the percentage of users connected to a WiFi network as a function of WiFi-LTE coverage percentage and backhaul capacity for the scenario of 7 WiFi APs and 100 users. For WF and PDR, the network selection criterion is based solely on WiFi coverage and physical data rate respectively; a change of WiFi backhaul capacity has no effect on the number of WiFi users. Figure B.4 shows that the percentage of admitted WiFi users for both NSSs is proportional to the total WiFi coverage size and inherently WF admitted a much larger number of WiFi users compared to PDR.

DyBaCS is a more intelligent algorithm that dynamically responds to changes in both WiFi coverage size and WiFi backhaul capacity. As shown in Figure B.4, when the WiFi backhaul capacity is limited (1 Mbps), no user is connected to a WiFi network. However, as backhaul capacity increases, the number of WiFi users increases gradually but saturates at 15 Mbps. Furthermore as the WiFi-LTE coverage ratio increases from 14% to 57%, the number of WiFi users also increases correspondingly, reaching a peak at 57% of WiFi-LTE coverage overlap. Further increments in WiFi coverage beyond 57% actually decrease the number of WiFi

users. The reason for this behaviour is that with more WiFi coverage, APs will service some users previously covered only by the LTE but at the same time APs will offload some WiFi users to the LTE BS for higher average user throughput and fairness. In this case, the number of dropped WiFi users is higher than the number of WiFi users services; hence overall number of WiFi users decreases.

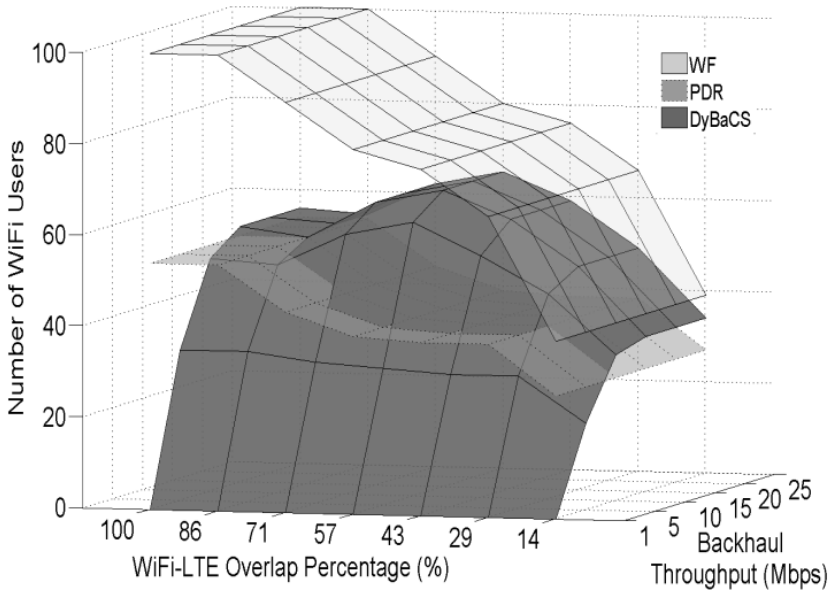

Figure B.4: Number of WiFi users as a function of WiFi-LTE coverage ratio and backhaul capacity (7 Nodes; total users = 100).